Compact steep-spectrum and peaked-spectrum radio sources

Christopher P. O'Dea · D. J. Saikia

the date of receipt and acceptance should be inserted later

Abstract Compact steep-spectrum (CSS) and peaked spectrum (PS) radio sources are compact, powerful radio sources. The multi-frequency observational properties and current theories are reviewed with emphasis on developments since the earlier review of O'Dea (1998). There are three main hypotheses for the nature of PS and CSS sources. (1) The PS sources might be very young radio galaxies which will evolve into CSS sources on their way to becoming large radio galaxies. (2) The PS and CSS sources might be compact because they are confined (and enhanced in radio power) by interaction with dense gas in their environments. (3) Alternately, the PS sources might be transient or intermittent sources. Each of these hypotheses may apply to individual objects. The relative number in each population will have significant implications for the radio galaxy paradigm. Proper motion studies over long time baselines have helped determine hotspot speeds for over three dozen sources and establish that these are young objects. Multifrequency polarization observations have demonstrated that many CSS/PS sources are embedded in a dense interstellar medium and vigorously interacting with it. The detection of emission line gas aligned with the radio source, and blue-shifted HI absorption and [OIII] emission lines indicates that AGN feedback is present in these objects - possibly driven by the radio source. Also, CSS/PS sources with evidence of episodic AGN over a large range of time-scales have been discussed. The review closes with a discussion of open questions and prospects for the future.

C. P. O'Dea

Dept of Physics & Astronomy, University of Manitoba, Winnipeg MB R3T 2N2 Canada

Tel.: +1 204-474-9863Fax: +1 204-474-7622E-mail: odeac@umanitoba.ca

D. J. Saikia

Inter-University Centre for Astronomy and Astrophysics, Savitribai Phule Pune University Campus, Ganeshkind P.O., Pune 411007, India

 $\hbox{E-mail: dhrubasaikia.tifr.ccsu@gmail.com, dhrubasaikia@iucaa.in}$

Keywords galaxies: active – galaxies: jets – radio continuum: galaxies

Contents

L	Intr	oduction	3
2	Sam	nples	5
3	Rad	io properties	0
	3.1	• •	0
			3
	3.2		5
	0.2		6
			18
	2.2	- 0	
	3.3	3	21
	3.4		24
			28
			29
	3.5	•	30
	3.6	What causes the turnover in the radio spectrum?	37
1	Infra	ared properties	88
5	Hos	t galaxies	12
	5.1		12
	5.2		13
	5.3		15
	5.4		15
	0.4		15
			17
			ε <i>ι</i> [7
			18
		v 11 111	18
	5.5		19
			19
			52
	5.6	Jet-induced Star Formation	53
	5.7	Black-hole Masses, Eddington ratios, the black-hole fundamental plane, and	
		jet production efficiency	55
3	High		66
	6.1		66
	-	V 1 1	66
			57
		3.00	8
			59
	6.2		50
	6.2		
_			32
1			32
	7.1	1 1 1	32
			32
		1 1	3
		7.1.3 Are CSS sources related to radio loud Narrow-Line Seyfert 1s? 6	64
	7.2	What are the PS and CSS sources?	55
		7.2.1 Transient or episodic sources	35
		7.2.2 Frustrated sources	35
			66
			39
	7.3		39
	7.4		70
2		•	73
,	rutt	uic work	J

Table 1 Nomenclature for Compact Radio Sources

Acronym	Text	Definition	ref	Notes
GPS	GHz-Peaked Spectrum	$0.5 \le \nu_p \le 5 \text{ GHz}$	1,2	a
HFP	High Frequency Peakers	$\nu_p > 5 \text{ GHz}$	3	a
MPS	MHz-Peaked Spectrum	$\nu_p < 1 \; \mathrm{GHz}$	4	
PS	Peaked Spectrum	All GPS, HFP, MPS	5	
CSO	Compact Symmetric Object	$LS < 1 \ \mathrm{kpc}$	6,7	b
CSS	Compact Steep Spectrum	$1 \le LS \le 20 \text{ kpc}$	8,9,10	c
MSO	Medium Symmetric Object	$1 \le LS \le 20 \text{ kpc}$	11	d

Columns. (1) Acronym. (2) Text. (3) Definition. ν_p is the observed frequency of the peak in the spectrum. LS is projected linear size. (4) Reference for initial recognition of this class of sources and/or use of the acronym. (5) Notes. a. The GPS and HFP are also very small (< 500 pc in size). b. The CSOs tend to have a core and two lobes and are preferentially associated with GPS and HFP galaxies, while core-jet morphology is more typical in GPS and HFP quasars. The description "compact symmetric object" replaced the earlier description "compact double" which was suggested by Phillips and Mutel (1982). c. The CSS sources also have a requirement for a steep spectrum at high frequencies ($\alpha \geq 0.5$). d. The MSOs and CSS sources are really the same objects, but the name MSO is meant to emphasize that they are larger versions of the CSOs. References. 1. Spoelstra et al. (1985); 2. Gopal-Krishna et al. (1983); 3. Dallacasa et al. (2000); 4. Coppejans et al. (2015); 5. This work; 6. Wilkinson et al. (1994); 7. Readhead et al. (1994); 8. Fanti et al. (1985); 9. Peacock and Wall (1982); 10. Kapahi (1981); 11. Fanti et al. (1995).

1 Introduction

Among the different types of active galactic nuclei (AGN), the radio luminous extragalactic radio sources associated with massive elliptical galaxies and referred to as radio AGN, continue to pose a number of interesting astrophysical questions (e.g., Padovani et al., 2017). These include the triggering of radio AGN activity, the formation of jets squirting out from the AGN with relativistic speeds, its effect on the host galaxy and its subsequent evolution, and relationship of the different radio and optical classification schemes to modes of accretion onto the supermassive black holes which are believed to fuel the AGN activity (e.g., Tadhunter, 2016a; Hardcastle and Croston, 2020). Radio AGN extend in their overall projected linear size from parsec-scales to over a few Mpc, with the largest known radio galaxy so far having a size of about 4.7 Mpc (Machalski et al., 2008). The extended sources inclined at small angles to the line of sight may appear small due to projection effects. Such sources tend to have dominant flat-spectrum radio cores over a large frequency range due to relativistic beaming of the nuclear jets moving at velocities close to that of light. A flat-spectrum is defined to have a spectral index $\alpha < 0.5$ where flux density, S, varies with frequency ν as $S \propto \nu^{-\alpha}$. The flat and complex spectra of the dominant cores are largely due to synchrotron self absorption in the radio core and knots of emission in the nuclear jets. Intrinsically small sources are however not generally dominated by their nuclear or core radio emission, and are believed to represent the early stages of evolution of radio AGN while some may be confined to small dimensions by a dense interstellar medium (O'Dea, 1998).

The radio spectra of these small sources may appear peaked either due to synchrotron self absorption or free-free absorption. However their spectra are steep and optically thin above the peak frequency. The GHz-Peaked-Spectrum (GPS) sources are selected to have their radio spectra dominated by a peak in the flux density around 1 GHz, in practice in the range ~ 500 MHz to ~ 5 GHz (Gopal-Krishna et al., 1983); though Stanghellini et al. (1998b) used a slightly larger range of 400 MHz to 6 GHz. Sources that peak above 5 GHz are called High Frequency Peakers (HFPs) (Dallacasa et al., 2000). Here we will refer to GPS and HFP sources together as Peaked-Spectrum (PS) sources. See Table 1 for a summary of common nomenclature.

The frequency of the peak in a synchrotron self-absorbed source scales inversely with the angular size of the source as $\nu_m \propto \theta^{-4/5}$ (see Sect. 3). Thus, the requirement for a peak at high frequencies selects compact radio sources. The PS sources tend to have projected linear sizes less than 500 pc while Compact Steep Spectrum (CSS) sources tend to have sizes between 500 pc and 20 kpc (e.g., O'Dea, 1998; Fanti et al., 1990). Compact radio sources (called Compact Symmetric Objects or CSOs) have been defined to be those with radio lobe emission on both sides of an active nucleus and an overall size less than about a kpc. CSOs are found directly via VLBI imaging surveys (e.g., Wilkinson et al., 1994; Peck et al., 2000).

Sources which peak at frequencies below 400 MHz are the Compact Steep Spectrum (CSS) sources though they are not selected specifically on the basis of the location of the spectral peak (Fanti et al., 1990). The selection criteria of the Fanti sample of CSS sources include projected linear size less than 20 kpc and flux density at 178 MHz greater than 10 Jy (Fanti et al., 1990). The requirement that the sources are bright at 178 MHz tends to select sources which peak below ~ 400 MHz. Peaked-spectrum or PS sources with a peak below about 1 GHz in the observer's frame have also been referred to as Megahertz Peaked-Spectrum or MPS sources (Coppejans et al., 2015, 2016a,b). The MPS sources are likely to be a combination of relatively nearby CSS and/or GPS sources, or more distant, compact high-frequency peakers whose peak frequency has been shifted to low frequencies due to the cosmological redshift.

The turnover in the radio spectrum in CSS and PS sources likely requires an absorption mechanism (e.g., de Kool and Begelman, 1989; O'Dea, 1998; Tingay and de Kool, 2003). The physics of the absorption mechanism provides important constraints on physical conditions in and around the radio source which are typically not available for much larger radio sources.

The compact sizes mean that the radio sources interact with their host galaxy interstellar medium (ISM) on a range of size scales ranging from parsecs to about 10 kpc. Energy input from radio sources (radio mode feedback) may be important in regulating star formation in massive galaxies and determining the shape of the high end of the galaxy luminosity function and also determining the balance of heating and cooling in the intracluster medium (ICM) (e.g., Croton et al., 2006; Fabian, 2012). As the PS and CSS sources are propagating through their host galaxies, they can provide examples of ra-

dio mode feedback (e.g., Holt et al., 2008; Morganti et al., 2013; Tadhunter, 2016b; Hardcastle and Croston, 2020). Evidence of interaction with the cold component of the interstellar medium in these galaxies via HI absorption line studies has been reviewed recently by Morganti and Oosterloo (2018).

There are three main hypotheses for the nature of PS and CSS sources. (1) The PS sources might be very young radio galaxies which will evolve into CSS sources on their way to becoming large radio galaxies (e.g., Fanti et al., 1995; An and Baan, 2012). (2) The PS and CSS sources might be compact because they are confined by interaction with dense gas in their environments (e.g., van Breugel et al., 1984; Dicken et al., 2012). (3) Alternately, the PS sources might be transient or intermittent sources (e.g., Readhead et al., 1993; Reynolds and Begelman, 1997). Each of these hypotheses may apply to individual objects. Determining which hypotheses apply to which fractions of the population will have important implications for radio source origin and evolution.

In this review of PS and CSS sources we provide a comprehensive overview of the observational properties and theoretical understanding of these interesting objects. We will focus mainly on progress since the review of O'Dea (1998). We discuss the current samples in Sect. 2, radio properties in Sect. 3, infrared properties in Sect. 4, host galaxies in Sect. 5, high energy properties in Sect. 6. A discussion of current topics of interest and the nature of the PS and CSS sources is presented in Sect. 7 and potential future work is presented in Sect. 8. New topics include the relation of PS and CSS sources with FR0 sources (Sect. 3.1.1) and narrow-line Seyfert 1s (Sect. 7.1.3), black hole masses and accretion rates (Sect. 5.7), γ -ray emission (§6.2), a possible association between compact radio sources and star formation (Sect. 7.2.3), and the role of compact sources in AGN feedback (Sect. 7.4).

We adopt $H_0=70~{\rm km~s^{-1}~Mpc^{-1}}$, $\Omega_{m_0}=0.3,~\Omega_{\Lambda_0}=0.7$, and 20 kpc as the limiting size for CSS/PS sources.

2 Samples

Among the most significant developments in recent years have been surveys at low radio frequencies using telescopes which are not limited by narrow bandwidths, leading to increased sensitivity and more reliable determination of their low-frequency spectra. These include the GaLactic and Extragalactic All-sky Murchison Widefield Array survey (GLEAM; Wayth et al., 2015), the LOFAR Multifrequency Snapshot Sky Survey (MSSS; Heald et al., 2015), and more recently the LOFAR Two-Metre Sky Survey (LoTSS; Shimwell et al., 2017, 2019), and the TIFR GMRT Sky Survey (TGSS ADR1; Intema et al., 2017). At higher frequencies complete samples could be constructed in the near future at significantly lower flux density levels than has so far been possible from surveys with upgraded or newly constructed telescopes such as the Very Large Array Sky Survey (VLASS; Myers, 2019; Lacy et al., 2020); the Evolutionary Map of the Universe (EMU; Norris et al., 2011) with the Australian Square

Kilometre Array Pathfinder (ASKAP) and MeerKAT International GigaHertz Tiered Extragalactic Exploration (MIGHTEE; Jarvis et al., 2016).

These surveys when they come on-line will lead to much larger samples of CSS and PS sources. For this review we briefly summarize those that have been compiled and/or studied since the review of O'Dea (1998). We first describe briefly the different samples, starting with the low-frequency ones, and then discuss what we have learnt from studies of sources in these surveys.

GLEAM sample of peaked sources

Callingham et al. (2017) presented a sample of 1483 peaked-spectrum sources identified from the GLEAM extragalactic catalogue consisting of 307,456 sources with 20 flux density measurements between 72 and 231 MHz. They also used flux densities from the NRAO VLA Sky Survey at 1400 MHz (NVSS; Condon et al., 1998) and Sydney University Molonglo Sky Survey at 843 MHz (SUMSS; Bock et al., 1999; Mauch et al., 2003) to determine the overall spectra reliably and be sensitive to PS sources with peaks between 72 MHz and 843/1400 MHz. Coppejans et al. (2015) found 24 of the Megahertz PS sources with redshift measurements in their sample to have an average redshift of 1.3, with four having a redshift >2, and a further four fainter objects without a redshift measurement being possibly even farther. They suggest that highly compact MPS sources could be a useful way of finding high-redshift radio-loud AGN.

B3/VLA sample

Fanti et al. (2001) presented a new sample of 87 CSS objects selected from the B3-VLA survey with a flux density $S_{408\mathrm{MHz}} > 0.8$ Jy. The B3-VLA sample consisting of 1049 sources (Vigotti et al., 1989) is expected to contain about 275 CSS/GPS objects, although Fanti et al. (2001) have focussed on the bright subsample as these had more complete spectroscopic information.

Sample from the B2 survey

A small sample of 19 candidate CSSs from a complete sample of 52 sources of intermediate strength selected from the B2.1 catalogue with flux densities in the range $0.9 \le S_{408} < 2.5$ Jy (Padrielli et al., 1981), was studied by Saikia et al. (2002).

CORALZ sample

A sample of Compact Radio sources at Low Redshift (CORALZ) consisting of 28 sources, with $\rm S_{1400MHz} > 100$ mJy and angular size <2 arcsec, was compiled by Snellen et al. (2004). These were selected from the FIRST survey and cross-correlated with the APM Palomar Sky Survey catalogue, and span the redshift range 0.005 < z < 0.16. Although these have not been selected on the basis of their spectral indices, over 90 per cent of the objects are either CSS or GPS objects.

$Additional\ FIRST$ -based samples

To probe the nature of low-luminosity CSS objects, weaker samples were compiled from the FIRST survey. Kunert et al. (2002) started with the Green Bank (GB) survey (White and Becker, 1992) with $\alpha_{1.4}^5 > 0.5$ and $S_{5GHz} > 150$ mJy in a region which overlaps with the FIRST survey. They listed 60 CSS sources which are compact with the FIRST beam after excluding those with a peaked spectrum.

Using a somewhat similar approach, Kunert-Bajraszewska and Thomasson (2009) considered the GB6 survey at 4.85 GHz and the FIRST survey and compiled a sample of 44 CSS objects with $\alpha_{1.4}^{4.85} > 0.7$, 70 mJy $\leq S_{1400 \mathrm{MHz}} \leq 1$ Jy and appearing compact with the FIRST beam. This sample too focused on CSS sources.

Sample of GPS sources based on the Parkes survey

Snellen et al. (2003) compiled a sample of 49 GPS sources from the PKSCAT90 survey (Otrupcek and Wright, 1991) with $S_{2700 MHz} > 0.5$ Jy and located in the declination range $-40^{\circ} < \delta < +15^{\circ}$ and Galactic latitude | b |> 20°. This is the southern counterpart to GPS samples in the northern hemisphere. All the GPS sources in this sample are identified with galaxies with redshifts in the range from 0.17 to 1.54 (de Vries et al., 2007).

The GPS 1-Jy sample

A complete sample of 33 GPS sources with $S_{5000MHz} > 1$ Jy, a turn-over frequency in the range 0.4 to 6 GHz with $\alpha_{\rm thin} > 0.5$, and with declination $\delta > -25^{\circ}$ and $|b| > 10^{\circ}$ was compiled by (Stanghellini et al., 1998b).

CSSs from the S4 survey

Saikia et al. (2001) observed a sample of candidate CSSs from the S4 survey (Pauliny-Toth et al., 1978) with $S_{5000MHz} \ge 0.5$ Jy, which were earlier found to be either unresolved or partially resolved with the Westerbork Synthesis Radio Telescope (Kapahi, 1981).

The COINS sample

From large-scale VLBI continuum surveys, Peck and Taylor (2000) identified a sample of 52 compact symmetric objects or CSOs observed in the northern sky (COINS) with $S_{5000MHz}$ larger than about 100 mJy. This sample is not based on the spectra of the sources but on the observed VLBI-scale structure of the objects.

The VIPS sample

From the Very Long Baseline Array (VLBA) Imaging and Polarization Survey (VIPS; Taylor et al., 2005; Helmboldt et al., 2007) of 1127 sources, Tremblay et al. (2009) compiled a sample of 103 CSOs, making it one of the largest samples.

High-frequency peakers: GB and NVSS/FIRST

To identify sources where the peak of the spectrum may be higher than a few GHz, sources with a rising spectrum between 1.40 and 4.85 GHz were identified by cross-correlating the 87GB and NVSS catalogues for a 'bright' sample (Dallacasa et al., 2000). These were selected to have $S_{5000MHz} > 300$ mJy. Similarly a 'faint' sample was compiled by comparing with the FIRST survey at 1400 MHz and limiting it to those with $S_{5000MHz} > 50$ mJy (Dallacasa et al., 2002; Orienti and Dallacasa, 2012, 2020).

High-frequency peakers: AT20G sample

From the Australia Telescope Compact Array survey at 20 GHz (AT20G survey) consisting of 5450 radio sources, Hancock (2009) compiled a sample of 656 radio sources with peaks above 5 GHz. Of these 466 were identified with optical objects, 104 with galaxies and 362 with quasars. HFPs are discussed further in Sect. 7.1.2.

Several of the surveys summarized here extend the radio power of the compact sources to significantly lower values since the review by O'Dea (1998). For example the log of median radio power of O'Dea (1998) samples at 5 GHz in units of W Hz⁻¹ consisting of bright 3CR sources (Fanti et al., 1990) and PS sources (Stanghellini et al., 1998b) is 27.6. For a sample of faint PS sources compiled by Snellen et al. (1998b), the log of median radio power at 5 GHz of 26.2 is marginally lower than that for the GLEAM sample which has a value of 26.5. The radio power of the B3-VLA sample selected at 408 MHz has a similar value of 26.6 when extrapolated to 5 GHz assuming a spectral index of 1. As one goes to fainter samples, lower-luminosity sources are selected. For example in the CORALZ sample (Snellen et al., 2004), the log of radio power at 5 GHz in W $\rm Hz^{-1}$ ranges from 22.96 to 25.03 with a median value of about 24.4. The log of median radio power of the galaxies in the AT20G-6dFGS sample at 1.4 GHz is 24.5 (Sadler, 2016), corresponding to 23.95 at 5 GHz assuming a spectral index of 1. The log of radio power of the FR0 sources many of which are likely to be CSS and PS sources range from 22 to 24 at 1.4 GHz in units of W Hz^{-1} (Capetti et al., 2020; Baldi et al., 2018).

The local 1.4 GHz radio luminosity function of AGN extends down to about $\log_{10}\sim 20.5~\rm W~Hz^{-1}$ (Mauch and Sadler, 2007). The current samples of PS and CSS have radio powers which extend down to about $\log_{10}\sim 23~\rm W~Hz^{-1}$ which is within about 1.5 orders of magnitude of the faintest radio AGN. The distribution of 1.4 GHz radio powers of Seyfert galaxies range from $\log_{10}\sim 20.5\text{--}24.0~\rm W~Hz^{-1}$ (e.g., Ulvestad and Wilson, 1989). There is overlap of the PS and CSS radio powers with the high power end of the Seyfert galaxies. Thus, the physics of the PS and CSS radio sources may extrapolate to the faintest radio AGN, including Seyferts.

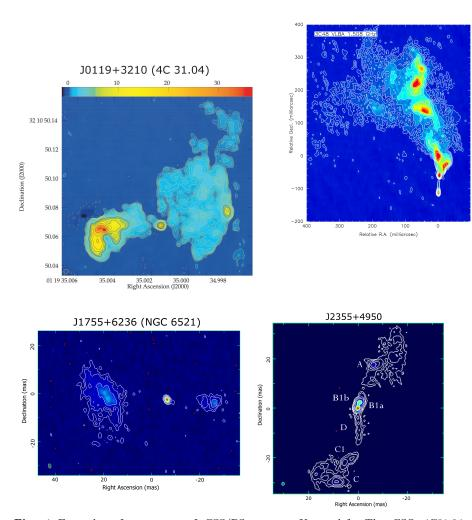


Fig. 1 Examples of structures of CSS/PS sources. Upper left: The CSO 4C31.04 (J0119+3210) which is associated with a galaxy at a redshift of 0.0602, has a peaked spectrum, and shows bright compact hotspots and extended emission on both sides along with a radio core (Giroletti et al., 2003). The projected linear size defined by the outer peaks of emission is 107 pc. Upper right: The CSS quasar 3C48 (J0137+3309) at a redshift of 0.367 which shows a disrupted jet indicating strong interaction with the interstellar medium of the host quasar (An et al., 2010). The total projected size seen in this image is $2.6~\mathrm{kpc}$ from the nucleus, although an extended envelope extends to about 5 kpc from the nucleus, the southernmost component seen in this image (An et al., 2010). Lower left: The CSS galaxy NGC6521 (J1755+6236) at a redshift of 0.0275 shows diffuse outer lobes with no prominent hot spots indicating that the energy supply may have stopped (Polatidis, 2009). The total projected size of the source defined by the outer lobes is 29 pc. Lower right: J2355+4950 associated with a galaxy at a redshift of 0.2379 shows hot spots along with diffuse emission on opposite sides and a well-defined radio jet (Polatidis et al., 1999; Taylor et al., 2000; Polatidis and Conway, 2003; Polatidis, 2009). The total projected size of the source defined by the outer lobes is 240 pc.

3 Radio properties

3.1 Radio structures

A study of the structures of radio sources could provide valuable insights towards understanding the formation, evolution and interaction with the ambient medium of these compact radio sources. For example if the PS and CSS sources are young objects advancing outwards through a dense inhomogeneous and asymmetric external medium on opposite sides of the nucleus, one may find evidence of this in their structural and polarization asymmetries. On the other hand for sources confined to small dimensions by a dense interstellar medium, one may find evidence of disruption of a radio jet as seen in 3C48, or deflection of a jet to form complex structures. To clarify the structures of these sources, one needs high-resolution observations ranging from mas scale for the most compact ones to the sub-arcsec scales. Figure 1 illustrates some of the structures observed in CSS/PS sources which include double-lobed sources with or without a detected radio core but well-defined hotspot(s) which could sometimes be significantly misaligned, jets which may be disrupted or appear quite collimated, as well as lobes which appear diffuse with no significant hotspots in them.

The extended structure of radio sources has traditionally been classified into the Fanaroff-Riley or FR Class I and II sources. The latter are characterized by prominent hotspots at the outer edges and narrow collimated asymmetric jets, while the former have more diffuse lobes of emission with more symmetric jets on kpc scales, and are less luminous than the FRII type sources. Ledlow and Owen (1996) suggested that the dividing luminosity between these two classes is not fixed but increases with optical luminosity of the host galaxy, although Best (2009), Wing and Blanton (2011), Gendre et al. (2013) and Mingo et al. (2019) have questioned this sharp division. From a large sample of 5805 sources from the LoTSS survey Mingo et al. (2019) find FRII sources about 3 orders of magnitude lower in luminosity compared to the traditional FR break. They also find the host galaxies of these low-luminosity FRIIs to be fainter than high-luminosity FRIIs and FRIs matched in luminosity. The FRI/II classification has traditionally been based on radio images of sources initially from the 3CR but generally from bright radio source samples. Deep sensitive surveys at radio frequencies as well as finding radio counterparts from optical surveys such as the Sloan Digital Sky Survey (SDSS) have also revealed sources which have similar core luminosity to those of FRI sources, but the extended emission is weaker by factors of ~ 100 (Baldi and Capetti, 2009). These have been christened as FR0s, and their relationship to the more extended sources need to be understood (Baldi et al., 2015; Sadler, 2016; Cheng and An, 2018). The FR0 sources, a significant fraction of which are likely to be CSS/PS sources are discussed further in Sect. 3.1.1.

Based on their optical spectra radio AGN have been classified into High Excitation Radio Galaxies (HERGs) and Low Excitation Radio Galaxies (LERGs) which appear related to different modes of fuelling the AGN (Hardcastle et al.,

2007; Buttiglione et al., 2010; Best and Heckman, 2012; Heckman and Best, 2014; Tadhunter, 2016a). This has been discussed further in Sect. 5.5.1. The LERGs tend to be of lower luminosity than the HERGs, and have an FRI-type structure while the radio structure of HERGS are predominantly of FRII type (Best and Heckman, 2012; Heckman and Best, 2014; Tadhunter, 2016a).

Another significant input in our understanding of AGN during the last decade has been the Wide-field Infrared Survey Explorer (WISE) measurements at 3.4 (W1), 4.6 (W2), 12 (W3) and 22 (W4) μ m (Wright et al., 2010). A colour-colour plot W1-W2 vs W2-W3 (e.g., Wright et al., 2010; Donoso et al., 2012) can help distinguish between quiescent galaxies, star-forming ones and different types of AGN. The WISE bands provide valuable information on host galaxies, tracing stellar light as well as from the interstellar medium associated with star formation. While the WISE W1 and W2 bands appear to be good tracers of stellar mass distribution, longer wavelengths trace cooler emission from the interstellar medium (e.g., Jarrett et al., 2013). The W2-W3 colour correlates well with the specific star formation rate with the stronger or more luminous AGN being close to the high star-forming galaxies. Weaker or less luminous AGN extend the relationship to lower specific star formation rate and smaller values of W2-W3 (e.g., Donoso et al., 2012). For those referred to as WISE early-type with W2-W3<2 most are LERGs in samples of sources of intermediate radio luminosity, while those with W2-W3>2 are a mixture of both LERGs and HERGs, but a majority appear to be HERGs. The brighter or more luminous source samples although contain both LERGs and HERGs are dominated by the HERGs (e.g., Hardcastle et al., 2007; Tadhunter, 2016a).

Early studies of CSS and PS sources, which includes the CSOs, usually defined to be two-sided with an overall projected linear size <1 kpc and the medium symmetric objects or MSOs defined to be >1 kpc, were based on bright source samples such as the 3CR (Laing et al., 1983), PW (Peacock and Wall, 1982) and S4 samples (Kapahi, 1981; Stickel and Kuehr, 1994) selected at both low and high frequencies. Detailed high-resolution images of these sources with both sub-arcsec and mas resolutions (Fig. 1) showed that (i) they often, but not always had a double-lobed structure either with or without a detected radio core and could be classified as a CSO/MSO depending on its size. The median values of the relative strength of the radio cores for the CSS/PS radio galaxies and quasars, were similar to those of the larger radio galaxies and quasars respectively. This is consistent with the expectations of the unified scheme with the quasar cores being more prominent. (ii) Large misalignments, where the two oppositely-directed axes are misaligned by more than 20° were often seen which could be due to a combination of interaction with an asymmetric external environment and the effects of projection. While those seen in quasars with strong cores could be due to projection effects, these are also seen in sources with weak cores, including galaxies. In more extreme cases, the source may appear quite complex. (iii) The effects of an ambient medium are also visible in the arm length and flux density ratios of the CSS sources, which are both significantly larger than the corresponding values for the larger sources. The brighter components are often closer to the nucleus suggesting the effects of an asymmetric environment with which the jets interact rather than relativistic beaming effects where the approaching beamed component would appear further (for e.g. Saikia et al., 1995, 2001, 2003).

In addition to these high-luminosity compact sources, it is relevant to investigate whether there is a large population of lower-luminosity compact sources and how do their properties compare with the higher-luminosity ones. One of the early lower-luminosity samples, the CORALZ sample, was compiled by Snellen et al. (2004) from the FIRST survey with $S_{1400MHz} > 100$ mJy, overall deconvolved angular diameter < 2 arcsec and lying in the redshift range 0.005 < z < 0.16. These sources which are on average over two orders of magnitude less luminous than the high-luminosity compact sources were also found to predominantly have a CSO or double structure (de Vries et al., 2009a,b). They also find the turnover frequency in the spectra of these weaker sources to be inversely related to their linear size, and suggest that the turnover in their spectra is consistent with synchrotron self absorption. Kunert-Bajraszewska and collaborators (Kunert-Bajraszewska et al., 2010; Kunert-Bajraszewska and Labiano, 2010; Kunert-Bajraszewska et al., 2014; Kunert-Bajraszewska, 2016) considered a sample of 44 low-luminosity compact sources (LLCs) with their luminosity at 1400 MHz ranging from 10²³ to 10²⁶ W Hz⁻¹ with a median value of $\sim 5 \times 10^{25} \text{ W Hz}^{-1}$. For those with a radio core, they reported significant asymmetries on opposite sides, as seen for the strong source samples. This is also likely to be due to asymmetries in the external environment. They also reported the LLC sources to have more dominant cores compared with both the higher-luminosity FRI and FRII sources, somewhat analogous to the FRO objects, suggesting their difficulties in forming prominent extended emission. Several CSS/PS sources in the nearby Universe have been studied in some detail. For those within about 100 Mpc detailed studies of the host galaxies are possible (see e.g., Labiano et al., 2007). An example of a nearby PS source is B1718-649 (NGC6328, J1723-6500) at a distance of $\sim 60 \text{ Mpc}$ with a double-lobed radio structure and an optical galaxy formed possibly by the merger of two systems (Tingay et al., 1997, 2015). Although NGC1052 (J0241-0815) and IC1459 (J2257-3627) have been suggested to be nearby GPS sources (Tingay et al., 2003; Tingay and Edwards, 2015), these sources are variable, with NGC1052 having a nearly flat spectrum and two-sided jets traversing outwards at sub-relativistic speeds (Vermeulen et al., 2003). IC1459 also has similar oppositely-directed jets and a dominant core component (Tingay and Edwards, 2015). Their possible relationship to the archetypal PS sources need to be understood.

Sadler et al. (2014) have further probed the low-luminosity region. They compiled a sample of 202 sources by cross matching the AT20G sample with the 6dF Galaxy Survey (Jones et al., 2009). The median redshift of this sample is 0.058, while the median luminosity at 1.4 GHz is 3.2×10^{24} W Hz⁻¹, with 55 of the objects below 10^{24} W Hz⁻¹ (Sadler, 2016). Although detailed high-resolution images are not available, based on the ATCA observations as well as comparisons with NVSS and SUMSS images, Sadler et al. find \sim 68%

to be compact FR0s, most of which are either candidate CSS or PS objects, 8% are FRIIs and 24% FRIs. They find their results for FRI and FRII sources consistent with the Ledlow-Owen trend by considering the 20 GHz radio luminosity and the absolute K-band magnitude, with the CSS and PS objects (which are included in their FR0s) spanning about 3 orders of magnitude in luminosity and overlapping with their FRI and FRII sources. For the entire ATG20-6dFGS sample, the majority (\sim 77%) are LERGs while \sim 23% are HERGs. This is also true for the CSS and PS (FR0) sources, the percentages being \sim 75 and 25 respectively. In the WISE colour-colour plot, the FRIs are almost entirely WISE early type with W2-W3<2.0, the FRIIs of WISE late type with W2-W3>2.0, while the FR0s are largely (\sim 67%) of WISE early type, with \sim 33% being of late type. These trends have significant implications in our understanding of the evolution of radio sources (Sadler et al., 2014; Sadler, 2016).

The evolution scenario in the 1990s revolved around GPS sources evolving into CSS and then on to the larger-sized extended sources (Fanti et al., 1995; Readhead et al., 1996; O'Dea, 1998). The classification of radio sources into LERGs and HERGs and the recognition of two possible accretion modes, suggest two parallel paths, one for LERGs and one for HERGs: PS_{LERGs} – CSS_{LERGs} – Ext_{LERGs}, and a similar track at a higher luminosity for HERGs (e.g., Kunert-Bajraszewska, 2016). The higher luminosity HERGs could be evolving largely into FRII sources, while the lower-luminosity LERGs into FRIs. Several authors have considered evolutionary models along these lines (An and Baan, 2012). However, the large number of low-luminosity compact sources suggests that many of them may not evolve into larger sources, being confined to the small dimensions by the dense interstellar medium of the host galaxies (Sect. 7.2.2), or may represent sources going through intermittent cycles of low-level activity (Sect. 7.2.1).

3.1.1 The FR0 sources

In this section, we discuss possible relationship between the FR0 sources which are weak compact radio sources characterized by the deficit of extended emission and the CSS/PS sources. The FR0s have been seen in large numbers in sensitive radio and optical surveys. Those with a steep or peaked spectrum are analogues of weak CSS/PS sources and pose similar questions related to the formation and evolution of these objects. What fraction of these sources may be young objects and what fraction may evolve into larger objects? Do the FR0s represent transient AGN activity? Is their inability to launch large-scale jets related to their black hole mass and spin?

The FR0 sources are easily discernible in sensitive radio surveys. For example, the availability of radio surveys with the VLA and large-area optical surveys such as the SDSS led to the compilation of \sim 18000 radio sources upto redshifts of \sim 0.3 and stronger than \sim 5 mJy at 1400 MHz (Best and Heckman, 2012). These span a range of luminosity from 10^{22} – 10^{26} W Hz⁻¹ at 1400 MHz, and although these exhibit a wide range of structures including those seen in

the stronger 3CR sources, the majority of these are compact. The resolution of the FIRST observations of 5 arcsec would correspond to a size of ~ 20 kpc at at redshift of 0.3. These objects christened as FR0s have been identified from both low- and high-frequency surveys and dominate the radio source population at low radio luminosities (e.g., Baldi and Capetti, 2009, 2010; Sadler et al., 2014; Baldi et al., 2015; Whittam et al., 2016; Miraghaei and Best, 2017). However detailed spectral information would be required to determine what fraction may be similar to CSS/PS sources.

At high frequencies, Sadler (2016) note that the FR0s which make up most of the AT20G-6dfGS sample are a mixed lot with \sim 75% being LERGs and 25% HERGs, and \sim 67% being WISE early-type and 33 per cent late-type galaxies. Their luminosity at 1.4 GHz ranges from 10^{22} to 10^{26} W Hz⁻¹ and many of these could be PS/CSS type sources. For a complete sample of 96 sources (S > 0.5 Jy) chosen from the Cambridge 10C survey at 15.7 GHz, 65 have been classified as compact or FR0s with 13 as CSS, 10 as PS and the remaining 42 as unclassified (Whittam et al., 2016). In both the samples, the number of FR0s are in the range of 70–80%, although the mean radio spectral indices and optical properties may exhibit dependence on the flux density of the radio sources, with the radio spectra exhibiting a variety of shapes.

At low radio frequencies which is expected to be dominated by optically thin emission, ~70% of the radio sources in LoTSS (Shimwell et al., 2017, 2019) appear to be unresolved with an angular resolution of ~6 arcsec. These sources which dominate the low-frequency radio Universe are likely to give rise to thousands of FR0 candidates (c.f. Hardcastle et al., 2019; Sabater et al., 2019; Mingo et al., 2019). Deep radio observations of well-studied fields have also yielded large numbers of compact steep-spectrum sources, as seen for example in the ELAIS-N1 field (e.g., Sirothia et al., 2009; Ishwara-Chandra et al., 2020). Of the 6400 sources found in a wide-area deep survey of this region at 610 MHz, the vast majority are compact with a median spectral index of ~0.85 between 610 and 1400 MHz (Ishwara-Chandra et al., 2020).

Baldi et al. (2018) have compiled a catalogue of 108 FR0 sources (FR0CAT) with a redshift <0.05 and a size less than ~ 5 kpc starting with the Best and Heckman (2012) sample. These FR0s are found to reside in massive luminous early type galaxies (-21 > M_r > -23) with black hole masses in the range of \sim $10^{7.5}$ – $10^9 M_{\odot}$, which are less massive than FRI radio galaxies by a ~1.6. Their mid-IR colours are also consistent with those of elliptical galaxies (Wright et al., 2010). The most striking feature is the deficit of extended radio emission. Considering sources of similar [OIII] luminosity which is an indicator for AGN power, the radio luminosity of FR0s is lower than 3CR sources by ~ 100 (Baldi et al., 2018). Capetti et al. (2019) found no evidence of extended emission in these sources in the TIFR GMRT Sky Survey (TGSS), and noted that although \sim 75 per cent have a convex spectrum the steepening is more gradual than the high-luminosity PS sources. Besides the deficit of extended radio emission the FR0s appear to reside in environments where the galaxy density is lower than for FRIs by a factor of ~ 2 (Capetti et al., 2020). The association of a Fermi source Tol1326-379 with an FR0 galaxy (Grandi et al., 2016) has aroused interest in their high-energy properties which has been reviewed recently by Baldi et al. (2019b).

As a significant fraction of these FR0 objects are likely to be PS and CSS sources, although of much lower luminosity, it is important to understand their nature which may provide insights towards understanding the diverse structures of radio sources and the possible evolutionary scenarios (e.g., Sadler, 2016; Miraghaei and Best, 2017; Baldi et al., 2019b). Possible scenarios for the FR0 sources are as follows. (i) Are these radio sources inclined at small angles to the line of sight, being low-luminosity blazars with highly-relativistic jets? This seems unlikely. High-resolution radio observations with both the VLA and VLBI techniques often exhibit reasonably symmetric structure on opposite sides of the nuclear component (Cheng and An, 2018; Baldi et al., 2019a). Of the 14 sources observed by Cheng and An (2018) on parsec scale, 4 show Doppler boosting factors from 1.7 to 6, and 2 with multiple epoch observations indicate velocities between 0.23 and 0.49c. Mild variability is found in only one source, while three others exhibit no significant variability over a few years. These observations are consistent with mildly relativistic jets. This is also consistent with the ratio of [OIII] to X-ray luminosity for FR0s and FRIs which have a similar value of ~ -1.6 , while it is significantly lower for BL Lacs due to a beamed X-ray component (Torresi et al., 2018). (ii) As has been suggested for the luminous PS and CSS sources, are the FR0s likely to evolve into larger FRI and FRII radio sources? This appears unlikely given the much larger space density of FR0s but it is difficult to rule out a small fraction of FR0s evolving into larger sources. (iii) Are these sources compact because of the intrinsic properties of the supermassive black holes which are unable to launch large-scale jets or these are smothered by dense gaseous environment? The similarity of optical host magnitudes and [OIII] luminosity of FR0s and FRIs does not suggest that the jets in FR0s are frustrated by a dense environment. Miraghaei and Best (2017) suggest that due to a lower black hole mass, FR0s find it difficult to launch large-scale radio jets and may be able to support jet activity for only short periods of time. The launching of jets could be due to a low black hole spin limiting its ability to extract energy to launch the jets, consistent with a relation between black hole spin and bulk jet Lorentz factor (e.g., Tchekhovskoy et al., 2010; Maraschi et al., 2012). This would provide a natural explanation for the mild bulk Lorentz factors determined from VLBI observations. Garofalo and Singh (2019) explore a theoretical scenario where the evolution of FR0s is governed both by spin of the black hole and availability of fuelling gas.

3.2 Polarization observations

As both CSS and PS sources are confined well within the interstellar medium of their host galaxies, multifrequency polarization observations could provide a valuable probe of the magnetoionic plasma in which these are embedded as well as of interactions of the radio jets and lobes with the ambient medium.

The magnetized plasma causes a rotation of the plane of polarization which is given by $\chi(\lambda) = \chi_0 + RM\lambda^2$ where $RM = 812 \int_0^l n_e B_{\parallel} dl$, where $\chi(\lambda)$ is the position angle (PA) of the E-vector at a wavelength λ , χ_0 is the PA at zero wavelength, RM defined as the Rotation Measure is in units of radian m⁻², n_e is the electron density in cm⁻³, B_{\parallel} in mG and l in parsec. The degree of rotation is a strong function of the wavelength, leading to depolarization of emission at longer wavelengths. If radio emitting plasma is mixed with the magnetized thermal plasma, the E-vector from regions of greater Faraday depth will be rotated more relative to the regions of smaller Faraday depth, leading to depolarization. Also in the case of a screen of thermal plasma in front of the radio source, adjacent regions within the resolution element of the observations may traverse through regions of differing Faraday depth, again leading to depolarization. As high RMs in the range of 1000s of radian m⁻² are expected, especially closer to the nucleus (e.g., O'Dea, 1989), one needs to probe over a wide bandwidth at high frequencies and with high angular resolution to disentangle the different effects.

One of the early studies of polarization properties of CSS and PS sources based on VLA A-array observations at $\lambda 20$ and 6 cm showed that for these sources (i) those associated with galaxies tend to be unpolarized or weakly polarized with the percentage polarization <0.5% at both wavelengths; (ii) the quasars from this sample of CSS and PS sources have a wider distribution with a median value of ~2% at $\lambda 6$ cm and show significant depolarization at the longer wavelengths; (iii) several of these compact sources have large rotation measures (RMs) although those with low rotation measures are also known; (iv) strong polarization and total intensity variations were not common, although in some cases flat-spectrum sources could be classified as CSS/PS sources from a few frequency measurements due to variability at the different frequencies (Saikia et al., 1987; Saikia, 1988) (and see Sect. 3.5). This was broadly the situation at the time of the O'Dea (1998) review. These studies were largely confined to bright source samples such as the VLA Calibrator Survey and the well-studied 3CR sample.

Since then there have been detailed studies of fainter or lower-luminosity sources, such as the B3-VLA CSS sample with lower resolution using the Westerbork and Effelsberg telescopes to examine integrated properties, and the VLA and MERLIN with higher resolution to examine polarization distribution and relationship to structure and environment. Several well-known 3CR as well as weaker sources have also been studied extensively with high resolution using VLBI techniques to probe polarization properties closer to the nucleus. We summarize these results and possible implications in our understanding of CSS/PS sources.

3.2.1 Integrated properties

The PS sources are more compact than the CSS sources and are expected to show stronger Faraday effects due to larger column densities of the magnetoionic medium. Cotton et al. (2003b) examined the polarization properties of

the sample of GPS sources compiled by Stanghellini et al. (1998a) at $\lambda 20$ cm using the NVSS survey. They found the galaxies to be more weakly polarized than the quasars in this sample, consistent with earlier results. Cotton et al. (2003b) also reported from the dependence of polarization on linear size in a sample of CSS and PS sources (Fanti et al., 2001) that sources smaller than 6 kpc tend to be weakly polarized, usually less than ~ 0.5 per cent, while those larger could be polarized up to several per cent. This suggests a change in the properties of the magnetoionic medium on this scale. A similar trend was also reported by Fanti et al. (2004) for the B3-VLA sample of compact sources which they had observed at 4.9 and 8.5 GHz with the VLA and used the NVSS results at 1.4 GHz. Rossetti et al. (2008) who observed this sample with the Westerbork telescope at 2.64 GHz also reported a similar trend. However, this trend was not seen for the entire sample of 3CR+PW sample by Mantovani et al. (2009) who observed the bright-source sample with the Effelsberg telescope at 2.64, 4.85, 8.35 and 10.45 GHz and also used the NVSS results and previous single-dish measurements from the catalogue by Tabara and Inoue (1980). They found that this trend was seen when only galaxies were considered alone. It may be mentioned that the samples considered by Cotton et al. (2003b) and the B3-VLA sample (Fanti et al., 2004; Rossetti et al., 2008) are dominated by galaxies. Among galaxies too there could be outliers (Rossetti et al., 2008). This difference suggests a polarized component in the quasars, such as a beamed jet, which may be less affected by the magnetoionic plasma.

A fainter source sample than say the 3CR one is the B3-VLA sample whose polarization properties have been studied extensively by Fanti et al. (2001), Fanti et al. (2004) and later by Rossetti et al. (2008), who reported Westerbork observations at 2.26 GHz (~13 cm) using 8 different intermediate frequencies (IFs), and combined these with earlier VLA observations at 1.4, 4.9 and 8.5 GHz (Fanti et al., 2004). Sources smaller than about 2.5 kpc usually appear depolarized at all frequencies; the critical size where depolarization sets in being 5 kpc at 2.26 GHz, intermediate between those at 1.4 GHz and 4.9/8.5 GHz (Cotton et al., 2003b; Fanti et al., 2004). As expected, Rossetti et al. (2008) find the degree of polarization to decrease between 8.5 and 2.6 GHz, which would be expected due to Faraday depolarization, but find a flattening between 2.6 and 1.4 GHz. They explore possible explanations using both the Burn (1966) and Tribble (1991) models, and find that a variation of the Burn model in which the concept of a 'covering factor' of the foreground screen is introduced appears to fit the data. Rossetti et al. (2008) also suggest that the 'covering factor' they introduced may be due to orientation effects with the receding component being more strongly depolarized compared to the approaching one as in the Laing-Garrington effect. If so one would expect a difference between galaxies and quasars. A more natural origin may be a clumpy, inhomogeneous medium as structural and polarization asymmetries appear to suggest.

The integrated rotation measure in the source frame, RM_{sf} varies from ~ 10 to 10^4 rad m⁻² with the dispersion in RM $\sigma_{RM,sf}$ spanning a somewhat smaller range. The total RM_{sf} suggests a large-scale ordered field as well in

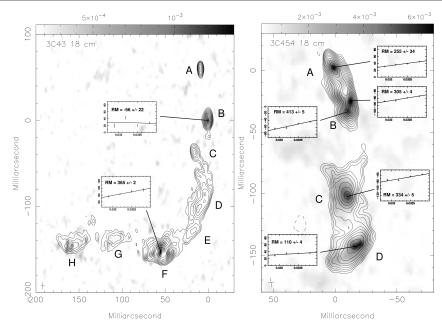


Fig. 2 VLBA total-intensity contours of the CSS sources 3C43 and 3C454 at 18cm overlaid on the images of the polarized intensity. The values of RM for different regions of the source as observed are shown. These have to be multiplied by 6.1 and 7.6 respectively to be in the source reference frame for the two sources. 3C43 is seen through a thick Faraday screen with the sharp bend being due to jet-ISM interaction, while in 3C454 thermal plasma appears to be mixed along with the radiating relativistic particles (Cotton et al., 2003a).

addition to a random component, and there are suggestions of both RM_{sf} and $\sigma_{RM,sf}$ increasing with redshift and decreasing with projected linear size. For sources with $RM_{sf} > 100$ rad m⁻², for almost all of which $RM_{sf} > \sigma_{RM,sf}$, $RM_{sf} \propto l^{-2.2}$ where l is the projected size in kpc (Rossetti et al., 2008).

Similar results have been obtained for brighter sources. From observations of the 3CR and PW (Peacock and Wall, 1982) sample, Mantovani et al. (2009) report a rapid decrease in polarization at longer wavelengths although the degree of polarization does not usually go to 0 at $\lambda >$ 49 cm. Their estimated values of RM range from -20 rad m⁻² to ~ 3900 rad m⁻² with sources generally following the λ^2 law. They also suggest that a variation of the Tribble (1991) model incorporating a covering factor can explain their observations.

3.2.2 Higher-resolution observations

While low-resolution observations give us an overview of the properties of the source as a whole, higher-resolution observations reveal the variation of degree of polarization and rotation measure across the source. It also minimizes the effects of depolarization due to coarser resolution. For example, the median values of polarization at 8.5 GHz for the 'low-resolution' images of the B3-VLA sample varies from 0.1 per cent for sources <1 kpc, to 1.28, 3.95 and 3.6

per cent for those with sizes of 1-5, 5-10 and 10-20 kpc respectively. The median value for all the sources is ~ 1.6 per cent compared with ~ 4 per cent for the components inferred from the high-resolution images at 8.5 GHz (Fanti et al., 2001).

Sub-arcsec resolution images also reveal asymmetries in the polarization properties of the lobes on opposite sides of the nucleus or parent optical object. This has been reported for several of the resolved sources in the B3-VLA sample (Fanti et al., 2001), and also for a sample of largely 3CR and 4C CSS objects whose polarization properties have been well determined (Saikia and Gupta, 2003). The ratio of the degree of polarization of the oppositelydirected lobes has a median value of ~ 5 for the 3CR+4C CSS objects, while for the control sample of larger sources observed by Garrington et al. (1991) is ~ 1.5 , with only two of the sources dominated by one-sided jets having a value >5. This is unlikely to be due to effects of orientation as seen in the Laing-Garrington effect (Laing, 1988; Garrington et al., 1988) as about half the sources in the sample are galaxies (Saikia and Gupta, 2003) which should be inclined at large angles to the line of sight. Also the magnetoionic haloes envisaged to explain the Laing-Garrington depolarization asymmetry (Garrington and Conway, 1991) is likely to have a marginal effect on the scale of the compact objects. These asymmetries are more likely to be caused by interactions with dense clouds of gas which are asymmetrically located relative to the central engine. Structural asymmetries where the brighter component is on the jet side and closer to the nucleus as seen for example in the CSS quasar 3C147 (Junor et al., 1999) and in a number of galaxies (Saikia et al., 2001), including the highly-asymmetric radio galaxy 3C459 on a slightly larger scale (Thomasson et al., 2003), are consistent with this scenario. Whether these clouds of gas are related to the fuelling process of the central active galactic nucleus remains unclear.

Detailed imaging at both sub-arcsec and milli-arcsec resolution has been used to study the total intensity and polarization structure to probe possible interactions with the external environment. A number of 3CR sources have been studied in some detail. The CSS quasar 3C147 which was found to have a high observed RM value of ~ -1600 rad m⁻² (Kato et al., 1987; Inoue et al., 1995) exhibited a huge differential Faraday rotation with the RMs in the rest frame being -3140 and +630 rad m⁻² for the southern and northern components respectively (Junor et al., 1999). With the southern component nearer the core and facing the jet, this was interpreted to be due to jet-cloud interaction. VLBA observations of 3C 147 show large variations in RM with observed values ranging from ~ -1200 to -2400 rad m⁻² in the inner portion of the jet on parsec scale (Zhang et al., 2004; Rossetti et al., 2009).

Besides 3C147, the other CSS sources usually used as primary flux density calibrators are 3C48, 3C138 and 3C286. From VLA observations at the highest available frequencies (20–45 GHz) Cotton et al. (2016) estimate an RM of ~ 10000 rad m⁻² for 3C48 but with a significant scatter suggesting complex Faraday effects. This is significantly higher than RM ~ -64 rad m⁻² determined by Mantovani et al. (2009) from Effelsberg observations and NVSS data

between 1.4 and 10.85 GHz. This suggests that the RM could be frequency dependent affected by opacity and complex Faraday effects. A detailed polarization study of the pc-scale structure of 3C48 between 1.5 and 8.3 GHz has been presented by An et al. (2010) with RM values consistent with those of Mantovani et al. (2009). The core appears unpolarized at all frequencies, while the most strongly polarized feature is at \sim 0.25 arcsec north of the core where the jet bends towards the north east. The polarization properties suggest interaction of the jet with the interstellar medium and/or changes in the magnetic field structure. A prominent knot in the jet, labelled B, exhibits a higher RM and no significant proper motion, suggesting a stationary shock, while a feature closer to the core exhibits superluminal motion.

The CSS quasar 3C138 was earlier found to have a low RM along the bulk of the jet which is strongly polarized and contributes most of the flux density, but high values of RM close to the core (Cotton et al., 1997a). This is consistent with the integrated RM value close to ~ 0 rad m⁻². More recent VLBA observations at 5 GHz show the inner jet to have an RM $\sim -5000~{\rm rad~m}^{-2}$ (a lower value of $\sim -3000 \text{ rad m}^{-2}$ was reported by Cotton et al. (2016) from higher frequency VLA observations between 20 and 48 GHz) in the source frame, with the polarization in the inner jet being seen through holes in a thick Faraday screen (Cotton et al., 2003a). They also monitored time variation in RM and suggest that the observed variations in RM are likely to be due to jet-ISM interaction. Their data were interpreted to be due to a moving component seen behind a Faraday screen with structure on pc or sub-pc scales (Cotton et al., 2003a). The standard polarization calibrator, the CSS quasar 3C286 which has a low integrated RM was shown to have a high degree of polarization of ~ 8.9 and 11 per cent respectively at 5 GHz for two knots in the inner jet. The E-vector was aligned along the jet indicating a perpendicular magnetic field in the inner jet following a bend in the jet (for e.g. and references in Cotton et al., 1997b). An inverted-spectrum radio core has been identified recently by An et al. (2017).

Several well-studied sources show regions of high RM near where the source bends, but sources may also exhibit a high RM without an obvious relationship with structural changes. In the case of 3C43, the observed RM in a component close to the core is small (-56 ± 22 rad m⁻²) while for the polarized region near the bend it increases to 365 ± 2 rad m⁻² or ~ 680 rad m⁻² in the source frame (Cotton et al., 2003a). However, the jet in 3C454 does not exhibit a brightening near the westward bend, suggesting it may not be due to a collision, and exhibits a high RM all along the jet (Cotton et al., 2003a). The VLBA results for both these sources are shown in Fig. 2. Similarly Mantovani et al. (2002) who studied the CSS sources with strongly bent jets B0548+165 and B1524-136 found high RM ranging from ~ 1000 to 10^4 rad m⁻², but enhanced RM only near the bend in B0548+165 which also exhibits a brightening in this region. CSSs with complex structure such as 3C119, 3C318 and 3C343 have been found to have RMs in the range of ~ 3000 to 10^4 rad m⁻². In the case of 3C119 the highest RM is where the jet bends at a projected distance of ~ 325 pc from the core (Mantovani et al., 2005, 2010).

3.3 Rejuvenated radio sources

Over the years there has been evidence of episodic nuclear jet activity from radio observations, based on both structures and spectral index information, and later from X-ray observations as well. For example in the radio galaxy 3C338 a radio jet south of the nucleus has been interpreted to be due to episodic jet activity (Burns et al., 1983), while the extended emission of 3C388 show a sharp discontinuity in spectral index which has been again interpreted to be due to intermittent jet activity (Roettiger et al., 1994). 3C388 has been studied over a much wider frequency range by Brienza et al. (2020) who suggest a duty cycle of ~60 per cent. A sharp gradient in spectral index is also seen in the case of Her A, another example of a galaxy with recurrent activity (Gizani et al., 2005). Evidence of earlier cycle of activity has also been reported from X-ray observations such as in Cygnus A where old electrons are scattered by inverse-Compton scattering to high energies (Steenbrugge et al., 2008). Multiple generations of X-ray cavities in radio-loud AGN suggest a mean outburst interval of $\sim 6 \times 10^7$ yr (Vantyghem et al., 2014). Although evidence of episodic AGN activity may manifest itself in a variety of ways (see also Jurlin et al., 2020; Shabala et al., 2020), one of the most striking evidence of episodic activity is when two or more pairs of distinct radio lobes are seen on opposite sides of the nucleus which are due to different cycles of jet activity. Such objects have been christened as double-double radio galaxies or ddrgs (Schoenmakers et al., 1999; Saikia and Jamrozy, 2009; Kuźmicz et al., 2017).

In this review we consider whether PS and CSS sources tend to have diffuse extended emission from an earlier cycle of activity. One of the earliest examples of extended radio emission associated with a CSS/PS source is B0108+388. Baum et al. (1990) reported an extended lobe of emission which could be a relic of an earlier cycle of activity. Although Kuźmicz et al. (2017) mentions a faint optical object in the vicinity of the diffuse lobe, its association with the lobe is unclear, and we consider the diffuse radio lobe to be associated with the PS source as there appears to be bridge of emission connecting the two. In a search for extended emission in a sample of PS sources, Stanghellini et al. (2005) found, in addition to B0108+388 with extended emission ~ 125 kpc away, the GPS radio galaxy B0941-080 to be a good candidate with extended radio emission located \sim 70 kpc away and B1345+125 (4C12.50), a GPS radio galaxy with double nuclei, to have extended emission on a scale of ~ 130 kpc in addition to the pc-scale structure. 4C12.50 shows evidence of fast outflows of ionized, atomic (HI) and molecular (CO) gas with velocities of ${\sim}1000~\mathrm{km}$ s⁻¹ largely driven by the radio jet (Holt et al., 2003a; Morganti et al., 2005b; Holt et al., 2011; Dasyra and Combes, 2012; Morganti et al., 2013; Fotopoulou et al., 2019). Interpreting the more extended radio components to be from an earlier cycle of activity, these relics were estimated to be $\sim 10^7 - 10^8$ yr ago (Stanghellini et al., 2005).

On smaller scales Jeyakumar et al. (2000) found evidence of larger-scale structure compared with the known VLBI-scale structures for 8 CSS and PS sources from interplanetary scintillation observations at 327 MHz using the

Ooty Radio Telescope, but the detailed structures remained unclear. Candidate rejuvenated sources have also been suggested from the detection of extended emission around PS sources (Hancock et al., 2010), large radio sources with PS cores (Bruni et al., 2019), and suggestions of both extended emission and PS cores from the integrated spectra of several sources from the GLEAM survey (Callingham et al., 2017). However detailed observations are required to establish the structure of the sources on all scales to firmly establish their episodic nuclear activity (Hancock et al., 2009). We illustrate here a couple of examples of rejuvenated sources to illustrate the range of structures. Figure 3 shows the inner and outer doubles of the giant radio source J1247+6723 with sizes of ~ 0.02 and 1200 kpc respectively with the inner double having a peaked spectrum (Marecki et al., 2003a; Bondi et al., 2004). Evidence of episodic activity is seen over a large range of size scales. Figure 4 shows the well-studied CSS source B2 0258+35 (J0301+3512) in the nearby galaxy NGC1167 where Westerbork observations have revealed diffuse emission possibly from an earlier cycle of activity but not with very steep spectra (Shulevski et al., 2012; Giroletti et al., 2005; Brienza et al., 2018; Murthy et al., 2019). Here the CSS and outer radio emission have sizes of ~ 0.7 and 230 kpc respectively.

There is also direct evidence of diffuse emission on small scales from VLBI observations. For example in OQ208 in addition to the double-lobed structure, there is weak diffuse emission about ~ 30 mas (40 pc) to the west as shown in Fig. 5 (Luo et al., 2007; Wu et al., 2013). Another good example is the galaxy J1511+0518 which in addition to a well-defined triple source has diffuse extended lobe $\sim 30 \text{ mas } (\sim 50 \text{ pc})$ significantly misaligned from the triple (Orienti and Dallacasa, 2008a). It has also been speculated that the range of VLBI-scale structures in the well-studied GPS source CTA21 (4C16.09) may be due to multiple cycles of nuclear activity (Salter et al., 2010). The VLBIscale relics are from more recent activity $\sim 10^3$ – 10^4 yr ago, suggesting short bursts of activity in the initial phases. An intriguing feature of these diffuse lobes is that they are often one-sided both on kpc and pc scales, somewhat reminiscent of the northern middle lobe of Cen A. In the small scales it may be due to short outbursts or sputtering, while on the larger scales the oppositely directed diffuse lobe may be below the detection threshold due to radiative losses or rapid expansion on one side due to an inhomogeneous, asymmetric environment on opposite sides of the nucleus.

In a recent compilation of extragalactic radio sources with evidence of recurrent jet activity there are 74 radio sources of which 67 are galaxies, 2 are quasars and 5 are unidentified sources (Kuźmicz et al., 2017). Sensitive low-frequency observations such as with LOFAR are likely to reveal many more ddrgs, as has been demonstrated by Mahatma et al. (2019) in the HETDEX field. Candidate rejuvenated radio galaxies have also been identified from deep LOFAR images of the Lockman Hole region, constituting ~15 per cent of the sample (Jurlin et al., 2020). Of the 74 sources compiled by Kuźmicz et al. (2017) only 12 are listed to have a size of the inner double which is less than 20 kpc, falling in the category of either PS or CSS objects. Of these 12 the nuclear structure in the quasar B0738+313 is more likely to be that of a core-

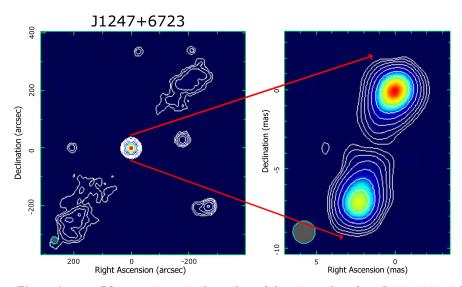


Fig. 3 A young PS source is seen in the nucleus of the giant radio galaxy J1247+6723 with the sizes of the inner and outer doubles being \sim 0.02 and 1200 kpc respectively (Marecki et al., 2003a; Bondi et al., 2004; Polatidis, 2009).

jet type rather than a compact double (Stanghellini et al., 2001a). The size of the inner double in Cen A is \sim 12 kpc (Israel, 1998; Feain et al., 2011) and is included in our list. The CSS/PS sources with evidence of recurrent activity including the ones from Kuźmicz et al. (2017) are summarized in Table 2.

Time scales of interruption of jet activity covers a wide range from $\sim 10^7$ to 10^8 yr for larger sources based on dynamical and spectral ageing arguments as in the case of 3C236 (O'Dea et al., 2001) and 4C34.09 (Shulevski et al., 2012) to $\sim 10^5$ yr for 3C293 (Joshi et al., 2011). In the case of CTA21, Salter et al. (2010) suggested that there may be repeated cycles of activity based on the radio structure on different scales in VLBI observations of varying resolutions. This appears consistent with the suggestion by Reynolds and Begelman (1997) that jet activity may be intermittent on time scales on 10^{4-5} yr for the CSS/PS sources.

Statistical studies of samples of radio sources based on their luminosity functions suggest that the time scales of the active phase are dependent on luminosity and mass of the optical host galaxy, with the time scales of jets being off are $\sim 10^7$ – 10^8 yr (Shabala et al., 2008; Best et al., 2005). In a study of dying radio sources Parma et al. (2007) find the typical age of the active phase to be $\sim 10^7$ – 10^8 yr. In the case of double-double radio galaxies the suggestion by Kaiser et al. (2000) that the formation of the inner double could be due to the dispersion of hot clouds of the inter-galactic medium into the cocoon on time scales of $\sim 10^7$ yr may work for the large sources, but not for the small CSS/PS sources. For the smaller time scales one needs to understand the fuelling process in the central regions of these sources. In

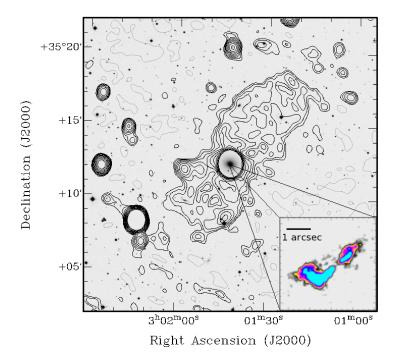


Fig. 4 Diffuse radio emission likely to be from an earlier cycle of activity in the CSS source B2 0258+35 which was imaged with the Westerbork Synthesis Radio Telescope is shown overlaid on a DSS2 image (Shulevski et al., 2012). The inset shows a high-resolution VLA image of the CSS source whose structure indicates interaction with the external interstellar medium (Giroletti et al., 2005).

this context it is interesting to note that the rejuvenated sources appear to have a higher incidence of detection of HI in absorption than the general population of CSS/PS sources (Saikia and Jamrozy, 2009; Chandola et al., 2010), although this needs further investigation using larger samples. The HI properties of CSS/PS sources are discussed briefly in Sect. 5 and have been reviewed recently by Morganti and Oosterloo (2018).

3.4 Proper motion

Determination of the proper motion of the hotspots from high-resolution observations of these compact sources provides us with estimates of their velocities and kinematic ages. Among the early measurements, Tzioumis et al. (1989) found no significant evidence of changes in structure of the southern CSS source B1934-638 over a 12-year time scale, although evidence of expansion was reported later by Ojha et al. (2004) over a 32-year time scale. Taylor

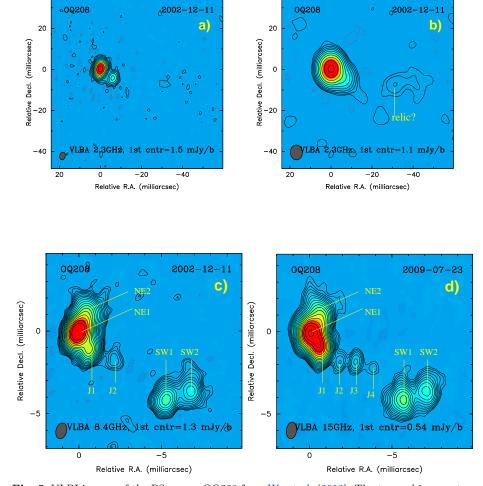


Fig. 5 VLBI images of the PS source OQ208 from Wu et al. (2013). The tapered image at 2.3 GHz (panel b) shows evidence of relic emission from an earlier cycle of activity similar to what was seen in B0108+388 (Baum et al., 1990). The lower panels (c and d) show the high-resolution structure revealing each mini lobe splitting into two hotspots. NE1 and SW1 are moving apart at a velocity of \sim 0.13c implying a hot-spot advance speed of 0.065c, while the knot in the jet is advancing with a significantly higher and mildly relativistic speed of 0.23c relative to the systemic centre. The kinematic age was estimated to be \sim 255 yr (Wu et al., 2013).

Table 2 Rejuvenated radio sources associated with CSS/PS sources

Source	Alt.	Opt.	Z	$l_{ m in}$	$l_{ m out}$	Refs.	Notes
		Id.		kpc	kpc		
J0111+3906	B0108+388	G	0.6685	0.07	126	1,4	GPS; a
J0301 + 3512	4C34.09	\mathbf{G}	0.0165	0.66	234	2,26,27	CSS
J0318+1628	CTA21	Q	0.907	0.09	2.4	17,18,19	GPS; a
J0405 + 3803	B30402 + 379	G	0.0550	0.04	~ 10	24,25	CSS; c
J0821 + 2117	B0818 + 214	G	0.4180	2.7	210	3	CSS
J0943 - 0819	B0941-080	G	0.228	0.18	72	4	GPS; a
J1006 + 3454	3CR 236	G	0.101	1.8	4248	5,6	CSS
J1247 + 6723		G	0.107	0.02	1196	7,8	GPS
J1325 - 4301	Cen A	G	0.0018	~ 12	~ 600	28,29	CSS
J1347+1217	4C12.50	G	0.1217	~ 0.3	130	5,30	GPS
J1352+3126	3CR293	G	0.045	1.1	180	9,10,11	CSS
J1407 + 2827	OQ + 208	Q	0.0766	0.01	0.04	20, 21	GPS, a
J1511+0518		G	0.084	0.01	0.05	22, 23	PS, a
J1513 + 2607	3CR315	G	0.1083	5.9	262	12	CSS?
J1516+0701	3CR317	G	0.0345	0.05	51	$13,\!14$	GPS; b
J1528 + 0544		G	0.0401	15	645	15	CSS
J1628 + 3933	3CR338	G	0.0304	7.8	48	16	CSS

a. extended emission is one-sided; b. Venturi et al. (2004) show the bright central component to have a peaked spectrum with outer steep-spectrum lobes; c. radio source with double nuclei (Bansal et al., 2017)

1. Baum et al. (1990); 2. Shulevski et al. (2012); 3. Marecki and Szablewski (2009); 4. Stanghellini et al. (2005); 5. Schilizzi et al. (2001); 6. O'Dea et al. (2001); 7. Marecki et al. (2003a); 8. Bondi et al. (2004); 9. Bridle et al. (1981); 10. Akujor et al. (1996); 11. Joshi et al. (2011); 12. Saripalli and Subrahmanyan (2009); 13. Venturi et al. (2004); 14. Zhao et al. (1993); 15. Kuźmicz et al. (2017); 16. Ge and Owen (1994); 17. Jones (1984); 18. Kellermann et al. (1998); 19. Dallacasa et al. (1995); 20. Luo et al. (2007); 21. Wu et al. (2013); 22. Orienti and Dallacasa (2008a); 23. An et al. (2012); 24. Maness et al. (2004); 25. Bansal et al. (2017); 26. Brienza et al. (2018); 27. Murthy et al. (2019); 28. Israel (1998); 29. Feain et al. (2011); 30. Morganti et al. (2013)

and Vermeulen (1997) also found no evidence of significant hotspot advance motion in the CSS/PS source with bi-directional jets B1946+708. However, Conway et al. (1994) reported possible motion in B0108+388 and B2021+614 and transverse motion in B0711+356. The first clear evidences of proper motion of hotspots in CSS/PS sources were reported by Owsianik and Conway (1998) for B0710+439 and Owsianik et al. (1998) for B0108+388. These were based on VLBI observations stretching over a decade. Since then, observations of outward proper motions or upper limits to these for CSS/PS sources have been reported for about 40 sources with the observations being largely at 5, 8– 10 and 15 GHz (Polatidis et al., 1999; Taylor et al., 2000; Tschager et al., 2000; Polatidis et al., 2002; Polatidis and Conway, 2003; Giroletti et al., 2003; Ojha et al., 2004; Gugliucci et al., 2005; Nagai et al., 2006; Giroletti and Polatidis, 2009; Stanghellini et al., 2009b; An et al., 2012; Wu et al., 2013; Rastello et al., 2016). In PKS1155+251, the components appear to be moving inwards resulting in the source shrinking in size (Tremblay et al., 2008). Yang et al. (2017) observed the source with the VLBA at 24 and 43 GHz and suggested that the southern component may harbour another black hole. Further observations are required to clarify the nature of this source. Apparent contraction has also been noticed between the core and the southern component in J0650+6001 which could be due to a knot in the jet moving south (Orienti and Dallacasa, 2010). The CSO J1755+6236 associated with the nearby galaxy NGC6521 has no prominent hotspots in the outer lobes, suggesting that energy supply from the nucleus may have stopped, and exhibits no radial motion (Polatidis, 2009). It is relevant to note that the measurements of proper motion and hence velocities could be affected by opacity and resolution, as well as intrinsic variations in the velocities of components or birth of new radio components in the core.

The velocities of separation of the hotspots from the nucleus of the galaxy range from ~ 0.04 c to about 0.4c with a median value of ~ 0.1 c. The corresponding kinematic ages range from as low as 20 yr to several thousand years with a median value of ~ 600 yr. Estimates of the radiative age of these sources from a spectral break due to synchrotron ageing (Murgia et al., 1999; Murgia, 2003) also yield similar values given the uncertainties, clearly suggesting that most CSS/PS sources are young objects. Considering a few specific examples, the radiative age of B1943+546 (Murgia, 2003) is very similar to the kinematic age listed here. Among the well-studied sources, Giroletti et al. (2003) find the radiative age of 4C31.04 to be \sim 4000 yr, but as they note this could reduce to \sim 1000 yr depending on the assumptions, which is within a factor of 2 of the kinematic age. In the case of CTD93, Nagai et al. (2006) estimate the radiative age only in the northern lobe due to complex spectral break behaviour in the southern one and find the estimated hotspot speed to be similar to that estimated from proper motion. Many of the CSS/PS sources exhibit prominent radio jets, especially in those associated with quasars. High-resolution observations of knots of emission in the jets yield velocities which are usually higher than those observed for the hotspots as for example in OQ208 (Wu et al., 2013), with some of the features exhibiting superluminal motion as in the inner jet knot of 3C48 (An et al., 2010). Proper motion measurements of CSS/PS sources are summarized in Table 3. For those with a significantly different value of Hubble's constant, the values have been listed for $H_o=70$ km s⁻¹ Mpc⁻¹. The notes indicate whether the velocity has been estimated between two hotspots (hs-hs), a core and a hotspot (c-hs) or of components in a jet (c-j, hs-j, j). Evidence of non-radial motion has been denoted by nr and the references are listed at the bottom of Table 3.

Polatidis and Conway (2003) explored possible correlations with other source parameters such as redshift and size. They reported a possible correlation with redshift, but also noted that this could be affected by the difficulty of measuring proper motion in high redshift objects. With the new measurements since, which are often over longer baselines, there does not appear to be a significant correlation with either redshift or size. For a redshift of about 0.5 or above, the lowest radial velocity from proper motion measurements is 0.12±0.04c for J1324+4048 (An et al., 2016b). The lack of a dependence of velocity of advance on size or separation from the core is not surprising, as large radio galaxies have also been estimated to have similar advancement velocities (Scheuer, 1995). de Vries et al. (2010) determined the expansion velocities of two low-luminosity radio AGN from the CORALZ sample to be

within ~ 0.1 c, and suggested that expansion velocities may be positively correlated with radio source luminosities. It would be interesting to determine the expansion velocities for a larger sample of low-luminosity radio AGN for comparison with the higher-luminosity ones.

At present over \sim 75 per cent of the sources monitored show evidence of motion including those which show non-radial motion, with a median expansion velocity of \sim 0.1c. The time range over which the sources have been monitored ranges from about 3 to 30 years with a median value of about 5 years. Almost all the sources which do not exhibit evidence of motion have been monitored for not more than about 5 years. Considering that B1934–638 showed evidence of expansion when observed over about a 32-year time scale (Ojha et al., 2004), the ones with upper limits are also likely to exhibit expansion when observed over a longer time scale. Monitoring over long time scales approaching about a decade or more has often revealed complex and interesting motion of the hot spots (e.g. An et al., 2012), and it would be desirable to extend such studies to larger samples of sources of varying luminosity.

3.4.1 Non-radial motion

Although velocities of separation are measured along the source axis, a number of sources are seen to exhibit motion transverse to the source axis. Stanghellini et al. (2009b) reported evidence of transverse motion surprisingly in all the three sources they observed, namely J0706+4647, J1335+5844 and J1823+7938. Similarly, An et al. (2012) find evidence of a wandering hotspot in the CSO quasar J1324+4048 which has a loop-like motion, initially moving towards the north and then abruptly moving towards the south-west, reminiscent of the dentist drill model of Scheuer (1982) for multiple hotspots. An et al. (2012) also confirm the transverse motion in the CSO galaxy J1335+5844 from measurements spanning about 12.2 years, which was reported earlier by Stanghellini et al. (2009b) from a time range of \sim 2 year. The dominant transverse motion of the hotspots B1 and B2, and component B3 which is possibly part of a jet are illustrated in Fig. 6.

When observed with sufficient angular resolution the lobes on opposite sides of the nucleus of the CSS/PS sources often show multiple hotspots. Such features are also seen in larger sources and could arise due to a number of effects. For example the head of the jet could be interacting at different points at different times as in the dentist-drill model (Scheuer, 1982), with the primary hotspot being the present location and the secondary hotspot an earlier one. This has been suggested to be the case for J1324+4048 (An et al., 2012). Alternatively these may be due to precession of the jet axis (Gower et al., 1982) or redirected outflows from the primary hotspot to a secondary one (Laing, 1981; Lonsdale and Barthel, 1986). In the latter case the secondary hotspot is being continuously fed from the primary one, and radiative ageing is not likely to be significant. A deflected outflow has been suggested for the double hotspots in J1511+058 where the secondary one appears to move away from the primary one (An et al., 2012). Both precession and redirected outflows

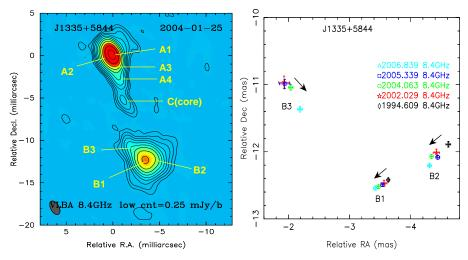


Fig. 6 VLBI images of the PS source J1335+5844 with a compact symmetric structure showing the motion of the components B1, B2 and B3 relative to A1. The dominant motion of the hot spots B1 and B2 are transverse to the source axis. The slow radial motion of the primary hotspot B1, which suggests a kinematic age of $\sim 1800 \pm 1150$ yr, and the dominant transverse motion reflects interaction with the external medium (An et al., 2012). B3 has the highest radial velocity and is possibly part of a jet.

have been explored for the multiple hotspots of OQ208 (Fig. 5) which exhibits complex motion and advances with a significantly smaller velocity than the jet (Wu et al., 2013). While the dentist-drill scenario and redirected outflows suggest inhibition in the advancement of the jet, these do not imply that the source would be confined to small dimensions for its lifetime.

3.4.2 Structural asymmetries and hotspot velocities

In sources with a radio core, the velocities could be determined for each of the outer hotspots on opposite sides relative to the core. In such cases it is possible to examine any relationship between hotspot speed and structural asymmetries as the radio jets plough their way outwards through a dense and inhomogeneous external medium. The effects may be more apparent in the most asymmetric sources. Orienti et al. (2007b) considered two very asymmetric sources, B0147+400 and B0840+424, and found from their radiative ages that the hotspot velocities range from 0.005 to 0.05c for the closer one, and from 0.03 to 0.3c for the farther one. This suggests that the closer hotspot is propagating through a denser medium leading to higher dissipation of energy and leading to greater hotspot pressure (Jeyakumar et al., 2005; Bicknell et al., 2003), consistent with studies based on structural asymmetries of the sources (Saikia et al., 2001, 2003; Saikia and Gupta, 2003). A denser medium on the side of the closer hotspot may also be probed by the detection of HI absorption towards the brighter and closer lobe (e.g., Orienti et al., 2007b). Labiano et al. (2006) find the brighter and closer hotspot in 3C49 and 3C268.3 to be

detected in H_I absorption, be depolarized and show evidence of line-emitting gas, although they cannot rule out similar amount of H_I gas in the opposite lobe. High-resolution H_I absorption measurements of a large sample of CSS/PS objects would be helpful to examine this further.

Direct measurements of velocities of hotspots relative to the core have also been made in a number of asymmetric sources. The closer and brighter hotspots in J0111+3906 and J1944+5448 are moving with smaller velocities compared with the opposite ones, the one in the more asymmetric source J1944+5448 being lower by more than a factor of 2 (Rastello et al., 2016; Polatidis et al., 2002). In sources which are reasonably symmetric, the difference in velocity may not be as striking as seen for example in 4C31.04 (Giroletti et al., 2003) and J1511+0518 (An et al., 2012).

3.5 Variability, orientation and unification schemes

The most dramatic examples of variability in radio AGN in both total intensity and polarization are seen in the core-dominated flat-spectrum radio sources, especially the class of blazars. These can be understood via shocks-in-jet scenario in relativistic jets on parsec scales embedded in largely turbulent magnetic fields (Aller et al., 2017). Interstellar scintillation (ISS) which is sensitive to microarcsec scale structure and properties of the interstellar medium (ISM) provides an explanation for the intraday variability (IDV) seen in flat-spectrum AGN. The Micro-Arcsecond Scintillation Induced Variability (MASIV) Survey shows that more than half of their sample of 500 compact flat-spectrum AGN show evidence of IDV (e.g., Jauncey et al., 2020). Variability may also be seen due to gravitational lensing of for example relativistically moving features in the AGN jets (e.g., Vedantham et al., 2017).

Variability in CSS/PS sources, although low compared with flat-spectrum AGN, may be caused by expansion of the compact outer components as they expand and traverse outwards with the turnover frequency shifting to lower frequencies, variations in optical depth, interstellar scintillation (ISS) and effects of Doppler boosting, although the latter is more likely to be significant in flat-spectrum radio sources (see Fig. 7 for an illustration of variability in PS sources). Although there have been a number of monitoring programmes and several genuine PS sources are known to exhibit variability, the overall trend for genuine CSS/PS sources to exhibit low variability (O'Dea, 1998) still holds. For example intensive monitoring of a small sample of 7 CSOs on an average every 2.7 days for about 8 months at 8.5 GHz showed their variability in flux density to be only ~0.7 per cent (Fassnacht and Taylor, 2001). Monitoring of a sample of 33 southern PS sources also showed low incidence of variability with a few exceptions (Jauncey et al., 2003). An interesting PS source in their sample is PKS1519-273 which in spite of its variability maintains a PS from 0.4 to 22 GHz and exhibits intraday variability in all Stokes parameters. This has been interpreted to be due to ISS of a 15–35 μ as component which is -3.8±0.4 per cent circularly polarized at 4.8 GHz (Macquart et al., 2000). ISS

 ${\bf Table~3~~Proper~motions~of~CSS~and~PS~sources}$

J0003+2129 J0003+4807 J0005+0524 J0038+2303 J0111+3906 J0119+3210 J0132+5620 J0204+0903 J0405+3803 J0427+4133 J0518+4730 J0620+2102 J0650+6001 J0713+4349 J0754+5324 J0831+4608	B2 0035+22 S4 0108+388 4C 31.04 B3 0402+379 B3 0710+439 CORALZ TXS 1031+567	0.45 1.887 0.0960 0.6685 0.0602 0.0550 0.455 0.5180	pc (mas) (40) 21 (4.8) 15 31 32 41 60 (12.2) (11.5) (10.5) (2.4) (18) 23 7.3 (1.3) (3.1) (1.9) (27) 40 17 152	c (mas/yr) (<0.144) 0.15 (<0.014) 0.7 0.17 0.26 0.04 0.33 (-0.005) (0.028) (0.060) (-0.073) (0.070) 0.14 0.0054 (0.060) (-0.026) (0.030) (<0.013) 0.39	>280 500 >340 140 567 417 1080 550 >4700 410 180 240 502 20 ~1200 >2060 360	6 18 6 18 12,9 12,1,3,4 13 5 15 15 15 21 22 6 15 15 6	hs-hs hs-hs c-hs hs-hs hs-hs hs-hs c-hs hs-hs;nr j-hs j-hs c-hs c1-hs c2-hs;nr c-hs;nr
J0003+2129 J0003+4807 J0005+0524 J0038+2303 J0111+3906 J0119+3210 J0132+5620 J0204+0903 J0405+3803 J0427+4133 J0518+4730 J0620+2102 J0650+6001 J0713+4349 J0754+5324 J0831+4608	B2 0035+22 S4 0108+388 4C 31.04 B3 0402+379 B3 0710+439 CORALZ	1.887 0.0960 0.6685 0.0602 0.0550	(40) 21 (4.8) 15 31 32 41 60 (12.2) (11.5) (10.5) (2.4) (18) 23 7.3 (1.3) (3.1) (1.9) (27) 40 17	$ \begin{array}{c} (<0.144) \\ 0.15 \\ (<0.014) \\ 0.7 \\ 0.17 \\ 0.26 \\ 0.04 \\ 0.33 \\ (-0.005) \\ (0.028) \\ (0.060) \\ (-0.073) \\ (0.070) \\ 0.14 \\ 0.0054 \\ (0.060) \\ (-0.026) \\ (0.030) \\ (<0.013) \\ 0.39 \\ \end{array} $	500 >340 140 567 417 1080 550 >4700 410 180 240 502 20 ~1200 >2060	18 6 18 12,9 12,1,3,4 13 5 15 15 15 21 22 6 15 15 6	hs-hs c-hs hs-hs hs-hs hs-hs c-hs hs-hs;nr j-hs j-hs c-hs c1-hs c1-c2 c-hs;nr c-hs;nr
J0003+4807 J0005+0524 J0038+2303 J0111+3906 J0119+3210 J0132+5620 J0204+0903 J0405+3803 J0427+4133 J0518+4730 J0620+2102 J0650+6001 J0713+4349 J0754+5324 J0831+4608	S4 0108+388 4C 31.04 B3 0402+379 B3 0710+439 CORALZ	1.887 0.0960 0.6685 0.0602 0.0550	(4.8) 15 31 32 41 60 (12.2) (11.5) (10.5) (2.4) (18) 23 7.3 (1.3) (3.1) (1.9) (27) 40 17	$(<0.014)\\0.7\\0.17\\0.26\\0.04\\0.33\\(-0.005)\\(0.028)\\(0.060)\\(-0.073)\\(0.070)\\0.14\\0.0054\\(0.060)\\(-0.026)\\(0.030)\\(<0.013)\\0.39$	>340 140 567 417 1080 550 >4700 410 180 240 502 20 ~1200 >2060	6 18 12,9 12,1,3,4 13 5 15 15 15 22 6 21 22 6 15 15	c-hs hs-hs hs-hs hs-hs c-hs hs-hs;nr j-hs j-hs c-hs c1-hs c1-c2 c-hs;nr c-hs;nr
J0005+0524 J0038+2303 J0111+3906 J0119+3210 J0132+5620 J0204+0903 J0405+3803 J0427+4133 J0518+4730 J0620+2102 J0650+6001 J0713+4349 J0754+5324 J0831+4608	S4 0108+388 4C 31.04 B3 0402+379 B3 0710+439 CORALZ	0.0960 0.6685 0.0602 0.0550	15 31 32 41 60 (12.2) (11.5) (10.5) (2.4) (18) 23 7.3 (1.3) (3.1) (1.9) (27) 40 17	0.7 0.17 0.26 0.04 0.33 (-0.005) (0.028) (0.060) (-0.073) (0.070) 0.14 0.0054 (0.060) (-0.026) (0.030) (<0.013) 0.39	140 567 417 1080 550 >4700 410 180 240 502 20 ~1200 >2060	18 12,9 12,1,3,4 13 5 15 15 15 22 6 15 15 15	hs-hs hs-hs hs-hs c-hs hs-hs;nr j-hs j-hs c-hs c1-hs c1-c2 c-hs;nr c-hs;nr
J0038+2303 J0111+3906 J0119+3210 J0132+5620 J0204+0903 J0405+3803 J0427+4133 J0518+4730 J0620+2102 J0650+6001 J0713+4349 J0754+5324 J0831+4608	S4 0108+388 4C 31.04 B3 0402+379 B3 0710+439 CORALZ	0.0960 0.6685 0.0602 0.0550	31 32 41 60 (12.2) (11.5) (10.5) (2.4) (18) 23 (1.3) (3.1) (1.9) (27) 40 17	$\begin{array}{c} 0.17 \\ 0.26 \\ 0.04 \\ 0.33 \\ (-0.005) \\ (0.028) \\ (0.060) \\ (-0.073) \\ (0.070) \\ 0.14 \\ 0.0054 \\ (0.060) \\ (-0.026) \\ (0.030) \\ (<0.013) \\ 0.39 \end{array}$	567 417 1080 550 >4700 410 180 240 502 20 ~1200 >2060	12,9 12,1,3,4 13 5 15 15 15 15 22 6 15 15 6	hs-hs hs-hs c-hs hs-hs;nr j-hs j-hs c-hs c1-hs c1-c2 c-hs;nr c-hs;nr
J0111+3906 J0119+3210 J0132+5620 J0204+0903 J0405+3803 J0427+4133 J0518+4730 J0620+2102 J0650+6001 J0713+4349 J0754+5324 J0831+4608	S4 0108+388 4C 31.04 B3 0402+379 B3 0710+439 CORALZ	0.6685 0.0602 0.0550	32 41 60 (12.2) (11.5) (10.5) (2.4) (18) 23 7.3 (1.3) (3.1) (1.9) (27) 40 17	$\begin{array}{c} 0.26 \\ 0.04 \\ 0.33 \\ (-0.005) \\ (0.028) \\ (0.060) \\ (-0.073) \\ (0.070) \\ 0.14 \\ 0.0054 \\ (0.060) \\ (-0.026) \\ (0.030) \\ (<0.013) \\ 0.39 \end{array}$	417 1080 550 >4700 410 180 240 502 20 ~1200 >2060	12,1,3,4 13 5 15 15 15 15 6 21 22 6 15 15 6	hs-hs hs-hs c-hs hs-hs;nr j-hs j-hs c-hs c1-hs c1-c2 c-hs;nr c-hs;nr
J0119+3210 J0132+5620 J0204+0903 J0405+3803 J0427+4133 J0518+4730 J0620+2102 J0650+6001 J0713+4349 J0754+5324 J0831+4608	4C 31.04 B3 0402+379 B3 0710+439 CORALZ	0.0602 0.0550 0.455	41 60 (12.2) (11.5) (10.5) (2.4) (18) 23 7.3 (1.3) (3.1) (1.9) (27) 40 17	$\begin{array}{c} 0.04 \\ 0.33 \\ (-0.005) \\ (0.028) \\ (0.060) \\ (-0.073) \\ (0.070) \\ 0.14 \\ 0.0054 \\ (0.060) \\ (-0.026) \\ (0.030) \\ (<0.013) \\ 0.39 \end{array}$	1080 550 >4700 410 180 240 502 20 ~1200 >2060	13 5 15 15 15 15 15 6 21 22 6 15 15 6	hs-hs c-hs hs-hs;nr j-hs j-hs c-hs c1-hs c1-c2 c-hs;nr c-hs;nr
J0132+5620 J0204+0903 J0405+3803 J0427+4133 J0518+4730 J0620+2102 J0650+6001 J0713+4349 J0754+5324 J0831+4608	B3 0402+379 B3 0710+439 CORALZ	0.0550 0.455	60 (12.2) (11.5) (10.5) (2.4) (18) 23 7.3 (1.3) (3.1) (1.9) (27) 40 17	$\begin{array}{c} 0.33 \\ (-0.005) \\ (0.028) \\ (0.060) \\ (-0.073) \\ (0.070) \\ 0.14 \\ 0.0054 \\ (0.060) \\ (-0.026) \\ (0.030) \\ (<0.013) \\ 0.39 \end{array}$	550 >4700 410 180 240 502 20 ~1200 >2060	5 15 15 15 15 6 21 22 6 15 15 6	c-hs hs-hs;nr j-hs j-hs c-hs c1-hs c1-c2 c-hs;nr c-hs;nr
J0132+5620 J0204+0903 J0405+3803 J0427+4133 J0518+4730 J0620+2102 J0650+6001 J0713+4349 J0754+5324 J0831+4608	B3 0402+379 B3 0710+439 CORALZ	0.0550 0.455	(12.2) (11.5) (10.5) (2.4) (18) 23 7.3 (1.3) (3.1) (1.9) (27) 40 17	$ \begin{array}{c} (-0.005) \\ (0.028) \\ (0.060) \\ (-0.073) \\ (0.070) \\ 0.14 \\ 0.0054 \\ (0.060) \\ (-0.026) \\ (0.030) \\ (<0.013) \\ 0.39 \end{array} $	>4700 410 180 240 502 20 ~1200 >2060	15 15 15 15 6 21 22 6 15 15 6	hs-hs;nr j-hs j-hs j-hs c-hs c1-hs c1-c2 c-hs? c-hs;nr c-hs;nr
J0204+0903 J0405+3803 J0427+4133 J0518+4730 J0620+2102 J0650+6001 J0713+4349 J0754+5324 J0831+4608	B3 0710+439 CORALZ	0.455	(11.5) (10.5) (2.4) (18) 23 7.3 (1.3) (3.1) (1.9) (27) 40 17	(0.028) (0.060) (-0.073) (0.070) 0.14 0.0054 (0.060) (-0.026) (0.030) (<0.013) 0.39	410 180 240 502 20 ~1200 >2060	15 15 15 6 21 22 6 15 15	j-hs j-hs j-hs c-hs c1-hs c1-c2 c-hs? c-hs;nr c-hs;nr
J0405+3803 J0427+4133 J0518+4730 J0620+2102 J0650+6001 J0713+4349 J0754+5324 J0831+4608	B3 0710+439 CORALZ	0.455	(10.5) (2.4) (18) 23 7.3 (1.3) (3.1) (1.9) (27) 40 17	(0.060) (-0.073) (0.070) 0.14 0.0054 (0.060) (-0.026) (0.030) (<0.013) 0.39	240 502 20 ~1200 >2060	15 15 6 21 22 6 15 15	j-hs j-hs c-hs c1-hs c1-c2 c-hs? c-hs;nr c-hs;nr
J0405+3803 J0427+4133 J0518+4730 J0620+2102 J0650+6001 J0713+4349 J0754+5324 J0831+4608	B3 0710+439 CORALZ	0.455	(2.4) (18) 23 7.3 (1.3) (3.1) (1.9) (27) 40 17	(-0.073) (0.070) 0.14 0.0054 (0.060) (-0.026) (0.030) (<0.013) 0.39	240 502 20 ~ 1200 >2060	15 6 21 22 6 15 15	j-hs c-hs c1-hs c1-c2 c-hs? c-hs;nr c-hs;nr
J0405+3803 J0427+4133 J0518+4730 J0620+2102 J0650+6001 J0713+4349 J0754+5324 J0831+4608	B3 0710+439 CORALZ	0.455	(18) 23 7.3 (1.3) (3.1) (1.9) (27) 40 17	(0.070) 0.14 0.0054 (0.060) (-0.026) (0.030) (<0.013) 0.39	502 20 ~ 1200 >2060	6 21 22 6 15 15	c-hs c1-hs c1-c2 c-hs? c-hs;nr c-hs;nr
J0427+4133 J0518+4730 J0620+2102 J0650+6001 J0713+4349 J0754+5324 J0831+4608	B3 0710+439 CORALZ	0.455	7.3 (1.3) (3.1) (1.9) (27) 40 17	$\begin{array}{c} 0.0054 \\ (0.060) \\ (-0.026) \\ (0.030) \\ (< 0.013) \\ 0.39 \end{array}$	$20 \\ \sim 1200 \\ > 2060$	22 6 15 15 6	c1-c2 c-hs? c-hs;nr c-hs;nr
J0518+4730 J0620+2102 J0650+6001 J0713+4349 J0754+5324 J0831+4608	CORALZ		(1.3) (3.1) (1.9) (27) 40 17	$ \begin{array}{c} (0.060) \\ (-0.026) \\ (0.030) \\ (<0.013) \\ 0.39 \end{array} $	~ 1200 > 2060	6 15 15 6	c-hs? c-hs;nr c-hs;nr
J0518+4730 J0620+2102 J0650+6001 J0713+4349 J0754+5324 J0831+4608	CORALZ		(3.1) (1.9) (27) 40 17	(-0.026) (0.030) (<0.013) 0.39	~ 1200 > 2060	15 15 6	c-hs;nr c-hs;nr
J0620+2102 J0650+6001 J0713+4349 J0754+5324 J0831+4608	CORALZ		(1.9) (27) 40 17	(0.030) (<0.013) 0.39	>2060	15 6	c-hs;nr
J0650+6001 J0713+4349 J0754+5324 J0831+4608	CORALZ		(27) 40 17	(<0.013) 0.39		6	
J0650+6001 J0713+4349 J0754+5324 J0831+4608	CORALZ		40 17	0.39			ha h-
J0713+4349 J0754+5324 J0831+4608	CORALZ		17		360		hs-hs
J0754+5324 J0831+4608	CORALZ	0.5180				20	hs-hs
J0754+5324 J0831+4608	CORALZ	0.5180	137	-0.37	020	20	c-hs
J0831+4608				0.43	932	12,2,3,4	hs-hs
			(20) (~ 8)	(<0.009) (0.060)	>2220	6 6	hs-hs j-hs
		0.1311	10	0.14	245	25	hs-hs
		0.4597	198	0.27	1836	12,3	hs-hs;nı
01000 0020		0.100.	190	0.86	1000	12,3	hs-j?
J1111+1955	PKS 1108+201	0.2991	71	<0.14c	>1620	6	hs-hs
			78	< 0.19c	> 1360	6	hs-hs
J1143+1834			(6.9)	(<0.010)	>690	6	hs-hs
J1247+6723	B 1245+676	0.1073	15	0.23	190	12,9,23	hs-hs
J1317+4115	CORALZ	0.0662	4.2	< 0.11	> 130	25	hs-hs
J1324+4048		0.496	33	0.12	870	15	hs-hs
			28	2.2		15	hs-j
J1335+5844	4C 58.26	(0.57)	85	0.16	1800	15	hs-hs;ni
			84	0.45	600	15	hs-hs;nı
T1407 2027	00 200	0.0766	75 11	2.86	90	15	j-hs;nr hs-hs;nı
J1407+2827	OQ 208	0.0766	11	0.108	255	16,12	,
			$9.5 \\ 1.8$	$0.134 \\ -0.168$	255	16,12 16	hs-hs;nı hs-j
J1414+4554	B3 1412+461	0.186	89	-0.103 < 0.14	>2030	6	hs-hs
	PKS1413+135	0.2467	31	0.80	130	6	c-j
01110 1020	11101110 100	0.2101	7.6	1.10	22	6	c-j
J1511+0518		0.084	3.4	0.04	300	15,18	c-hs
·			4.0			15,18	c-hs;nr
			5.3	0.15		15,18	c-hs;nr
J1546+0026		0.55	~ 35	-1.1		6	c-hs
	CTD 93	0.473	300	0.34	2200	7	hs-hs
	NGC 6328	0.0144	3	~ 0.1	91	24,12,9	hs-hs
	PKS 1732+094	0.735	96	< 0.18	>1780	6	hs-hs
	PKS	0.735	101	0.25	1300	15	hs-hs;nı
	NGC6521	0.0274	20	< 0.04		19	hs-hs
	B2 1814+34	0.245	~ 140	(0.027)	200	6	hs-hs;nı
J1826+1831			(14) (42)	(0.037) (0.013)	380 3000	6 6	c-j c-hs
J1845+3541	B 1843+356	0.7640	$\frac{(42)}{32}$	(0.013) 0.57	180	12,9	hs-hs
·	PKS 1934-63	0.1813	130	0.26	1600	8,12	hs-hs
	B 1943+546	0.1613 0.2630	153	0.20	1306	12,13,4,9	hs-hs
		5.2000	166	0.27	1800	13	hs-hs
J1945+7055	TXS 1946+708	0.1008	56	< 0.14		12	hs-hs
	,			< 0.57	>200	11	hs-c
				0.29		12,11	j
				0.7 - 1.3		12,11	j
J2022+6136	B 2021+614	0.2270	25	0.2	440	10,9	hs-hs
J2203+1007		1.005	82	0.53	500	15,6	hs-hs;n
			76	1.13	220	15	hs-j
J2355+4950	TXS 2352+495	0.2379	190	$0.17 \\ 0.4-1$	300	$12,3,4 \\ 3,12$	hs-hs hs-j

^{1.} Owsianik et al. (1998); 2. Owsianik and Conway (1998); 3. Taylor et al. (2000); 4. Polatidis et al. (1999); 5. Giroletti et al. (2003); 6. Gugliucci et al. (2005); 7. Nagai et al. (2006); 8. Ojha et al. (2004); 9. Polatidis et al. (2002); 10. Tschager et al. (2000); 11. Taylor and Vermeulen (1997); 12. Polatidis and Conway (2003); 13. Rastello et al. (2016); 15. An et al. (2012); 16. Wu et al. (2013); 17. Giroletti and Polatidis (2009); 18. Orienti and Dallacasa (2008a); 19. Polatidis (2009); 20. Orienti and Dallacasa (2010); 21. Maness et al. (2004); 22. Bansal et al. (2017); 23. Marecki et al. (2003a); 24. Giroletti and Polatidis (2009); 25. de Vries et al. (2010)

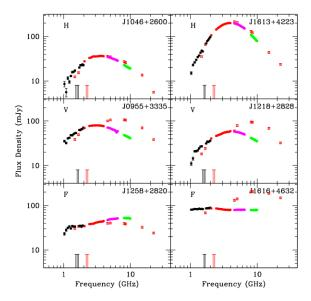


Fig. 7 Variability of the integrated flux density of PS sources illustrating those where the spectrum remains convex without showing significant variability (upper panel) and those which show significant variability due to evolution of source components (middle panel). The bottom panel shows flat-spectrum objects which may exhibit a convex or peaked spectrum due to variability (Dallacasa and Orienti, 2016). The filled circles in different colours denote their observations with the Jansky Very Large Array in 2012 May in different bands: L (1–2 GHz) in black, S (2–4 GHz) in red, C(4.5–6.5 GHz) in violet and X (8–10 GHz) in green. The open squares denote earlier-epoch VLA data.

has also been invoked to explain longer term variability at low frequencies in a sample of GLEAM peaked spectrum sources (Ross et al., 2020). Aller et al. (2002) present flux density and polarization monitoring of the 32 sources in the Stanghellini sample that are observable by the Michigan radio telescope. About 10 sources show flux density variability at some level though generally with longer time scales than found in other AGN studied by the Michigan group (Aller et al., 2002). Even during times of variability, the overall peaked spectrum is generally maintained (Aller et al., 2002).

Blazars in the act of flaring can have peaked radio spectra at high frequencies (e.g., Dent and Balonek, 1980; O'Dea et al., 1983; Wills et al., 1983; O'Dea et al., 1986; Kovalev et al., 2002; Kovalev, 2005). This is one of the reasons why blazars can contaminate samples of PS sources. Consistent with this, while many of the PS sources with a peak frequency greater than about 3 GHz seem to vary, their spectra usually appear peaked only during an outburst (Jauncey et al., 2003). For a sample of 21 PS sources selected from the ATCA 20 GHz (AT20G) survey, Hancock et al. (2010) suggest only ~60 per cent of the sources showed low-level variability over times scales of ~1-3 yr at 20GHz and are likely to be genuine PS sources. Tinti et al. (2005) also suggested that most PS sources associated with quasars and peaking at high frequencies

are likely to be flaring blazars. For a sample of 'bright' high-frequency peakers (Dallacasa et al., 2000), multifrequency observations at different epochs showed that only ~ 56 per cent are genuine PS candidates (Orienti et al., 2007a). Similarly for a sample of 'faint' high-frequency peakers (Stanghellini et al., 2009a), about 56 per cent mostly associated with galaxies are candidate young sources, while the remaining largely quasars belong to the flat-spectrum blazar population (Orienti et al., 2010a). Long-term multi-frequency monitoring of high-frequency peaked sources is necessary to determine whether peakedspectrum sources identified from limited observations are indeed genuine candidates for young sources. From long-term well-sampled data sets spread over about two decades Torniainen et al. (2005) showed that PS quasars are largely flat-spectrum sources having a peaked spectrum during a flare, although a few have a quiescent convex spectrum along with low variability. A similar study for PS galaxies showed that contamination by flat-spectrum objects is far smaller (Torniainen et al., 2007, 2008). Similar results were obtained from multi-frequency monitoring of a sample of 122 sources with the RATAN600 telescope over four years, with only \sim 29 per cent identified as PS candidates and the majority of quasars as not genuine PS sources (Mingaliev et al., 2012, 2013). These studies underline the importance of long-term multi-frequency monitoring, preferably simultaneously with adequate sampling to identify the genuine PS sources (Tornikoski et al., 2001, 2009).

Besides identifying genuine PS sources which are likely to be young objects, long-term monitoring could also provide insights towards understanding the early evolution of these young objects. In the optically thick region of the spectrum adiabatic expansion is likely to play a major role in the case of synchrotron self absorption, and variations in optical depth in the case of free-free absorption. In the case of a self-absorbed component, the opacity decreases as the source expands with the turn-over frequency decreasing and flux density below the turn-over frequency increasing (van der Laan, 1966). In the optically thin region above the turn-over frequency spectral evolution would be determined by both expansion and radiative losses, and injection of fresh particles from the nucleus. The spectral peak in the extreme PS source RXJ1459+3337 has decreased from \sim 24 GHz in 1996 to \sim 12.5 GHz in 2003, accompanied by an increase in flux density below the spectral peak and a decrease above it. Orienti and Dallacasa (2008b) explain their observations of RXJ1459+3337 in terms of an adiabatically expanding homogeneous component and estimate the age of the radio emission to be ~ 50 years. Dallacasa and Orienti (2016) besides reviewing earlier work present their results on three variable PS sources, J0754+3033, J0955+3335 and J1218+2828, which show similar behaviour for which detailed modelling would be useful. In the well-studied PS source PKS1718-649 (NGC 6328) variability was found both below and above the peak, where variations in the optically thick part have been attributed to variations in optical depth while in the optically thin part to adiabatic losses of the synchrotron-emitting lobes (Tingay and de Kool, 2003; Tingay et al., 2015).

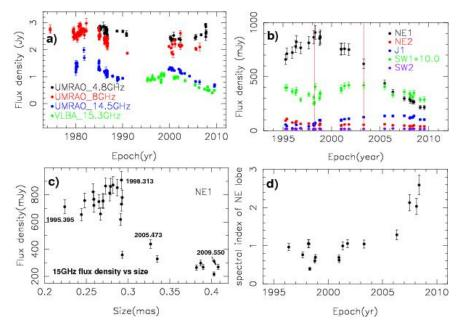


Fig. 8 Variability of the integrated flux density and of the components observed by VLBI observations for the PS source OQ208. Upper left: The total flux density variability of the source as measured with the UMRAO 26-m telescope at 4.8 GHz (black), 8 GHz (red) and 14.5 GHz (blue) is shown along with the sum of the flux densities of the VLBI components at 15.3 GHz (green). Upper right: The flux density variability of the different VLBI components, with the north-eastern components NE1 and NE2 shown in black and red respectively, while the jet component J1 and the south-western components SW1 and SW2 are shown in blue, green and purple respectively. The flux density of SW1 has been multiplied by a factor of 10. The vertical lines mark the peak epochs of NE1 and SW1. Lower left: This shows the variation of the 15-GHz flux density of hotspot NE1 and its component size. The flux density of NE1 increased till 1998.313 followed by a decline. The component size was found to increase during the entire period. Lower right: This shows the temporal variation of the spectral index of the north-eastern lobe between 8 and 15 GHz (Wu et al., 2013).

In addition, high-resolution VLBI-scale monitoring observations would help reveal variability of individual features such as hotspots and cores. These reveal more complex and interesting variations which we illustrate with a couple of examples. OQ 208 (Mrk 0668 with Seyfert 1 type spectra) consists of two lobes with multiple hotspots and an overall separation of ~ 10 pc (Fig. 5) with both hotspots exhibiting variability, the maximum levels being ~ 62 and 19 per cent for the north-eastern and south-western hotspots respectively (Fig. 8). The complex variability pattern requires in addition to expansion and radiative losses, periodic feeding and acceleration of fresh relativistic electrons (Wu et al., 2013). Evidence of feeding is also seen in J1324+4048 a PS source associated with a quasar and with two steep-spectrum, resolved components, A and B, separated by ~ 32 pc with no flat-spectrum core component. The flux densities of both components appear to decrease from 1993, reaching a minimum at 2005, consistent with expansion losses, and then found to increase by

 \sim 40 per cent in 2009. In 1998 a new component was observed at the beginning of hotspot B which appears to be advancing with a superluminal velocity \sim 2.2c along the axis, possibly feeding energy to the lobe (An et al., 2012). The radio core and inner jet component in the CSS quasar 3C48 was also found to exhibit significant variability over a 8-year period (An et al., 2010). Long-term VLBI-scale monitoring of a large sample of CSS/PS sources is required to understand their systematics and the rich and diverse phenomena these may reveal. At radio frequencies, differences in the prominence and variability of the radio core, detection of superluminal motion and source asymmetries could in principle be useful tests of the unified scheme for CSS/PS radio galaxies and quasars. Superluminal motion is observed when the jet axis is inclined at a small angle to the line of sight with features in the jet appearing to move at velocities greater than than of light. The apparent velocity of such a feature is given by $\beta_{app} = \beta \sin \theta/(1 - \beta \cos \theta)$, where θ is the angle of inclination of the jet axis to the line of sight. The apparent transverse velocity has a maximal value $\beta_{\rm app, max} = \beta \gamma$ for $\sin \theta = 1/\gamma$ where γ is the Lorentz factor corresponding to β .

In the unified schemes for radio AGN, the FRII radio galaxies which also tend to have strong emission lines are believed to be inclined at large angles to the line of sight while the quasars are inclined at small angles, the dividing angle being $\sim 45^{\circ}$ (Barthel, 1989). Effects of relativistic motion such as Doppler boosting of the flux density of the extended and nuclear jets in the cores, detection of superluminal motion, as well as apparent structural asymmetries for intrinsically symmetric sources would be more apparent in those observed at small angles to the line of sight. In this scenario a dusty, clumpy torus obstructs a direct view of the broad-line region in the case of radio galaxies, while the orientation independent parameters such as the extended lobes of radio emission should be similar for both classes of objects. An FRII radio source cannot be changed to an FRI by orientation effects. The relativistically beamed counterparts of the FRI sources which also tend to have weak emission lines have been suggested to be BL Lac type objects. The unified schemes for radio AGN have been reviewed by a number of authors over the years (e.g., Antonucci, 1993, 2012; Urry and Padovani, 1995), and more recently by Tadhunter (2016b).

Barthel (1989) compared the projected radio sizes of FRII radio galaxies and quasars, and found the radio galaxies to be larger as would be expected if these are inclined at larger angles to the line of sight. However as CSS/PS sources have been defined to be <20 kpc, size comparisons may not be very meaningful. Also, asymmetries in both total intensity (Saikia et al., 2001, 2002, 2003; Rossetti et al., 2006) and linear polarization (Saikia and Gupta, 2003) are more strongly affected by local inhomogeneities in the immediate environment of the CSS/PS sources rather than the differences in orientation, making it difficult to use these aspects for testing the unified scheme. At radio frequencies one could for example investigate the relative strengths of the cores due to relativistic beaming, core variability, detection of jets and superluminal motion which would depend on orientation. The cores of radio galaxies have

been found to be less prominent than those of quasars in CSS/PS sources as expected in the unified scheme (Saikia et al., 2001; Fanti, 2009), consistent with earlier studies for both small and large sources. Although there have been reports of core variability in individual sources, a systematic study to examine differences between galaxies and quasars is required even though there could be an unavoidable bias towards observing brighter cores. The candidate PS source J1324+4048 associated with a quasar exhibits superluminal motion of a jet component of 2.2±0.5c (An et al., 2012). Clear evidence of superluminal motion of jet components have been reported in the CSS source 3C48 with $v\sim3.7c$ (An et al., 2010), 3C138 with velocities of $\sim2.6c$ and 7.2c for different components (Cotton et al., 1997a; Shen et al., 2005) and 3C309.1 with superluminal velocities ranging from ~ 1.4 to 6.6c for the different components (Lister et al., 2013). 3C216 earlier listed as a CSS has a velocity of ~4c (Paragi et al., 2000) but has since been known to have extended emission larger than 20 kpc. These sources are all associated with quasars consistent with the unified scheme (Barthel, 1989; Antonucci, 1993; Urry and Padovani, 1995), although there is a natural bias towards monitoring sources with bright cores. In the case of the CSS quasar 3C286, An et al. (2017) have identified a core from multi-frequency VLBA data and determined the jet speed to be subluminal with a value of ~0.5c and an inclination angle of 48°. Clearly more data and measurements for a larger sample with varied core strengths are required. Although only a few CSS and PS sources have been monitored in order to study the motion of the nuclear jets, large samples of sources with prominent cores have been monitored for example by the VLBA (e.g. Lister et al., 2013, 2019). These studies show that the apparent speeds range from subluminal ones to over 40c, with the galaxies having small values, consistent with the unified scheme.

Besides the radio band, unified schemes may be tested across different wavebands using both orientation independent properties which should be similar and also the orientation-dependent ones. Properties which have been studied include their environments, narrow emission line and mid-infrared luminosity, detection of polarized broad emission lines, host galaxy properties, high-energy emission which could be due to Doppler boosting and inverse-Compton scattering of lower energy photons. The infrared properties suggest that compact sources appear to have similar structure of the central region with black holes, accretion disks and obscuring tori as in the case of the larger sources (as discussed in Sect. 4). However, there may be additional obscuration for the CSS/PS sources if the triggering of radio sources is associated with significant infall of gas and dust from a merger. In the context of differences between quasars and radio galaxies Tadhunter (2016b) notes that traditional indicators of bolometric luminosity of AGN such as [OIII] emission line luminosity and 24μ continuum luminosity may also suffer attenuation in narrow-line objects due to circumnuclear dust. In PS and CSS sources, the [OIII] emission line luminosity can be affected by a significant contribution from shocks (Sect. 5.5.2). At X-ray wavelengths observations of a few PS/CSS quasars suggest that at least some of the X-ray emission is due to relativistic beaming (see Sect. 6.1.3), consistent with the unified scheme. Tadhunter (2016b) shows in his review that a wide range of observations can be explained in terms of the unified schemes for radio AGN although there are aspects that need to be understood further. These studies have been done for well-defined samples of luminous radio sources which include CSS/PS sources, but could be extended to larger samples of CSS/PS sources, including the low-luminosity ones.

3.6 What causes the turnover in the radio spectrum?

The peak in the radio spectrum is a defining characteristic of all PS and even many CSS sources. The mechanism responsible for the turnover in the spectrum is of great importance because it will constrain either the internal properties (e.g., magnetic field, thermal electron density) or external environment (e.g., thermal electron density) of the radio source (e.g., de Kool and Begelman, 1989; O'Dea, 1998; Tingay and de Kool, 2003). The two mechanisms currently favored are synchrotron self-absorption (SSA) and external free-free absorption (FFA).

O'Dea (1998) noted that the magnetic field which would produce the observed turnover in GPS sources due to SSA was in agreement with the magnetic field calculated assuming minimum pressure. Snellen et al. (2000) noted that the relation between source size and turnover frequency could be reproduced if the turnover was due to SSA and the sources evolved in a self-similar way while remaining in equipartition. de Vries et al. (2009a) confirm that SSA is a better explanation than FFA for the relation between peak frequency and angular size in the CORALZ sample. Jeyakumar (2016) found that by adding synchrotron opacity effects into the evolution model of Kaiser (2000), it is possible to fit the relation of frequency at the spectral peak vs. linear size, and the relation of luminosity of the spectral peak vs. linear size. These results are consistent with the turnover in the radio spectrum being due to SSA. Uniform source models are unrealistic and non-uniform source models may give better fits to SSA (e.g., Artyukh et al., 2008).

FFA has been suggested to occur in a disk (Marr et al., 2001), a torus (Peck et al., 1999; Kameno et al., 2000, 2001, 2003), and in ambient clouds shocked by the expanding radio source, producing a power-law distribution of electron density in the ionized ambient clouds (Bicknell et al., 1997, 2018). There is supporting evidence from individual sources whose spectra are better fit by FFA rather than by SSA (e.g., Bicknell et al., 1997; Peck et al., 1999; Kameno et al., 2000, 2001, 2003; Marr et al., 2001, 2014; Tingay et al., 2015; Callingham et al., 2015; Mhaskey et al., 2019a) and see Krishna et al. (2014), Callingham et al. (2017) and Mhaskey et al. (2019b) for additional candidates. The FFA is generally consistent with an ionized medium with a temperature $T \sim 10^4$ K, path length $\sim 1-100$ pc, and an electron density $n_e \sim 10^3-10^4$ cm⁻³.

Thus, typically, the FFA scenario requires high thermal electron density in the environment of compact radio sources. In the models of Bicknell and

collaborators, these thermal electrons are generated by shock heating dense ambient clouds. However, there is evidence for dense clouds in the environments of some but not all compact radio sources (Sect. 5.4, Sect. 7.2.2). The evidence for large gas masses in individual sources succeed of FFA is mixed – Table 5 shows high molecular gas masses (> $10^{10}\,M_{\odot}$) for 0108+388 and OQ208, but not for PKS 1718–649 and TXS 1946+708. Given that the link between dense molecular gas clouds and high thermal electron densities is still uncertain, these limits should not be considered restrictive.

Mutoh et al. (2002) suggest that the polarization behavior is more consistent with FFA in some sources. However, the Bicknell model does less well in reproducing the relation between the frequency of the peak and the linear size over the large range (over 3.5 dex) in linear size (Bicknell et al., 2018).

In summary, there is evidence in some individual sources that the turnover is due to FFA. However, the global relationship between frequency of the peak and the linear size is best described by SSA. Thus, we suggest that in most sources the turnover is due to SSA; while in some sources possibly interacting with dense ambient clouds, the turnover is due to FFA.

4 Infrared properties

The infrared properties of GPS and CSS sources can constrain the AGN bolometric luminosity, the covering factor of the obscuring material (do they have higher covering factor than large radio galaxies?), the properties of the circumnuclear region (e.g., torus), and the star formation rate (SFR) averaged over about 200 Myr. See Tadhunter (2016a) for a discussion of caveats in the determination of SFR in galaxies with AGN. We list SFR, where available, in Table 4.

IRAS and ISO did not detect many GPS and CSS sources and the initial results obtained were consistent with no difference in mid-far Infrared properties between GPS/CSS and large radio galaxies (Heckman et al., 1994; Fanti et al., 2000; Hes et al., 1995).

Willett et al. (2010) obtained Spitzer IRS spectra of eight low redshift CSOs. Willett et al. (2010) detect the 11.3 μ m PAH feature in \sim 87% of the CSOs. They find that the sources are heterogeneous in the mid-IR properties, displaying a varying mixture of AGN and dusty star formation properties. Clumpy torus AGN models can fit the silicate features in most of the CSOs. Based on the PAH strength, silicate features, fine-structure lines, and H₂ lines, they find that 4 categories are necessary to classify the CSOs. A slight majority (5/8) CSOs show moderately dusty environments and moderate ($< 10\,M_{\odot}$ yr⁻¹) levels of star formation.

Dicken et al. (2012) compared Spitzer observations of the 2Jy and 3CRR radio galaxies including 8 GPS or CSS objects. Similar to Willett et al. (2010) they find that the GPS and CSS sources are heterogeneous in their mid-IR properties (PAH strength, silicate features, fine-structure lines, and H₂ lines). In addition Dicken et al. (2012) find a high fraction (6/8) with PAH emission

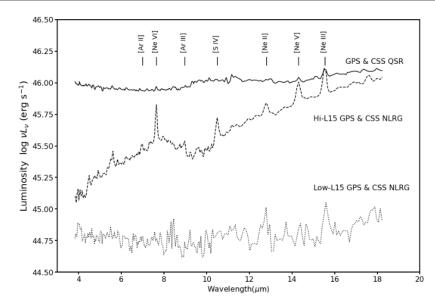


Fig. 9 The median MIR spectra of QSRs and NLRGs. These spectra reflect the difference in luminosity seen in Fig. 10. The NLRG population are split into low-luminosity and high luminosity subsamples, νL_{ν} (15 μ m) $< 1.3 \times 10^{45}$ erg s⁻¹, and νL_{ν} (15 μ m) $> 1.3 \times 10^{45}$ erg s⁻¹, respectively. The Hi-L15 NLRGs have very red spectra with strong silicate absorption and high-EW emission lines, consistent with quasars viewed at a high inclination or through a high dust column. The Low-L15 NLRGs have much weaker MIR continuum and emission lines, consistent with their 10x lower luminosity. (Figure from Ogle et al., priv, comm.)

indicating the presence of moderate star formation. Dicken et al. point out that the fraction of compact sources with star formation (75%) is higher than found for the extended (2 Jy + 3 CRR) radio galaxies (21%).

Note that Dicken et al. (2012) do not provide any estimates of star formation rate, however, they do provide the flux of the 11.3 μ m PAH feature. Farrah et al. (2007) give a SFR calibration using the luminosity of the 6.2 μ m + 11.3 μ m PAH features,

$$SFR(M_{\odot} \text{ yr}^{-1}) = 1.18 \times 10^{-41} L_{PAH} (\text{ergs s}^{-1})$$
 (1)

where $L_{\rm PAH}$ is the combined luminosity of the 6.2 μ m and 11.3 μ m PAH features. We note that the 6.2 μ m and 11.3 μ m fluxes are approximately equal in starburst galaxies (Brandl et al., 2006), and double the 11.3 μ m flux to estimate an approximate SFR which are included in Table 4. Note that the 11.3 μ m PAH is easily excited and probably gives an upper limit to the SFR (Ogle et al., 2010).

Ogle et al. (in preparation) present Spitzer IRS and MIPS observations of 24 GPS and CSS sources at z=0.4–1.0 and compare them to large FRII radio sources. Median MIR SEDs are shown in Fig. 9. CSS and PS quasars have similar mid-IR spectra to the FR II quasars studied by Ogle et al. (2006). Most of the GPS and CSS radio galaxies show strong high ionization lines such as [Ne

V] and [Ne VI] that must be photoionized by obscured AGNs. The distribution of 15 μ m luminosity is similar between the GPS and CSS and the large FRII sources, with $\nu L_{\nu}(15\mu m) = 10^{45} - 10^{46}$ erg s⁻¹. The Spitzer results from Ogle et al. and the Herschel results from Podigachoski et al. (2016b) indicate that the compact sources have similar central engines (BHs, accretion structures, obscuring tori) as the large sources.

There is evidence for additional obscuration in the PS and CSS sources (Ogle et al. 2020). High-luminosity CSS and PS NLRGs (HERGs) have heavily reddened MIR spectra (Fig. 9). The greater obscuration compared to FR II NLRGs indicates a larger column density of cold dust in the circumnuclear region or host galaxy. Lower-luminosity CSS and PS NLRGs (log $\nu L_{\nu} < 45.0$) may host a mix of obscured and unobscured AGNs, which are difficult to separate based on their low-quality MIR and optical spectra. The MIR spectra of obscured CSS quasars are also heavily reddened and have high-equivalent width emission lines, presumably from the extended narrow-line region.

PS and CSS quasars seem to have systematically higher 15 μ m luminosity than radio galaxies (Fig. 9, 10), even after accounting for dust obscuration. This is consistent with known problems with unifying PS and CSS quasars with radio galaxies (Sect. 3.5). It is unclear whether the type 1 fraction increases with luminosity or if it is just more difficult to detect broad lines in the optical spectra of the lower luminosity radio galaxies. A difference in intrinsic luminosity between the quasars and radio galaxies is consistent with the galaxies containing a mixture of intrinsically luminous AGN and a population of intrinsically weaker AGN whose radio power has been increased via interaction with the ambient medium (See Sect. 7.2.3).

The detection of 7.7 μ m PAH in 4 compact sources indicates star formation rates of $10\text{--}60\,M_{\odot}~\mathrm{yr^{-1}}$. Upper limits on an additional 10 sources do not rule out similar star formation rates. Thus, these data are also consistent with a majority of the compact sources showing moderate star formation as suggested by Willett et al. (2010) and Dicken et al. (2012).

Westhues et al. (2016) present Herschel photometry of a sample of 87 3CR sources with z < 1. They list 12 CSS, but we remove 3C216 and 3C380 because they have extended emission which makes them larger than 20 kpc (O'Dea, 1998) and we add 3C305 (e.g., Hardcastle et al., 2012) for a total of 11 CSS. Westhues et al. (2016) calculate SFR from the FIR luminosity. If we adopt SFR $> 10 \, M_{\odot} \, \text{yr}^{-1}$ to indicate substantial star formation, then 11/12 = 91% of the CSS sources are star forming, and 42/76 = 55% of the extended 3CR are star forming. This is a higher fraction of extended sources with star formation than found by Dicken et al. (2012), but Dicken et al. did not use FIR luminosity to calculate SFR because of concerns of an AGN contribution to the FIR. Nevertheless, the Westhues et al. (2016) results continue the trend of the GPS/CSS forming stars more often than the large radio sources.

Podigachoski et al. (2015) present Hershel photometry of z>1 3CR sources, and present SFR and dust mass. This sample includes 10 CSS out of a total of 62 objects. There are a significant number of 3C sources undetected with Herschel with corresponding upper limits on SFR of up to $100\,M_{\odot}$

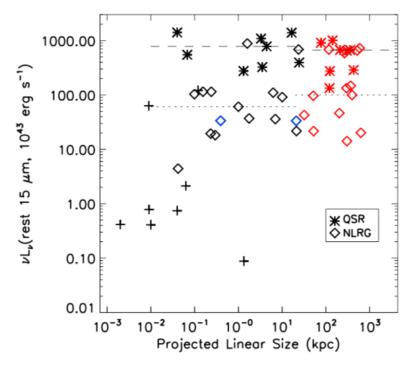


Fig. 10 Rest frame MIR luminosities of GPS and CSS quasars (asterisks) and radio galaxies (diamonds) compared to FR II quasars and radio galaxies, vs. projected linear size (Ogle et al. priv, comm). The weakest sources (+ symbols) are nearby CSOs from Willett et al. (2010). Red = FRII data from Ogle et al. (2006). Black = Ogle et al. CSS+GPS data. Blue= CSS/GPS NLRGs with silicate emission. The luminosities are given as νL_{ν} (rest 15 μ m), measured from Spitzer IRS spectra. Quasars of all sizes have high MIR luminosities. NLRGs, on the other hand show a wider range of MIR luminosity, suggesting that they are a more heterogeneous population. Regardless of size, there are very few NLRGs (only 4 in the sample) with MIR luminosities as high as quasars. It seems unlikely that the factor of 10 difference in median luminosity (dashed lines for quasars, dotted for NLRGs) is caused by extinction at 15 microns. Instead, they may be drawn from an intrinsically less luminous population.

yr⁻¹, so we don't merge the statistics with the Westhues et al. (2016) sample. Star formation rates of at least $100 M_{\odot} \text{ yr}^{-1}$ are detected in 7/10 (70%) of the CSS and 16/52 (31%) of the large radio sources (Podigachoski et al., 2015).

Kosmaczewski et al. (2020) consider the WISE colors of a sample of 29 GPS and CSOs and compare them to other samples of galaxies and AGN. They find that the WISE colors suggest less star formation in the GPS/CSOs than in starburst and ULIRG galaxies, but more star formation than in extended FRII radio galaxies. They find that the WISE colors and implied star formation in GPS/CSOs are similar to those in a sample of double-double radio galaxies. ¹

 $^{^{1}\,}$ See Section 3.3 for a discussion of the double-double radio galaxies.

Thus, the small samples of GPS/CSS studied so far consistently suggest that compact radio sources exhibit star formation more often than large-scale radio sources. This has implications for the population of compact radio sources (Sect. 7.2.3) and should be investigated with a larger sample of compact radio sources.

5 Host galaxies

Here we discuss the host galaxy properties and environments of the PS and CSS sources. See Holt (2009) for a previous discussion. Star formation is also discussed in Sect. 4 and 7.2.3.

5.1 Host types, stellar populations, and magnitudes

In general, the hosts of PS and CSS sources tend to be large, bright elliptical galaxies dominated by an old stellar population and with magnitudes around M*² (e.g., de Vries et al., 1998, 2000a; Snellen et al., 1998a, 1999, 2002; Perlman et al., 2001; Drake et al., 2004; de Vries et al., 2007; Labiano et al., 2007; Orienti et al., 2010a; Kosmaczewski et al., 2020). There are several examples of sources hosted by galaxies with significant disk components - the HFP J1530+2705 (Orienti et al., 2010a) and the CSS sources MRC B1221-423 ((Johnston et al., 2010; Anderson et al., 2013), Duggal et al., in preparation), 3C305 (Heckman et al., 1982), PKS1814-637 (Morganti et al., 2011), and the CSS sources B0258+35 and B1128+455 (Duggal et al., in preparation). The existence of some spiral hosts strengthens the case for a link between CSS and NLSy1s (Sect. 7.1.3). Note that AGN with lower radio power tend to be found in hosts with less luminous stellar bulges (Best et al., 2005; Brown et al., 2011; Vaddi et al., 2016) and/or lower bulge/disk ratios (Pierce et al., 2019).

The hosts tend not to be brightest cluster galaxies (e.g., de Vries et al., 2000a; Drake et al., 2004). These host galaxy properties are consistent with those of the large radio galaxies at lower redshift (z < 0.6), especially FRII hosts (e.g., de Vries et al., 1998, 2000a, 2007). However, at higher redshift (z > 0.6) the hosts of the 3C are more luminous than the hosts of the GPS radio galaxies likely due to the additional aligned light in the larger sources (O'Dea, 1998; Snellen et al., 2002; de Vries et al., 2007).

In addition to the dominant old stellar population, there is often a younger stellar population in the host galaxy due to recent or ongoing star formation (e.g., Holt et al., 2007; Holt, 2009; Labiano et al., 2008; Hancock et al., 2010; Fanti et al., 2011; Tadhunter et al., 2011), and Duggal et al. (in preparation). SFRs are tabulated in Table 4 and a histogram is plotted in Fig. 11. As discussed in Sect. 4, PS and CSS sources can have moderate SFR of a few to tens of M_{\odot} yr⁻¹, but there is also a subset above $100 M_{\odot}$ yr⁻¹. The number

 $^{^2\,}$ M* is the magnitude at the break of the Schechter luminosity function (Schechter, 1976).

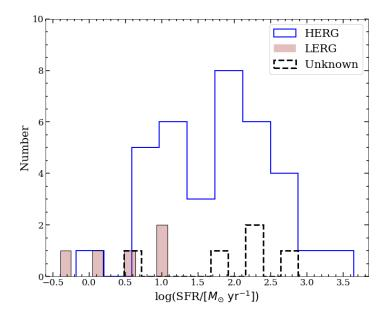


Fig. 11 SFR from Table 4. If there are more than one estimate for a given source, the estimates were averaged. The values are shaded using the emission line class (HERG/LERG).

of LERGs with estimates of SFR is small, but there is a possible trend for the LERGs to have lower SFR than the HERGs.

5.2 Merging and interaction

There are examples of well-studied mergers, e.g., 3C48 (e.g., Kirhakos et al., 1999; Canalizo and Stockton, 2000; Zuther et al., 2004; Scharwächter et al., 2004; Stockton et al., 2007), MRC B1221–423 (Johnston et al., 2010; Anderson et al., 2013), and 4C12.50 (PKS 1345+12) (e.g., Evans et al., 1999; Batcheldor et al., 2007; Emonts et al., 2016). In addition, a few systematic studies show that mergers and interactions in PS and CSS soures are common - with a range of measured fractions of sources that have either close companions and/or distorted isophotes from about 40% (Randall et al., 2011) to about 70% (e.g., O'Dea et al., 1996; de Vries et al., 1997; Drake et al., 2004), and Duggal et al. (in preparation). This is within the range of previous studies of interaction in large powerful radio galaxies (e.g., Smith and Heckman, 1989; Ramos Almeida et al., 2011, 2012; Chiaberge et al., 2015; Storchi-Bergmann and Schnorr-Müller, 2019). Based on deep optical observations, all 7 of the CSS/GPS in the 0.05 < z < 0.7 2Jy sample of Ramos Almeida et al. (2011, 2012) show evidence for galaxy interactions/mergers, but the rate is also high for the extended radio

Table 4 Star formation rates

Source	Alt.	z	ID	H/L	Tracer	SFR	Refs.
(1)	(a)	(0)	(4)	(=)	(a)	$M_{\odot} \text{ yr}^{-1}$	(0)
(1)	(2)	(3)	(4)	(5)	(6)	(7)	(8)
J0025-2602	PKS 0023-26	0.322	G	Н	PAH	270	1
J0111+3906	S4 0108+388	0.668	G	L	PAH	12	2
J0119+3210	4C 31.04	0.0602	G	Η	FIR	4.9	3
					PAH	6.4	4
			_		Ne	7.8	4
J0137 + 3309	3C48	0.3670	Q	Η	FIR	573	7
J0141+1353	3C49	0.6207	G	H	FIR	54	7
J0252 - 7104	PKS 0252-71	0.566	G	H	PAH	< 200	1
J0405 + 3803	4C 37.11	0.055	G	H	Ne	11	4
					PAH	0.8 - 1.6	4
J0432+4138	3C119	1.023	G		FIR	150	8
J0503+0203	PKS 0500+019	0.58457	G	H	PAH	23	2
J0521+1638	3C138	0.7590	Q	H	FIR	174	7
J0542+4951	3C147	0.5450	Q	Н	FIR	125	7
J0713+4349	B3 0710+439	0.518	G	H	PAH	< 10	2
J0741+3112	0738+313	0.6314	Q	H	PAH	< 20	2
J0745-0044	0743-006	0.994	Q	H	PAH	<100	2
J0801+1414	3C190	1.196	Q	Н	FIR	470	8
J1035+5628	TXS 1031+567	0.4590	G	H	PAH	<6	2
J1148 + 5924	1146+59	0.0108	G	L	Ne	0.5	4
.	NGC3894				PAH	0.3	4
J1154-3505	PKS 1151-34	0.258	Q	H	PAH	140	1
J1206+6413	3C268.3	0.3717	В	H	FIR	17	7
J1223-4235	MRC B1221-423	0.1706	G	H	$H\alpha$	>54	5
J1308-0950	PKS 1306-09	0.464	G	H	PAH	<120	1
J1331+3030	3C286	0.8499	Q	H	FIR	226	7
J1347+1217	$4C\ 12.50$	0.1234	G	Н	Ne PAH	159	4
$J1352+2126^a$	3C293	0.045	G	L	$H\alpha + 24 \mu m$	$31.5 \\ 3.2$	$\frac{4}{10}$
J1400+6210	1358+624	0.431	G	H	PAH	<4	2
J1400+0210 J1407+2827	OQ 208	0.431	В	H	Ne	54	4
31401-2021	OQ 200	0.07056	Ь	11	PAH	47.8	4
J1419+0628	3C298	1.438	Q	Н	FIR	930	8
J1447+7656	3C305.1	1.132	Ğ		FIR	$\frac{330}{220}$	8
J1449+6316	3C305	0.042	G	H	PAH	14	1
31443+0310	30300	0.042	G	11	FIR	2.4	7
J1459+7140	3C309.1	0.9050	Q	Н	FIR	120	7
J1520+2016	3C318	1.574	Q	H	FIR	580	8, 9
J1609+2641	1607+268	0.473	G		PAH	<3	2
J1634+6245	3C343	0.9880	G	Н	FIR	261	7
J1638+6234	3C343.1	0.7500	G	Н	FIR	61	7
J1723-6500	PKS 1718-649	0.014428	G	L	Ne	1.8	4
01120 0000	1110 1110 010	0.011120	Ŭ.	ь	PAH	0.8	4
J1744 - 5144	PKS 1740-517	0.44	G	Н	[OII] $\lambda 3727$	< 0.66	6
J1819-6345	PKS 1814-63	0.063	Ğ	Н	PAH	18	1
J1945+7055	1946+708	0.101	G	L	Ne	11.1	4
J1939-6342	PKS 1934-63	0.18129	Ğ	H	PAH	29	1
01000 0012	1115 1001 00	0.10120	Ŭ.		PAH	1.7-3.1	4
J2130+0502	2128+048	0.990	G		PAH	<60	2
J2130+0302 $J2137-2042$	PKS 2135-20	0.635	В	H	PAH	4400	1
J2251+1848	3C454	1.757	Q	Н	FIR	620	8
J2250+7129	3C454.1	1.841	Ğ		FIR	750	8
J2255+1313	3C455	0.5430	G	Н	FIR	17	7
J2344+8226	2342+821	0.735	Q	Н	PAH	<40	2
	O Source name Colu						

Column 1, J2000 Source name. Column 2, Alternate name. Column 3, redshift. Column 4, host identification (G) Galaxy, (B) Broad Line Radio Galaxy, or (Q) Quasar. Column 5, Emission line excitation class – (H) high excitation, (L) – low excitation. Column 6, Tracer used to determine the SFR. Equation 1 is used to calculate the SFR from the 11.3 μ m PAH fluxes from Dicken et al. (2012). Column 7, SFR (M_{\odot} yr⁻¹). Column 8, Reference for the SFR or data used to calculate SFR. References. Dicken et al. (2012) using equation 1. 2. Ogle et al., in preparation. Upper limits are 2 σ . 3. Ocaña Flaquer et al. (2010). 4. Willett et al. (2010). 5. Anderson et al. (2013). 6. Allison et al. (2019). 7. Westhues et al. (2016). 8. Podigachoski et al. (2015). 9. Podigachoski et al. (2016a). 10. Labiano et al. (2014). Footnotes. a 3C293 is the inner CSS in a double-double radio source. (Sect. 3.3).

sources in the same sample (95% for the HERG sources). Thus, it appears the compact and extended radio sources have similar merging rates. Additional studies with larger samples of compact sources would be useful.

5.3 Environments

Wold et al. (2000) selected 21 radio-loud quasars (including 6 CSS) from the 7C and Molonglo/APM Quasar Surveys. They find that the data are consistent with CSS quasars having the same clustering environments as the other quasars studied. Ramos Almeida et al. (2013) studied the clustering environments of the 46 powerful radio galaxies in the 2-Jy sample (including 1 GPS and 6 CSS). They find that the GPS and CSS sources have similar clustering environments as the FRII radio galaxies; and both FRII and GPS/CSS are less clustered than the FRI sources. Optical imaging of the fields of PS sources shows the presence of either candidate or confirmed companion galaxies suggestive of a group environment (Stanghellini et al., 1993; Snellen et al., 2002; Orienti et al., 2006, 2010a). Thus, results so far indicate that the powerful GPS and CSS sources seem to be in similar environments as powerful large radio sources. Both of these studies included relatively powerful sources and included small samples of PS and CSS sources. Follow-up studies should be done for larger samples and also extended to lower radio power PS and CSS sources.

5.4 Gas content

The gas content of the host galaxies of PS and CSS sources is relevant to the issue of the triggering and fueling of activity. It is also relevant to the hypothesis that some subset of the PS and CSS source are confined by dense gas (Sect. 7.2.2). Estimates of the molecular gas masses are presented in Table 5 and plotted in Fig. 12. We caution that the objects in Table 5 are not a complete sample. There is a broad range of masses from 10^7 to $10^{11}~M_{\odot}$. The independent estimates of the gas mass in 3C 48, 4C 12.50, and 3C 318 give consistent results. The gas mass estimates based on N_H from X-ray absorption (Sect. 5.4.4) tend to be lower than other estimates, possibly because the estimates using the other tracers (CO, dust) require higher gas masses to ensure a detection.

5.4.1 Atomic gas

Overall, the detection rate of HI absorption in compact sources is about twice that of the extended sources (32% vs. 16%, e.g., (Maccagni et al., 2017)). This might be due to the presence of bright radio emission on galaxy scales (where the atomic hydrogen is preferentially located) in the compact sources (e.g. Conway, 1997; Pihlström et al., 2003; Gupta et al., 2006; Chandola et al., 2011).

The properties of HI absorption in PS and CSS sources have been reviewed by Morganti and Oosterloo (2018) as part of their comprehensive review of HI absorption in AGN. Since then a major survey for HI absorption in a sample of 145 CSS, PS and flat-spectrum objects over a redshift range of 0.02 < z < 3.8using the Green Bank Telescope was reported by Grasha et al. (2019). Besides re-detecting H_I absorption in 6 known systems, they surprisingly did not detect any new system in the spectra of 108 sources free from RFI, and none beyond a redshift of 0.7. In contrast, for a sample of 11 compact (mostly CSS/PS) sources in the intermediate redshift range 0.7 < z < 1, 4 were detected in H_I absorption using the uGMRT by Aditya (2019). This suggests that the detection rate at intermediate redshifts of ~ 30 per cent could be similar to those at lower redshifts, without consideration of WISE colours (Chandola and Saikia, 2017). Beyond a redshift of 1, the detection rate is much smaller. The tendency of compact sources with WISE colours W2-W3>2.0 having a detection rate of ~60 per cent (Chandola and Saikia, 2017) has been confirmed for a much larger sample of ~240 sources combining the results of Westerbork (Maccagni et al., 2017) and new GMRT observations (Chandola et al., 2020). Chandola et al. (2020) also find that while LERGs have a lower detection rate compared with HERGs, there is no significant difference between these two classes when they are all chosen to have WISE colours W2-W3>2.0. HERGs and LERGs are believed to differ in their accretion modes, with the Eddington³ ratio being > 0.01 for HERGs and < 0.01 for LERGS (Heckman and Best, 2014). A similar HI detection rate for those with W2-W3>2.0 indicates that detection of HI alone does not imply a high accretion mode AGN (Chandola et al., 2020). Besides the properties of the supermassive black hole and the accretion disk, a more detailed understanding of inflow in the circumnuclear region is required to understand the fuelling mechanisms (Martini, 2004; Storchi-Bergmann and Schnorr-Müller, 2019).

There have also been new studies of individual sources. HI and $^{12}\text{CO}(2-1)$ absorption towards the young southern PS source PKSB1740-517 show that it has $\sim 10^7-10^8~M_{\odot}$ of cold gas (Allison et al., 2019). They argue that this reservoir of cold gas was accreted ~ 50 Myr ago, lending support to the hypothesis that luminous radio sources are powered by minor mergers.

The gas content of PKS 1718-643 is also discussed in detail (Maccagni et al., 2014, 2016a,b, 2018). The gas has three main components - an outer (15 kpc) warped disk of atomic and molecular gas, an inner (< 700 pc) circumnuclear molecular disk perpendicular to the outer disk, and individual molecular clouds which are infalling and could contribute to the fueling of the AGN.

VLA and EVN HI observations of the rejuvenated CSS source B0258+350 show that the cold gas in the circumnuclear region is very turbulent, due to interaction of the jet with the interstellar medium of the host galaxy NGC1167 (Murthy et al., 2019), the results being broadly consistent with the expec-

 $^{^3}$ The Eddington ratio (or fraction) is the ratio of the AGN bolometric luminosity to the Eddington luminosity $\lambda_{\rm Edd} = L_{\rm bol}/L_{\rm Edd}$. The Eddington luminosity is the maximum possible luminosity due to accretion onto a compact object, assuming spherical accretion and a balance between gravity and radiation pressure.

tations of numerical simulations (Mukherjee et al., 2018b,a). This provides evidence of the importance of AGN feedback. We discuss H_I absorption further in Sect. 5.4.5 and Sect. 7.4.

5.4.2 Molecular gas

CO has been detected in a few objects in merging/interacting systems – 3C48 (Krips et al., 2005), 3C318 (Willott et al., 2007), 4C 12.50 (Evans et al., 1999; Dasyra and Combes, 2012; Fotopoulou et al., 2019), PKS 1549–79 (Oosterloo et al., 2019), and B1740–517 (Allison et al., 2019), the possible cool-core CSS PKS 0023–26 (Morganti et al., 2020), and two nearby CSOs – 4C 31.04 (García-Burillo et al., 2007; Ocaña Flaquer et al., 2010) and PKS B1718–649 (Maccagni et al., 2018). Given the small number of sources with CO detections, the focus has been on the "interesting" sources; thus the current trends are preliminary. The merging systems tend to have more gas mass (> $10^{10} M_{\odot}$) and a more irregular distribution of gas, while the CSOs have smaller gas mass (< $10^{10} M_{\odot}$) with most of the molecular gas in a disk.

Other tracers of molecular gas have been used to place upper limits on gas content. Gupta et al. (2006) observed a sample of 17 GPS and CSS sources in OH, and O'Dea et al. (1994, 2005) observed 7 GPS sources in a variety of tracers (CO, OH, CS, and NH₃) obtaining upper limits to the molecular gas.

Near-IR observations of ro-vibrational transitions of $\rm H_2$ provide a probe of warm molecular hydrogen in 3C305, OQ208, PKS 1549–79 (Guillard et al., 2012), 4C 31.04 (Zovaro et al., 2019b), 4C 12.50 (Dasyra and Combes, 2011; Dasyra et al., 2014; Guillard et al., 2012), 3C293 (Ogle et al., 2010), and PKS B1718–649 (Maccagni et al., 2016b). In these sources, the warm $\rm H_2$ is heated to temperatures of $\sim 500-1000$ K, likely due to shocks from the radio jet (Dasyra and Combes, 2011; Dasyra et al., 2014; Guillard et al., 2012). In PKS 1549–79 (Guillard et al., 2012; Morganti et al., 2020) and 4C 12.50 (Dasyra and Combes, 2011; Dasyra et al., 2014; Guillard et al., 2012; Fotopoulou et al., 2019) both the warm molecular gas measured with the near-IR lines of $\rm H_2$ and the colder phase traced by CO are participating in the gaseous outflow. Multiphase outflows are discussed further in Sect. 7.4.

Baker et al. (2002) suggested that there was evidence for dense gas in the environment of compact radio sources due to the preferential presence of strong CIV absorption in CSS quasars. However, this result was not confirmed by subsequent work (e.g., Vestergaard, 2003; Stone and Richards, 2019).

5.4.3 Dust

Tadhunter et al. (2014) summarize the dust masses of the 2Jy sample, but do not give values for individual objects. They adopt a gas-to-dust conversion of $M_{\rm gas}=140M_{\rm dust}$ (Draine et al., 2007; Parkin et al., 2012). Westhues et al. (2016) present dust masses for 11 CSS sources based on Herschel photometry as part of a study of a sample of 87 3CR sources with z<1. Podigachoski

et al. (2015) present dust masses for an additional 7 CSS sources from a study of 3C sources with z > 1. We convert dust mass to gas mass using the adopted factor of 140 and list the gas masses in Table 5.

5.4.4 X-ray absorption column densities $N_{\rm H}$

See Sect. 6.1 for a discussion of X-ray properties. The column densities found in X-ray absorption in GPS and CSO sources cover a broad range from 10²¹ to 10^{23} cm^{-2} with values in a few sources approaching the Compton thick limit of $10^{24}~\rm cm^{-2}$ (e.g., Vink et al., 2006; Tengstrand et al., 2009; Siemiginowska et al., 2016; Ostorero et al., 2017; Sobolewska et al., 2019). There is some evidence that CSOs with higher N_H have smaller linear size for a given 5 GHz power (Sobolewska et al., 2019). If this is confirmed with a larger sample, it would be consistent with a denser environment, possibly keeping these CSOs compact (i.e., the frustration scenario, Sect. 7.2.2), or increasing radio power for a given source size (Sect. 7.2.3). The sources with high N_H have a maximum linear size of 40 pc, and this might represent the size of the region of high density (Sobolewska et al., 2019). Since N_H is related to N_{HI} (see Sect. 5.4.5), it would be good to look for a similar relation using trends in radio size vs radio power for different values of N_{HI}. Also, it would be good to search for independent evidence of a dense ISM in galaxies with high $N_{\rm H}$. Important questions are: how much gas mass is associated with the high values of N_H, and how is the gas mass distributed in the host galaxy?

We obtain a rough estimate of the amount of gas associated with the X-ray absorption by assuming that the absorbing column is distributed uniformly over some surface area. Then, $M_{\rm gas} \sim N_{\rm H} \pi r^2 m_{\rm p}$, where r is the radius of the region containing the X-ray absorbing gas, and $m_{\rm p}$ is the mass of the proton. We choose r=1 kpc based on the high detection fraction of HI absorption in compact radio sources out to sizes of about 1 kpc (Sect. 5.4.5). This gives

$$M_{\rm gas} \sim 2.5 \times 10^8 \, M_{\odot} \left(\frac{N_{\rm H}}{10^{22} \, {\rm cm}^{-2}} \right) \left(\frac{r}{1 \, {\rm kpc}} \right)^2$$
 (2)

which is given in Table 5.

5.4.5 The relation between X-ray $N_{\rm H}$ and HI $N_{\rm HI}$

In GPS sources, the column densities measured in the X-rays $N_{\rm H}$ are typically 1–2 orders of magnitude larger than those estimated by HI absorption $N_{\rm HI}$ (Vink et al., 2006; Tengstrand et al., 2009; Ostorero et al., 2017), and see also the review by Morganti and Oosterloo (2018). $N_{\rm HI}$ is likely measured towards a compact radio lobe (e.g., Araya et al., 2010; Morganti et al., 2013). Recall that $N_{\rm H}$ measures the column through all phases of the gas, and $N_{\rm HI}$ is the column though the atomic hydrogen only. $N_{\rm HI}$ is directly proportional to the Spin Temperature, which if underestimated, could also result in a lower value for $N_{\rm HI}$.

The two column densities are correlated, but with large scatter (Ostorero et al., 2010, 2017). Consistent with this, Glowacki et al. (2017) and Moss et al. (2017) note that H_I absorption is preferentially found in galaxies with high N_H, but do not explicitly test for a correlation. Also, Moss et al. (2017) find a correlation between H_I optical depth and X-ray hardness (where harder spectra are missing the softer photons due to absorption). In Sect. 6.1.4 we discuss the possibility that in the LERG GPS galaxies the X-ray emission comes from the radio lobes (via synchrotron or inverse Compton scattering (Stawarz et al., 2008; Ostorero et al., 2010)), and in the HERG GPS galaxies, the X-ray emission is dominated by the accretion structure (e.g., disk-corona, Hardcastle et al. (2009)). This would cause the total path length for X-ray absorption through the galaxy to be different in the LERGs and HERGs. The detection of possible Compton thick absorption in four sources (Guainazzi et al., 2004; Tengstrand et al., 2009; Ostorero et al., 2017) is consistent with the X-ray emission being produced in the nucleus in these four sources. Is the correlation between N_H and N_{HI} different for HERGs and LERGs?

The correlation between $N_{\rm H}$ and $N_{\rm HI}$ suggests that the two absorbing columns are physically connected. There is a peak in the HI absorption detection rate of over 50% in compact radio sources in the size range 0.1 to 1 kpc, suggesting that the size of the absorbing structure is roughly this scale (Curran et al. (2013) and references therein). Upper limits on spin temperature are obtained by setting $N_{\rm H}=N_{\rm HI}$ and assuming a covering factor for the HI of unity, obtaining upper limits in the range 100–5000 (Allison et al., 2015; Glowacki et al., 2017; Moss et al., 2017). The estimated spin temperatures might be more accurate if restricted to LERGs where the X-ray and radio emission likely both originate in the lobes, resulting in the column densities probing the same lines of sight.

5.5 Emission lines

5.5.1 Nuclear emission lines, HERG and LERG

A significant development in the last decade or so has been the realization of a dichotomy in their optical spectroscopic properties and relationship to the nature of fuelling the AGN (Heckman and Best, 2014; Tadhunter, 2016b). Starting with the early work by Hine and Longair (1979), Laing et al. (1994), and Baum et al. (1995), and more recent work by, for example, Ogle et al. (2006), Hardcastle et al. (2007), Leipski et al. (2009), Buttiglione et al. (2010) and Best and Heckman (2012) and references therein, radio AGN could be divided into High Excitation Radio Galaxies (HERGs) and Low Excitation Radio Galaxies (LERGs). As summarized by Heckman and Best (2014), in the high-excitation or radiative mode AGN, the Eddington ratio is greater than 1 per cent, while in the low-excitation or jet-mode AGN the Eddington ratio is less that 1 per cent. Accretion in the radiative mode AGN is characterized by the classical optically thin, geometrically thick accretion disk,

Table 5 Molecular Gas Masses

Source	Alt.	\mathbf{z}	ID	H/L	Tracer	$Mass$ M_{\odot}	Refs.
J0025-2602	PKS 0023-26	0.32188	G	Н	CO(2-1)	$\frac{5 \times 10^{10}}{5 \times 10^{10}}$	15
J0038+2303	B2 0035+22	0.0960	Ğ		N _H	3.5×10^{8}	1
J0111+3906	S4 0108+388	0.66847	G	L	N_{H}	1.4×10^{10}	1
J0111+3300 J0119+3210	4C 31.04	0.0602	G	H	12CO(2-1)	6×10^{9}	2,3
J0432+4138	3C119	1.023	G		dust	9.8×10^{9}	13
J0137+3309	3C48	0.367	Q	H	12CO(1-0)	1×10^{10}	4
30131 +3303	3040	0.507	Q.	11	dust	3.7×10^{10}	5
J0141+1353	3C49	0.6207	G	Н	dust	5.7×10^9	5
J0503+0203	PKS 0500+019	0.58457	G	Н	N_{H}	1.3×10^{8}	1
J0521+1638	3C138	0.7590	Q	H	dust	2.0×10^{10}	5
J0542+4951	3C138 3C147	0.7330	Q	H	dust	6.8×10^9	5
J0713+4349	B3 0710+439	0.5430	G	Н	N _H	2.5×10^{8}	6
J0801+1414	3C190	1.196	Q	H	dust	6.9×10^{10}	13
J1035+5628	TXS 1031+567	0.4590	G		N _H	1.3×10^{8}	1
•	3C268.3	0.4590 0.3717	В	Н	dust	2.0×10^9	5
J1206+6413	B2 1323+32		G	11		3×10^{7}	1
J1326+3154	·	0.370		TT	N _H	6.1×10^{10}	5
J1331+3030	3C286	0.8499	Q	H H	dust	1.2×10^{9}	о 1
J1347+1217	$4C\ 12.50$	0.1234	G	п	N _H		7
11950 019 <i>0</i> 0	9.0009	0.045	a	т.	12CO(1-0)	1.0×10^{10}	
J1352+2126 ^a	3C293	0.045	G	L	12CO(1-0)	2.2×10^{10}	16, 17
J1400+6210	4C 62.22	0.431	G	Н	N_{H}	7.3×10^{8}	1
J1407+2827	OQ 208	0.07658	В	Н	N_{H}	2.2×10^{10}	1
J1419+0628	3C298	1.438	Q	Н	dust	5.3×10^{10}	13
J1447+7656	3C305.1	1.132	G		dust	2.0×10^{10}	13
J1449+6316	3C305	0.0416	G	H	dust	1.2×10^9	5
J1459+7140	3C309.1	0.9050	Q	H	dust	9.0×10^{10}	5
J1511+0518		0.084	G		N _H	9.5×10^{9}	6
J1520+2016	3C318	1.574	Q	H	12CO(2-1)	3×10^{10}	8,12
T4 F F O F O 4 4	DIIG 4740 F0	0.4504	~	**	dust	2.4×10^{10}	13, 14
J1556-7914	PKS 1549-79	0.1521	G	H	12CO(1-0)	1×10^{10}	9
J1634+6245	3C343	0.9880	G	Н	dust	1.8×10^{11}	5
J1638+6234	3C343.1	0.7500	G	H	dust	2.6×10^{9}	5
J1723 - 6500	PKS 1718-649	0.014428	G	\mathbf{L}	H_2	2×10^{9}	10
					N _H	1.3×10^{8}	6
			~		12CO(2-1)	1.9×10^9	18
J1744-5144	PKS 1740-517	0.44	G	H	12CO(2-1)	$1 - 10 \times 10^7$	11
J1845 + 3541	1843+356	0.764	G		N_{H}	2×10^{8}	1
J1939 - 6342	PKS 1934-63	0.18129	G	Η	N_{H}	3×10^{7}	1
J1944+5448	1943 + 546	0.263	G		N_{H}	2.8×10^{8}	1
J1945 + 7055	1946 + 708	0.101	G		N_{H}	4.0×10^{8}	1
J2022+6136	2021+614	0.227	G	H	N_{H}	9.0×10^{9}	1
J2251+1848	3C454	1.757	Q	Η	dust	3.2×10^{10}	13
J2250+7129	3C454.1	1.841	G		dust	3.4×10^{10}	13
J2255+1313	3C455	0.5430	G	Η	dust	4.0×10^{9}	5
J2355+4950	TXS $2352+495$	0.2379	G	Η	N_{H}	1.7×10^{8}	6

Column 1, J2000 Source name. Column 2, Alternate name. Column 3, redshift. Column 4, host identification (G) Galaxy, (B) Broad Line Radio Galaxy, or (Q) Quasar. Column 5, Emission line excitation class – (H) high excitation, (L) – low excitation. Column 6, Tracer used to determine the gas mass. Equation 2 is used to calculate the mass from the X-ray column density N_H. Column 7, Mass of gas (M_{\odot}). Column 8, Reference for the gas mass or data used to calculate gas mass. Cold Hydrogen is the default mass. However, N_H is sensitive to all phases of the gas along the line of sight to the X-ray emission. References. 1. Ostorero et al. (2017). 2. García-Burillo et al. (2007). 3. Ocaña Flaquer et al. (2010). 4. Krips et al. (2005). 5. Westhues et al. (2016). 6. Sobolewska et al. (2019). 7. Dasyra and Combes (2012). 8. Willott et al. (2007). 9. Oosterloo et al. (2019). 10. Maccagni et al. (2016b). 11. Allison et al. (2019). 12. Heywood et al. (2013). 13. Podigachoski et al. (2015). 14. Podigachoski et al. (2016a). 15. Morganti et al. (2020). 16. Evans et al. (1999). 17. Labiano et al. (2014). 18. Maccagni et al. (2018). Footnotes. ^a 3C293 is the inner CSS in a double-double radio source (Sect. 3.3).

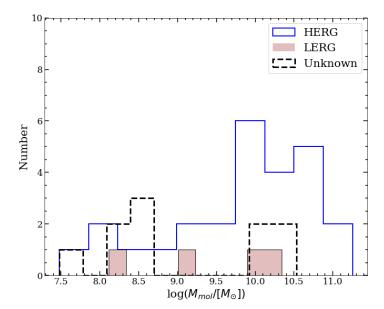


Fig. 12 Mass of molecular gas from Table 5. If there are more than one estimate for a given source, the estimates were averaged. The values are shaded using the emission line class (HERG/LERG).

the ultraviolet radiation from which gives rise to prominent emission lines in both the broad- and narrow-line regions. In this class of objects, namely the HERGs, an obscuring torus of dust and molecular gas could obstruct a view of the broad-line region giving rise to Type 2 AGN, while closer to the jet axis one would get a direct view of the broad-line region giving rise to Type 1 AGN. On the other hand for LERGs, the inner disk is not there resulting in weak or no emission lines, with the inner region being dominated by a "geometrically thick advection-dominated accretion flow" (Heckman and Best, 2014). LERGs tend to have higher black hole masses, occur in more massive early-type galaxies and have lower specific star-formation rates approaching the red sequence, compared with the HERGs (Heckman and Best, 2014). Recent studies of the LOFAR-Boötes sample by Williams et al. (2018) and the Stripe 82 1–2 GHz JVLA survey by Whittam et al. (2018) are consistent with these trends. Most of the HERGs have an FRII morphology while LERGs predominantly appear to have an FRI structure. LERGs are on average of lower luminosity than the HERGs (Best and Heckman, 2012; Heckman and Best, 2014). Whittam et al. (2018) find mechanical feedback to be significant for both LERGs and HERGs, although there is a scatter of about 2 dex in the fraction of accreted power deposited in the ISM.

Optical spectroscopy is available for PS (e.g., Snellen et al., 1999; de Vries et al., 2000b, 2007; Labiano et al., 2007) and CSS (e.g., Gelderman and Whittle, 1994; Morganti et al., 1997; Hirst et al., 2003; Labiano et al., 2005) sources. Current results suggest that the nuclear emission line spectra are very similar for compact radio sources and larger radio sources (e.g., Morganti et al., 1997; Hirst et al., 2003; Kunert-Bajraszewska and Labiano, 2010). The CSS and PS sources can be classified as HERGs and LERGs similar to the large radio sources (Buttiglione et al., 2010; Kunert-Bajraszewska and Labiano, 2010). The compact and large HERGs lie on the same correlation of [OIII] $\lambda 5007$ luminosity with radio power (Kunert-Bajraszewska and Labiano, 2010). A parallel correlation is found for the compact and large LERGs. In addition, as discussed here in Sect. 6.1.4, Kunert-Bajraszewska et al. (2014) show that the compact and large HERGs lie on the same correlation of X-ray luminosity with radio power. And a similar correlation is found for the compact and large LERGs. These optical - radio - X-ray correlations for HERGs and LERGs argue that the compact and large radio sources have similar central engines. They also make it plausible that at least some of the compact sources evolve to become large radio sources. They also imply (but do not require) continuity, i.e., compact sources start as HERG or LERG and then evolve to become large radio sources while maintaining their HERG or LERG nature. If some of the compact sources are short-lived (Sect. 7.2.1), then they must fade without disrupting the observed correlations.

O'Dea (1998) showed that GPS radio galaxies tend to have lower [OIII] $\lambda 5007$ luminosities than CSS radio galaxies. Labiano (2008) confirmed this for a larger sample of sources. Vink et al. (2006) find that the ratio of [OIII]/X-ray luminosity is lower for the GPS sources than for larger sources. Vink et al. (2006) suggest that if the emission line gas is photo-ionized, the young age of the GPS sources means that the Stromgren⁴ sphere which determines the size and luminosity of the ionized NLR is still small and growing. Alternately, if there is a strong contribution to the emission line luminosity from jet-driven shocks, the small size of the GPS radio source means that only a small volume of gas has been shocked (e.g., Moy and Rocca-Volmerange, 2002).

The smaller radio sources have larger [OIII] $\lambda 5007$ line FWHM than the larger radio sources (Gelderman and Whittle, 1994; Best et al., 2000; Labiano, 2008; Holt et al., 2008). As discussed in Sect. 5.5.2 and 7.4, this is consistent with strong jet interaction with the clouds producing the emission line gas.

5.5.2 Extended emission lines and the alignment effect

GPS radio sources are generally too small to be resolved in the optical, thus, the detection of the alignment effect has been mostly restricted to CSS radio sources (but see Batcheldor et al. (2007) for an example of two nearby GPS sources slightly resolved by HST). Extended emission lines in CSS are almost

⁴ The Stromgren sphere is an idealized representation of the size of a nebula which has been ionized by a compact source of high energy photons.

always aligned with and co-spatial with the radio source (de Vries et al., 1997, 1999; Axon et al., 2000; Privon et al., 2008). The alignment effect is seen in CSS sources at all redshifts (de Vries et al., 1997; Privon et al., 2008), while extended radio sources display the alignment effect only at z>0.6 (McCarthy, 1993). Spatially resolved spectroscopy reveals that the kinematics of the emission line gas are consistent with the emission line clouds having been shocked by the radio source and accelerated outwards (Chatzichristou et al., 1999; O'Dea et al., 2002; Holt et al., 2008; Shih et al., 2013; Reynaldi and Feinstein, 2013). The excitation of the aligned emission line gas is generally consistent with shocks combined with AGN photoionization (De Breuck et al., 2000; Best et al., 2000; Moy and Rocca-Volmerange, 2002; Inskip et al., 2002, 2006; Labiano et al., 2005; Holt et al., 2009; Shih et al., 2013; Reynaldi and Feinstein, 2013, 2016). Thus, the alignment effect in CSS sources is a signature of radio-jet feedback to the host galaxy ISM and is discussed further in Sect. 7.4.

5.6 Jet-induced Star Formation

Jet-induced star formation⁵ is expected to be a natural consequence of radio jets propagating though the ISM (e.g., Rees, 1989; Begelman and Cioffi, 1989; De Young, 1989; Daly, 1990; Tortora et al., 2009; Gaibler et al., 2012; Dugan et al., 2014, 2017; Fragile et al., 2017). Because of this, jet-induced star formation should be a key signature of radio jet feedback (e.g., Gaibler et al., 2012; Fragile et al., 2017).

There is observational evidence for jet-induced star formation associated with several extended radio sources, e.g., Minkowski's Object (Brodie et al., 1985; van Breugel et al., 1985; Croft et al., 2006; Salomé et al., 2015; Lacy et al., 2017; Zovaro et al., 2020), Centaurus A (Graham, 1998; Mould et al., 2000; Rejkuba et al., 2002; Oosterloo and Morganti, 2005; Crockett et al., 2012; Santoro et al., 2015, 2016; Morganti et al., 2016; Salomé et al., 2017), 3C285 (van Breugel and Dey, 1993; Salomé et al., 2015), 4C 41.17 (Dey et al., 1997; Nesvadba et al., 2020), and 3C441 (Lacy et al., 1998). Jet-induced star formation is also supported by statistical studies of large samples of radio sources (e.g., Zinn et al., 2013; Kalfountzou et al., 2017).

GPS/CSO radio sources are too small for current facilities to show jet-induced star formation on the scale of the radio source. However, there is growing evidence for jet-induced star formation in CSS radio sources. Labiano et al. (2008) obtained HST ACS/HRC observations through the F330W filter of 3 CSS sources and detected extended UV light in one object, 3C303.1. The

⁵ This process is commonly referred to as jet-induced star formation, though it is expected that in powerful radio sources, the bow shock driven by the over-pressured cocoon is responsible for compressing the ambient clouds and triggering star formation (e.g., Rees, 1989; Begelman and Cioffi, 1989; De Young, 1989; Daly, 1990). However, there is also evidence for star formation triggered by direct jet impact, e.g., Minkowski's Object (Brodie et al., 1985; van Breugel et al., 1985; Croft et al., 2006; Salomé et al., 2015; Lacy et al., 2017; Zovaro et al., 2020).

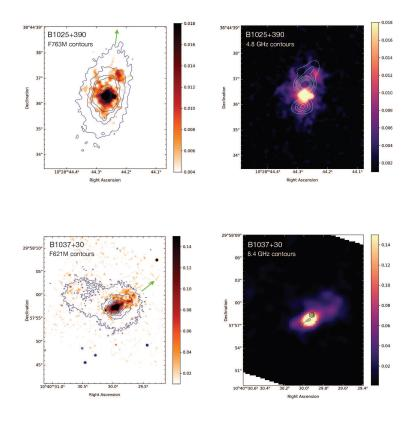


Fig. 13 Possible jet-induced star formation in 2 CSS radio galaxies. (Left Panels) HST WFC3/UVIS data. Contours of R-band superposed on image of UV continuum. The green arrow shows the orientation of the radio source axis. (Right Panels). HST WFC3/UVIS UV continuum image on contours of radio image. (Top) J1028+3844 (4C 39.32). (Bottom) J1040+2957 (4C 30.19). (Figure from Duggal, private communication).

UV light in 3C303.1 is along the radio axis and seems associated with the brighter southern radio lobe. Duggal et al. (in preparation) obtained HST WFC3/UVIS imaging of the UV continuum in the region between rest-frame [CIII] λ 1909 and MgII λ 2798. This region is free of bright emission lines (e.g., McCarthy, 1993). Duggal et al. find extended UV continuum aligned with the radio source in 6 of 9 CSS sources observed. Two examples are shown in

Figure 13. Combining the two studies, extended UV light aligned with the radio source is found in 7/12 (58%) of CSS radio sources. If the UV light is confirmed to be due to star formation, this would indicate that jet-induced star formation is common in CSS radio galaxies. There may be a contribution to the UV light from scattered AGN light, which is identified by its polarization (di Serego Alighieri et al., 1988, 1989, 1993; Antonucci, 1984; Fabian, 1989; Dey et al., 1996; Cimatti et al., 1997; Tran et al., 1998; Tadhunter et al., 1992, 1996, 2002). There may also be a contribution from nebular continuum (Dickson et al., 1995; Cimatti et al., 1997; Wills et al., 2002; Tadhunter et al., 2002; Inskip et al., 2006).

5.7 Black-hole Masses, Eddington ratios, the black-hole fundamental plane, and jet production efficiency

Estimates of the masses of the central supermassive black holes in PS and CSS sources have been made (Wu, 2009b; Son et al., 2012; Liao and Gu, 2020; Wójtowicz et al., 2020). The mass estimates range from $\log_{10}(M/M_{\odot}) \sim 7.32$ to 9.84, with a median value of 8.72 (Liao and Gu, 2020). Liao and Gu (2020) compare the black hole mass estimates with those of low redshift large-scale radio galaxies studied by Hu et al. (2016). There is good overlap of the black masses at the high end. However, none of the large-scale radio galaxies (and 11% of the PS and CSS sources) have estimated black hole masses less than $\log_{10}(M/M_{\odot}) = 8$. The subset of PS and CSS sources with low black hole masses ($\log_{10}(M/M_{\odot}) < 8$) may represent a population which will not evolve to become large-scale radio galaxies (Sect. 7.2).

Estimates of the Eddington ratio in PS and CSS surces have also been made (Holt et al., 2006, 2011; Wu, 2009b; Son et al., 2012; Liao and Gu, 2020; Wójtowicz et al., 2020). Son et al. (2012) show that the high Eddington ratio sources tend to be HERGs and the low ratio sources tend to be LERGs as found for large-scale radio sources (e.g., Best and Heckman, 2012). The Eddington ratios for the PS and CSS sources are in a broad range $R_{\rm Edd} \sim 10^{-4.93} - 10^{0.37}$ (Liao and Gu, 2020). The Eddington ratios tend to be a bit higher for the PS and CSS sources (mean value $R_{\rm Edd} \sim 10^{-2.26}$) than the Hu et al. (2016) large-scale radio galaxies (mean value $R_{\rm Edd} \sim 10^{-3.05}$) (Liao and Gu, 2020). If the PS and CSS evolve into these large-scale radio sources, the accretion rates must decline as the sources age.

Note the following two cavaets. (1) The black hole masses, bolometric luminosities, and Eddington ratios have considerable uncertainty. (2) The PS and CSS sample is heterogeneous and may not be well matched with the Hu et al. (2016) sample of low redshift large-scale radio sources. Thus, these interesting results deserve further study.

AGN with estimates of black hole mass can be placed on the black hole fundamental plane which is defined by nuclear radio luminosity, nuclear X-ray luminosity, and black hole mass (Merloni et al., 2003; Falcke et al., 2004a). The existence of the fundamental plane is consistent with the radio luminosity

being produced in a jet whose power is related to black hole mass and accretion rate, and the X-ray emission being produced in a disk-corona system (whose power is related to black hole mass and accretion rate) and/or the jet (Merloni et al., 2003; Falcke et al., 2004a). PS and CSS sources have been placed on the black hole fundamental plane (Fan and Bai, 2016; Liao et al., 2020; Wójtowicz et al., 2020). Their results are consistent with the X-ray emission containing a contribution from the radio source, e.g., synchrotron or inverse Compton (Stawarz et al., 2008; Ostorero et al., 2010; Migliori et al., 2012) (and see discussion in Sect. 6.1).

The jet production efficiency, $\eta_{\rm jet}$, is defined to be the ratio of the jet kinetic power to the accretion power (e.g., Wójtowicz et al., 2020). Wójtowicz et al. (2020) find a broad range ($10^{-3} < \eta_{\rm jet} < 0.2$) for jet production efficiency in a sample of 17 CSOs. Wójtowicz et al. (2020) point out that these values for $\eta_{\rm jet}$ are below those expected for magnetically arrested disks around maximally spinning black holes and consistent with those of a sample of extended FRII quasars. Wójtowicz et al. (2020) suggest that the jets in these CSOs are produced most efficiently in high/hard states in analogy with Galactic XRBs (Homan and Belloni, 2005; McClintock and Remillard, 2006).

6 High-energy properties

6.1 X-ray properties

At the time of the previous review (O'Dea, 1998), some PS and CSS quasars had been detected in X-rays at luminosities consistent with those of other quasars. However, few PS and CSS galaxies had been detected. X-ray studies of PS and CSS sources have been previously reviewed by Siemiginowska (2009) and Migliori (2016). Currently, nearly all powerful extragalactic radio sources (both compact and extended) are detected in X-rays in the 2Jy (Mingo et al., 2014) and 3CR samples (Stuardi et al., 2018; Jimenez-Gallardo et al., 2020). Nearly all (91%) of CSOs are detected (Siemiginowska et al., 2016), while detection rates for CSS galaxies are lower with 4/7 (57%) of low power CSS galaxies detected (Kunert-Bajraszewska et al., 2014).

6.1.1 X-rays from PS and CSO galaxies

Recent studies with ASCA, BeppoSAX, XMM-Newton and Chandra have greatly increased the detections of PS and CSO galaxies (O'Dea et al., 2000; Risaliti et al., 2003; Guainazzi et al., 2006; Vink et al., 2006; Tengstrand et al., 2009; Siemiginowska et al., 2016; Beuchert et al., 2018; Sobolewska et al., 2019). Tengstrand et al. (2009) discussed a sample of 16 PS galaxies detected in X-rays. Siemiginowska et al. (2016) presented new Chandra observations of 10 CSOs and archival Chandra observations of another 6. Sobolewska et al. (2019) presented XMM-Newton observations of 3 CSOs thought to have high column densities and compiled a list of 24 CSOs with X-ray data. In general,

the X-ray spectra of PS and CSO galaxies can be described by an absorbed power-law with photon index in the range $\Gamma \sim 1.4-1.7$. The absorbing column in the PS and CSO galaxies lies in the range $N_{\rm H} \sim 10^{21}-10^{24}~{\rm cm}^{-2}$ and Sobolewska et al. (2019) confirm that 5 sources have $N_{\rm H} > 10^{23}~{\rm cm}^{-2}$. Sobolewska et al. (2019) show that the 5 heavily absorbed sources have a smaller radio size for a given 5 GHz luminosity than the less absorbed sources and suggest that the small, heavily absorbed sources are confined by a dense environment.

There are two main hypotheses for the origin of the X-ray emission in PS and CSOs. It is possible that the X-ray emission in HERGs is produced primarily by the accretion disk and corona (e.g., Tengstrand et al., 2009). Note that the attribution of the X-ray emission to a disk/corona is not meant to imply that these systems are well understood or well modelled (e.g., Blaes, 2007). However, it is also possible that the X-ray emission is produced in the radio source via inverse Compton scattering (Stawarz et al., 2008; Ostorero et al., 2010). Both mechanisms may contribute in individual sources. Depending on the origin of the X-ray emission, the measured $N_{\rm H}$ samples a different line of sight through the host galaxy. Demanding that the X-ray derived $N_{\rm H}$ matches that derived from the 21-cm line in absorption against the radio source (e.g., Vermeulen et al., 2003) requires a ratio of spin temperature to covering factor of $T_s/c_f \sim 100$ –5000 K in the atomic gas (Ostorero et al., 2010; Allison et al., 2015; Glowacki et al., 2017; Moss et al., 2017). (See also Sect. 5.4.5.)

6.1.2 X-rays from CSS galaxies

Because the radio source size is well matched to the size of the host galaxy, CSS galaxies probe the process of energy transfer from the radio source to the host galaxy ISM (Sect. 7.4). X-ray emission is expected from hot gas which has been shocked by the expanding radio source (Heinz et al., 1998; Bicknell and Sutherland, 2006; Sutherland and Bicknell, 2007).

O'Dea et al. (2006) present XMM observations of 3C303.1. There is no evidence in the X-ray spectrum for absorption at the redshift of the galaxy, suggesting that the emission is not dominated by the nucleus. They detect a thermal component with a temperature kT ~ 0.8 keV which they attribute to the ISM of the host galaxy. There is also evidence for an additional component contributing to the spectrum. The component could be synchrotron self-Compton from the southern radio lobe if the magnetic field is below the equipartition value by a factor of ~ 3.5 . Alternately, the second component could be hot gas which has been shocked by the expansion of the radio source. If due to hot gas, the fit to the spectrum gives a temperature of kT ~ 45 keV which corresponds to a shock Mach number $M \sim 13$. The kinematics of the optical emission line gas are consistent with shock acceleration (O'Dea et al., 2002; Reynaldi and Feinstein, 2016) and the excitation is consistent with shocks contributing to the heating of the emission line gas (Labiano et al., 2005; Holt et al., 2009; Shih et al., 2013; Reynaldi and Feinstein, 2016).

Chandra observations show the soft X-ray emission in 3C305 is spatially extended over 5" (4 kpc) and has a closer correspondence with the optical emission line gas than with the radio emission (Massaro et al., 2009; Balmaverde et al., 2012; Hardcastle et al., 2012). This implies the X-ray emission is thermal rather than non-thermal (Massaro et al., 2009). Deeper Chandra observations confirm that the X-ray gas is shock-heated (Hardcastle et al., 2012). The data are consistent with the hypothesis that the X-ray gas is part of a gaseous outflow driven by the radio source (Hardcastle et al., 2012). The kinematics and excitation of the optical emission line gas are also consistent with acceleration and heating by shocks (Reynaldi and Feinstein, 2013).

Chandra observations of the double-double source 3C293 (Sect. 3.3) are presented by Lanz et al. (2015). The Chandra data show evidence for hot (10⁷ K) shock-heated gas associated with the nucleus and the inner jets in the central CSS source. Combined with the observations of warm H₂ (Ogle et al., 2010), this suggests that the radio jet is driving shocks into both the hot and cold gas in the host galaxy (Lanz et al., 2015).

Observations of 7 low radio power CSS galaxies detected 4 and showed that one of them (1321+045) is in a cool core cluster (Kunert-Bajraszewska et al., 2013, 2014). 1321+045 (z=0.263) has a projected size of 17 kpc and a radio power $L_{5GHz} \sim 10^{25}$ W Hz⁻¹ (Kunert-Bajraszewska et al., 2013). This source does not show evidence for strong interaction with the environment; e.g., the optical emission lines are consistent with AGN photoionization, and the extended X-ray emission does not show any distortions which could be attributed to interaction with the radio source (Kunert-Bajraszewska et al., 2013).

O'Dea et al. (2017) compiled selected radio and X-ray properties of the nine CSS radio galaxies with X-ray detections so far. They found that 2/9 CSS radio galaxies show X-ray spectroscopic evidence for hot shocked gas (3C303.1 (O'Dea et al., 2006) and 3C305 (Massaro et al., 2009; Hardcastle et al., 2012)) and 3 CSS sources (with 2 overlap) show X-ray emission aligned with the radio source (3C237 (Massaro et al., 2018), 3C303.1 (Massaro et al., 2010), and 3C305 (Massaro et al., 2009; Balmaverde et al., 2012; Hardcastle et al., 2012)). These detections of hot shocked gas and aligned emission in the X-rays are consistent with the results of numerical simulations (Heinz et al., 1998; Bicknell and Sutherland, 2006; Sutherland and Bicknell, 2007) and suggest significant jet-mode feedback to the ISM (see Sect. 7.4). O'Dea et al. (2017) suggest that hot shocked gas may be typical of CSS radio galaxies due to their propagation through their host galaxies. More data are needed (deep Chandra and XMM-Newton observations on a sample of CSS galaxies) in order to improve our understanding of the interaction of CSS radio galaxies with their host galaxies.

6.1.3 X-rays from PS and CSS quasars

About 13 PS and CSS quasars have been studied so far with Chandra and XMM (e.g., Worrall et al., 2004; Siemiginowska et al., 2008; Salvesen et al.,

2009; Migliori et al., 2012). The Chandra study by Siemiginowska et al. (2008) includes new observations and summarizes previous work on 6 objects classified as PS quasars and 7 classified as CSS quasars. Two of the "GPS quasars" have large scale jets detected by Chandra (B2 0738+313 Siemiginowska et al. (2003), although note that Stanghellini et al. (2001b) suggest it to be a corejet source, and PKS 1127–145 Siemiginowska et al. (2002, 2007)) indicating that these are extended quasars with GPS-shaped nuclei. The X-ray spectra of the PS and CSS quasars are generally well fit by an absorbed power-law (e.g., Worrall et al., 2004; Siemiginowska et al., 2008; Salvesen et al., 2009). Siemiginowska et al. (2008) note that the power-law indexes of the PS and CSS quasars are steeper (median $\Gamma = 1.84$) than those of typical radio loud quasars ($\Gamma = 1.5$) (Elvis et al., 1994; Richards et al., 2006). If this is confirmed with a larger sample, it would suggest that there is an additional component to the X-ray emission in the PS/CSS sources that is not seen in the typical radio loud quasars (or vice versa). Siemiginowska et al. (2008) also find that the absorbing columns towards the GPS/CSS quasars are no more than \sim few $\times 10^{21}$ cm⁻², suggesting that the higher absorbing columns seen in two high z GPS quasars (Elvis et al., 1994) are not common. Observations of some PS/CSS quasars are consistent with relativistic beaming of at least some of the X-ray emission (e.g., 3C48 Worrall et al. (2004), 3C287 Salvesen et al. (2009), and 3C186 Migliori et al. (2012)).

6.1.4 X-ray-radio relations and the origin of the X-ray emission

See Sect. 5.5.1 for an introduction to HERGs and LERGs. In extended radio galaxies, at a given radio luminosity, the HERG galaxies have more luminous X-ray emission than the LERG galaxies (e.g., Hardcastle et al., 2009). This is interpreted to mean that the X-rays in the HERGs are produced in the accreting gas (e.g., a disk-corona system), while the X-rays in the LERGS (which are missing a bright accretion structure) are produced in the radio source, possibly in the base of the jet (e.g., Hardcastle et al., 2009). Though in the CSOs, the X-ray emission might be produced in the radio lobes (Stawarz et al., 2008; Ostorero et al., 2010).

Kunert-Bajraszewska et al. (2014) compiled X-ray and radio fluxes for GPS, CSS, FRI, and FRII radio sources in order to study relations on the radio-X-ray plane. The GPS and CSS sources lie on the same radio X-ray correlation as the FRI and FRII radio sources (extending 6 decades in X-ray power and 5 decades in radio power, Fig. 14) consistent with Tengstrand et al. (2009). Thus, there is continuity in the properties of the small and large sources.

In addition, at a given radio power, the objects with high excitation emission lines have X-ray powers about an order of magnitude higher than the objects with low excitation emission lines (Fig 15). This indicates the presence of an additional source of X-rays in the HERG sources and is consistent with the X-ray emission being dominated by the accretion disk-corona in the high excitation galaxies (e.g., Hardcastle et al., 2009). Note that there are

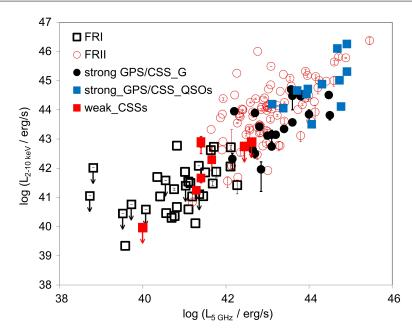


Fig. 14 2–10 keV luminosity vs. 5 GHz luminosity for GPS, CSS, FRI and FRII radio sources from Kunert-Bajraszewska et al. (2014). Strong and weak refer to high and low radio power, respectively.

only 3 GPS/CSS LERGs in Figure 15, so it remains to be confirmed that the GPS/CSS LERGs show the same trend as the extended radio galaxies which are LERGs.

Based on the above results, we suggest the following scenario for X-ray emission in GPS and CSS sources. In LERG galaxies the X-ray emission comes from the radio source (via synchrotron or inverse Compton scattering), in HERG galaxies, the X-ray emission is dominated by the accretion structure (e.g., disk-corona). In the quasars, because the radio emission is beamed, but the accretion flow is not, the radio source will make a relatively larger contribution to the X-ray emission. If this scenario is correct, it will assist the interpretation of the relation between X-ray $N_{\rm H}$ and Hi $N_{\rm HI}$ (Sect. 5.4.5).

6.2 γ -ray emission

The status of γ -ray observations of PS and CSS sources was previously reviewed by Migliori (2016). Inverse Compton (IC) scattering of ambient photons by the relativistic electrons in lobes and cocoons (e.g., Stawarz et al., 2008; Ito et al., 2011; Kino et al., 2013), and jets (Migliori et al., 2014) of compact radio sources are predicted to produce luminous γ -ray emission. Other mechanisms for producing γ -ray emission include bremsstrahlung (Kino et al., 2007, 2009) and synchrotron emission from protons and secondary electrons/positrons pro-

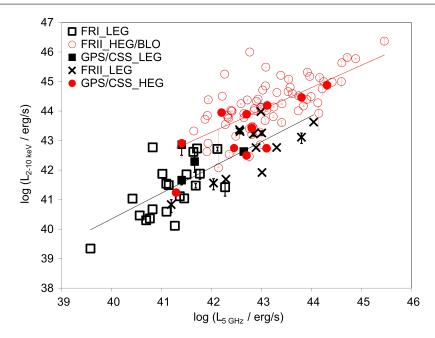


Fig. 15 2–10 keV luminosity vs. 5 GHz luminosity for GPS, CSS, FRI and FRII radio sources from Kunert-Bajraszewska et al. (2014). High Excitation (HERG, in this figure called HEG) and Low Excitation (LERG, in this figure called LEG) emission line objects are noted.

duced via the photo-pion cascade (e.g., Kino and Asano, 2011). Thus, γ -ray emission is potentially an important diagnostic of conditions in the compact radio sources.

Migliori et al. (2014) report upper limits on γ -ray emission from a sample of 6 GPS quasars and 7 CSS quasars which have X-ray observations from Siemiginowska et al. (2008). D'Ammando et al. (2016) report upper limits on a sample of 51 HFPs from the sample of Dallacasa et al. (2000) from which obvious blazars have been removed as discussed by Orienti and Dallacasa (2008b). Likely γ -ray detections include the CSOs PKS 1413+135 (Gugliucci et al., 2005) and 2234+282 (An et al., 2016b), and the CSS quasars 0202+149 (An et al., 2016a), 3C138 (Zhang et al., 2020), 3C286 (An et al., 2017; Yao and Komossa, 2020; Zhang et al., 2020), and 3C309.1 (Zhang et al., 2020). However, some may require confirmation that they are either true (unconfused) γ -ray sources or true (non-blazar) PS and CSS sources (e.g., D'Ammando et al., 2016; Migliori et al., 2016).

The detection of γ -ray emission from the nearby CSO PKS 1718-649 is consistent with IC scattering of ambient emission by the relativistic electrons in the compact lobes (Migliori et al., 2016). The γ -ray detection of the CSO PMN J1603-4904 also seems reliable (Müller et al., 2014, 2016; Goldoni et al., 2016; Krauß et al., 2018). Two additional γ -ray detections in nearby, young CSOs have been reported - NGC 3894 (Principe et al., 2020) and TXS 0128+554

(Lister et al., 2020). Principe et al. (2020) and Lister et al. (2020) note the young kinematic ages (< 100 yr) of the CSOs with γ -ray detections and suggest that in these two CSOs, the γ -rays are produced in the inner jet rather than the lobes. Kosmaczewski et al. (2020) reach similar conclusions.

6.3 Ultra-high energy cosmic rays from PS and CSS sources?

Ultra-High Energy Cosmic Rays (UHECR) have energies above 10^{18} eV. UHECR in large-scale radio sources are discussed by Hardcastle and Croston (2020). Here we focus on compact radio sources. Elbert and Sommers (1995) noted that the CSS quasar 3C147 was in the direction of a UHECR event with energy $> 10^{20}$ eV. This led Farrar and Biermann (1998) to suggest an association between the highest energy UHECR and compact (e.g., GPS and CSS) quasars based on 5 events. This association was challenged by Hoffman (1999) (but see the reply by Farrar and Biermann (1999)) and by Sigl et al. (2001), but supported by Virmani et al. (2002). We regard this result as requiring confirmation. Takami and Horiuchi (2011) show that UHECR protons might be accelerated to energies up to 10²⁰ eV in the hot spots of CSOs. If compact quasars (or any distant source) was found to be the origin of the highest energy UHECR, this would have profound implications. The interaction of UHECR protons or heavy nuclei with the cosmic microwave background results in loss of the particle energy due to production of pions (the GZK effect, (Greisen, 1966; Zatsepin and Kuz'min, 1966)). So, UHECR with energies $> 10^{20}$ eV cannot have an origin more than about 100 Mpc from Earth (e.g., Dermer et al., 2009). Thus, the association of UHECR of energy $> 10^{20}$ eV with distant AGN would require a new particle or new physics.

7 Discussion

7.1 Implications for PS and CSS sources in selected AGN populations

Compact and/or peaked spectrum radio sources are found in many populations of AGN. Here we discuss the presence and implications of these sources in several important populations.

7.1.1 PS and CSS sources in the infrared faint radio sources

The Infrared Faint Radio Sources (IFRS) are selected to have a ratio of 20 cm flux density/3.6 μ m flux density > 500 and a 3.6 μ m flux density < 30 μ Jy (e.g., Norris et al., 2006; Zinn et al., 2011). This selection tends to find powerful radio sources at high redshift ($z \sim 2-4$) (e.g., Collier et al., 2014; Singh et al., 2017; Orenstein et al., 2019). Note that at these redshifts, the rest frame is closer to 1 μ m and so 3.6 μ m is not a rest-frame IR selection. Some of the IFRS are found to be GPS and CSS sources (e.g., Middelberg et al., 2011;

Collier et al., 2014; Herzog et al., 2015). Since the IFRS are a subset of the high-z radio galaxies, it is not clear how representative the relative fractions of GPS and CSS sources are. Herzog et al. (2016) find that at least 18% of the IFRS are GPS and CSS sources and suggest that this is consistent with the fractions in the general radio source population noted by O'Dea (1998). This could also be consistent with a lack of strong evolution in the relative fractions of PS and CSS sources in the radio source population out to redshift $z \sim 4$.

7.1.2 The population of PS sources at mm wavelengths

There are now several wide field surveys at high frequencies, e.g., AT20G (Murphy et al., 2010) and Planck (Planck Collaboration et al., 2011a). This allows us to address the issue of the contribution of PS sources to the population of sources at mm wavelengths (See Sect. 2). PS sources at mm wavelengths are of interest because of their potential contribution to observations of the cosmic microwave background (e.g., de Zotti et al., 2005). In addition, sources which peak at mm wavelengths are likely to be extremely compact and/or have extreme physical properties. As discussed in Sect. 2, there is a population of PS sources with spectral peaks above 5 GHz - the high-frequency peakers (Dallacasa et al., 2000, 2002; Hancock, 2009; Orienti and Dallacasa, 2012, 2020). Many candidate HFPs identified with quasars turn out to be blazars based on variability of the shape of the radio spectrum (Sect. 3.5), very compact radio size suggesting Doppler boosting (e.g., Bolton et al., 2006; Orienti and Dallacasa, 2012), or high polarization from jet-dominated emission (e.g., Orienti and Dallacasa, 2008b).

Hancock (2009) presents a sample of 656 candidate PS sources with observed peaks above 5 GHz, drawn from a sample of 4404 AT20G sources with data at three frequencies. Follow-up studies on a sample of 21 candidates suggest that 75% of the sources identified with galaxies are non-blazar PS sources, and 25% of the sources identified with stellar objects are non-blazar PS objects (Hancock et al., 2010). The likely fraction of non-blazar PS sources in the AT20G depends on the identifications, but may be something like half of the 656 sources or $\sim 7\%$ of the AT20G sample of 4404 sources.

About 10% of the compact extragalactic sources detected by Planck and listed in the Early Release Compact Source Catalog (ERCSC) have a peaked spectrum (Planck Collaboration et al., 2011a). However nearly all of these are identified with known blazars (Planck Collaboration et al., 2011a; Volvach et al., 2016); though Massardi et al. (2016) suggest nine Planck sources are good HFP candidates. One of the nine, J114553–695404, is contained in a sample of Planck point sources studied by Rocha et al. (in preparation). The source shows a factor of \sim 2 variability in the Planck data and is probably a blazar.

The general lack of non-blazar PS sources in the Planck ERCSC is puzzling given their presence in the AT20G survey. One explanation could be the much poorer sensitivity of Planck. The flux density limit at 20 GHz for the AT20G sample is 40 mJy (Murphy et al., 2010), while the flux density limit for the

ERCSC at 30 GHz is at least an order of magnitude higher (Planck Collaboration et al., 2011b). This would be consistent with the beamed emission from the blazars dominating over the unbeamed emission from the non-blazar PS sources. At this time it appears that study of the high frequency population of PS sources should focus on the AT20G sample.

7.1.3 Are CSS sources related to radio loud Narrow-Line Seyfert 1s?

The properties of Narrow Line Seyfert 1s (NLS1s) are reviewed by Komossa (2008) and D'Ammando (2019), and the latter has an emphasis on γ -ray emitting NLS1s. NLS1s have narrower Balmer lines (FWHM (H β) < 2000 km s⁻¹) than regular Sy 1s (e.g., Osterbrock and Pogge, 1985, 1987; Goodrich, 1989). Other emission line properties tend to include weak [OIII] $\lambda 5007/H\beta$ and strong Fe II/H β (e.g., Osterbrock and Pogge, 1985; Goodrich, 1989). NLS1s have less massive host galaxies (Krongold et al., 2001) and less massive black holes (e.g., Peterson, 2011; Mathur et al., 2012; Xu et al., 2012) than regular Sy 1s, but appear to be accreting near the Eddington limit (e.g., Boroson, 2002; Xu et al., 2012). About 4.5 - 7% of NLS1s are radio loud (Komossa et al., 2006; Singh and Chand, 2018). The radio properties of RL NLS1s have been compared to those of CSS radio sources (Oshlack et al., 2001; Komossa et al., 2006; Gallo et al., 2006; Yuan et al., 2008; Gu and Chen, 2010; Gu et al., 2015, 2016; Caccianiga et al., 2014, 2017; Schulz et al., 2016; Berton et al., 2017; Singh and Chand, 2018; Yao and Komossa, 2020). It has also been suggested that the NLS1s are young AGN (e.g., Grupe, 2000; Mathur, 2000) similar to a subset of PS and CSS sources.

Caccianiga et al. (2014); Berton et al. (2016); Liao and Gu (2020) consider the possibility that the CSS/HERGs are the parent population for the beamed (flat spectrum) RL NLS1s. As Berton et al. (2016) note, the two populations are nominally hosted by different galaxies. CSSs are predominantly in elliptical galaxy hosts though there are a few examples of hosts with a disk component (Sect. 5) and NLS1s are found in disk galaxies, sometimes with a pseudobulge (e.g., Crenshaw et al., 2003; Mathur et al., 2012; Kotilainen et al., 2016; Olguín-Iglesias et al., 2017). However, Berton et al. (2016) note that the host galaxies of the flat spectrum RL NLS1s are not yet well studied. D'Ammando (2019) note that the hosts have been determined for four γ -ray emitting NLS1s and two are hosted by elliptical galaxies. If the flat spectrum RL NLS1s turn out to be in elliptical galaxies, similar to the CSS, this would support the hypothesis that the CSS/HERGs are the parent population of the flat spectrum RL NLS1s. It would also suggest that the flat spectrum RL and RQ NLS1s are different populations of objects. Based on radio and X-ray properties, D'Ammando (2019) argues against a relationship between CSS and the γ -ray emitting NLS1s. Thus, the issue of whether the CSS sources are the parent population of the flat spectrum RL NLS1s is still an interesting open question. Nevertheless, the similarity in the radio properties between CSS sources and RL NLS1s makes it clear that compact radio sources can form in a variety of AGN.

7.2 What are the PS and CSS sources?

Here we provide updates on the main hypotheses for PS and CSS sources since the review of O'Dea (1998).

7.2.1 Transient or episodic sources

A strong motivation for considering short lifetimes for PS sources is the excess number of sources with sizes below 1 kpc over an extrapolation from large sizes (O'Dea and Baum, 1997; Reynolds and Begelman, 1997; Alexander, 2000; Marecki et al., 2003b; Kunert-Bajraszewska et al., 2010). In addition, there is recent evidence that some compact sources are turning off and fading (e.g., Kunert-Bajraszewska et al., 2005; Giroletti et al., 2005; Giroletti, 2008; Orienti et al., 2010b; Callingham et al., 2015). Kunert-Bajraszewska et al. (2010) suggest that many of the low luminosity CSS sources could be short-lived objects. A possible link between short-lived CSS sources and changing look AGN has been suggested by Wołowska et al. (2017). The double-double sources also provide strong support to the hypothesis of episodic activity in radio sources (Sect. 3.3). In addition, the existence of AGN with X-ray nuclei but no extended emission-line nebulae argues for AGN time scales of $\sim 10^5$ yr (Schawinski et al., 2015).

Radiation pressure instabilities in accretion disks may provide the timescales needed for intermittent activity (Czerny et al., 2009). In this scenario, activity lasts $\sim 10^3-10^4$ yr and episodes are separated by $\sim 10^4-10^6$ yr (Czerny et al., 2009; Wu, 2009a; Siemiginowska et al., 2010). Jet disruption is another way of producing short-lived radio sources (e.g., De Young, 1991; Higgins et al., 1999; Wang et al., 2000; Wiita, 2004; Sutherland and Bicknell, 2007; Wagner and Bicknell, 2011; Mukherjee et al., 2016, 2017, 2018b,a; Bicknell et al., 2018; Aditya, 2019). If the jets in some sources disrupt (and the source fades quickly) before the radio source propagates out of the core, the distribution of number vs source size (O'Dea and Baum, 1997) can be reproduced (Alexander, 2000; Kaiser and Best, 2007; Kunert-Bajraszewska et al., 2010; An and Baan, 2012).

7.2.2 Frustrated sources

One of the possible scenarios for the PS and CSS radio sources is that they are confined to their host galaxies through interaction with dense clouds in the host galaxy ISM (van Breugel, 1984; Wilkinson et al., 1984; O'Dea et al., 1991). This has been called the frustration scenario and is motivated by the observation that PS and CSS radio sources are much more asymmetric than the large-scale radio sources, suggesting interaction with a dense medium (Sect. 3.1, Sect. 3.4.2). As discussed in Sect. 6.1.1, Sobolewska et al. (2019) show that the 5 CSOs with very large X-ray derived $N_{\rm H}$ have a smaller radio size for a given 5 GHz luminosity than the less absorbed sources and suggest that the small, heavily absorbed sources are confined by a dense environment. Confinement

of radio sources on small scales could also help to explain the excess of sources at small sizes.

Table 5 presents the available molecular gas masses. The objects in the Table are not a complete sample. However, there is a broad range of masses from 10^7 to $10^{11} M_{\odot}$. The total gas mass required to confine a radio source is still uncertain and depends on the mass and distribution of the individual dense clouds, though rough estimates are that masses of at least 10^9 to $10^{10} M_{\odot}$ would be required (De Young, 1993; Carvalho, 1994, 1998; O'Dea, 1998). These gas masses are present in the PS and CSS sources, so it remains possible that some fraction of the sources are confined to the ISM of their host galaxies by interaction of the radio source with dense gas.

Simulations show that interaction of jets with large dense clouds can disrupt the jets and/or impede their progress (e.g., De Young, 1991; Higgins et al., 1999; Wang et al., 2000; Wiita, 2004). In simulations of jets propagating through a clumpy ISM, the weaker jets can be confined for a long time, while the more powerful jets can break through (or around) the clouds (e.g., Bicknell and Sutherland, 2006; Wagner and Bicknell, 2011; Mukherjee et al., 2016, 2017, 2018b,a; Bicknell et al., 2018). These simulations suggest that in sufficiently dense environments with mean densities of $\sim 300~{\rm cm}^{-3}$, jets can remain frustrated for 1 to 2 Myr. It is also possible that the sources which show intense star formation are in dense environments and might be frustrated Sect. 7.2.3. Note that some GPS sources show gaseous outflows suggesting that the jet-cloud interactions are removing gas from the galactic nucleus (Sect. 7.4).

The proper motions of CSOs (Table 3) are plotted against the molecular gas masses (Table 5) in Fig. 16 for sources in common. There is a trend for the CSOs to have lower proper motions in galaxies with larger molecular gas mass. The numbers are still small, so this should be confirmed with a larger sample. If confirmed, this would be consistent with the frustration scenario, i.e., the interaction with ambient gas clouds slows the propagation of compact radio sources.

7.2.3 Imposters: Star-forming, radio-enhanced, compact sources?

Gopal-Krishna and Wiita (1991) suggest that intrinsically weak radio sources propagating through a dense ISM (possibly from a merger) will have their radio luminosity enhanced. O'Dea (1998) noted that PS and CSS sources which are interacting with dense gas from a merger should also have significant star formation. This could result in a population of intrinsically weak, but radio-enhanced, compact radio sources in hosts which are forming stars.

Morganti et al. (2011); Tadhunter et al. (2011); Dicken et al. (2012) have noted the evidence for enhanced star formation in compact radio sources (see discussion in Sect. 4, and O'Dea (2016)) and suggested that this scenario is indeed occurring. They suggest that the enhanced radio emission lifts the compact sources above the sample flux density limits, so that compact radio sources in star forming galaxies are over-represented in radio selected samples.

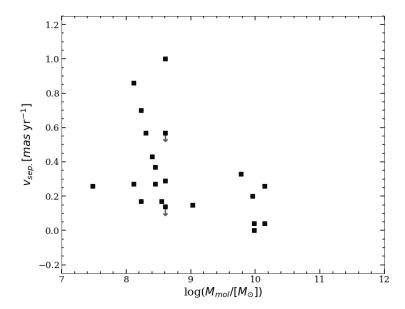


Fig. 16 Proper motions of CSOs (Table 3) are plotted against the molecular gas masses (Table 5) for sources in common. For sources with multiple measurements of proper motion, all measurements are plotted. The CSOs tend to have higher proper motions in hosts with less molecular gas.

Here we call these sources imposters. The radio enhancement is qualitatively consistent with the excess of compact radio sources compared to an extrapolation of the number vs size relation from the extended radio galaxies (O'Dea and Baum, 1997). Thus, the imposter scenario competes with the transient and frustrated source scenarios to explain the excess of compact sources. If the radio-enhanced sources are really intrinsically weaker AGN, then ratios of AGN bolometric luminosity to radio luminosity (for HERGs) should reveal this. Kunert-Bajraszewska et al. (2014) show that the compact and large HERGs lie on the same correlation of X-ray luminosity with radio power. And a similar correlation is found for the compact and large LERGs. Thus, so far there is no evidence for enhancement of radio luminosity relative to AGN bolometric luminosity (as probed by X-ray emission). One caveat to this argument is that in sources interacting strongly with their environments, it is possible that the X-ray emission will also be enhanced (Sect. 6.1.2). If the contribution to the X-ray emission is significant, the X-ray emission is no longer a reliable proxy for the AGN luminosity.

As discussed in Sect. 5.7, the black hole fundamental plane plots nuclear radio power against a combination of nuclear X-ray luminosity and black hole mass. Wójtowicz et al. (2020) find that some CSOs have higher radio power

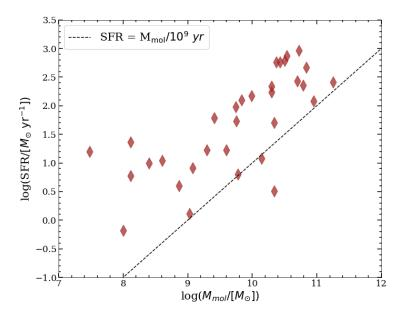


Fig. 17 SFR from Table 4 is shown against the mass of molecular gas from Table 5. If there are more than one estimate for a given source, the estimates were averaged. The SFR lie above a line which assumes a gas depletion time scale of 10^9 yr. This indicates that the PS and CSS sources have enhanced star formation.

than expected on the black hole fundamental plane, which they attribute to a higher radiative efficiency in the radio.

Note that optical emission line (e.g., [OIII]) luminosity is problematic as a proxy for AGN luminosity if there is a significant contribution from jet-induced shocks (e.g., Labiano et al., 2005; Labiano, 2009; Holt et al., 2009; Shih et al., 2013; Reynaldi and Feinstein, 2013, 2016) or if the emission line luminosity increases with time (e.g., Vink et al., 2006).

We show SFR vs mass of molecular gas in Fig. 17. Above a mass of $10^9\,M_\odot$, the SFR is correlated with the total gas mass as is generally found in star forming galaxies (e.g., Young et al., 1986; Gao and Solomon, 2004; O'Dea et al., 2008). The gas depletion time scale is defined to be the total molecular gas mass divided by the SFR. The dotted line shows the SFR expected with a gas depletion time scale of 10^9 yr which is typical in a broad range of star forming galaxies (e.g., Young et al., 1986; Rownd and Young, 1999; O'Dea et al., 2008). The SFR of the PS and CSS sources lie above the line, showing that they have a relatively high star formation efficiency. Thus, star formation is enhanced in PS and CSS sources. We suggest that this is due to star formation triggered via interaction with the radio source.

7.2.4 Young, dynamic sources

It is clear that while some PS and CSS sources may be transient (Sect. 7.2.1), radio-enhanced (Sect. 7.2.3), or frustrated (Sect. 7.2.2), there is very likely a subset which are young, dynamic sources which will grow to become large radio galaxies and quasars. We list the arguments here. (1) The PS and CSS sources live in the same host galaxies as the large sources (Sect. 5). (2) There is continuity in the properties from small to large sources (e.g., Sect. 6.1.4). (3) There is evidence so far for a dense clumpy ISM which could confine the radio source in just a subset of PS and CSS (Sect. 5). (4) Models for compact radio source evolution provide a plausible scenario for growth of CSOs to become CSS and large scale FRIs and FRIIs and are consistent with currently available data (Sect. 7.3). (5) Observed proper motions of CSOs show the radio sources are indeed propagating through the host ISM (even in galaxies with substantial masses of molecular gas, Figure 16) and give plausible dynamical ages which are consistent with spectral aging (Sect. 3.4). Below we discuss analytical models for propagation of young radio sources.

7.3 Analytical models for compact source propagation

Numerical simulations of compact radio sources are discussed in Sect. 7.4. Here we discuss analytical models because they can make predictions for radio source populations which can be compared with observations. Assuming that dense clouds in the ISM do not confine the radio source (Sect. 5,7.2.2), and the jet remains stable and long-lived, the compact radio sources will propagate through their host galaxies (e.g., Begelman, 1999).

Self-similar analytical dynamical models with a constant density 1 kpc core and a power-law decline in density on larger scales results in radio power that increases with distance from the nucleus out to 1 kpc and then declines on larger scales (Snellen et al., 2000; Alexander, 2000). Note, that while the assumption of self-similar behavior is very useful, numerical simulations suggest significant departures from self-similarity (Carvalho and O'Dea, 2002; Cielo et al., 2014). Improvements to the models include adding a non-self-similar phase to the evolution on the smallest scales (Alexander, 2006), and adding radiative losses (Carvalho and O'Dea, 2003; Maciel and Alexander, 2014). Synchrotron losses are significant in compact sources and modify the evolution of the source (Maciel and Alexander, 2014). Since the observational properties of hot spots are relatively easy to measure, some analytical models focus on the evolution of the hot spots (Perucho and Martí, 2002; Kawakatu and Kino, 2006; Kawakatu et al., 2008). An alternate set of models has been used to estimate the GPS luminosity function and the contribution of HFPs to high frequency surveys (De Zotti et al., 2000; Tinti and de Zotti, 2006). In these models, the radio power always decreases with increasing size.

An and Baan (2012) compare the results of the dynamical models with data on a sample of 24 CSOs (radio power, separation between two hotspots,

hotspot separation velocity, and kinematic age of the source). Overall, the properties of CSOs are consistent with the models. However, the excess of small (< 100 pc) and young (< 1000 yr) CSOs is consistent with some sources not surviving to become large sources.

Stawarz et al. (2008) include radiative processes in their dynamical model in order to calculate the broad-band SED of the sources. Ostorero et al. (2010) fit these models to eleven GPS sources with CSO radio sources. The fits are consistent with the X-rays being produced by IC scattering of ambient photons by the relativistic electrons in the radio lobes. Ostorero et al. (2010) note that correlation between X-ray absorbing column $N_{\rm H}$ and 21 cm absorption column density $N_{\rm HI}$ (Sect. 5) is consistent with the X-ray emission originating in the radio lobes.

7.4 The role of compact radio sources in AGN feedback

We note that AGN feedback is a broad topic, including different mechanisms (accretion disk-driven and radio jet-driven) and a wide range of size scales from galaxies to clusters of galaxies (e.g., Croton et al., 2006; McNamara and Nulsen, 2007, 2012; Fabian, 2012; Somerville and Davé, 2015; Harrison et al., 2018). Here we focus on feedback to the host galaxy ISM from compact radio sources (CSO and CSS) (and see also Tadhunter (2016b,a); Wagner et al. (2016); Hardcastle and Croston (2020)).

We have previously discussed several lines of evidence for AGN feedback in CSO and CSS sources: (1) The asymmetric radio morphology of CSO and CSS sources suggests interaction with dense clouds in the host galaxy ISM (Sect. 3.1, Sect. 3.4.2). (2) The kinematics (and to some extent the excitation) of aligned optical emission line gas is consistent with shocks being driven by the radio source (Sect. 5.5.2). (3) X-ray observations of shocked and aligned hot gas are consistent with shocks driven by the radio source (Sect. 6.1.2). (4) There is evidence for jet-induced star formation (Sect. 5.6).

There are clear examples of multi-phase outflows in CSO and CSS radio sources. The outflows are seen in neutral atomic hydrogen (e.g., Morganti et al., 2003, 2005a,b, 2013; Holt et al., 2008; Geréb et al., 2015; Maccagni et al., 2017; Morganti and Oosterloo, 2018) (and possibly also (Labiano et al., 2006; Vermeulen et al., 2006)). About 23% of compact sources with an HI absorption detection show a blue wing in the HI with an outflow velocity > 100 km s⁻¹ (Maccagni et al., 2017; Morganti and Oosterloo, 2018).

In addition, outflows are seen in warm ionized gas seen in optical (mainly [OIII] $\lambda5007$) emission lines (e.g., Tadhunter et al., 2001; Holt et al., 2003b, 2006, 2008; Buchanan et al., 2006; Nesvadba et al., 2007; Roche et al., 2016; Santoro et al., 2018; Liao and Gu, 2020), and IR lines (Dasyra and Combes, 2011; Guillard et al., 2012), and in absorption in the UV (De Breuck et al., 2000; Gupta et al., 2005). About 22% of a set of 68 PS and CSS sources with SDSS data show blue shifted wings in the [OIII] line (Liao and Gu, 2020). Holt et al. (2008) detect warm outflows in 10 (71%) of a sample of 14 compact

sources, and 8 of the 10 detections are in sources with outflows in H_I. Thus, the detection rate for warm outflows seems to be higher in objects with outflows in H_I.

The HI outflows are seen in galaxies with a rich supply of gas which can be transported outwards (Morganti et al., 2005b; Guillard et al., 2012; Maccagni et al., 2017). Outflows of molecular gas are rare so far in compact radio sources, but are detected in PKS 1549–79 (Guillard et al., 2012; Oosterloo et al., 2019) and in the ULIRG 4C 12.50 (PKS 1345+12) (Dasyra and Combes, 2011, 2012; Dasyra et al., 2014; Guillard et al., 2012; Spoon et al., 2013; Fotopoulou et al., 2019). A significant fraction of the H₂ in the outflow in 4C 12.50 has been heated to a temperature of about 400 K (Dasyra et al., 2014). In other compact radio sources with HI outflows, the near-IR H₂ lines do not display the same kinematics as the out-flowing HI and warm gas (Guillard et al., 2012). However, the symmetric line width and excitation diagrams of the H₂ lines suggest that the radio source is shocking the molecular gas instead of entraining it in an outflow (Ogle et al., 2010; Guillard et al., 2012).

There is evidence that these outflows are driven by the radio source rather than by radiation pressure. In CSS sources, the close spatial relationship between the [OIII] $\lambda5007$ emission and the radio source (alignment effect, Section 5.5.2) suggests that the radio source is driving the outflow. In some sources the out-flowing emission line gas is seen on scales which are too small to be driven by a kpc scale starburst wind (Batcheldor et al., 2007; Santoro et al., 2018). In 4C 12.50, a radio component (hotspot?) 100 pc from the nucleus appears to be pushing an HI cloud with a blue-shifted velocity of 1000 km s⁻¹ providing the direct link between the radio jet and the outflow (Morganti et al., 2013). In addition, the high velocity [OIII] $\lambda5007$ gas in 3C48 is associated with the base of the radio jet (Stockton et al., 2007; Shih and Stockton, 2014).

Best et al. (2000) showed that smaller radio sources had emission line nebulae with lower ionization, higher luminosity, and broader line widths than in larger radio sources, consistent with shocks driven by the radio source in the smaller sources. These results are confirmed by subsequent studies (De Breuck et al., 2000; Moy and Rocca-Volmerange, 2002; Inskip et al., 2002), though Moy and Rocca-Volmerange (2002) suggest that the emission line region in the very smallest sources (< 2 kpc) are dominated by AGN photoionization because the size of the region shocked by the radio source is still very small. Note that Best et al. (2000) defined small to be < 125 (< 90, correcting for cosmology) kpc, suggesting that the importance of shocks (and thus radio mode feedback) is not limited to the scale of CSS sources (< 20 kpc) and/or that the effects of feedback continue even after the radio source has propagated beyond the host galaxy. If feedback remains active while the radio source propagates for an additional 35 kpc beyond the CSS phase at a lobe advance speed of 10^4 km s⁻¹ (e.g., O'Dea et al., 2002), the additional time corresponds to $\sim 3 \times 10^6$ yr.

The observed correlations between Eddington ratio or AGN bolometric luminosity and outflow properties such as outflow velocity or kinetic power in large samples of AGN (e.g., Greene and Ho, 2005; Woo et al., 2016; Fiore et al., 2017; Rakshit and Woo, 2018) support the hypothesis that the outflows

are driven by radiation pressure. There is also a correlation between AGN bolometric luminosity and radio power (e.g., de Bruyn and Wilson, 1978; Baum and Heckman, 1989; Xu et al., 1999). Thus, we might expect to see a correlation of outflow properties and radio power. However, the relationship with the radio source appears to be complicated (Mullaney et al. (2013) and references therein).

Mullaney et al. (2013) studied [OIII] λ 5007 line profiles using SDSS spectra of a sample of 24,264 optically selected AGN. They find the broadest [OIII] λ 5007 line widths (i.e., fastest outflows) in the subset of AGN with compact (< 2 arcsec in size) radio sources with moderate radio power $P_{1.4 \mathrm{GHz}} \sim 10^{23} - 10^{25}$ W $\mathrm{Hz^{-1}}$ (Mullaney et al., 2013). Using FWHM > 500 km/s as the criterion, 25% of all AGN and 50% of sources with radio power $P_{1.4} > 10^{23}~\rm W~Hz^{-1}$ have broadened [OIII] lines indicative of outflow. However, see Woo et al. (2016) and Rakshit and Woo (2018) for differing conclusions regarding the influence of radio power. The detection of ionized outflows in a large sample of compact radio sources by Mullaney et al. (2013) supports earlier work that showed that compact radio sources display more extreme [OIII] $\lambda 5007$ kinematics than larger radio sources (Gelderman and Whittle, 1994; Best et al., 2000; Holt et al., 2008) and indicates that compact radio sources do indeed drive outflows. Singha et al. (in preparation) point out that the preference for outflows in compact radio sources found by Mullaney et al. (2013) might be because at least 80% of the radio sources in the low redshift (z < 0.4) sample considered by Mullaney et al. (2013) are compact (see also Sect. 3.1.1). At this point the statistics of outflows in compact vs. extended radio sources needs to be clarified.

The mass outflow rates and kinetic powers of the *ionized* outflows are generally too low to have a significant effect on star formation in their host galaxies (e.g., Holt et al., 2006, 2011; Tadhunter, 2007; Santoro et al., 2018, 2020) or even to shock-ionize the optical emission lines (Santoro et al., 2020). However, the other components of the multiphase outflows can carry more mass and dominate the kinetic power of the outflows (e.g., Holt et al., 2011; Hardcastle et al., 2012; Dasyra et al., 2014). The outflows of molecular gas tend to be more massive and carry more kinetic power, but do not seem to extend beyond the inner kpc of the host galaxy (e.g., Dasyra et al., 2014; Morganti et al., 2020). We note that the sources discussed here are at relatively low redshift (z < 0.5). The outflow energetics scale with AGN luminosity (e.g., Mullaney et al., 2013; Woo et al., 2016). We speculate that during Cosmic Noon, when AGN luminosity is much higher, the outflows would be capable of significantly suppressing star formation. However, confirmation requires observations of compact radio sources at high redshift (e.g., Nesvadba et al., 2007; Kim et al., 2013; Lonsdale et al., 2015; Patil et al., 2020).

Arguments based on numerical simulations and estimates of jet power also suggest that compact radio sources can drive outflows out to size scales of several times the radio source size (Zovaro et al., 2019b,a). Numerical simulations which include radiative cooling of the gas show that ISM clouds which are shocked by the jet can collapse and cool and may form stars, consistent with

the positive feedback required for jet-induced star formation (e.g., Mellema et al., 2002; Fragile et al., 2004, 2017; Antonuccio-Delogu and Silk, 2008; Gaibler et al., 2012). Nevertheless, AGN feedback must be globally negative in order to suppress star formation in galaxies. Numerical simulations have been used to explore the interaction of jets in compact radio sources with the ISM and the impact on both the jet and the ISM (e.g., Steffen et al., 1997; Bicknell and Sutherland, 2006; Sutherland and Bicknell, 2007; Wagner and Bicknell, 2011; Cielo et al., 2014; Bicknell et al., 2018). When the jet interacts with a distribution of small, dense clouds, the jet tends to split and follow the path of least resistance between the clouds producing a diffuse, spherical radio source (Sutherland and Bicknell, 2007; Wagner and Bicknell, 2011; Bicknell et al., 2018). If the jets are sufficiently powerful, they are able to accelerate and disperse clouds (Wagner and Bicknell, 2011; Cielo et al., 2014; Mukherjee et al., 2016, 2017, 2018b,a; Bicknell et al., 2018). Independent simulations find that a significant fraction of the jet kinetic energy and momentum are deposited in the galaxy ISM (Wagner and Bicknell, 2011; Cielo et al., 2014). In practice, the observations indicate much lower fractions for the outflows of warm gas (e.g., Holt et al., 2006, 2011; Tadhunter, 2007; Santoro et al., 2018). A higher fraction of the jet energy (more comparable to the simulations) is deposited in the ISM in the full multiphase outflows in three well-studied sources (Hardcastle et al., 2012; Dasyra et al., 2014; Oosterloo et al., 2019).

8 Future work

The motivation for studies of PS and CSS sources has been presented for ASKAP (Norris et al., 2011; Allison et al., 2016), LOFAR (Snellen et al., 2009; Shimwell et al., 2019), ngVLA (Patil et al., 2018), and SKA (Falcke et al., 2004b; Kapinska et al., 2015; Afonso et al., 2015). Norris et al. (2011) note that the EMU survey with ASKAP will detect millions of GPS and CSS sources down to very faint levels, allowing the creation of large, complete samples. Deep surveys with MeerKAT will also add to the samples of CSS/PS sources at faint flux density levels (Jonas and MeerKAT Team, 2016; Mauch et al., 2020). Allison et al. (2016) discuss systematic H_I absorption studies with ASKAP of PS/CSS sources which will probe the interaction of compact radio sources with their environments and the properties of HI outflows driven by the radio source. The HI observations will be extended with the more sensitive SKA (Morganti et al., 2015). Snellen et al. (2009) highlight 3 areas to be addressed with LOFAR: determining the origin of the spectral turnover (FFA/SSA), the search for extended emission from previous cycles of activity, and discovery of z > 6 GPS sources which are compact because of a dense environment (as suggested by Falcke et al. (2004b)). Shimwell et al. (2019) discuss the LOFAR detection of low luminosity peaked-spectrum sources which might be shortlived radio sources. Patil et al. (2018) discuss the potential contributions of the ngVLA to three areas: sub-arcsec resolution radio imaging, determining spectral ages, and constraining the spectral turnover. Kapinska et al. (2015)

highlight the ability of SKA to detect many radio sources (over a large range of redshift and luminosity) at all stages of the life cycle, allowing comprehensive statistical studies. Afonso et al. (2015) discuss the detection of powerful, young AGN at high redshift (the first generation of AGN) with SKA and the effects of inverse Compton scattering of the hot, bright CMB.

Here we list some interesting areas for future research.

- Origin of PS and CSS Sources In this review, we discuss four scenarios for the origin of the PS and CSS sources. It is possible that they each describe a subset of the population. We would like to know the relative contributions to the population, and if possible determine the origin of individual objects. It will be important to measure SFR and molecular gas mass in a large sample of objects. The ratio of AGN bolometric luminosity to radio luminosity is also an important diagnostic. The distribution of sizes and proper motions for a large sample of CSOs will help constrain radio source propagation models.
- Radio Sources Driving Shocks Deep Chandra and XMM-Newton observations of CSS sources to search for hot shocked gas will constrain the impact of the radio source on the host galaxy ISM.
- Jet Induced Star Formation High resolution UV imaging to search for jet-induced star formation should also be done.
- $-\gamma$ -rays There are confirmed γ -ray detections of several CSOs and CSS quasars at the present time. It is important to continue the search for γ -ray emission from PS and CSS sources.
- AGN Feedback Compact radio sources may contribute to AGN feedback by driving gaseous outflows. Given the high detection rate for HI absorption, this is a promising approach. Detections of HI in outflow by e.g., ASKAP, SKA, WSRT, uGMRT and MeerKAT should be followed up by VLBI HI absorption measurements to locate the components which are driving the outflow, and combined with VLBI measurements of proper motion of the radio components. This will provide a unique data set for advancing our understanding of the interaction of the radio sources with their environments.
- Numerical Simulations High resolution, 3-D numerical simulations may help to clarify the propagation of compact radio sources and their interaction with their environments.
- Mechanism for the Spectral Turnover Determinations of the radio spectrum at multiple wavelengths near the spectral peak will allow the nature of the spectral turnover to be determined (FFA vs. SSA) and its relationship to the environment of the radio source.
- Larger Samples There are currently many samples of PS and CSS sources selected in different ways. Current and future deep radio surveys over a broad range of wavelengths by, e.g., ASKAP, AT, uGMRT, LOFAR, SKA, (ng)VLA, WSRT and MeerKAT will allow construction of large, uniform samples of PS and CSS sources.

- Low-luminosity sources and formation of jets The lower end of the luminosity distribution of CSS and PS sources, including those classified as FR0s, overlaps with those of Seyfert galaxies. The radio structures of Seyfert galaxies also tend to be of sub-galactic dimensions. It would be important to clarify the precise properties of the central engine and its environment that give rise to a wide range of observed properties of these compact sources of varying luminosity and different host galaxies.

Acknowledgements We are very grateful to colleagues who provided thoughtful comments on the manuscript and/or figures for the review, especially T. An, G. Bicknell, J. Conway, W. Cotton, D. Dallacasa, C. Duggal, M. Giroletti, Y. Gordon, M. Kunert-Bajraszewska, A. Marecki, G. Migliori, R. Morganti, D. Mukherjee, P. Ogle, M. Orienti, T. Oosterloo, A. Polatidis and L. Stawarz. We thank our referee, C. Tadhunter, for helpful comments which improved the paper. CO is grateful to M. Singha for help with some of the figures and to R. Antonucci for interesting discussions. CO is grateful to the Natural Sciences and Engineering Research Council (NSERC) of Canada for support. This research has made use of NASA/s Astrophysics Data System Bibliographic Services. This research has made use of the NASA/IPAC Extragalactic Database (NED), which is funded by the National Aeronautics and Space Administration and operated by the California Institute of Technology.

References

- Aditya JNHS (2019) uGMRT detections of H I 21-cm absorption associated with intermediate redshift galaxies. MNRAS482(4):5597–5605. https://doi.org/10.1093/mnras/sty3062. arXiv:1811.03048 [astro-ph.GA]
- Afonso J, Casanellas J, Prandoni I, Jarvis M, Lorenzoni S, Magliocchetti M, Seymour N (2015) Identifying the first generation of radio powerful AGN in the Universe with the SKA. In: Advancing Astrophysics with the Square Kilometre Array (AASKA14). p 71. arXiv:1412.6040 [astro-ph.GA]
- Akujor CE, Leahy JP, Garrington ST, Sanghera H, Spencer RE, Schilizzi RT (1996) A two-sided jet structure in the 'steep-spectrum core' of 3C293. MNRAS278:1–5. https://doi.org/10.1093/mnras/278.1.1
- Alexander P (2000) Evolutionary models for radio sources from compact sources to classical doubles. MNRAS319:8–16. https://doi.org/10.1046/j. 1365-8711.2000.03711.x
- Alexander P (2006) Models of young powerful radio sources. MNRAS368:1404–1410. https://doi.org/10.1111/j.1365-2966.2006.10225.x
- Aller M, Aller H, Hughes P (2017) The University of Michigan Centimeter-Band All Stokes Blazar Monitoring Program: Single-Dish Polarimetry as a Probe of Parsec-Scale Magnetic Fields. Galaxies 5(4):75. https://doi.org/10.3390/galaxies5040075. arXiv:1711.05763 [astro-ph.HE]
- Aller MF, Aller HD, Hughes PA, Plotkin RM (2002) Centimeter-band Variability in GPS Sources. In: Proceedings of the 6th EVN Symposium. p 131. arXiv:astro-ph/0210562 [astro-ph]
- Allison JR, Sadler EM, Moss VA, Whiting MT, Hunstead RW, Pracy MB, Curran SJ, Croom SM, Glowacki M, Morganti R, Shabala SS, Zwaan MA,

- Allen G, Amy SW, Axtens P, Ball L, Bannister KW, Barker S, Bell ME, Bock DCJ, Bolton R, Bowen M, Boyle B, Braun R, Broadhurst S, Brodrick D, Brothers M, Brown A, Bunton JD, Cantrall C, Chapman J, Cheng W, Chippendale AP, Chung Y, Cooray F, Cornwell T, DeBoer D, Diamond P, Edwards PG, Ekers R, Feain I, Ferris RH, Forsyth R, Gough R, Grancea A, Gupta N, Guzman JC, Hampson G, Harvey-Smith L, Haskins C, Hay S, Hayman DB, Heywood I, Hotan AW, Hoyle S, Humphreys B, Indermuehle BT, Jacka C, Jackson C, Jackson S, Jeganathan K, Johnston S, Joseph J, Kendall R, Kesteven M, Kiraly D, Koribalski BS, Leach M, Lenc E, Lensson E, Mackay S, Macleod A, Marquarding M, Marvil J, McClure-Griffiths N, McConnell D, Mirtschin P, Norris RP, Neuhold S, Ng A, O'Sullivan J, Pathikulangara J, Pearce S, Phillips C, Popping A, Qiao RY, Reynolds JE, Roberts P, Sault RJ, Schinckel A, Serra P, Shaw R, Shields M, Shimwell T, Storey M, Sweetnam T, Troup E, Turner B, Tuthill J, Tzioumis A, Voronkov MA, Westmeier T, Wilson CD (2015) Discovery of H I gas in a young radio galaxy at z = 0.44 using the Aus-//doi.org/10.1093/mnras/stv1532. arXiv:1503.01265
- Allison JR, Sadler EM, Moss VA, Harvey-Smith L, Heywood I, Indermuehle BT, McConnell D, Sault RJ, Whiting MT (2016) Tracing the neutral gas environments of young radio AGN with ASKAP. Astron Nachr 337:175. https://doi.org/10.1002/asna.201512288. arXiv:1511.03067
- Allison JR, Mahony EK, Moss VA, Sadler EM, Whiting MT, Allison RF, Bland-Hawthorn J, Curran SJ, Emonts BHC, Lagos CDP, Morganti R, Tremblay G, Zwaan M, Anderson CS, Bunton JD, Voronkov MA (2019) PKS B1740-517: an ALMA view of the cold gas feeding a distant interacting young radio galaxy. MNRAS482:2934-2949. https://doi.org/10.1093/mnras/sty2852. arXiv:1810.08507
- An T, Baan WA (2012) The Dynamic Evolution of Young Extragalactic Radio Sources. ApJ760:77. https://doi.org/10.1088/0004-637X/760/1/77. arXiv:1211.1760 [astro-ph.CO]
- An T, Hong XY, Hardcastle MJ, Worrall DM, Venturi T, Pearson TJ, Shen ZQ, Zhao W, Feng WX (2010) Kinematics of the parsec-scale radio jet in 3C 48. MNRAS402:87–104. https://doi.org/10.1111/j.1365-2966.2009.15899.x. arXiv:0910.3782
- An T, Wu F, Yang J, Taylor GB, Hong X, Baan WA, Liu X, Wang M, Zhang H, Wang W, Chen X, Cui L, Hao L, Zhu X (2012) VLBI Observations of 10 Compact Symmetric Object Candidates: Expansion Velocities of Hot Spots. ApJS198:5. https://doi.org/10.1088/0067-0049/198/1/5.arXiv:1111.3710 [astro-ph.CO]
- An T, Cui YZ, Baan WA, Wang WH, Mohan P (2016a) The Gamma-Ray-emitting Quasar 0202+149: A CSS Revisited. ApJ826:190. https://doi.org/10.3847/0004-637X/826/2/190. arXiv:1605.08488 [astro-ph.HE]
- An T, Cui YZ, Gabányi KÉ, Frey S, Baan WA, Zhao W (2016b) Radio properties of the γ -ray emitting CSO candidate 2234+282. Astron Nachr 337:65. https://doi.org/10.1002/asna.201512266. arXiv:1601.03859 [astro-ph.HE]

- An T, Lao BQ, Zhao W, Mohan P, Cheng XP, Cui YZ, Zhang ZL (2017) Parsec-scale jet properties of the gamma-ray quasar 3C 286. MNRAS466:952–959. https://doi.org/10.1093/mnras/stw2887.arXiv:1611.01234
- Anderson CS, Johnston HM, Hunstead RW (2013) Galactic interaction as the trigger for the young radio galaxy MRC B1221-423. MNRAS431(4):3269–3281. https://doi.org/10.1093/mnras/stt406. arXiv:1304.1293 [astro-ph.GA]
- Antonucci R (1993) Unified models for active galactic nuclei and quasars. ARA&A31:473–521. https://doi.org/10.1146/annurev.aa.31.090193.002353
- Antonucci R (2012) A panchromatic review of thermal and nonthermal active galactic nuclei. Astronomical and Astrophysical Transactions 27:557–602. arXiv:1210.2716 [astro-ph.CO]
- Antonucci RRJ (1984) Optical spectropolarimetry of radio galaxies. ApJ278:499–520. https://doi.org/10.1086/161816
- Antonuccio-Delogu V, Silk J (2008) Active galactic nuclei jet-induced feedback in galaxies I. Suppression of star formation. MNRAS389(4):1750–1762. https://doi.org/10.1111/j.1365-2966.2008.13663.x. arXiv:0806.4570 [astro-ph]
- Araya ED, Rodríguez C, Pihlström Y, Taylor GB, Tremblay S, Vermeulen RC (2010) VLBA Observations of H I in the Archetype Compact Symmetric Object B2352+495. AJ139:17-26. https://doi.org/10.1088/0004-6256/139/1/17. arXiv:0910.5035
- Artyukh VS, Chernikov PA, Tyul'Bashev SA (2008) Synchrotron self-absorption in the GPS radio galaxy B0108+388. A&A486:735-739. https://doi.org/10.1051/0004-6361:20079301
- Axon DJ, Capetti A, Fanti R, Morganti R, Robinson A, Spencer R (2000) The Morphology of the Emission-Line Region Of Compact Steep-Spectrum Radio Sources. AJ120:2284–2299. https://doi.org/10.1086/316838. astro-ph/0006355
- Baker JC, Hunstead RW, Athreya RM, Barthel PD, de Silva E, Lehnert MD, Saunders RDE (2002) Associated Absorption in Radio Quasars. I. C IV Absorption and the Growth of Radio Sources. ApJ568:592–609. https://doi.org/10.1086/339033. astro-ph/0112141
- Baldi RD, Capetti A (2009) Radio and spectroscopic properties of miniature radio galaxies: revealing the bulk of the radio-loud AGN population. A&A508:603–614. https://doi.org/10.1051/0004-6361/200913021. arXiv:0910.4261
- Baldi RD, Capetti A (2010) Spectro-photometric properties of the bulk of the radio-loud AGN population. A&A519:A48. https://doi.org/10.1051/0004-6361/201014446. arXiv:1005.3223 [astro-ph.CO]
- Baldi RD, Capetti A, Giovannini G (2015) Pilot study of the radio-emitting AGN population: the emerging new class of FR 0 radio-galaxies. A&A576:A38. https://doi.org/10.1051/0004-6361/201425426.arXiv:1502.00427
- Baldi RD, Capetti A, Massaro F (2018) FR0CAT: a FIRST catalog of FR 0

- radio galaxies. A&A609:A1. https://doi.org/10.1051/0004-6361/201731333. arXiv:1709.00015 [astro-ph.GA]
- Baldi RD, Capetti A, Giovannini G (2019a) High-resolution VLA observations of FR0 radio galaxies: the properties and nature of compact radio sources. MNRAS482(2):2294–2304. https://doi.org/10.1093/mnras/sty2703. arXiv:1810.01894 [astro-ph.GA]
- Baldi RD, Torresi E, Migliori G, Balmaverde B (2019b) The High Energy View of FR0 Radio Galaxies. Galaxies 7(3):76. https://doi.org/10.3390/galaxies7030076. arXiv:1909.04113 [astro-ph.HE]
- Balmaverde B, Capetti A, Grandi P, Torresi E, Chiaberge M, Rodriguez Zaurin J, Tremblay GR, Axon DJ, Baum SA, Giovannini G, Kharb P, Macchetto FD, O'Dea CP, Sparks W (2012) Extended soft X-ray emission in 3CR radio galaxies at z < 0.3: high excitation and broad line galaxies. A&A545:A143. https://doi.org/10.1051/0004-6361/201219561. arXiv:1208.6515 [astro-ph.CO]
- Bansal K, Taylor GB, Peck AB, Zavala RT, Romani RW (2017) Constraining the Orbit of the Supermassive Black Hole Binary 0402+379. ApJ843(1):14. https://doi.org/10.3847/1538-4357/aa74e1. arXiv:1705.08556 [astro-ph.GA]
- Barthel PD (1989) Is Every Quasar Beamed? ApJ336:606. https://doi.org/10. 1086/167038
- Batcheldor D, Tadhunter C, Holt J, Morganti R, O'Dea CP, Axon DJ, Koekemoer A (2007) Dominant Nuclear Outflow Driving Mechanisms in Powerful Radio Galaxies. ApJ661:70–77. https://doi.org/10.1086/515391. astro-ph/0702498
- Baum SA, Heckman T (1989) Extended Optical Line Emitting Gas in Powerful Radio Galaxies: What is the Radio Emission-Line Connection? ApJ336:702. https://doi.org/10.1086/167044
- Baum SA, O'Dea CP, Murphy DW, de Bruyn AG (1990) 0108 + 388 A compact double source with surprising properties. A&A232:19–26
- Baum SA, Zirbel EL, O'Dea CP (1995) Toward Understanding the Fanaroff-Riley Dichotomy in Radio Source Morphology and Power. ApJ451:88. https://doi.org/10.1086/176202
- Begelman MC (1999) Young radio galaxies and their environments. In: Röttgering HJA, Best PN, Lehnert MD (eds) The Most Distant Radio Galaxies. p 173
- Begelman MC, Cioffi DF (1989) Overpressured Cocoons in Extragalactic Radio Sources. ApJ345:L21. https://doi.org/10.1086/185542
- Berton M, Caccianiga A, Foschini L, Peterson BM, Mathur S, Terreran G, Ciroi S, Congiu E, Cracco V, Frezzato M, La Mura G, Rafanelli P (2016) Compact steep-spectrum sources as the parent population of flat-spectrum radio-loud narrow-line Seyfert 1 galaxies. A&A591:A98. https://doi.org/10.1051/0004-6361/201628171. arXiv:1601.06165
- Berton M, Foschini L, Caccianiga A, Ciroi S, Congiu E, Cracco V, Frezzato M, La Mura G, Rafanelli P (2017) An orientation-based unification of young jetted active galactic nuclei: the case of 3C 286. Frontiers in As-

- tronomy and Space Sciences 4:8. $https://doi.org/10.3389/fspas.2017.00008. \\ arXiv:1705.07905$
- Best PN (2009) Radio source populations: Results from SDSS. Astron Nachr 330(2):184–189. https://doi.org/10.1002/asna.200811152
- Best PN, Heckman TM (2012) On the fundamental dichotomy in the local radio-AGN population: accretion, evolution and host galaxy properties. MNRAS421:1569–1582. https://doi.org/10.1111/j.1365-2966.2012.20414.x. arXiv:1201.2397
- Best PN, Röttgering HJA, Longair MS (2000) Ionization, shocks and evolution of the emission-line gas of distant 3CR radio galaxies. MNRAS311(1):23–36. https://doi.org/10.1046/j.1365-8711.2000.03028.x. arXiv:astro-ph/9908211 [astro-ph]
- Best PN, Kauffmann G, Heckman TM, Brinchmann J, Charlot S, Ivezić Ž, White SDM (2005) The host galaxies of radio-loud active galactic nuclei: mass dependences, gas cooling and active galactic nuclei feedback. MNRAS362(1):25–40. https://doi.org/10.1111/j.1365-2966.2005.09192.x. arXiv:astro-ph/0506269 [astro-ph]
- Beuchert T, Rodríguez-Ardila A, Moss VA, Schulz R, Kadler M, Wilms J, Angioni R, Callingham JR, Gräfe C, Krauß F, Kreikenbohm A, Langejahn M, Leiter K, Maccagni FM, Müller C, Ojha R, Ros E, Tingay SJ (2018) Extended X-ray emission in PKS 1718-649. A&A612:L4. https://doi.org/10.1051/0004-6361/201833064. arXiv:1804.04188 [astro-ph.HE]
- Bicknell GV, Sutherland RS (2006) Evolutionary models of powerful radio galaxies. Astron Nachr 327:235–240. https://doi.org/10.1002/asna. 200510514
- Bicknell GV, Dopita MA, O'Dea CP (1997) Unification of the Radio and Optical Properties of Gigahertz Peak Spectrum and Compact Steep-Spectrum Radio Sources. ApJ485:112–124. https://doi.org/10.1086/304400
- Bicknell GV, Saxton CJ, Sutherland RS (2003) GPS and CSS Sources Theory and Modelling. PASA20:102–109. https://doi.org/10.1071/AS02042
- Bicknell GV, Mukherjee D, Wagner AY, Sutherland RS, Nesvadba NPH (2018) Relativistic jet feedback II. Relationship to gigahertz peak spectrum and compact steep spectrum radio galaxies. MNRAS475:3493–3501. https://doi.org/10.1093/mnras/sty070. arXiv:1801.06518
- Blaes O (2007) Accretion Disks in AGNs. In: Ho LC, Wang JW (eds) The Central Engine of Active Galactic Nuclei. ASP Conference Series, vol 373. Astronomical Society of the Pacific, p 75
- Bock DCJ, Large MI, Sadler EM (1999) SUMSS: A Wide-Field Radio Imaging Survey of the Southern Sky. I. Science Goals, Survey Design, and Instrumentation. AJ117:1578–1593. https://doi.org/10.1086/300786. astro-ph/9812083
- Bolton RC, Chandler CJ, Cotter G, Pearson TJ, Pooley GG, Readhead ACS, Riley JM, Waldram EM (2006) 5-GHz MERLIN and VLBA observations of compact 9C sources. MNRAS367(1):323–330. https://doi.org/10.1111/j.1365-2966.2005.09952.x
- Bondi M, Marchã MJM, Polatidis A, Dallacasa D, Stanghellini C, Antón S

- (2004) VLBA polarization observations of BL Lac objects and passive elliptical galaxies. MNRAS352(1):112–124. https://doi.org/10.1111/j.1365-2966. 2004.07903.x
- Boroson TA (2002) Black Hole Mass and Eddington Ratio as Drivers for the Observable Properties of Radio-loud and Radio-quiet QSOs. ApJ565(1):78–85. https://doi.org/10.1086/324486. arXiv:astro-ph/0109317 [astro-ph]
- Brandl BR, Bernard-Salas J, Spoon HWW, Devost D, Sloan GC, Guilles S, Wu Y, Houck JR, Weedman DW, Armus L, Appleton PN, Soifer BT, Charmandaris V, Hao L, Higdon JA, Marshall SJ, Herter TL (2006) The Mid-Infrared Properties of Starburst Galaxies from Spitzer-IRS Spectroscopy. ApJ653(2):1129–1144. https://doi.org/10.1086/508849.arXiv:astro-ph/0609024 [astro-ph]
- Bridle AH, Fomalont EB, Cornwell TJ (1981) The large and small-scale structure of 3C 293. AJ86:1294–1305. https://doi.org/10.1086/113010
- Brienza M, Morganti R, Murgia M, Vilchez N, Adebahr B, Carretti E, Concu R, Govoni F, Harwood J, Intema H, Loi F, Melis A, Paladino R, Poppi S, Shulevski A, Vacca V, Valente G (2018) Duty cycle of the radio galaxy B2 0258+35. A&A618:A45. https://doi.org/10.1051/0004-6361/201832846. arXiv:1807.07280
- Brienza M, Morganti R, Harwood J, Duchet T, Rajpurohit K, Shulevski A, Hardcastle MJ, Mahatma V, Godfrey LEH, Prandoni I, Shimwell TW, Intema H (2020) Radio spectral properties and jet duty cycle in the restarted radio galaxy 3C388. A&A638:A29. https://doi.org/10.1051/0004-6361/202037457. arXiv:2003.13476 [astro-ph.GA]
- Brodie JP, Bowyer S, McCarthy P (1985) A radio and optical study of a jet/cloud interaction in the galaxy cluster A 194. ApJ293:L59–L63. https://doi.org/10.1086/184491
- Brown MJI, Jannuzi BT, Floyd DJE, Mould JR (2011) The Ubiquitous Radio Continuum Emission from the Most Massive Early-type Galaxies. ApJ731(2):L41. https://doi.org/10.1088/2041-8205/731/2/L41. arXiv:1103.2828 [astro-ph.CO]
- Bruni G, Panessa F, Bassani L, Chiaraluce E, Kraus A, Dallacasa D, Bazzano A, Hernández-García L, Malizia A, Ubertini P, Ursini F, Venturi T (2019) A Discovery of Young Radio Sources in the Cores of Giant Radio Galaxies Selected at Hard X-Rays. ApJ875(2):88. https://doi.org/10.3847/1538-4357/ab1006. arXiv:1903.05922 [astro-ph.GA]
- Buchanan CL, McGregor PJ, Bicknell GV, Dopita MA (2006) Radio-Excess IRAS Galaxies. IV. Optical Spectroscopy. AJ132:27–49. https://doi.org/10.1086/504409. astro-ph/0604478
- Burn BJ (1966) On the depolarization of discrete radio sources by Faraday dispersion. MNRAS133:67. https://doi.org/10.1093/mnras/133.1.67
- Burns JO, Schwendeman E, White RA (1983) CD galaxy dynamics and an aged ridge (jet) in 3C 338. ApJ271:575–585. https://doi.org/10.1086/161224
- Buttiglione S, Capetti A, Celotti A, Axon DJ, Chiaberge M, Macchetto FD, Sparks WB (2010) An optical spectroscopic survey of the 3CR sample of radio galaxies with z < 0.3. II. Spectroscopic classes and ac-

- cretion modes in radio-loud AGN. A&A509:A6. https://doi.org/10.1051/0004-6361/200913290. arXiv:0911.0536
- Caccianiga A, Antón S, Ballo L, Dallacasa D, Della Ceca R, Fanali R, Foschini L, Hamilton T, Kraus A, Maccacaro T, Mack KH, Marchã MJ, Paulino-Afonso A, Sani E, Severgnini P (2014) SDSS J143244.91+301435.3: a link between radio-loud narrow-line Seyfert 1 galaxies and compact steep-spectrum radio sources? MNRAS441:172–186. https://doi.org/10.1093/mnras/stu508. arXiv:1403.3229
- Caccianiga A, Dallacasa D, Antón S, Ballo L, Berton M, Mack KH, Paulino-Afonso A (2017) SDSSJ143244.91+301435.3 at VLBI: a compact radio galaxy in a narrow-line Seyfert 1. MNRAS464:1474–1480. https://doi.org/10.1093/mnras/stw2471. arXiv:1609.09501 [astro-ph.HE]
- Callingham JR, Gaensler BM, Ekers RD, Tingay SJ, Wayth RB, Morgan J, Bernardi G, Bell ME, Bhat R, Bowman JD, Briggs F, Cappallo RJ, Deshpande AA, Ewall-Wice A, Feng L, Greenhill LJ, Hazelton BJ, Hindson L, Hurley-Walker N, Jacobs DC, Johnston-Hollitt M, Kaplan DL, Kudrayvtseva N, Lenc E, Lonsdale CJ, McKinley B, McWhirter SR, Mitchell DA, Morales MF, Morgan E, Oberoi D, Offringa AR, Ord SM, Pindor B, Prabu T, Procopio P, Riding J, Srivani KS, Subrahmanyan R, Udaya Shankar N, Webster RL, Williams A, Williams CL (2015) Broadband Spectral Modeling of the Extreme Gigahertz-peaked Spectrum Radio Source PKS B0008-421. ApJ809:168. https://doi.org/10.1088/0004-637X/809/2/168. arXiv:1507.04819
- Callingham JR, Ekers RD, Gaensler BM, Line JLB, Hurley-Walker N, Sadler EM, Tingay SJ, Hancock PJ, Bell ME, Dwarakanath KS, For BQ, Franzen TMO, Hindson L, Johnston-Hollitt M, Kapińska AD, Lenc E, McKinley B, Morgan J, Offringa AR, Procopio P, Staveley-Smith L, Wayth RB, Wu C, Zheng Q (2017) Extragalactic Peaked-spectrum Radio Sources at Low Frequencies. ApJ836:174. https://doi.org/10.3847/1538-4357/836/2/174. arXiv:1701.02771
- Canalizo G, Stockton A (2000) 3C 48: Stellar Populations and the Kinematics of Stars and Gas in the Host Galaxy. ApJ528:201–218. https://doi.org/10.1086/308165. astro-ph/9908020
- Capetti A, Baldi RD, Brienza M, Morganti R, Giovannini G (2019) The low-frequency properties of FR 0 radio galaxies. A&A631:A176. https://doi.org/10.1051/0004-6361/201936254. arXiv:1910.06618 [astro-ph.GA]
- Capetti A, Massaro F, Baldi RD (2020) Large-scale environment of FR 0 radio galaxies. A&A633:A161. https://doi.org/10.1051/0004-6361/201935962
- Carvalho JC (1994) The age of GHz-peaked-spectrum radio sources. A & A 292:392–394
- Carvalho JC (1998) The evolution of GHz-peaked-spectrum radio sources. A&A329:845–852
- Carvalho JC, O'Dea CP (2002) Evolution of Global Properties of Powerful Radio Sources. I. Hydrodynamical Simulations in a Constant Density Atmosphere and Comparison with Self-similar Models. ApJS141:337–370. https://doi.org/10.1086/340645

- Carvalho JC, O'Dea CP (2003) Luminosity Evolution of Double Radio Sources. PASA20(1):98–101. https://doi.org/10.1071/AS03002
- Chandola Y, Saikia DJ (2017) H I absorption towards low-luminosity radio-loud active galactic nuclei of different accretion modes and WISE colours. MNRAS465(1):997–1007. https://doi.org/10.1093/mnras/stw2705.arXiv:1607.00841 [astro-ph.GA]
- Chandola Y, Saikia DJ, Gupta N (2010) HI gas in the rejuvenated radio galaxy 4C29.30. MNRAS403(1):269–273. https://doi.org/10.1111/j. 1365-2966.2009.15854.x. arXiv:0910.4427 [astro-ph.CO]
- Chandola Y, Sirothia SK, Saikia DJ (2011) H I absorption towards nearby compact radio sources. MNRAS418:1787–1795. https://doi.org/10.1111/j. 1365-2966.2011.19607.x. arXiv:1108.2242
- Chandola Y, Saikia DJ, Li D (2020) H i absorption towards radio Active Galactic Nuclei of different accretion modes. MNRAShttps://doi.org/10.1093/mnras/staa1029
- Chatzichristou ET, Vanderriest C, Jaffe W (1999) Spectroscopic mapping of the quasar 3C 48 at sub-arcsec resolution. A&A343:407–419
- Cheng XP, An T (2018) Parsec-scale Radio Structure of 14 Fanaroff-Riley Type 0 Radio Galaxies. ApJ863(2):155. https://doi.org/10.3847/1538-4357/aad22c. arXiv:1807.02505 [astro-ph.HE]
- Chiaberge M, Gilli R, Lotz JM, Norman C (2015) Radio Loud AGNs are Mergers. ApJ806(2):147. https://doi.org/10.1088/0004-637X/806/2/147. arXiv:1505.07419 [astro-ph.GA]
- Cielo S, Antonuccio-Delogu V, Macciò AV, Romeo AD, Silk J (2014) 3D simulations of the early stages of AGN jets: geometry, thermodynamics and backflow. MNRAS439:2903–2916. https://doi.org/10.1093/mnras/stu161. arXiv:1311.5562 [astro-ph.HE]
- Cimatti A, Dey A, van Breugel W, Hurt T, Antonucci R (1997) Keck Spectropolarimetry of Two High-z Radio Galaxies: Discerning the Components of the Alignment Effect. ApJ476(2):677–684. https://doi.org/10.1086/303660
- Collier JD, Banfield JK, Norris RP, Schnitzeler DHFM, Kimball AE, Filipović MD, Jarrett TH, Lonsdale CJ, Tothill NFH (2014) Infrared-faint radio sources: a new population of high-redshift radio galaxies. MNRAS439:545–565. https://doi.org/10.1093/mnras/stt2485. arXiv:1312.1002
- Condon JJ, Cotton WD, Greisen EW, Yin QF, Perley RA, Taylor GB, Broderick JJ (1998) The NRAO VLA Sky Survey. AJ115:1693–1716. https://doi.org/10.1086/300337
- Conway J (1997) HI absorption in CSO and SSC Radio Sources. In: Snellen IAG, Schilizzi RT, Roettgering HJA, Bremer MN (eds) Gigahertz Peaked Spectrum and Compact Steep Spectrum Radio Sources. pp 198–207
- Conway JE, Myers ST, Pearson TJ, Readhead ACS, Unwin SC, Xu W (1994) Evidence for two classes of parsec-scale radio double source in active galactic nuclei. ApJ425:568–581. https://doi.org/10.1086/174006
- Coppejans R, Cseh D, Williams WL, van Velzen S, Falcke H (2015) Megahertz peaked-spectrum sources in the Boötes field I a route towards finding high-redshift AGN. MNRAS450:1477–1485. https://doi.org/10.1093/

mnras/stv681

- Coppejans R, Cseh D, van Velzen S, Falcke H, Intema HT, Paragi Z, Müller C, Williams WL, Frey S, Gurvits LI, Körding EG (2016a) What are the megahertz peaked-spectrum sources? MNRAS459:2455–2471. https://doi.org/10.1093/mnras/stw799. arXiv:1604.00171
- Coppejans R, Frey S, Cseh D, Müller C, Paragi Z, Falcke H, Gabányi KÉ, Gurvits LI, An T, Titov O (2016b) On the nature of bright compact radio sources at z > 4.5. MNRAS463:3260-3275. https://doi.org/10.1093/mnras/stw2236. arXiv:1609.00575
- Cotton WD, Dallacasa D, Fanti C, Fanti R, Foley AR, Schilizzi RT, Spencer RE (1997a) Dual frequency VLBI polarimetric observations of 3C 138. A&A325:493–501
- Cotton WD, Fanti C, Fanti R, Dallacasa D, Foley AR, Schilizzi RT, Spencer RE (1997b) VLBA polarimetric observations of 3C 286 at 5 GHz. A&A325:479–483
- Cotton WD, Dallacasa D, Fanti C, Fanti R, Foley AR, Schilizzi RT, Spencer RE (2003a) The Faraday screen near the nucleus of the CSS quasar 3C 138. A&A406:43–50. https://doi.org/10.1051/0004-6361:20030523
- Cotton WD, Spencer RE, Saikia DJ, Garrington S (2003b) Faraday rotation in the CSS QSOs 3C 43 and 3C 454. A&A403:537–546. https://doi.org/10.1051/0004-6361:20030347
- Cotton WD, Kravchenko E, Kovalev YY, Fomalont E (2016) Search for extreme rotation measures in CSS sources. Astron Nachr 337(1-2):87. https://doi.org/10.1002/asna.201512270. arXiv:1511.05055 [astro-ph.GA]
- Crenshaw DM, Kraemer SB, Gabel JR (2003) The Host Galaxies of Narrow-Line Seyfert 1 Galaxies: Evidence for Bar-Driven Fueling. AJ126(4):1690–1698. https://doi.org/10.1086/377625. arXiv:astro-ph/0306404 [astro-ph]
- Crockett RM, Shabala SS, Kaviraj S, Antonuccio-Delogu V, Silk J, Mutchler M, O'Connell RW, Rejkuba M, Whitmore BC, Windhorst RA (2012) Triggered star formation in the inner filament of Centaurus A. MNRAS421(2):1603–1623. https://doi.org/10.1111/j.1365-2966. 2012.20418.x. arXiv:1201.3369 [astro-ph.CO]
- Croft S, van Breugel W, de Vries W, Dopita M, Martin C, Morganti R, Neff S, Oosterloo T, Schiminovich D, Stanford SA, van Gorkom J (2006) Minkowski's Object: A Starburst Triggered by a Radio Jet, Revisited. ApJ647(2):1040–1055. https://doi.org/10.1086/505526. arXiv:astro-ph/0604557 [astro-ph]
- Croton DJ, Springel V, White SDM, De Lucia G, Frenk CS, Gao L, Jenkins A, Kauffmann G, Navarro JF, Yoshida N (2006) The many lives of active galactic nuclei: cooling flows, black holes and the luminosities and colours of galaxies. MNRAS365:11–28. https://doi.org/10.1111/j.1365-2966. 2005.09675.x. astro-ph/0508046
- Curran SJ, Allison JR, Glowacki M, Whiting MT, Sadler EM (2013) On the H I column density-radio source size anticorrelation in compact radio sources. MNRAS431:3408–3413. https://doi.org/10.1093/mnras/stt438.arXiv:1303.1604

- Czerny B, Siemiginowska A, Janiuk A, Nikiel-Wroczyński B, Stawarz L (2009) Accretion Disk Model of Short-Timescale Intermittent Activity in Young Radio Sources. ApJ698:840–851. https://doi.org/10.1088/0004-637X/698/1/840. arXiv:0903.3940 [astro-ph.CO]
- Dallacasa D, Orienti M (2016) Radio spectra of High Frequency Peakers. Astron Nachr 337:120. https://doi.org/10.1002/asna.201512756
- Dallacasa D, Fanti C, Fanti R, Schilizzi RT, Spencer RE (1995) A sample of small size compact steep-spectrum radio sources. 1: VLBI images at 18 CM. A&A295:27–42
- Dallacasa D, Stanghellini C, Centonza M, Fanti R (2000) High frequency peakers. I. The bright sample. A&A363:887–900. astro-ph/0012428
- Dallacasa D, Stanghellini C, Centonza M, Furnari G (2002) High frequency peakers. New A Rev.46:299–302. https://doi.org/10.1016/S1387-6473(01) 00198-1
- Daly RA (1990) A Model to Explain the Correlation between the Optical and Radio Properties of High-Redshift Galaxies. ApJ355:416. https://doi.org/10.1086/168775
- D'Ammando F (2019) Relativistic Jets in Gamma-Ray-Emitting Narrow-Line Seyfert 1 Galaxies. Galaxies 7(4):87. https://doi.org/10.3390/galaxies7040087. arXiv:1911.03500 [astro-ph.HE]
- D'Ammando F, Orienti M, Giroletti M, Fermi Large Area Telescope Collaboration (2016) The Fermi-LAT view of young radio sources. Astron Nachr 337:59. https://doi.org/10.1002/asna.201512265. arXiv:1510.06763 [astro-ph.HE]
- Dasyra KM, Combes F (2011) Turbulent and fast motions of H₂ gas in active galactic nuclei. A&A533:L10. https://doi.org/10.1051/0004-6361/201117730. arXiv:1108.2888 [astro-ph.CO]
- Dasyra KM, Combes F (2012) Cold and warm molecular gas in the outflow of 4C 12.50. A&A541:L7. https://doi.org/10.1051/0004-6361/201219229. arXiv:1203.3452
- Dasyra KM, Combes F, Novak GS, Bremer M, Spinoglio L, Pereira Santaella M, Salomé P, Falgarone E (2014) Heating of the molecular gas in the massive outflow of the local ultraluminous-infrared and radioloud galaxy 4C12.50. A&A565:A46. https://doi.org/10.1051/0004-6361/201323070. arXiv:1402.3187
- De Breuck C, Röttgering H, Miley G, van Breugel W, Best P (2000) A statistical study of emission lines from high redshift radio galaxies. A&A362:519–543. arXiv:astro-ph/0008264 [astro-ph]
- de Bruyn AG, Wilson AS (1978) The radio properties of Seyfert galaxies. A&A64(3):433–444
- de Kool M, Begelman MC (1989) Effects of Thermal Plasma on Self-absorbed Synchrotron Sources in Active Galactic Nuclei. ApJ345:135. https://doi.org/10.1086/167887
- de Vries N, Snellen IAG, Schilizzi RT, Lehnert MD, Bremer MN (2007) Complete identification of the Parkes half-Jansky sample of GHz peaked spectrum radio galaxies. A&A464:879–883. https://doi.org/10.1051/0004-6361:

20066506. astro-ph/0701316

- de Vries N, Snellen IAG, Schilizzi RT, Mack KH (2009a) Further evidence for synchrotron self-absorption from the CORALZ sample of young radio-loud AGN. Astron Nachr 330:214. https://doi.org/10.1002/asna.200811159
- de Vries N, Snellen IAG, Schilizzi RT, Mack KH, Kaiser CR (2009b) VLBI observations of the CORALZ sample: young radio sources at low redshift. A&A498:641–659. https://doi.org/10.1051/0004-6361/200811145.arXiv:0901.2124
- de Vries N, Snellen IAG, Schilizzi RT, Mack KH (2010) The dynamical ages of two low-luminosity young radio sources. A&A521:A2. https://doi.org/10.1051/0004-6361/200912706
- de Vries WH, O'Dea CP, Baum SA, Sparks WB, Biretta J, de Koff S, Golombek D, Lehnert MD, Macchetto F, McCarthy P, Miley GK (1997) Hubble Space Telescope Imaging of Compact Steep-Spectrum Radio Sources. ApJS110(2):191–211. https://doi.org/10.1086/313001
- de Vries WH, O'Dea CP, Baum SA, Perlman E, Lehnert MD, Barthel PD (1998) Hosts of Powerful Radio Galaxies in the Near-Infrared: Implications for Radio Source Evolution. ApJ503:156–167. https://doi.org/10.1086/305963
- de Vries WH, O'Dea CP, Baum SA, Barthel PD (1999) Optical-Radio Alignment in Compact Steep-Spectrum Radio Sources. ApJ526:27–39. https://doi.org/10.1086/307967
- de Vries WH, O'Dea CP, Barthel PD, Fanti C, Fanti R, Lehnert MD (2000a) Hubble Space Telescope NICMOS Observations of the Host Galaxies of Powerful Radio Sources: Does Size Matter? AJ120:2300–2330. https://doi.org/10.1086/316825.astro-ph/0007424
- de Vries WH, O'Dea CP, Barthel PD, Thompson DJ (2000b) Identifications and spectroscopy of Gigahertz Peaked Spectrum sources. II. A&AS143:181–192. https://doi.org/10.1051/aas:2000175
- De Young DS (1989) Star Formation in Radio Galaxies at Large Redshift. ApJ342:L59. https://doi.org/10.1086/185484
- De Young DS (1991) The Deflection of Cosmic Jets. ApJ371:69. https://doi.org/10.1086/169871
- De Young DS (1993) The evolution of compact steep spectrum sources. ApJ402:95–108. https://doi.org/10.1086/172115
- De Zotti G, Granato GL, Silva L, Maino D, Danese L (2000) An evolutionary model for GHz peaked spectrum sources. Predictions for high frequency surveys. A&A354:467–472. astro-ph/9912282
- de Zotti G, Ricci R, Mesa D, Silva L, Mazzotta P, Toffolatti L, González-Nuevo J (2005) Predictions for high-frequency radio surveys of extragalactic sources. A&A431:893–903. https://doi.org/10.1051/0004-6361:20042108.astro-ph/0410709
- Dent WA, Balonek TJ (1980) A dramatic radio outburst in the quasar 1921 29. Nature283(5749):747-748. https://doi.org/10.1038/283747a0
- Dermer CD, Razzaque S, Finke JD, Atoyan A (2009) Ultra-high-energy cosmic rays from black hole jets of radio galaxies. New Journal

- of Physics 11(6):065016. https://doi.org/10.1088/1367-2630/11/6/065016. arXiv:0811.1160 [astro-ph]
- Dey A, Cimatti A, van Breugel W, Antonucci R, Spinrad H (1996) On the Origin of the Ultraviolet Continuum Emission from the High-Redshift Radio Galaxy 3C 256. ApJ465:157. https://doi.org/10.1086/177409. arXiv:astro-ph/9601099 [astro-ph]
- Dey A, van Breugel W, Vacca WD, Antonucci R (1997) Triggered Star Formation in a Massive Galaxy at z=3.8: 4C 41.17. ApJ490(2):698–709. https://doi.org/10.1086/304911. arXiv:astro-ph/9707166 [astro-ph]
- di Serego Alighieri S, Binette L, Courvoisier TJL, Fosbury RAE, Tadhunter CN (1988) A blue, polarized continuum source near radio galaxy PKS2152-69. Nature334(6183):591-593. https://doi.org/10.1038/334591a0
- di Serego Alighieri S, Fosbury RAE, Quinn PJ, Tadhunter CN (1989) Polarized light in high-redshift radio galaxies. Nature341(6240):307–309. https://doi.org/10.1038/341307a0
- di Serego Alighieri S, Cimatti A, Fosbury RAE (1993) Imaging Polarimetry of High-Redshift Radio Galaxies. ApJ404:584. https://doi.org/10.1086/172311
- Dicken D, Tadhunter C, Axon D, Morganti R, Robinson A, Kouwenhoven MBN, Spoon H, Kharb P, Inskip KJ, Holt J, Ramos Almeida C, Nesvadba NPH (2012) Spitzer Mid-IR Spectroscopy of Powerful 2 Jy and 3CRR Radio Galaxies. I. Evidence against a Strong Starburst-AGN Connection in Radio-loud AGN. ApJ745:172. https://doi.org/10.1088/0004-637X/745/2/172. arXiv:1111.4476
- Dickson R, Tadhunter C, Shaw M, Clark N, Morganti R (1995) The nebular contribution to the extended UV continua of powerful radio galaxies. MNRAS273(2):L29–L33. https://doi.org/10.1093/mnras/273.1.L29
- Donoso E, Yan L, Tsai C, Eisenhardt P, Stern D, Assef RJ, Leisawitz D, Jarrett TH, Stanford SA (2012) Origin of 12 μ m Emission across Galaxy Populations from WISE and SDSS Surveys. ApJ748(2):80. https://doi.org/10.1088/0004-637X/748/2/80. arXiv:1201.2943 [astro-ph.CO]
- Draine BT, Dale DA, Bendo G, Gordon KD, Smith JDT, Armus L, Engelbracht CW, Helou G, Kennicutt J R C, Li A, Roussel H, Walter F, Calzetti D, Moustakas J, Murphy EJ, Rieke GH, Bot C, Hollenbach DJ, Sheth K, Teplitz HI (2007) Dust Masses, PAH Abundances, and Starlight Intensities in the SINGS Galaxy Sample. ApJ663(2):866–894. https://doi.org/10.1086/518306. arXiv:astro-ph/0703213 [astro-ph]
- Drake CL, McGregor PJ, Dopita MA (2004) Radio-Excess IRAS Galaxies. II. Host Galaxies. AJ128:955–968. https://doi.org/10.1086/422921
- Dugan Z, Bryan S, Gaibler V, Silk J, Haas M (2014) Stellar Signatures of AGN-jet-triggered Star Formation. ApJ796(2):113. https://doi.org/10.1088/0004-637X/796/2/113. arXiv:1404.0381 [astro-ph.GA]
- Dugan Z, Gaibler V, Silk J (2017) Feedback by AGN Jets and Wideangle Winds on a Galactic Scale. ApJ844(1):37. https://doi.org/10.3847/ 1538-4357/aa7566. arXiv:1608.01370 [astro-ph.GA]
- Elbert JW, Sommers P (1995) In Search of a Source for the 320 EeV Fly's Eye Cosmic Ray. ApJ441:151. https://doi.org/10.1086/175345. arXiv:astro-

- ph/9410069 [astro-ph]
- Elvis M, Fiore F, Wilkes B, McDowell J, Bechtold J (1994) Absorption in X-ray spectra of high-redshift quasars. ApJ422:60–72. https://doi.org/10.1086/173703
- Emonts BHC, Morganti R, Villar-Martín M, Hodgson J, Brogt E, Tadhunter CN, Mahony E, Oosterloo TA (2016) From galaxy-scale fueling to nuclear-scale feedback. The merger-state of radio galaxies 3C 293, 3C 305, and 4C 12.50. A&A596:A19. https://doi.org/10.1051/0004-6361/201628592. arXiv:1609.06539
- Evans AS, Kim DC, Mazzarella JM, Scoville NZ, Sanders DB (1999) Molecular Gas in the Powerful Radio Nucleus of the Ultraluminous Infrared Galaxy PKS 1345+12. ApJ521(2):L107-L110. https://doi.org/10.1086/312198. arXiv:astro-ph/9907397 [astro-ph]
- Fabian AC (1989) The alignment of the optical continuum and radio axes of high-redshift radio galaxies: electron scattering in intracluster gas? MNRAS238:41P-44. https://doi.org/10.1093/mnras/238.1.41P
- Fabian AC (2012) Observational Evidence of Active Galactic Nuclei Feedback. ARA&A50:455–489. https://doi.org/10.1146/annurev-astro-081811-125521. arXiv:1204.4114
- Falcke H, Körding E, Markoff S (2004a) A scheme to unify low-power accreting black holes. Jet-dominated accretion flows and the radio/X-ray correlation. A&A414:895–903. https://doi.org/10.1051/0004-6361:20031683.arXiv:astro-ph/0305335 [astro-ph]
- Falcke H, Körding E, Nagar NM (2004b) Compact radio cores: from the first black holes to the last. New A Rev.48:1157–1171. https://doi.org/10.1016/j.newar.2004.09.029. astro-ph/0409125
- Fan XL, Bai JM (2016) The Radio/X-Ray Correlation and Black Hole Fundamental Plane for Young Radio Sources: Implications for X-Ray Origin and Accretion Mode. ApJ818:185. https://doi.org/10.3847/0004-637X/818/2/185
- Fanti C (2009) Radio properties of CSSs and GPSs. Astron Nachr 330:120–127. https://doi.org/10.1002/asna.200811137
- Fanti C, Fanti R, Parma P, Schilizzi RT, van Breugel WJM (1985) Compact Steep Spectrum 3CR radio sources VLBI observations at 18 CM. A&A143:292–306
- Fanti C, Fanti R, Dallacasa D, Schilizzi RT, Spencer RE, Stanghellini C (1995) Are compact steep-spectrum sources young? A&A302:317
- Fanti C, Pozzi F, Fanti R, Baum SA, O'Dea CP, Bremer M, Dallacasa D, Falcke H, de Graauw T, Marecki A, Miley G, Rottgering H, Schilizzi RT, Snellen I, Spencer RE, Stanghellini C (2000) ISO observations of a sample of Compact Steep Spectrum and GHz Peaked Spectrum radio galaxies. A&A358:499–513. astro-ph/0005035
- Fanti C, Pozzi F, Dallacasa D, Fanti R, Gregorini L, Stanghellini C, Vigotti M (2001) Multi-frequency VLA observations of a new sample of CSS/GPS radio sources. A&A369:380–420. https://doi.org/10.1051/0004-6361:20010051
- Fanti C, Branchesi M, Cotton WD, Dallacasa D, Fanti R, Gregorini L, Murgia

- M, Stanghellini C, Vigotti M (2004) The B3-VLA CSS sample. IV. kpc-scale polarization properties. A&A427:465–483. https://doi.org/10.1051/0004-6361:20040460
- Fanti C, Fanti R, Zanichelli A, Dallacasa D, Stanghellini C (2011) The B3-VLA CSS sample. VIII. New optical identifications from the Sloan Digital Sky Survey The ultraviolet-optical spectral energy distribution of the young radio sources. A&A528:A110. https://doi.org/10.1051/0004-6361/201015379.arXiv:1102.1619
- Fanti R, Fanti C, Schilizzi RT, Spencer RE, Nan Rendong, Parma P, van Breugel WJM, Venturi T (1990) On the nature of compact steep spectrum radio sources. A&A231:333–346
- Farrah D, Bernard-Salas J, Spoon HWW, Soifer BT, Armus L, Brandl B, Charmandaris V, Desai V, Higdon S, Devost D, Houck J (2007) High-Resolution Mid-Infrared Spectroscopy of Ultraluminous Infrared Galaxies. ApJ667:149–169. https://doi.org/10.1086/520834. arXiv:0706.0513
- Farrar GR, Biermann PL (1998) Correlation between Compact Radio Quasars and Ultrahigh Energy Cosmic Rays. Physical Review Letters 81:3579–3582. https://doi.org/10.1103/PhysRevLett.81.3579. astro-ph/9806242
- Farrar GR, Biermann PL (1999) Farrar and Biermann Reply:. Physical Review Letters 83:2472. https://doi.org/10.1103/PhysRevLett.83.2472. astro-ph/9901315
- Fassnacht CD, Taylor GB (2001) Compact Symmetric Objects as Radio Flux Density Calibrators. AJ122:1661–1668. https://doi.org/10.1086/322112.astro-ph/0106001
- Feain IJ, Cornwell TJ, Ekers RD, Calabretta MR, Norris RP, Johnston-Hollitt M, Ott J, Lindley E, Gaensler BM, Murphy T, Middelberg E, Jiraskova S, O'Sullivan S, McClure-Griffiths NM, Bland-Hawthorn J (2011) The Radio Continuum Structure of Centaurus A at 1.4 GHz. ApJ740(1):17. https://doi.org/10.1088/0004-637X/740/1/17. arXiv:1104.0077 [astro-ph.CO]
- Fiore F, Feruglio C, Shankar F, Bischetti M, Bongiorno A, Brusa M, Carniani S, Cicone C, Duras F, Lamastra A, Mainieri V, Marconi A, Menci N, Maiolino R, Piconcelli E, Vietri G, Zappacosta L (2017) AGN wind scaling relations and the co-evolution of black holes and galaxies. A&A601:A143. https://doi.org/10.1051/0004-6361/201629478. arXiv:1702.04507 [astro-ph.GA]
- Fotopoulou CM, Dasyra KM, Combes F, Salomé P, Papachristou M (2019) Complex molecular gas kinematics in the inner 5 kpc of 4C12.50 as seen by ALMA. A&A629:A30. https://doi.org/10.1051/0004-6361/201834416.arXiv:1908.01011 [astro-ph.GA]
- Fragile PC, Murray SD, Anninos P, van Breugel W (2004) Radiative Shock-induced Collapse of Intergalactic Clouds. ApJ604(1):74–87. https://doi.org/10.1086/381726. arXiv:astro-ph/0311298 [astro-ph]
- Fragile PC, Anninos P, Croft S, Lacy M, Witry JWL (2017) Numerical Simulations of a Jet-Cloud Collision and Starburst: Application to Minkowski's Object. ApJ850(2):171. https://doi.org/10.3847/1538-4357/aa95c6. arXiv:1701.00024 [astro-ph.GA]

- Gaibler V, Khochfar S, Krause M, Silk J (2012) Jet-induced star formation in gas-rich galaxies. MNRAS425(1):438–449. https://doi.org/10.1111/j.1365-2966.2012.21479.x. arXiv:1111.4478 [astro-ph.CO]
- Gallo LC, Edwards PG, Ferrero E, Kataoka J, Lewis DR, Ellingsen SP, Misanovic Z, Welsh WF, Whiting M, Boller T, Brinkmann W, Greenhill J, Oshlack A (2006) The spectral energy distribution of PKS 2004-447: a compact steep-spectrum source and possible radio-loud narrow-line Seyfert 1 galaxy. MNRAS370(1):245–254. https://doi.org/10.1111/j.1365-2966.2006.10482.x. arXiv:astro-ph/0604480 [astro-ph]
- Gao Y, Solomon PM (2004) The Star Formation Rate and Dense Molecular Gas in Galaxies. ApJ606(1):271–290. https://doi.org/10.1086/382999. arXiv:astro-ph/0310339 [astro-ph]
- García-Burillo S, Combes F, Neri R, Fuente A, Usero A, Leon S, Lim J (2007) Fueling the central engine of radio galaxies. I. The molecular/dusty disk of 4C 31.04. A&A468(3):L71–L75. https://doi.org/10.1051/0004-6361: 20077599. arXiv:0704.3581 [astro-ph]
- Garofalo D, Singh CB (2019) FR0 Radio Galaxies and Their Place in the Radio Morphology Classification. ApJ871(2):259. https://doi.org/10.3847/1538-4357/aaf056. arXiv:1811.05383 [astro-ph.HE]
- Garrington ST, Conway RG (1991) The interpretation of asymmetric depolarization in extragalactic radio sources. MNRAS250:198. https://doi.org/10.1093/mnras/250.1.198
- Garrington ST, Leahy JP, Conway RG, Laing RA (1988) A systematic asymmetry in the polarization properties of double radio sources with one jet. Nature331(6152):147–149. https://doi.org/10.1038/331147a0
- Garrington ST, Conway RG, Leahy JP (1991) Asymmetry depolarization in double radio sources with one sided jets. MNRAS250:171. https://doi.org/10.1093/mnras/250.1.171
- Ge J, Owen FN (1994) Faraday Rotation in Cooling Flow Clusters of Galaxies. II. Survey. AJ108:1523. https://doi.org/10.1086/117173
- Gelderman R, Whittle M (1994) An optical study of compact steep-spectrum radio sources. 1: The spectroscopic data. ApJS91:491–505. https://doi.org/10.1086/191946
- Gendre MA, Best PN, Wall JV, Ker LM (2013) The relation between morphology, accretion modes and environmental factors in local radio AGN. MNRAS430(4):3086–3101. https://doi.org/10.1093/mnras/stt116. arXiv:1301.1526 [astro-ph.CO]
- Giroletti M (2008) Jet Properties and Evolution in Small and Intermediate Scale Objects. In: Rector TA, De Young DS (eds) Extragalactic Jets: Theory and Observation from Radio to Gamma Ray. Astronomical Society of the Pacific Conference Series, vol 386. p 176. arXiv:0707.3516
- Giroletti M, Polatidis A (2009) Samples and statistics of CSS and GPS sources. Astron Nachr 330:193. https://doi.org/10.1002/asna.200811154.

- arXiv:0904.1068 [astro-ph.CO]
- Giroletti M, Giovannini G, Taylor GB, Conway JE, Lara L, Venturi T (2003) Lobe advance velocities in the extragalactic compact symmetric object ¡ASTROBJ¿4C 31.04¡/ASTROBJ¿. A&A399:889–897. https://doi.org/10.1051/0004-6361:20021821. astro-ph/0212232
- Giroletti M, Giovannini G, Taylor GB (2005) Low power compact radio galaxies at high angular resolution. A&A441:89–101. https://doi.org/10.1051/0004-6361:20053347. astro-ph/0506497
- Gizani NAB, Cohen A, Kassim NE (2005) First results of the 74-MHz Very Large Array-Pie Town link. Hercules A at low frequencies. MNRAS358(3):1061–1068. https://doi.org/10.1111/j.1365-2966.2005. 08849.x. arXiv:astro-ph/0501470 [astro-ph]
- Glowacki M, Allison JR, Sadler EM, Moss VA, Curran SJ, Musaeva A, Deng C, Parry R, Sligo MC (2017) H I absorption in nearby compact radio galaxies. MNRAS467:2766–2786. https://doi.org/10.1093/mnras/stx214. arXiv:1701.07036
- Goldoni P, Pita S, Boisson C, Müller C, Dauser T, Jung I, Krauß F, Lenain JP, Sol H (2016) Optical-NIR spectroscopy of the puzzling γ -ray source 3FGL 1603.9-4903/PMN J1603-4904 with X-Shooter. A&A586:L2. https://doi.org/10.1051/0004-6361/201527582. arXiv:1510.06234 [astro-ph.HE]
- Goodrich RW (1989) Spectropolarimetry of "Narrow-Line" Seyfert 1 Galaxies. ApJ342:224. https://doi.org/10.1086/167586
- Gopal-Krishna, Wiita PJ (1991) Gaseous halos of elliptical galaxies, the cosmic evolution of their radio sizes, and the phenomenon of compact steep-spectrum sources. ApJ373:325–335. https://doi.org/10.1086/170054
- Gopal-Krishna, Patnaik AR, Steppe H (1983) A sample of 25 extragalactic radio sources having a spectrum peaked around 1 GHz. A&A123:107–110
- Gower AC, Gregory PC, Unruh WG, Hutchings JB (1982) Relativistic precessing jets in quasars and radio galaxies: models to fit high resolution data. ApJ262:478–496. https://doi.org/10.1086/160442
- Graham JA (1998) Shocked Gas and Star Formation in the Centaurus A Radio Galaxy. ApJ502(1):245–252. https://doi.org/10.1086/305888
- Grandi P, Capetti A, Baldi RD (2016) Discovery of a Fanaroff-Riley type 0 radio galaxy emitting at γ -ray energies. MNRAS457(1):2–8. https://doi.org/10.1093/mnras/stv2846. arXiv:1512.01242 [astro-ph.GA]
- Grasha K, Darling J, Bolatto A, Leroy AK, Stocke JT (2019) A Search for Intrinsic H I 21 cm and OH 18 cm Absorption toward Compact Radio Sources. ApJS245(1):3. https://doi.org/10.3847/1538-4365/ab4906.arXiv:1909.12422 [astro-ph.GA]
- Greene JE, Ho LC (2005) A Comparison of Stellar and Gaseous Kinematics in the Nuclei of Active Galaxies. ApJ627(2):721–732. https://doi.org/10.1086/430590. arXiv:astro-ph/0503675 [astro-ph]
- Greisen K (1966) End to the Cosmic-Ray Spectrum? Phys. Rev. Lett.16(17):748–750. https://doi.org/10.1103/PhysRevLett.16. 748
- Grupe D (2000) Statistical properties of narrow-line Seyfert 1 galax-

- ies. New A Rev.44(7-9):455-460. https://doi.org/10.1016/S1387-6473(00) 00080-4. arXiv:astro-ph/0005139 [astro-ph]
- Gu M, Chen Y (2010) The Compact Radio Structure of Radio-loud Narrow Line Seyfert 1 Galaxies. AJ139:2612–2619. https://doi.org/10.1088/0004-6256/139/6/2612. arXiv:1004.3058
- Gu M, Chen Y, Komossa S, Yuan W, Shen Z, Wajima K, Zhou H, Zensus JA (2015) The Radio Properties of Radio-loud Narrow-line Seyfert 1 Galaxies on Parsec Scales. ApJS221(1):3. https://doi.org/10.1088/0067-0049/221/1/3. arXiv:1509.01889 [astro-ph.GA]
- Gu M, Chen Y, Komossa S, Yuan W, Shen Z (2016) The compact radio structure of radio-loud NLS1 galaxies and the relationship to CSS sources. Astron Nachr 337(1-2):125. https://doi.org/10.1002/asna.201512277
- Guainazzi M, Siemiginowska A, Rodriguez-Pascual P, Stanghellini C (2004) XMM-Newton discovery of a Compton-thick AGN in the GPS galaxy Mkn 668. A&A421:461–471. https://doi.org/10.1051/0004-6361:20047051. astro-ph/0402639
- Guainazzi M, Siemiginowska A, Stanghellini C, Grandi P, Piconcelli E, Azubike Ugwoke C (2006) A hard X-ray view of giga-hertz peaked spectrum radio galaxies. A&A446:87–96. https://doi.org/10.1051/0004-6361:20053374.astro-ph/0509043
- Gugliucci NE, Taylor GB, Peck AB, Giroletti M (2005) Dating COINS: Kinematic Ages for Compact Symmetric Objects. ApJ622:136–148. https://doi.org/10.1086/427934. astro-ph/0412199
- Guillard P, Ogle PM, Emonts BHC, Appleton PN, Morganti R, Tadhunter C, Oosterloo T, Evans DA, Evans AS (2012) Strong Molecular Hydrogen Emission and Kinematics of the Multiphase Gas in Radio Galaxies with Fast Jet-driven Outflows. ApJ747:95. https://doi.org/10.1088/0004-637X/747/2/95. arXiv:1201.1503
- Gupta N, Srianand R, Saikia DJ (2005) Outflowing material in the compact steep-spectrum source quasar 3C 48: evidence of jet-cloud interaction? MNRAS361:451–459. https://doi.org/10.1111/j.1365-2966.2005.09169.x. astro-ph/0505125
- Gupta N, Salter CJ, Saikia DJ, Ghosh T, Jeyakumar S (2006) Probing radio source environments via HI and OH absorption. MNRAS373:972–992. https://doi.org/10.1111/j.1365-2966.2006.11064.x. astro-ph/0605423
- Hancock PJ (2009) High frequency GPS sources in the AT20G survey. Astron Nachr 330:180. https://doi.org/10.1002/asna.200811151. arXiv:0901.4592 [astro-ph.GA]
- Hancock PJ, Tingay SJ, Sadler EM, Phillips C, Deller AT (2009) e-VLBI observations of GHz-peaked spectrum radio sources in nearby galaxies from the AT20G survey. MNRAS397:2030–2036. https://doi.org/10.1111/j.1365-2966.2009.15055.x. arXiv:0905.3219
- Hancock PJ, Sadler EM, Mahony EK, Ricci R (2010) Observations and properties of candidate high-frequency GPS radio sources in the AT20G survey. MNRAS408:1187–1206. https://doi.org/10.1111/j.1365-2966.2010.17199.x. arXiv:1008.1401

- Hardcastle MJ, Croston JH (2020) Radio galaxies and feedback from AGN jets. New A Rev.88:101539. https://doi.org/10.1016/j.newar.2020.101539. arXiv:2003.06137 [astro-ph.HE]
- Hardcastle MJ, Evans DA, Croston JH (2007) Hot and cold gas accretion and feedback in radio-loud active galaxies. MNRAS376(4):1849–1856. https://doi.org/10.1111/j.1365-2966.2007.11572.x. arXiv:astro-ph/0701857 [astro-ph]
- Hardcastle MJ, Evans DA, Croston JH (2009) The active nuclei of z < 1.0 3CRR radio sources. MNRAS396:1929–1952. https://doi.org/10.1111/j.1365-2966.2009.14887.x. arXiv:0904.1323
- Hardcastle MJ, Massaro F, Harris DE, Baum SA, Bianchi S, Chiaberge M, Morganti R, O'Dea CP, Siemiginowska A (2012) The nature of the jet-driven outflow in the radio galaxy 3C 305. MNRAS424:1774–1789. https://doi.org/10.1111/j.1365-2966.2012.21247.x. arXiv:1205.0962
- Hardcastle MJ, Williams WL, Best PN, Croston JH, Duncan KJ, Röttgering HJA, Sabater J, Shimwell TW, Tasse C, Callingham JR, Cochrane RK, de Gasperin F, Gürkan G, Jarvis MJ, Mahatma V, Miley GK, Mingo B, Mooney S, Morabito LK, O'Sullivan SP, Prandoni I, Shulevski A, Smith DJB (2019) Radio-loud AGN in the first LoTSS data release. The lifetimes and environmental impact of jet-driven sources. A&A622:A12. https://doi.org/10.1051/0004-6361/201833893. arXiv:1811.07943 [astro-ph.GA]
- Harrison CM, Costa T, Tadhunter CN, Flütsch A, Kakkad D, Perna M, Vietri G (2018) AGN outflows and feedback twenty years on. Nat Astron 2:198–205. https://doi.org/10.1038/s41550-018-0403-6. arXiv:1802.10306 [astro-ph.GA]
- Heald GH, Pizzo RF, Orrú E, Breton RP, Carbone D, Ferrari C, Hardcastle MJ, Jurusik W, Macario G, Mulcahy D, Rafferty D, Asgekar A, Brentjens M, Fallows RA, Frieswijk W, Toribio MC, Adebahr B, Arts M, Bell MR, Bonafede A, Bray J, Broderick J, Cantwell T, Carroll P, Cendes Y, Clarke AO, Croston J, Daiboo S, de Gasperin F, Gregson J, Harwood J, Hassall T, Heesen V, Horneffer A, van der Horst AJ, Iacobelli M, Jelić V, Jones D, Kant D, Kokotanekov G, Martin P, McKean JP, Morabito LK, Nikiel-Wroczyński B, Offringa A, Pandey VN, Pandey-Pommier M, Pietka M, Pratley L, Riseley C, Rowlinson A, Sabater J, Scaife AMM, Scheers LHA, Sendlinger K, Shulevski A, Sipior M, Sobey C, Stewart AJ, Stroe A, Swinbank J, Tasse C, Trüstedt J, Varenius E, van Velzen S, Vilchez N, van Weeren RJ, Wijnholds S, Williams WL, de Bruyn AG, Nijboer R, Wise M, Alexov A, Anderson J, Avruch IM, Beck R, Bell ME, van Bemmel I, Bentum MJ, Bernardi G, Best P, Breitling F, Brouw WN, Brüggen M, Butcher HR, Ciardi B, Conway JE, de Geus E, de Jong A, de Vos M, Deller A, Dettmar RJ, Duscha S, Eislöffel J, Engels D, Falcke H, Fender R, Garrett MA, Grießmeier J. Gunst AW, Hamaker JP, Hessels JWT, Hoeft M, Hörandel J, Holties HA, Intema H, Jackson NJ, Jütte E, Karastergiou A, Klijn WFA, Kondratiev VI, Koopmans LVE, Kuniyoshi M, Kuper G, Law C, van Leeuwen J, Loose M, Maat P, Markoff S, McFadden R, McKay-Bukowski D, Mevius M, Miller-Jones JCA, Morganti R, Munk H, Nelles A, Noordam JE, Norden

- MJ, Paas H, Polatidis AG, Reich W, Renting A, Röttgering H, Schoenmakers A, Schwarz D, Sluman J, Smirnov O, Stappers BW, Steinmetz M, Tagger M, Tang Y, ter Veen S, Thoudam S, Vermeulen R, Vocks C, Vogt C, Wijers RAMJ, Wucknitz O, Yatawatta S, Zarka P (2015) The LOFAR Multifrequency Snapshot Sky Survey (MSSS). I. Survey description and first results. A&A582:A123. https://doi.org/10.1051/0004-6361/201425210.arXiv:1509.01257 [astro-ph.IM]
- Heckman TM, Best PN (2014) The Coevolution of Galaxies and Supermassive Black Holes: Insights from Surveys of the Contemporary Universe. ARA&A52:589–660. https://doi.org/10.1146/annurev-astro-081913-035722. arXiv:1403.4620 [astro-ph.GA]
- Heckman TM, Miley GK, Balick B, van Breugel WJM, Butcher HR (1982) An optical and radio investigation of the radio galaxy 3C 305. ApJ262:529–553. https://doi.org/10.1086/160445
- Heckman TM, O'Dea CP, Baum SA, Laurikainen E (1994) Obscuration, orientation, and the infrared properties of radio-loud active galaxies. ApJ428:65–81. https://doi.org/10.1086/174221
- Heinz S, Reynolds CS, Begelman MC (1998) X-Ray Signatures of Evolving Radio Galaxies. ApJ501:126–136. https://doi.org/10.1086/305807. astroph/9801268
- Helmboldt JF, Taylor GB, Tremblay S, Fassnacht CD, Walker RC, Myers ST, Sjouwerman LO, Pearson TJ, Readhead ACS, Weintraub L, Gehrels N, Romani RW, Healey S, Michelson PF, Blandford RD, Cotter G (2007) The VLBA Imaging and Polarimetry Survey at 5 GHz. ApJ658:203–216. https://doi.org/10.1086/511005. astro-ph/0611459
- Herzog A, Middelberg E, Norris RP, Spitler LR, Deller AT, Collier JD, Parker QA (2015) Active galactic nuclei cores in infrared-faint radio sources. Very long baseline interferometry observations using the Very Long Baseline Array. A&A578:A67. https://doi.org/10.1051/0004-6361/201525997.arXiv:1504.03771
- Herzog A, Norris RP, Middelberg E, Seymour N, Spitler LR, Emonts BHC, Franzen TMO, Hunstead R, Intema HT, Marvil J, Parker QA, Sirothia SK, Hurley-Walker N, Bell M, Bernardi G, Bowman JD, Briggs F, Cappallo RJ, Callingham JR, Deshpande AA, Dwarakanath KS, For BQ, Greenhill LJ, Hancock P, Hazelton BJ, Hindson L, Johnston-Hollitt M, Kapińska AD, Kaplan DL, Lenc E, Lonsdale CJ, McKinley B, McWhirter SR, Mitchell DA, Morales MF, Morgan E, Morgan J, Oberoi D, Offringa A, Ord SM, Prabu T, Procopio P, Udaya Shankar N, Srivani KS, Staveley-Smith L, Subrahmanyan R, Tingay SJ, Wayth RB, Webster RL, Williams A, Williams CL, Wu C, Zheng Q, Bannister KW, Chippendale AP, Harvey-Smith L, Heywood I, Indermuehle B, Popping A, Sault RJ, Whiting MT (2016) The radio spectral energy distribution of infrared-faint radio sources. A&A593:A130. https://doi.org/10.1051/0004-6361/201527000. arXiv:1607.02707
- Hes R, Barthel PD, Hoekstra H (1995) The far infrared properties of 3CR quasars and radio galaxies. A&A303:8
- Heywood I, Martínez-Sansigre A, Willott CJ, Rawlings S (2013) Ground-state

- $^{12}\mathrm{CO}$ emission and a resolved jet at 115 GHz (rest frame) in the radio-loud quasar 3C 318. MNRAS435(4):3376–3384. https://doi.org/10.1093/mnras/stt1530. arXiv:1308.3360 [astro-ph.CO]
- Higgins SW, O'Brien TJ, Dunlop JS (1999) Structures produced by the collision of extragalactic jets with dense clouds. MNRAS309(2):273–286. https://doi.org/10.1046/j.1365-8711.1999.02779.x. arXiv:astro-ph/9904009 [astro-ph]
- Hine RG, Longair MS (1979) Optical spectra of 3CR radio galaxies. MNRAS188:111–130. https://doi.org/10.1093/mnras/188.1.111
- Hirst P, Jackson N, Rawlings S (2003) Near-infrared spectroscopy of powerful compact steep-spectrum radio sources. MNRAS346:1009–1020. https://doi.org/10.1111/j.1365-2966.2003.07155.x. astro-ph/0309055
- Hoffman CM (1999) Comment on "Correlation between Compact Radio Quasars and Ultrahigh Energy Cosmic Rays". Phys. Rev. Lett.83(12):2471. https://doi.org/10.1103/PhysRevLett.83.2471. arXiv:astro-ph/9901026 [astro-ph]
- Holt J (2009) The host galaxies of Compact Steep Spectrum and Gigahertz-Peaked Spectrum radio sources. Astron Nachr 330:226. https://doi.org/10.1002/asna.200811163. arXiv:0812.2812
- Holt J, Tadhunter CN, Morganti R (2003a) Extreme Emission Line Outflows in the GPS Source 4C12.50 (PKS1345+12). PASA20:25–27. https://doi.org/10.1071/AS02038. astro-ph/0210092
- Holt J, Tadhunter CN, Morganti R (2003b) Highly extinguished emission line outflows in the young radio source PKS 1345+12. MNRAS342:227-238. https://doi.org/10.1046/j.1365-8711.2003.06532.x. astro-ph/0302311
- Holt J, Tadhunter C, Morganti R, Bellamy M, González Delgado RM, Tzioumis A, Inskip KJ (2006) The co-evolution of the obscured quasar PKS 1549-79 and its host galaxy: evidence for a high accretion rate and warm outflow. MNRAS370:1633–1650. https://doi.org/10.1111/j.1365-2966.2006. 10604.x. astro-ph/0606304
- Holt J, Tadhunter CN, González Delgado RM, Inskip KJ, Rodriguez Zaurin J, Emonts BHC, Morganti R, Wills KA (2007) The properties of the young stellar populations in powerful radio galaxies at low and intermediate redshifts. MNRAS381(2):611–639. https://doi.org/10.1111/j.1365-2966.2007.12140.x.arXiv:0708.2605 [astro-ph]
- Holt J, Tadhunter CN, Morganti R (2008) Fast outflows in compact radio sources: evidence for AGN-induced feedback in the early stages of radio source evolution. MNRAS387:639–659. https://doi.org/10.1111/j. 1365-2966.2008.13089.x. arXiv:0802.1444
- Holt J, Tadhunter CN, Morganti R (2009) The ionization of the emission-line gas in young radio galaxies. MNRAS400:589–602. https://doi.org/10.1111/j.1365-2966.2009.15491.x. arXiv:0912.0665 [astro-ph.CO]
- Holt J, Tadhunter CN, Morganti R, Emonts BHC (2011) The impact of the warm outflow in the young (GPS) radio source and ULIRG PKS 1345+12 (4C 12.50). MNRAS410:1527-1536. https://doi.org/10.1111/j.1365-2966. 2010.17535.x. arXiv:1008.2846

- Homan J, Belloni T (2005) The Evolution of Black Hole States. Ap&SS300(1-3):107–117. https://doi.org/10.1007/s10509-005-1197-4. arXiv:astro-ph/0412597 [astro-ph]
- Hu JF, Cao XW, Chen L, You B (2016) Correlation between excitation index and Eddington ratio in radio galaxies. Research in Astronomy and Astrophysics 16(9):136. https://doi.org/10.1088/1674-4527/16/9/136
- Inoue M, Tabara H, Kato T, Aizu K (1995) Search for High Rotation Measures in Extragalactic Radio Sources I. Multi-Channel Observations at 10 GHz. PASJ47:725–737
- Inskip KJ, Best PN, Rawlings S, Longair MS, Cotter G, Röttgering HJA, Eales S (2002) Deep spectroscopy of z~1 6C radio galaxies I. The effects of radio power and size on the properties of the emission-line gas. MNRAS337(4):1381–1406. https://doi.org/10.1046/j.1365-8711.2002.06012.x. arXiv:astro-ph/0208548 [astro-ph]
- Inskip KJ, Lee D, Cotter G, Pearson TJ, Readhead ACS, Bolton RC, Chandler C, Pooley G, Riley JM, Waldram EM (2006) Deep spectroscopy of 9C J1503+4528: a very young compact steep spectrum radio source at z = 0.521. MNRAS370(4):1585-1598. https://doi.org/10.1111/j.1365-2966. 2006.10584.x. arXiv:astro-ph/0605460 [astro-ph]
- Intema HT, Jagannathan P, Mooley KP, Frail DA (2017) The GMRT 150 MHz all-sky radio survey. First alternative data release TGSS ADR1. A&A598:A78. https://doi.org/10.1051/0004-6361/201628536.arXiv:1603.04368
- Ishwara-Chandra CH, Taylor AR, Green DA, Stil JM, Vaccari M, Ocran EF (2020) A wide-area GMRT 610-MHz survey of ELAIS N1 field. MNRAS497(4):5383-5394. https://doi.org/10.1093/mnras/staa2341.arXiv:2008.02530
- Israel FP (1998) Centaurus A NGC 5128. A&A Rev.8(4):237–278. https://doi.org/10.1007/s001590050011. arXiv:astro-ph/9811051 [astro-ph]
- Ito H, Kino M, Kawakatu N, Yamada S (2011) Evolution of Non-thermal Shell Emission Associated with Active Galactic Nucleus Jets. ApJ730(2):120. https://doi.org/10.1088/0004-637X/730/2/120. arXiv:1101.2543 [astro-ph.HE]
- Jarrett TH, Masci F, Tsai CW, Petty S, Cluver ME, Assef RJ, Benford D, Blain A, Bridge C, Donoso E, Eisenhardt P, Koribalski B, Lake S, Neill JD, Seibert M, Sheth K, Stanford S, Wright E (2013) Extending the Nearby Galaxy Heritage with WISE: First Results from the WISE Enhanced Resolution Galaxy Atlas. AJ145(1):6. https://doi.org/10.1088/0004-6256/145/1/6. arXiv:1210.3628 [astro-ph.CO]
- Jarvis M, Taylor R, Agudo I, Allison JR, Deane RP, Frank B, Gupta N, Heywood I, Maddox N, McAlpine K, Santos M, Scaife AMM, Vaccari M, Zwart JTL, Adams E, Bacon DJ, Baker AJ, Bassett BA, Best PN, Beswick R, Blyth S, Brown ML, Bruggen M, Cluver M, Colafrancesco S, Cotter G, Cress C, Davé R, Ferrari C, Hardcastle MJ, Hale CL, Harrison I, Hatfield PW, Klockner HR, Kolwa S, Malefahlo E, Marubini T, Mauch T, Moodley K, Morganti R, Norris RP, Peters JA, Prandoni I, Prescott M, Oliver S, Oozeer

- N, Rottgering HJA, Seymour N, Simpson C, Smirnov O, Smith DJB (2016) The MeerKAT International GHz Tiered Extragalactic Exploration (MIGHTEE) Survey. In: Proceedings of MeerKAT Science: On the Pathway to the SKA. 25-27 May, 2016 Stellenbosch, South Africa (MeerKAT2016). p 6. URL https://pos.sissa.it/cgi-bin/reader/conf.cgi?confid=277. arXiv:1709.01901
- Jauncey DL, King EA, Bignall HE, Lovell JEJ, Kedziora-Chudczer L, Tzioumis AK, Tingay SJ, Macquart JP, McCulloch PM (2003) Variability in GPS Sources. PASA20:151–155. https://doi.org/10.1071/AS03023
- Jauncey DL, Koay JY, Bignall H, Macquart JP, Pursimo T, Giroletti M, Hovatta T, Kiehlmann S, Rickett B, Readhead A, Max-Moerbeck W, Vedantham H, Reynolds C, Lovell J, Ojha R, Kedziora-Chudczer L (2020) Interstellar scintillation, ISS, and intrinsic variability of radio AGN. Advances in Space Research 65(2):756-762. https://doi.org/10.1016/j.asr.2019.05.003
- Jeyakumar S (2016) Numerical calculations of spectral turnover and synchrotron self-absorption in CSS and GPS radio sources. MNRAS458:3786–3794. https://doi.org/10.1093/mnras/stw181. arXiv:1601.05406
- Jeyakumar S, Saikia DJ, Pramesh Rao A, Balasubramanian V (2000) Small-scale structures in compact steep-spectrum and GHz-peaked-spectrum radio sources. A&A362:27–41. astro-ph/0008288
- Jeyakumar S, Wiita PJ, Saikia DJ, Hooda JS (2005) Jet propagation and the asymmetries of CSS radio sources. A&A432:823–833. https://doi.org/10.1051/0004-6361:20041564. astro-ph/0411598
- Jimenez-Gallardo A, Massaro F, Prieto MA, Missaglia V, Stuardi C, Paggi A, Ricci F, Kraft RP, Liuzzo E, Tremblay GR, Baum SA, O'Dea CP, Wilkes BJ, Kuraszkiewicz J, Forman WR, Harris DE (2020) Completing the 3CR Chandra Snapshot Survey: Extragalactic Radio Sources at High Redshift. ApJS250(1):7. https://doi.org/10.3847/1538-4365/aba5a0.arXiv:2007.02945 [astro-ph.GA]
- Johnston HM, Broderick JW, Cotter G, Morganti R, Hunstead RW (2010) The extraordinary radio galaxy MRC B1221-423: probing deeper at radio and optical wavelengths. MNRAS407(2):721-733. https://doi.org/10.1111/j.1365-2966.2010.16950.x. arXiv:1005.0862 [astro-ph.CO]
- Jonas J, MeerKAT Team (2016) The MeerKAT Radio Telescope. In: MeerKAT Science: On the Pathway to the SKA. p 1
- Jones DH, Read MA, Saunders W, Colless M, Jarrett T, Parker QA, Fairall AP, Mauch T, Sadler EM, Watson FG, Burton D, Campbell LA, Cass P, Croom SM, Dawe J, Fiegert K, Frankcombe L, Hartley M, Huchra J, James D, Kirby E, Lahav O, Lucey J, Mamon GA, Moore L, Peterson BA, Prior S, Proust D, Russell K, Safouris V, Wakamatsu KI, Westra E, Williams M (2009) The 6dF Galaxy Survey: final redshift release (DR3) and southern large-scale structures. MNRAS399(2):683–698. https://doi.org/10.1111/j.1365-2966.2009.15338.x. arXiv:0903.5451 [astro-ph.CO]
- Jones DL (1984) The radio structure of CTA 21. ApJ276:L5–L8. https://doi.org/10.1086/184176
- Joshi SA, Nandi S, Saikia DJ, Ishwara-Chand ra CH, Konar C (2011) A radio

- study of the double-double radio galaxy 3C293. MNRAS414(2):1397–1404. https://doi.org/10.1111/j.1365-2966.2011.18472.x. arXiv:1102.3675 [astro-ph.CO]
- Junor W, Salter CJ, Saikia DJ, Mantovani F, Peck AB (1999) Large differential Faraday rotation in the compact steep-spectrum quasar 3C 147 and jet-medium interactions. MNRAS308:955–960. https://doi.org/10.1046/j. 1365-8711.1999.02774.x
- Jurlin N, Morganti R, Brienza M, Mandal S, Maddox N, Duncan KJ, Shabala SS, Hardcastle MJ, Prandoni I, Röttgering HJA, Mahatma V, Best PN, Mingo B, Sabater J, Shimwell TW, Tasse C (2020) The life cycle of radio galaxies in the LOFAR Lockman Hole field. A&A638:A34. https://doi.org/10.1051/0004-6361/201936955. arXiv:2004.09118 [astro-ph.GA]
- Kaiser CR (2000) The environments and ages of extragalactic radio sources inferred from multi-frequency radio maps. A&A362:447–464. arXiv:astro-ph/0007261 [astro-ph]
- Kaiser CR, Best PN (2007) Luminosity function, sizes and FR dichotomy of radio-loud AGN. MNRAS381(4):1548–1560. https://doi.org/10.1111/j. 1365-2966.2007.12350.x. arXiv:0708.3733 [astro-ph]
- Kaiser CR, Schoenmakers AP, Röttgering HJA (2000) Radio galaxies with a 'double-double' morphology II. The evolution of double-double radio galaxies and implications for the alignment effect in FRII sources. MNRAS315(2):381–394. https://doi.org/10.1046/j.1365-8711.2000.03431.x. arXiv:astro-ph/9912142 [astro-ph]
- Kalfountzou E, Stevens JA, Jarvis MJ, Hardcastle MJ, Wilner D, Elvis M, Page MJ, Trichas M, Smith DJB (2017) Observational evidence that positive and negative AGN feedback depends on galaxy mass and jet power. MNRAS471(1):28–58. https://doi.org/10.1093/mnras/stx1333.arXiv:1706.02334 [astro-ph.GA]
- Kameno S, Horiuchi S, Shen ZQ, Inoue M, Kobayashi H, Hirabayashi H, Murata Y (2000) Asymmetric Free-Free Absorption towards a Double Lobe of OQ 208. PASJ52:209. https://doi.org/10.1093/pasj/52.1.209
- Kameno S, Sawada-Satoh S, Inoue M, Shen ZQ, Wajima K (2001) The Dense Plasma Torus around the Nucleus of an Active Galaxy NGC1052. PASJ53(2):169–178. https://doi.org/10.1093/pasj/53.2.169. arXiv:astro-ph/0104039 [astro-ph]
- Kameno S, Inoue M, Wajima K, Sawada-Satoh S, Shen ZQ (2003) Dense Plasma Torus in the GPS Galaxy NGC 1052. PASA20:134–139. https://doi.org/10.1071/AS03003. astro-ph/0210467
- Kapahi VK (1981) Westerbork observations of radio sources in the 5GHz "S4" survey. A&AS43:381–393
- Kapinska AD, Hardcastle M, Jackson C, An T, Baan W, Jarvis M (2015) Unravelling lifecycles and physics of radio-loud AGN in the SKA Era. Advancing Astrophysics with the Square Kilometre Array (AASKA14) 173. arXiv:1412.5884
- Kato T, Tabara H, Inoue M, Aizu K (1987) Extragalactic radio sources with very large Faraday rotation. Nature329(6136):223–224. https://doi.org/10.

1038/329223a0

- Kawakatu N, Kino M (2006) On the dynamical evolution of hotspots in powerful radio-loud active galactic nuclei. MNRAS370:1513–1518. https://doi.org/10.1111/j.1365-2966.2006.10574.x. astro-ph/0605482
- Kawakatu N, Nagai H, Kino M (2008) The Fate of Young Radio Galaxies: Decelerations Inside Host Galaxies? ApJ687:141–155. https://doi.org/10.1086/591900. arXiv:0807.2103
- Kellermann KI, Vermeulen RC, Zensus JA, Cohen MH (1998) Sub-Milliarcsecond Imaging of Quasars and Active Galactic Nuclei. AJ115(4):1295–1318. https://doi.org/10.1086/300308. arXiv:astro-ph/9801010 [astro-ph]
- Kim M, Ho LC, Lonsdale CJ, Lacy M, Blain AW, Kimball AE (2013) Evidence for Active Galactic Nucleus Driven Outflows in Young Radio Quasars. ApJ768:L9. https://doi.org/10.1088/2041-8205/768/1/L9. arXiv:1303.7194
- Kino M, Asano K (2011) Mini-radio lobes in AGN core illumination and their hadronic gamma-ray afterlight. MNRAS412:L20–L24. https://doi.org/10.1111/j.1745-3933.2010.00996.x. arXiv:1012.5328 [astro-ph.HE]
- Kino M, Kawakatu N, Ito H (2007) Extragalactic MeV γ -ray emission from cocoons of young radio galaxies. MNRAS376:1630–1634. https://doi.org/10.1111/j.1365-2966.2007.11354.x. astro-ph/0611870
- Kino M, Ito H, Kawakatu N, Nagai H (2009) New prediction of extragalactic GeV γ -ray emission from radio lobes of young AGN jets. MNRAS395:L43–L47. https://doi.org/10.1111/j.1745-3933.2009.00638.x. arXiv:0812.1850
- Kino M, Ito H, Kawakatu N, Orienti M (2013) New Class of Very High Energy γ -Ray Emitters: Radio-dark Mini Shells Surrounding Active Galactic Nucleus Jets. ApJ764:134. https://doi.org/10.1088/0004-637X/764/2/134. arXiv:1302.0106 [astro-ph.HE]
- Kirhakos S, Bahcall JN, Schneider DP, Kristian J (1999) The Host Galaxies of Three Radio-loud Quasars: 3C 48, 3C 345, and B2 1425+267. ApJ520:67-77. https://doi.org/10.1086/307430. astro-ph/9902175
- Komossa S (2008) Narrow-line Seyfert 1 Galaxies. In: Revista Mexicana de Astronomia y Astrofisica Conference Series. Revista Mexicana de Astronomia y Astrofisica Conference Series, vol 32. pp 86–92. arXiv:0710.3326 [astro-ph]
- Komossa S, Voges W, Xu D, Mathur S, Adorf HM, Lemson G, Duschl WJ, Grupe D (2006) Radio-loud Narrow-Line Type 1 Quasars. AJ132(2):531–545. https://doi.org/10.1086/505043. arXiv:astro-ph/0603680 [astro-ph]
- Kosmaczewski E, Stawarz L, Siemiginowska A, Cheung CC, Ostorero L, Sobolewska M, Kozieł-Wierzbowska D, Wójtowicz A, Marchenko V (2020) Mid-infrared Diagnostics of the Circumnuclear Environments of the Youngest Radio Galaxies. ApJ897(2):164. https://doi.org/10.3847/1538-4357/ab9b1f. arXiv:2002.12870 [astro-ph.HE]
- Kotilainen JK, León-Tavares J, Olguín-Iglesias A, Baes M, Anórve C, Chavushyan V, Carrasco L (2016) Discovery of a Pseudobulge Galaxy Launching Powerful Relativistic Jets. ApJ832(2):157. https://doi.org/10.3847/0004-637X/832/2/157. arXiv:1609.02417 [astro-ph.GA]
- Kovalev YY (2005) "TEMPORARY GPS/HFP" Radio Sources. Baltic As-

- tronomy 14:413-416
- Kovalev YY, Kovalev YA, Nizhelsky NA, Bogdantsov AB (2002) Broad-band Radio Spectra Variability of 550 AGN in 1997-2001. PASA19(1):83–87. https://doi.org/10.1071/AS01109
- Krauß F, Kreter M, Müller C, Markowitz A, Böck M, Burnett T, Dauser T, Kadler M, Kreikenbohm A, Ojha R, Wilms J (2018) Investigating source confusion in PMN J1603-4904. A&A610:L8. https://doi.org/10.1051/0004-6361/201732338. arXiv:1801.01702 [astro-ph.HE]
- Krips M, Eckart A, Neri R, Zuther J, Downes D, Scharwächter J (2005) Molecular gas and continuum emission in 3C 48: evidence for two merger nuclei? A&A439:75–84. https://doi.org/10.1051/0004-6361:20052643. astro-ph/0505161
- Krishna G, Sirothia SK, Mhaskey M, Ranadive P, Wiita PJ, Goyal A, Kantharia NG, Ishwara-Chandra CH (2014) Extragalactic radio sources with sharply inverted spectrum at metre wavelengths. MNRAS443(3):2824–2829. https://doi.org/10.1093/mnras/stu1364. arXiv:1407.4255 [astro-ph.HE]
- Krongold Y, Dultzin-Hacyan D, Marziani P (2001) Host Galaxies and Circum-galactic Environment of "Narrow Line" Seyfert 1 Nuclei. AJ121(2):702–709. https://doi.org/10.1086/318768
- Kunert M, Marecki A, Spencer RE, Kus AJ, Niezgoda J (2002) FIRST-based survey of Compact Steep Spectrum sources. I. MERLIN images of arcsecond scale objects. A&A391:47–54. https://doi.org/10.1051/0004-6361: 20020532. astro-ph/0112511
- Kunert-Bajraszewska M (2016) Dichotomy in the population of young AGN: Optical, radio, and X-ray properties. Astron Nachr 337:27. https://doi.org/10.1002/asna.201512259. arXiv:1510.09061
- Kunert-Bajraszewska M, Labiano A (2010) A survey of low-luminosity compact sources and its implication for the evolution of radio-loud active galactic nuclei II. Optical analysis. MNRAS408:2279–2289. https://doi.org/10.1111/j.1365-2966.2010.17300.x. arXiv:1009.5237
- Kunert-Bajraszewska M, Thomasson P (2009) A survey of Low Luminosity Compact sources. Astron Nachr 330:210. https://doi.org/10.1002/asna. 200811158. arXiv:0903.3838 [astro-ph.CO]
- Kunert-Bajraszewska M, Marecki A, Thomasson P, Spencer RE (2005) FIRST-based survey of Compact Steep Spectrum sources. II. MERLIN and VLA observations of medium-sized symmetric objects. A&A440:93–105. https://doi.org/10.1051/0004-6361:20042496. astro-ph/0505435
- Kunert-Bajraszewska M, Marecki A, Thomasson P (2006) FIRST-based survey of compact steep spectrum sources. IV. Multifrequency VLBA observations of very compact objects. A&A450:945–958. https://doi.org/10.1051/0004-6361:20054428. astro-ph/0601288
- Kunert-Bajraszewska M, Gawroński MP, Labiano A, Siemiginowska A (2010) A survey of low-luminosity compact sources and its implication for the evolution of radio-loud active galactic nuclei I. Radio data. MNRAS408:2261–2278. https://doi.org/10.1111/j.1365-2966.2010.17271.x. arXiv:1009.5235
- Kunert-Bajraszewska M, Siemiginowska A, Labiano A (2013) An X-Ray

- Cooling-core Cluster Surrounding a Low-power Compact Steep Spectrum Radio Source 1321+045. ApJ772:L7. https://doi.org/10.1088/2041-8205/772/1/L7. arXiv:1306.5579
- Kunert-Bajraszewska M, Labiano A, Siemiginowska A, Guainazzi M (2014) First X-ray observations of low-power compact steep spectrum sources. MNRAS437:3063–3071. https://doi.org/10.1093/mnras/stt1978.arXiv:1311.6633
- Kuźmicz A, Jamrozy M, Kozieł-Wierzbowska D, Wezgowiec M (2017) Optical and radio properties of extragalactic radio sources with recurrent jet activity. MNRAS471(4):3806–3826. https://doi.org/10.1093/mnras/stx1830.arXiv:1709.01802 [astro-ph.GA]
- Labiano A (2008) Tracing jet-ISM interaction in young AGN: correlations between [O III] λ 5007 Å and 5-GHz emission. A&A488:L59–L62. https://doi.org/10.1051/0004-6361:200810399. arXiv:0807.2230
- Labiano A (2009) Relationship between the [O III] λ 5007 line and 5 GHz radio emission. Astron Nachr 330:241. https://doi.org/10.1002/asna.200811166. arXiv:0806.3899
- Labiano A, O'Dea CP, Gelderman R, de Vries WH, Axon DJ, Barthel PD, Baum SA, Capetti A, Fanti R, Koekemoer AM, Morganti R, Tadhunter CN (2005) HST/STIS low dispersion spectroscopy of three Compact Steep Spectrum sources. Evidence for jet-cloud interaction. A&A436:493–501. https://doi.org/10.1051/0004-6361:20042425. astro-ph/0504330
- Labiano A, Vermeulen RC, Barthel PD, O'Dea CP, Gallimore JF, Baum S, de Vries W (2006) H I absorption in 3C 49 and 3C 268.3. Probing the environment of compact steep spectrum and GHz peaked spectrum sources. A&A447:481–487. https://doi.org/10.1051/0004-6361: 20053856. astro-ph/0510563
- Labiano A, Barthel PD, O'Dea CP, de Vries WH, Pérez I, Baum SA (2007) GPS radio sources: new optical observations and an updated master list. A&A463:97–104. https://doi.org/10.1051/0004-6361:20066183. astro-ph/0611600
- Labiano A, O'Dea CP, Barthel PD, de Vries WH, Baum SA (2008) Star formation in the hosts of GHz peaked spectrum and compact steep spectrum radio galaxies. A&A477:491–501. https://doi.org/10.1051/0004-6361: 20077112. astro-ph/0701619
- Labiano A, García-Burillo S, Combes F, Usero A, Soria-Ruiz R, Piqueras López J, Fuente A, Hunt L, Neri R (2014) Fueling the central engine of radio galaxies. III. Molecular gas and star formation efficiency of ¡ASTROBJ¿3C 293¡/ASTROBJ¿. A&A564:A128. https://doi.org/10.1051/0004-6361/201323123. arXiv:1402.7208 [astro-ph.GA]
- Lacy M, Rawlings S, Blundell KM, Ridgway SE (1998) A radio-jet-galaxy interaction in 3C 441. MNRAS298(4):966-976. https://doi.org/10.1046/j. 1365-8711.1998.01591.x. arXiv:astro-ph/9803017 [astro-ph]
- Lacy M, Croft S, Fragile C, Wood S, Nyland K (2017) ALMA Observations of the Interaction of a Radio Jet with Molecular Gas in Minkowski's Object. ApJ838(2):146. https://doi.org/10.3847/1538-4357/

aa65d7. arXiv:1703.03006 [astro-ph.GA]

- Lacy M, Baum SA, Chandler CJ, Chatterjee S, Clarke TE, Deustua S, English J, Farnes J, Gaensler BM, Gugliucci N, Hallinan G, Kent BR, Kimball A, Law CJ, Lazio TJW, Marvil J, Mao SA, Medlin D, Mooley K, Murphy EJ, Myers S, Osten R, Richards GT, Rosolowsky E, Rudnick L, Schinzel F, Sivakoff GR, Sjouwerman LO, Taylor R, White RL, Wrobel J, Andernach H, Beasley AJ, Berger E, Bhatnager S, Birkinshaw M, Bower GC, Brandt WN, Brown S, Burke-Spolaor S, Butler BJ, Comerford J, Demorest PB, Fu H, Giacintucci S, Golap K, Güth T, Hales CA, Hiriart R, Hodge J, Horesh A, Ivezić Ž, Jarvis MJ, Kamble A, Kassim N, Liu X, Loinard L, Lyons DK, Masters J, Mezcua M, Moellenbrock GA, Mroczkowski T, Nyland K, O'Dea CP, O'Sullivan SP, Peters WM, Radford K, Rao U, Robnett J, Salcido J, Shen Y, Sobotka A, Witz S, Vaccari M, van Weeren RJ, Vargas A, Williams PKG, Yoon I (2020) The Karl G. Jansky Very Large Array Sky Survey (VLASS). Science Case and Survey Design. PASP132(1009):035001. https://doi.org/10.1088/1538-3873/ab63eb. arXiv:1907.01981 [astro-ph.IM] Laing RA (1981) Multifrequency observations of 40 powerful extragalactic
- Laing RA (1981) Multifrequency observations of 40 powerful extragalactic sources with the 5-km telescope. MNRAS195:261–324. https://doi.org/10.1093/mnras/195.2.261
- Laing RA (1988) The sidedness of jets and depolarization in powerful extragalactic radio sources. Nature331(6152):149–151. https://doi.org/10.1038/331149a0
- Laing RA, Riley JM, Longair MS (1983) Bright radio sources at 178 MHz: flux densities, optical identifications and the cosmological evolution of powerful radio galaxies. MNRAS204:151–187. https://doi.org/10.1093/mnras/204.1.151
- Laing RA, Jenkins CR, Wall JV, Unger SW (1994) Spectrophotometry of a Complete Sample of 3CR Radio Sources: Implications for Unified Models. In:
 Bicknell GV, Dopita MA, Quinn PJ (eds) The Physics of Active Galaxies.
 Astronomical Society of the Pacific Conference Series, vol 54. p 201
- Lanz L, Ogle PM, Evans D, Appleton PN, Guillard P, Emonts B (2015) Jet-ISM Interaction in the Radio Galaxy 3C 293: Jet-driven Shocks Heat ISM to Power X-Ray and Molecular H₂ Emission. ApJ801(1):17. https://doi.org/10.1088/0004-637X/801/1/17. arXiv:1501.01010 [astro-ph.GA]
- Ledlow MJ, Owen FN (1996) 20 CM VLA Survey of Abell Clusters of Galaxies. VI. Radio/Optical Luminosity Functions. AJ112:9. https://doi.org/10.1086/117985. arXiv:astro-ph/9607014 [astro-ph]
- Leipski C, Antonucci R, Ogle P, Whysong D (2009) The Spitzer View of FR I Radio Galaxies: On the Origin of the Nuclear Mid-Infrared Continuum. ApJ701(2):891–914. https://doi.org/10.1088/0004-637X/701/2/891.arXiv:0906.2152 [astro-ph.CO]
- Liao M, Gu M (2020) Investigation on young radio AGNs based on SDSS spectroscopy. MNRAS491(1):92–112. https://doi.org/10.1093/mnras/stz2981.arXiv:1910.09452 [astro-ph.GA]
- Liao M, Gu M, Zhou M, Chen L (2020) The X-ray emission in young radio active galactic nuclei. MNRAS497(1):482–497. https://doi.org/10.1093/

- mnras/staa1559. arXiv:2006.01079 [astro-ph.GA]
- Lister ML, Aller MF, Aller HD, Homan DC, Kellermann KI, Kovalev YY, Pushkarev AB, Richards JL, Ros E, Savolainen T (2013) MOJAVE. X. Parsec-scale Jet Orientation Variations and Superluminal Motion in Active Galactic Nuclei. AJ146(5):120. https://doi.org/10.1088/0004-6256/146/5/120. arXiv:1308.2713 [astro-ph.CO]
- Lister ML, Homan DC, Hovatta T, Kellermann KI, Kiehlmann S, Kovalev YY, Max-Moerbeck W, Pushkarev AB, Readhead ACS, Ros E, Savolainen T (2019) MOJAVE. XVII. Jet Kinematics and Parent Population Properties of Relativistically Beamed Radio-loud Blazars. ApJ874(1):43. https://doi.org/10.3847/1538-4357/ab08ee. arXiv:1902.09591 [astro-ph.GA]
- Lister ML, Homan DC, Kovalev YY, Mand al S, Pushkarev AB, Siemiginowska A (2020) TXS 0128+554: A Young Gamma-Ray-emitting Active Galactic Nucleus with Episodic Jet Activity. ApJ899(2):141. https://doi.org/10.3847/1538-4357/aba18d. arXiv:2006.16970 [astro-ph.GA]
- Lonsdale CJ, Barthel PD (1986) Double hotspots and flow redirection in the lobes of powerful extragalactic radio sources. AJ92:12–22. https://doi.org/10.1086/114130
- Lonsdale CJ, Lacy M, Kimball AE, Blain A, Whittle M, Wilkes B, Stern D, Condon J, Kim M, Assef RJ, Tsai CW, Efstathiou A, Jones S, Eisenhardt P, Bridge C, Wu J, Lonsdale CJ, Jones K, Jarrett T, Smith R (2015) Radio Jet Feedback and Star Formation in Heavily Obscured, Hyperluminous Quasars at Redshifts ~ 0.5-3. I. ALMA Observations. ApJ813:45. https://doi.org/10.1088/0004-637X/813/1/45. arXiv:1509.00342
- Luo WF, Yang J, Cui L, Liu X, Shen ZQ (2007) Seven-frequency VLBI Observations of the GHz-Peaked-Spectrum Source OQ 208. Chinese J. Astron. Astrophys.7:611–619. https://doi.org/10.1088/1009-9271/7/5/01.astro-ph/0703752
- Maccagni FM, Morganti R, Oosterloo TA, Mahony EK (2014) What triggers a radio AGN?. The intriguing case of PKS B1718-649. A&A571:A67. https://doi.org/10.1051/0004-6361/201424334. arXiv:1409.0566 [astro-ph.GA]
- Maccagni FM, Santoro F, Morganti R, Oosterloo TA, Oonk JBR, Emonts BHC (2016a) PKS B1718-649: An H I and H₂ perspective on the birth of a compact radio source. Astron Nachr 337:154. https://doi.org/10.1002/asna. 201512285. arXiv:1511.01628
- Maccagni FM, Santoro F, Morganti R, Oosterloo TA, Oonk JBR, Emonts BHC (2016b) The warm molecular hydrogen of PKS B1718-649. Feeding a newly born radio AGN. A&A588:A46. https://doi.org/10.1051/0004-6361/201528016. arXiv:1602.00701
- Maccagni FM, Morganti R, Oosterloo TA, Geréb K, Maddox N (2017) Kinematics and physical conditions of H I in nearby radio sources. The last survey of the old Westerbork Synthesis Radio Telescope. A&A604:A43. https://doi.org/10.1051/0004-6361/201730563. arXiv:1705.00492 [astro-ph.GA]
- Maccagni FM, Morganti R, Oosterloo TA, Oonk JBR, Emonts BHC (2018) ALMA observations of AGN fuelling. The case of PKS B1718-649. A&A614:A42. https://doi.org/10.1051/0004-6361/201732269.

arXiv:1801.03514

- Machalski J, Kozieł-Wierzbowska D, Jamrozy M, Saikia DJ (2008) J1420-0545: The Radio Galaxy Larger than 3C 236. ApJ679(1):149–155. https://doi.org/10.1086/586703. arXiv:0808.2742 [astro-ph]
- Maciel T, Alexander P (2014) Radio source evolution on galactic scales. MNRAS442:3469–3483. https://doi.org/10.1093/mnras/stu1111.arXiv:1406.1101
- Macquart JP, Kedziora-Chudczer L, Rayner DP, Jauncey DL (2000) Strong, Variable Circular Polarization in PKS 1519-273. ApJ538(2):623–627. https://doi.org/10.1086/309184
- Mahatma VH, Hardcastle MJ, Williams WL, Best PN, Croston JH, Duncan K, Mingo B, Morganti R, Brienza M, Cochrane RK, Gürkan G, Harwood JJ, Jarvis MJ, Jamrozy M, Jurlin N, Morabito LK, Röttgering HJA, Sabater J, Shimwell TW, Smith DJB, Shulevski A, Tasse C (2019) LoTSS DR1: Double-double radio galaxies in the HETDEX field. A&A622:A13. https://doi.org/10.1051/0004-6361/201833973. arXiv:1811.08194 [astro-ph.GA]
- Maness HL, Taylor GB, Zavala RT, Peck AB, Pollack LK (2004) Breaking All the Rules: The Compact Symmetric Object 0402+379. ApJ602:123–134. https://doi.org/10.1086/380919. astro-ph/0310663
- Mantovani F, Junor W, Ricci R, Saikia DJ, Salter C, Bondi M (2002) Milliarcsecond scale rotation measure in the CSS quasars 0548+165 and 1524-136. A&A389:58-67. https://doi.org/10.1051/0004-6361:20020482. astro-ph/0203338
- Mantovani F, Rossetti A, Junor W, Saikia DJ, Salter CJ (2005) VLBA Polarimetric Observations of Young Radio Sources. In: Romney J, Reid M (eds) Future Directions in High Resolution Astronomy. Astronomical Society of the Pacific Conference Series, vol 340. p 186
- Mantovani F, Mack KH, Montenegro-Montes FM, Rossetti A, Kraus A (2009) Effelsberg 100-m polarimetric observations of a sample of compact steep-spectrum sources. A&A502:61–65. https://doi.org/10.1051/0004-6361/200911815. arXiv:0906.1729
- Mantovani F, Rossetti A, Junor W, Saikia DJ, Salter CJ (2010) Radio polarimetry of 3C 119, 3C 318, and 3C 343 at milliarcsecond resolution. A&A518:A33. https://doi.org/10.1051/0004-6361/201014400.arXiv:1005.2950
- Maraschi L, Colpi M, Ghisellini G, Perego A, Tavecchio F (2012) On the role of black hole spin and accretion in powering relativistic jets in AGN. In: Journal of Physics Conference Series. vol 355. p 012016. https://doi.org/10.1088/1742-6596/355/1/012016
- Marecki A, Szablewski M (2009) Evidence of a double-double morphology in B 0818+214. A&A506:L33-L36. https://doi.org/10.1051/0004-6361/200912980. arXiv:0909.3741 [astro-ph.CO]
- Marecki A, Barthel PD, Polatidis A, Owsianik I (2003a) 1245+676 A CSO/GPS Source being an Extreme Case of a Double-Double Structure. PASA20:16–18. https://doi.org/10.1071/AS02032. astro-ph/0209212
- Marecki A, Spencer RE, Kunert M (2003b) Location of Weak CSS Sources

- on the Evolutionary Path of Radio-Loud AGN. PASA20:46–49. https://doi.org/10.1071/AS02051. astro-ph/0211253
- Marr JM, Taylor GB, Crawford F III (2001) Nonuniform Free-Free Absorption in the GPS Radio Galaxy 0108+388. ApJ550:160-171. https://doi.org/10.1086/319729. astro-ph/0011372
- Marr JM, Perry TM, Read J, Taylor GB, Morris AO (2014) Multi-frequency Optical-depth Maps and the Case for Free-Free Absorption in Two Compact Symmetric Radio Sources: The CSO Candidate J1324 + 4048 and the CSO J0029 + 3457. ApJ780:178. https://doi.org/10.1088/0004-637X/780/2/178. arXiv:1311.5762
- Martini P (2004) Why does low-luminosity AGN fueling remain an unsolved problem? In: Storchi-Bergmann T, Ho LC, Schmitt HR (eds) The Interplay Among Black Holes, Stars and ISM in Galactic Nuclei. IAU Symposium, vol 222. pp 235–241. https://doi.org/10.1017/S1743921304002170. arXiv:astro-ph/0404426 [astro-ph]
- Massardi M, Bonaldi A, Bonavera L, De Zotti G, Lopez-Caniego M, Galluzzi V (2016) The Planck-ATCA Co-eval Observations project: analysis of radio source properties between 5 and 217 GHz. MNRAS455:3249–3262. https://doi.org/10.1093/mnras/stv2561. arXiv:1511.02605
- Massaro F, Chiaberge M, Grandi P, Giovannini G, O'Dea CP, Macchetto FD, Baum SA, Gilli R, Capetti A, Bonafede A, Liuzzo E (2009) Extended X-Ray Emission in Radio Galaxies: The Peculiar Case of 3C 305. ApJ692:L123–L126. https://doi.org/10.1088/0004-637X/692/2/L123.arXiv:0901.1286 [astro-ph.HE]
- Massaro F, Harris DE, Tremblay GR, Axon D, Baum SA, Capetti A, Chiaberge M, Gilli R, Giovannini G, Grandi P, Macchetto FD, O'Dea CP, Risaliti G, Sparks W (2010) Chandra Observations of 3C Radio Sources with z < 0.3: Nuclei, Diffuse Emission, Jets, and Hotspots. ApJ714(1):589–604. https://doi.org/10.1088/0004-637X/714/1/589. arXiv:1003.2438 [astro-ph.HE]
- Massaro F, Missaglia V, Stuardi C, Harris DE, Kraft RP, Paggi A, Liuzzo E, Tremblay GR, Baum SA, O'Dea CP, Wilkes BJ, Kuraszkiewicz J, Forman WR (2018) The 3CR Chandra Snapshot Survey: Extragalactic Radio Sources with 0.5 < z < 1.0. ApJS234(1):7. https://doi.org/10.3847/1538-4365/aa8e9d. arXiv:1807.10774 [astro-ph.HE]
- Mathur S (2000) Narrow-line Seyfert 1 galaxies and the evolution of galaxies and active galaxies. MNRAS314(4):L17–L20. https://doi.org/10.1046/j. 1365-8711.2000.03530.x. arXiv:astro-ph/0003111 [astro-ph]
- Mathur S, Fields D, Peterson BM, Grupe D (2012) Supermassive Black Holes, Pseudobulges, and the Narrow-line Seyfert 1 Galaxies. ApJ754(2):146. https://doi.org/10.1088/0004-637X/754/2/146. arXiv:1102.0537 [astro-ph.CO]
- Mauch T, Sadler EM (2007) Radio sources in the 6dFGS: local luminosity functions at 1.4GHz for star-forming galaxies and radio-loud AGN. MNRAS375(3):931–950. https://doi.org/10.1111/j.1365-2966.2006.11353.x. arXiv:astro-ph/0612018 [astro-ph]
- Mauch T, Murphy T, Buttery HJ, Curran J, Hunstead RW, Piestrzynski B, Robertson JG, Sadler EM (2003) SUMSS: a wide-field radio imaging sur-

vey of the southern sky – II. The source catalogue. MNRAS342:1117–1130. https://doi.org/10.1046/j.1365-8711.2003.06605.x. astro-ph/0303188

Mauch T, Cotton WD, Condon JJ, Matthews AM, Abbott TD, Adam RM, Aldera MA, Asad KMB, Bauermeister EF, Bennett TGH, Bester H, Botha DH, Brederode LRS, Brits ZB, Buchner SJ, Burger JP, Camilo F, Chalmers JM, Cheetham T, de Villiers D, de Villiers MS, Dikgale-Mahlakoana MA, du Toit LJ, Esterhuyse SWP, Fadana G, Fanaroff BL, Fataar S, February S, Frank BS, Gamatham RRG, Geyer M, Goedhart S, Gounden S, Gumede SC, Heywood I, Hlakola MJ, Horrell JMG, Hugo B, Isaacson AR, Józsa GIG, Jonas JL, Julie RPM, Kapp FB, Kasper VA, Kenyon JS, Kotzé PPA, Kriek N, Kriel H, Kusel TW, Lehmensiek R, Loots A, Lord RT, Lunsky BM, Madisa K, Magnus LG, Main JPL, Malan JA, Manley JR, Marais SJ, Martens A, Merry B, Millenaar R, Mnyandu N, Moeng IPT, Mokone OJ, Monama TE, Mphego MC, New WS, Ngcebetsha B, Ngoasheng KJ, Ockards MTO, Oozeer N, Otto AJ, Patel AA, Peens-Hough A, Perkins SJ, Ramaila AJT, Ramudzuli ZR, Renil R, Richter LL, Robyntjies A, Salie S, Schollar CTG, Schwardt LC, Serylak M, Siebrits R, Sirothia SK, Smirnov OM, Sofeya L, Stone G, Taljaard B, Tasse C, Theron IP, Tiplady AJ, Toruvanda O, Twum SN, van Balla TJ, van der Byl A, van der Merwe C, Van Tonder V, Wallace BH, Welz MG, Williams LP, Xaia B (2020) The 1.28 GHz MeerKAT DEEP2 Image. ApJ888(2):61. https://doi.org/10.3847/1538-4357/ab5d2d. arXiv:1912.06212 [astro-ph.GA]

McCarthy PJ (1993) High redshift radio galaxies. ARA&A31:639–688. https://doi.org/10.1146/annurev.aa.31.090193.003231

McClintock JE, Remillard RA (2006) Black hole binaries. In: Lewin W, van der Klis M (eds) Compact stellar X-ray sources. vol 39. Cambridge University Press, Cambridge, UK, pp 157–213. https://doi.org/10.1017/CBO9780511536281.005

McNamara BR, Nulsen PEJ (2007) Heating Hot Atmospheres with Active Galactic Nuclei. ARA&A45(1):117–175. https://doi.org/10.1146/annurev.astro.45.051806.110625. arXiv:0709.2152 [astro-ph]

McNamara BR, Nulsen PEJ (2012) Mechanical feedback from active galactic nuclei in galaxies, groups and clusters. New Journal of Physics 14(5):055023. https://doi.org/10.1088/1367-2630/14/5/055023. arXiv:1204.0006 [astro-ph.CO]

Mellema G, Kurk JD, Röttgering HJA (2002) Evolution of clouds in radio galaxy cocoons. A&A395:L13–L16. https://doi.org/10.1051/0004-6361: 20021408. arXiv:astro-ph/0209601 [astro-ph]

Merloni A, Heinz S, di Matteo T (2003) A Fundamental Plane of black hole activity. MNRAS345(4):1057–1076. https://doi.org/10.1046/j. 1365-2966.2003.07017.x. arXiv:astro-ph/0305261 [astro-ph]

Mhaskey M, Gopal-Krishna, Dabhade P, Paul S, Salunkhe S, Sirothia SK (2019a) GMRT observations of extragalactic radio sources with steeply inverted spectra. MNRAS485(2):2447–2456. https://doi.org/10.1093/mnras/stz335. arXiv:1901.11217 [astro-ph.GA]

Mhaskey M, Gopal-Krishna, Paul S, Dabhade P, Salunkhe S, Bhagat S, Ben-

- dre A (2019b) GMRT observations of a first sample of 'Extremely Inverted Spectrum Extragalactic Radio Sources (EISERS)' candidates in the Northern sky. MNRAS489(3):3506–3518. https://doi.org/10.1093/mnras/stz2379. arXiv:1908.08883 [astro-ph.GA]
- Middelberg E, Norris RP, Hales CA, Seymour N, Johnston-Hollitt M, Huynh MT, Lenc E, Mao MY (2011) The radio properties of infrared-faint radio sources. A&A526:A8. https://doi.org/10.1051/0004-6361/201014926.arXiv:1011.2391 [astro-ph.CO]
- Migliori G (2016) The high-energy view of young radio sources: X-ray and gamma-ray observations. Astron Nachr 337:52. https://doi.org/10.1002/asna.201512264
- Migliori G, Siemiginowska A, Celotti A (2012) Broadband Jet Emission in Young and Powerful Radio Sources: The Case of the Compact Steep Spectrum Quasar 3C 186. ApJ749:107. https://doi.org/10.1088/0004-637X/749/2/107. arXiv:1202.3153 [astro-ph.HE]
- Migliori G, Siemiginowska A, Kelly BC, Stawarz L, Celotti A, Begelman MC (2014) Jet Emission in Young Radio Sources: A Fermi Large Area Telescope Gamma-Ray View. ApJ780:165. https://doi.org/10.1088/0004-637X/780/2/165. arXiv:1311.7647 [astro-ph.HE]
- Migliori G, Siemiginowska A, Sobolewska M, Loh A, Corbel S, Ostorero L, Stawarz L (2016) First Detection in Gamma-Rays of a Young Radio Galaxy: Fermi-LAT Observations of the Compact Symmetric Object PKS 1718-649. ApJ821:L31. https://doi.org/10.3847/2041-8205/821/2/L31. arXiv:1604.01987 [astro-ph.HE]
- Mingaliev MG, Sotnikova YV, Torniainen I, Tornikoski M, Udovitskiy RY (2012) Multifrequency study of GHz-peaked spectrum sources and candidates with the RATAN-600 radio telescope. A&A544:A25. https://doi.org/10.1051/0004-6361/201118506
- Mingaliev MG, Sotnikova YV, Mufakharov TV, Erkenov AK, Udovitskiy RY (2013) Gigahertz-peaked spectrum (GPS) galaxies and quasars. Astrophysical Bulletin 68:262–272. https://doi.org/10.1134/S1990341313030036
- Mingo B, Hardcastle MJ, Croston JH, Dicken D, Evans DA, Morganti R, Tadhunter C (2014) An X-ray survey of the 2 Jy sample I. Is there an accretion mode dichotomy in radio-loud AGN? MNRAS440(1):269–297. https://doi.org/10.1093/mnras/stu263. arXiv:1402.1770 [astro-ph.GA]
- Mingo B, Croston JH, Hardcastle MJ, Best PN, Duncan KJ, Morganti R, Rottgering HJA, Sabater J, Shimwell TW, Williams WL, Brienza M, Gurkan G, Mahatma VH, Morabito LK, Prandoni I, Bondi M, Ineson J, Mooney S (2019) Revisiting the Fanaroff-Riley dichotomy and radio-galaxy morphology with the LOFAR Two-Metre Sky Survey (LoTSS). MNRAS488(2):2701–2721. https://doi.org/10.1093/mnras/stz1901. arXiv:1907.03726 [astro-ph.GA]
- Miraghaei H, Best PN (2017) The nuclear properties and extended morphologies of powerful radio galaxies: the roles of host galaxy and environment. MNRAS466(4):4346–4363. https://doi.org/10.1093/mnras/stx007. arXiv:1701.00919 [astro-ph.GA]

- Morganti R, Oosterloo T (2018) The interstellar and circumnuclear medium of active nuclei traced by HI 21 cm absorption. A&A Rev.26(1):4. https://doi.org/10.1007/s00159-018-0109-x. arXiv:1807.01475 [astro-ph.GA]
- Morganti R, Tadhunter CN, Dickson R, Shaw M (1997) Clues on the nature of Compact Steep Spectrum radio sources from optical spectroscopy. A&A326:130–138
- Morganti R, Tadhunter CN, Oosterloo TA, Holt J, Tzioumis A, Wills K (2003) The Impact of the Early Stages of Radio Source Evolution on the ISM of the Host Galaxies. PASA20:129–133. https://doi.org/10.1071/AS02056.astro-ph/0212321
- Morganti R, Oosterloo TA, Tadhunter CN, van Moorsel G, Emonts B (2005a) The location of the broad HI absorption in 3C 305: clear evidence for a jet-accelerated neutral outflow. A&A439(2):521–526. https://doi.org/10.1051/0004-6361:20053175. arXiv:astro-ph/0505365 [astro-ph]
- Morganti R, Tadhunter CN, Oosterloo TA (2005b) Fast neutral outflows in powerful radio galaxies: a major source of feedback in massive galaxies. A&A444(1):L9–L13. https://doi.org/10.1051/0004-6361: 200500197. arXiv:astro-ph/0510263 [astro-ph]
- Morganti R, Holt J, Tadhunter C, Ramos Almeida C, Dicken D, Inskip K, Oosterloo T, Tzioumis T (2011) PKS 1814-637: a powerful radio-loud AGN in a disk galaxy. A&A535:A97. https://doi.org/10.1051/0004-6361/201117686. arXiv:1109.0630
- Morganti R, Fogasy J, Paragi Z, Oosterloo T, Orienti M (2013) Radio Jets Clearing the Way Through a Galaxy: Watching Feedback in Action. Science 341:1082–1085. https://doi.org/10.1126/science.1240436. arXiv:1309.1240
- Morganti R, Sadler EM, Curran S (2015) Cool Outflows and HI absorbers with SKA. In: Advancing Astrophysics with the Square Kilometre Array (AASKA14). p 134. arXiv:1501.01091 [astro-ph.GA]
- Morganti R, Oosterloo T, Oonk JBR, Santoro F, Tadhunter C (2016) The missing link: Tracing molecular gas in the outer filament of Centaurus A. A&A592:L9. https://doi.org/10.1051/0004-6361/201628950.arXiv:1605.06598 [astro-ph.GA]
- Morganti R, Oosterloo T, Tadhunter CN (2020) Taking snapshots of the jet-ISM interplay with ALMA. arXiv e-prints arXiv:2005.04765 [astro-ph.HE]
- Moss VA, Allison JR, Sadler EM, Urquhart R, Soria R, Callingham JR, Curran SJ, Musaeva A, Mahony EK, Glowacki M, Farrell SA, Bannister KW, Chippendale AP, Edwards PG, Harvey-Smith L, Heywood I, Hotan AW, Indermuehle BT, Lenc E, Marvil J, McConnell D, Reynolds JE, Voronkov MA, Wark RM, Whiting MT (2017) Connecting X-ray absorption and 21 cm neutral hydrogen absorption in obscured radio AGN. MNRAS471:2952–2973. https://doi.org/10.1093/mnras/stx1679. arXiv:1707.01542
- Mould JR, Ridgewell A, Gallagher I John S, Bessell MS, Keller S, Calzetti D, Clarke JT, Trauger JT, Grillmair C, Ballester GE, Burrows CJ, Krist J, Crisp D, Evans R, Griffiths R, Hester JJ, Hoessel JG, Holtzman JA, Scowen PA, Stapelfeldt KR, Sahai R, Watson A, Meadows V (2000) Jetinduced Star Formation in Centaurus A. ApJ536(1):266–276. https://doi.

org/10.1086/308927

- Moy E, Rocca-Volmerange B (2002) The balance between shocks and AGN photoionization in radio sources and its relation to the radio size. A&A383:46–55. https://doi.org/10.1051/0004-6361:20011727. astro-ph/0201139
- Mukherjee D, Bicknell GV, Sutherland R, Wagner A (2016) Relativistic jet feedback in high-redshift galaxies I. Dynamics. MNRAS461(1):967–983. https://doi.org/10.1093/mnras/stw1368. arXiv:1606.01143 [astro-ph.HE]
- Mukherjee D, Bicknell GV, Sutherland R, Wagner A (2017) Erratum: Relativistic jet feedback in high-redshift galaxies I. Dynamics. MNRAS471(3):2790–2800. https://doi.org/10.1093/mnras/stx1749
- Mukherjee D, Bicknell GV, Wagner AeY, Sutherland RS, Silk J (2018a) Relativistic jet feedback III. Feedback on gas discs. MNRAS479(4):5544–5566. https://doi.org/10.1093/mnras/sty1776. arXiv:1803.08305 [astro-ph.HE]
- Mukherjee D, Wagner AY, Bicknell GV, Morganti R, Oosterloo T, Nesvadba N, Sutherland RS (2018b) The jet-ISM interactions in IC 5063. MNRAS476(1):80–95. https://doi.org/10.1093/mnras/sty067.arXiv:1801.06875 [astro-ph.HE]
- Mullaney JR, Alexander DM, Fine S, Goulding AD, Harrison CM, Hickox RC (2013) Narrow-line region gas kinematics of 24,264 optically selected AGN: the radio connection. MNRAS433(1):622–638. https://doi.org/10.1093/mnras/stt751. arXiv:1305.0263 [astro-ph.CO]
- Müller C, Kadler M, Ojha R, Böck M, Krauß F, Taylor GB, Wilms J, Blanchard J, Carpenter B, Dauser T, Dutka M, Edwards PG, Gehrels N, Großberger C, Hase H, Horiuchi S, Kreikenbohm A, Lovell JEJ, McConville W, Phillips C, Plötz C, Pursimo T, Quick J, Ros E, Schulz R, Stevens J, Tingay SJ, Trüstedt J, Tzioumis AK, Zensus JA (2014) The unusual multiwavelength properties of the gamma-ray source PMN J1603-4904. A&A562:A4. https://doi.org/10.1051/0004-6361/201322827.arXiv:1312.4827 [astro-ph.HE]
- Müller C, Burd PR, Schulz R, Coppejans R, Falcke H, Intema H, Kadler M, Krauß F, Ojha R (2016) The MHz-peaked radio spectrum of the unusual γ -ray source PMN J1603-4904. A&A593:L19. https://doi.org/10.1051/0004-6361/201629547. arXiv:1609.01992 [astro-ph.HE]
- Murgia M (2003) Spectral Ages of CSOs and CSS Sources. PASA20:19–24. https://doi.org/10.1071/AS02033. astro-ph/0302376
- Murgia M, Fanti C, Fanti R, Gregorini L, Klein U, Mack KH, Vigotti M (1999) Synchrotron spectra and ages of compact steep spectrum radio sources. A&A345:769–777
- Murphy T, Sadler EM, Ekers RD, Massardi M, Hancock PJ, Mahony E, Ricci R, Burke-Spolaor S, Calabretta M, Chhetri R (2010) The Australia Telescope 20 GHz Survey: the source catalogue. MNRAS402(4):2403–2423. https://doi.org/10.1111/j.1365-2966.2009.15961.x. arXiv:0911.0002 [astro-ph.GA]
- Murthy S, Morganti R, Oosterloo T, Schulz R, Mukherjee D, Wagner AY, Bicknell G, Prandoni I, Shulevski Aa (2019) Feedback from low-luminosity radio

- galaxies: B2 0258+35. A&A629:A58. https://doi.org/10.1051/0004-6361/201935931. arXiv:1908.00374 [astro-ph.GA]
- Mutoh M, Inoue M, Kameno S, Asada K, Kenta F, Uchida Y (2002) A New Test for the Absorption Mechanism of GPS Radio Sources Using Polarization Properties. PASJ54:131–138. https://doi.org/10.1093/pasj/54.1.131.astro-ph/0201144
- Myers ST (2019) The VLA Sky Survey (VLASS): First Half-Epoch (1.1) Results and Future Prospects. In: American Astronomical Society Meeting Abstracts #233. American Astronomical Society Meeting Abstracts, vol 233. p 214.03
- Nagai H, Inoue M, Asada K, Kameno S, Doi A (2006) The Kinematic and Spectral Ages of the Compact Radio Source CTD 93. ApJ648:148–157. https://doi.org/10.1086/505793. astro-ph/0605312
- Nesvadba NPH, Lehnert MD, De Breuck C, Gilbert A, van Breugel W (2007) Compact radio sources and jet-driven AGN feedback in the early universe: constraints from integral-field spectroscopy. A&A475:145–153. https://doi.org/10.1051/0004-6361:20078175. arXiv:0708.4150
- Nesvadba NPH, Bicknell GV, Mukherjee D, Wagner AY (2020) Gas, dust, and star formation in the positive AGN feedback candidate 4C 41.17 at z = 3.8. A&A639:L13. https://doi.org/10.1051/0004-6361/202038269. arXiv:2006.10572 [astro-ph.GA]
- Norris RP, Afonso J, Appleton PN, Boyle BJ, Ciliegi P, Croom SM, Huynh MT, Jackson CA, Koekemoer AM, Lonsdale CJ (2006) Deep ATLAS Radio Observations of the Chandra Deep Field-South/Spitzer Wide-Area Infrared Extragalactic Field. AJ132(6):2409–2423. https://doi.org/10.1086/508275.arXiv:astro-ph/0610538 [astro-ph]
- Norris RP, Hopkins AM, Afonso J, Brown S, Condon JJ, Dunne L, Feain I, Hollow R, Jarvis M, Johnston-Hollitt M, Lenc E, Middelberg E, Padovani P, Prandoni I, Rudnick L, Seymour N, Umana G, Andernach H, Alexander DM, Appleton PN, Bacon D, Banfield J, Becker W, Brown MJI, Ciliegi P, Jackson C, Eales S, Edge AC, Gaensler BM, Giovannini G, Hales CA, Hancock P, Huynh MT, Ibar E, Ivison RJ, Kennicutt R, Kimball AE, Koekemoer AM, Koribalski BS, López-Sánchez ÁR, Mao MY, Murphy T, Messias H, Pimbblet KA, Raccanelli A, Randall KE, Reiprich TH, Roseboom IG, Röttgering H, Saikia DJ, Sharp RG, Slee OB, Smail I, Thompson MA, Urquhart JS, Wall JV, Zhao GB (2011) EMU: Evolutionary Map of the Universe. PASA28:215–248. https://doi.org/10.1071/AS11021. arXiv:1106.3219
- Ocaña Flaquer B, Leon S, Combes F, Lim J (2010) TANGO I: Interstellar medium in nearby radio galaxies. Molecular gas. A&A518:A9. https://doi.org/10.1051/0004-6361/200913392. arXiv:1001.5009 [astro-ph.CO]
- O'Dea CP (1989) Constraints on integrated nuclear rotation measures in coredominated active galactic nuclei. A&A210:35–41
- O'Dea CP (1998) The Compact Steep-Spectrum and Gigahertz Peaked-Spectrum Radio Sources. PASP110:493–532. https://doi.org/10.1086/316162
- O'Dea CP (2016) The infrared properties of the GPS and CSS radio sources.

- Astron Nachr 337:141. https://doi.org/10.1002/asna.201512280
- O'Dea CP, Baum SA (1997) Constraints on Radio Source Evolution from the Compact Steep Spectrum and GHz Peaked Spectrum Radio Sources. AJ113:148–161. https://doi.org/10.1086/118241
- O'Dea CP, Dent WA, Balonek TJ, Kapitzky JE (1983) 2.7-GHz observations of four radio polarization rotators. AJ88:1616–1625. https://doi.org/10.1086/113451
- O'Dea CP, Dent WA, Kinzel WM, Balonek TJ (1986) Multifrequency radio observations of the variable quasars 0133+476, 0235+164, 1749+096, and 2131-021. AJ92:1262-1271. https://doi.org/10.1086/114260
- O'Dea CP, Baum SA, Stanghellini C (1991) What are the gigahertz peaked-spectrum radio sources? ApJ380:66–77. https://doi.org/10.1086/170562
- O'Dea CP, Baum SA, Maloney PR, Tacconi LJ, Sparks WB (1994) Constraints on molecular gas in cooling flows and powerful radio galaxies. ApJ422:467–479. https://doi.org/10.1086/173742
- O'Dea CP, Stanghellini C, Baum SA, Charlot S (1996) On the Host Galaxies of the Gigahertz Peaked-Spectrum Radio Sources. ApJ470:806. https://doi.org/10.1086/177911
- O'Dea CP, De Vries WH, Worrall DM, Baum SA, Koekemoer A (2000) ASCA Observations of the Gigahertz-Peaked Spectrum Radio Galaxies 1345+125 and 2352+495. AJ119:478-485. https://doi.org/10.1086/301209
- O'Dea CP, Koekemoer AM, Baum SA, Sparks WB, Martel AR, Allen MG, Macchetto FD, Miley GK (2001) 3C 236: Radio Source, Interrupted? AJ121:1915–1926. https://doi.org/10.1086/319953. astro-ph/0101441
- O'Dea CP, de Vries WH, Koekemoer AM, Baum SA, Morganti R, Fanti R, Capetti A, Tadhunter CN, Barthel PD, Axon DJ, Gelderman R (2002) Hubble Space Telescope STIS Observations of the Kinematics of Emission-Line Nebulae in Three Compact Steep-Spectrum Radio Sources. AJ123:2333–2351. https://doi.org/10.1086/340076
- O'Dea CP, Gallimore J, Stanghellini C, Baum SA, Jackson JM (2005) A Search for Molecular Gas in GHz-peaked Spectrum Radio Sources. AJ129:610–614. https://doi.org/10.1086/427133. astro-ph/0411123
- O'Dea CP, Mu B, Worrall DM, Kastner J, Baum S, de Vries WH (2006) XMM-Newton Detection of X-Ray Emission from the Compact Steep-Spectrum Radio Galaxy 3C 303.1. ApJ653:1115–1120. https://doi.org/10.1086/508705.astro-ph/0608320
- O'Dea CP, Baum SA, Privon G, Noel-Storr J, Quillen AC, Zufelt N, Park J, Edge A, Russell H, Fabian AC, Donahue M, Sarazin CL, McNamara B, Bregman JN, Egami E (2008) An Infrared Survey of Brightest Cluster Galaxies. II. Why are Some Brightest Cluster Galaxies Forming Stars? ApJ681(2):1035–1045. https://doi.org/10.1086/588212.arXiv:0803.1772 [astro-ph]
- O'Dea CP, Worrall DM, Tremblay GR, Clarke TE, Rothberg B, Baum SA, Christiansen KP, Mullarkey CA, Noel-Storr J, Mittal R (2017) Testing for Shock-heated X-Ray Gas around Compact Steep Spectrum Radio Galaxies. ApJ851:87. https://doi.org/10.3847/1538-4357/aa9923. arXiv:1711.03157

- Ogle P, Whysong D, Antonucci R (2006) Spitzer Reveals Hidden Quasar Nuclei in Some Powerful FR II Radio Galaxies. ApJ647(1):161–171. https://doi.org/10.1086/505337. arXiv:astro-ph/0601485 [astro-ph]
- Ogle P, Boulanger F, Guillard P, Evans DA, Antonucci R, Appleton PN, Nesvadba N, Leipski C (2010) Jet-powered Molecular Hydrogen Emission from Radio Galaxies. ApJ724(2):1193–1217. https://doi.org/10.1088/0004-637X/724/2/1193. arXiv:1009.4533 [astro-ph.CO]
- Ojha R, Fey AL, Johnston KJ, Jauncey DL, Tzioumis AK, Reynolds JE (2004) VLBI Observations of the Gigahertz-Peaked Spectrum Galaxy PKS 1934-638. AJ127:1977–1981. https://doi.org/10.1086/382724
- Olguín-Iglesias A, Kotilainen JK, León Tavares J, Chavushyan V, Añorve C (2017) Evidence of bar-driven secular evolution in the gamma-ray narrow-line Seyfert 1 galaxy FBQS J164442.5+261913. MNRAS467(3):3712-3722. https://doi.org/10.1093/mnras/stx022. arXiv:1701.00911 [astro-ph.GA]
- Oosterloo T, Morganti R, Tadhunter C, Oonk JBR, Bignall HE, Tzioumis T, Reynolds C (2019) ALMA observations of PKS 1549-79: a case of feeding and feedback in a young radio quasar. arXiv e-prints arXiv:1910.07865 [astro-ph.GA]
- Oosterloo TA, Morganti R (2005) Anomalous HI kinematics in Centaurus A: Evidence for jet-induced star formation. A&A429:469–475. https://doi.org/10.1051/0004-6361:20041379. arXiv:astro-ph/0409500 [astro-ph]
- Orenstein BJ, Collier JD, Norris RP (2019) The redshift distribution of infrared-faint radio sources. MNRAS484(1):1021–1030. https://doi.org/10.1093/mnras/sty3259. arXiv:1811.11957 [astro-ph.GA]
- Orienti M, Dallacasa D (2008a) Are young radio sources in equipartition? A&A487:885–894. https://doi.org/10.1051/0004-6361:200809948. arXiv:0806.4831
- Orienti M, Dallacasa D (2008b) Constraining the nature of high frequency peakers. II. Polarization properties. A&A479:409–415. https://doi.org/10.1051/0004-6361:20078572. arXiv:0712.3207
- Orienti M, Dallacasa D (2010) Proper motion and apparent contraction in J0650+6001. MNRAS406:529-534. https://doi.org/10.1111/j.1365-2966. 2010.16687.x. arXiv:1003.2910
- Orienti M, Dallacasa D (2012) Parsec-scale morphology and spectral-index distribution in faint high-frequency peakers. MNRAS424:532–544. https://doi.org/10.1111/j.1365-2966.2012.21226.x. arXiv:1205.0395
- Orienti M, Dallacasa D (2020) Variability and parsec-scale radio structure of candidate compact symmetric objects. MNRAS499(1):1340–1355. https://doi.org/10.1093/mnras/staa2856. arXiv:2009.08995 [astro-ph.GA]
- Orienti M, Morganti R, Dallacasa D (2006) H I absorption in high-frequency peaker galaxies. A&A457:531–536. https://doi.org/10.1051/0004-6361:20064820. astro-ph/0607137
- Orienti M, Dallacasa D, Stanghellini C (2007a) Constraining the nature of high frequency peakers. The spectral variability. A&A475:813–820. https://doi.org/10.1051/0004-6361:20078105. arXiv:0708.3979
- Orienti M, Dallacasa D, Stanghellini C (2007b) Constraining the spectral

- age of very asymmetric CSOs. Evidence of the influence of the ambient medium. A&A461:923–929. https://doi.org/10.1051/0004-6361:20066122. astro-ph/0610359
- Orienti M, Dallacasa D, Stanghellini C (2010a) Spectral variability in faint high-frequency peakers. MNRAS408:1075–1088. https://doi.org/10.1111/j. 1365-2966.2010.17179.x. arXiv:1006.2049
- Orienti M, Murgia M, Dallacasa D (2010b) The last breath of the young gigahertz-peaked spectrum radio source PKS1518+047. MNRAS402:1892–1898. https://doi.org/10.1111/j.1365-2966.2009.16016.x. arXiv:0911.1723
- Oshlack AYKN, Webster RL, Whiting MT (2001) A Very Radio Loud Narrow-Line Seyfert 1: PKS 2004-447. ApJ558(2):578–582. https://doi.org/10.1086/322299. arXiv:astro-ph/0105213 [astro-ph]
- Osterbrock DE, Pogge RW (1985) The spectra of narrow-line Seyfert 1 galaxies. ApJ297:166–176. https://doi.org/10.1086/163513
- Osterbrock DE, Pogge RW (1987) Optical Spectra of Narrow Emission Line Palomar-Green Galaxies. ApJ323:108. https://doi.org/10.1086/165810
- Ostorero L, Moderski R, Stawarz L, Diaferio A, Kowalska I, Cheung CC, Kataoka J, Begelman MC, Wagner SJ (2010) X-ray-emitting GHz-peaked-spectrum Galaxies: Testing a Dynamical-Radiative Model with Broadband Spectra. ApJ715:1071–1093. https://doi.org/10.1088/0004-637X/715/2/1071. arXiv:0910.3611
- Ostorero L, Morganti R, Diaferio A, Siemiginowska A, Stawarz Ł, Moderski R, Labiano A (2017) Correlation between X-Ray and Radio Absorption in Compact Radio Galaxies. ApJ849:34. https://doi.org/10.3847/1538-4357/aa8ef6. arXiv:1709.08404 [astro-ph.HE]
- Otrupcek RE, Wright AE (1991) PKSCAT90 the Southern Radio Source Database. Proceedings of the Astronomical Society of Australia 9:170
- Owsianik I, Conway JE (1998) First detection of hotspot advance in a Compact Symmetric Object. Evidence for a class of very young extragalactic radio sources. A&A337:69–79. astro-ph/9712062
- Owsianik I, Conway JE, Polatidis AG (1998) Renewed Radio Activity of Age 370 years in the Extragalactic Source 0108+388. A&A336:L37-L40. astro-ph/9806388
- Padovani P, Alexander DM, Assef RJ, De Marco B, Giommi P, Hickox RC, Richards GT, Smolčić V, Hatziminaoglou E, Mainieri V, Salvato M (2017) Active galactic nuclei: what's in a name? A&A Rev.25(1):2. https://doi.org/10.1007/s00159-017-0102-9. arXiv:1707.07134 [astro-ph.GA]
- Padrielli L, Kapahi VK, Katgert-Merkelijn JK (1981) Compact and extended structure in B2 radio sources of intermediate strength. A&AS46:473–481
- Paragi Z, Frey S, Fejes I, Venturi T, Porcas RW, Schilizzi RT (2000) The Compact Core-Jet Region of the Superluminal Quasar 3C 216. PASJ52:983–L988. https://doi.org/10.1093/pasj/52.6.983. arXiv:astro-ph/0008508 [astro-ph]
- Parkin TJ, Wilson CD, Foyle K, Baes M, Bendo GJ, Boselli A, Boquien M, Cooray A, Cormier D, Davies JI, Eales SA, Galametz M, Gomez HL, Lebouteiller V, Madden S, Mentuch E, Page MJ, Pohlen M, Remy A,

- Roussel H, Sauvage M, Smith MWL, Spinoglio L (2012) The gas-to-dust mass ratio of Centaurus A as seen by Herschel. MNRAS422(3):2291–2301. https://doi.org/10.1111/j.1365-2966.2012.20778.x. arXiv:1202.5323 [astro-ph.CO]
- Parma P, Murgia M, de Ruiter HR, Fanti R, Mack KH, Govoni F (2007) In search of dying radio sources in the local universe. A&A470(3):875–888. https://doi.org/10.1051/0004-6361:20077592. arXiv:0705.3209 [astro-ph]
- Patil P, Nyland K, Harwood JJ, Kimball A, Mukherjee D (2018) Young Radio AGN in the ngVLA Era. In: Murphy E (ed) Science with a Next Generation Very Large Array. ASP Conference Series, vol 517. Astronomical Society of the Pacific, p 595
- Patil P, Nyland K, Whittle M, Lonsdale C, Lacy M, Lonsdale C, Mukherjee D, Trapp AC, Kimball AE, Lanz L, Wilkes BJ, Blain A, Harwood JJ, Efstathiou A, Vlahakis C (2020) High-resolution VLA Imaging of Obscured Quasars: Young Radio Jets Caught in a Dense ISM. arXiv e-prints arXiv:2004.07914. arXiv:2004.07914 [astro-ph.GA]
- Pauliny-Toth IIK, Witzel A, Preuss E, Kühr H, Kellermann KI, Fomalont EB, Davis MM (1978) The 5 GHz strong source surveys. IV Survey of the area between declination 35 and 70 degrees and summary of source counts, spectra and optical identifications. AJ83:451–474. https://doi.org/10.1086/112223
- Peacock JA, Wall JV (1982) Bright extragalactic radio sources at 2.7 GHz-II. Observations with the Cambridge 5-km telescope. MNRAS198:843–860. https://doi.org/10.1093/mnras/198.3.843
- Peck AB, Taylor GB (2000) The COINS Sample: VLBA Identifications of Compact Symmetric Objects. ApJ534:90–103. https://doi.org/10.1086/308746.astro-ph/9912189
- Peck AB, Taylor GB, Conway JE (1999) Obscuration of the Parsec-Scale Jets in the Compact Symmetric Object 1946+708. ApJ521:103–111. https://doi.org/10.1086/307535. astro-ph/9811386
- Peck AB, Taylor GB, Fassnacht CD, Readhead ACS, Vermeulen RC (2000) Redshifts and Neutral Hydrogen Observations of Compact Symmetric Objects in the COINS Sample. ApJ534:104–108. https://doi.org/10.1086/308745.astro-ph/9912188
- Perlman ES, Stocke JT, Conway J, Reynolds C (2001) Host Galaxies, Obscuration, and Nuclear Structure of Three Nearby Compact Symmetric Objects. AJ122:536–548. https://doi.org/10.1086/321149. astro-ph/0104439
- Perucho M, Martí JM (2002) Physical Parameters in the Hot Spots and Jets of Compact Symmetric Objects. ApJ568:639–650. https://doi.org/10.1086/338882. astro-ph/0111579
- Peterson BM (2011) Masses of Black Holes in Active Galactic Nuclei: Implications for NLS1s. arXiv e-prints arXiv:1109.4181. arXiv:1109.4181 [astro-ph.CO]
- Phillips RB, Mutel RL (1982) On symmetric structure in compact radio sources. A&A106:21–24
- Pierce JCS, Tadhunter CN, Ramos Almeida C, Bessiere PS, Rose M (2019)

- Do AGN triggering mechanisms vary with radio power? I. Optical morphologies of radio-intermediate HERGs. MNRAS487(4):5490–5507. https://doi.org/10.1093/mnras/stz1253. arXiv:1905.01315 [astro-ph.GA]
- Pihlström YM, Conway JE, Vermeulen RC (2003) The presence and distribution of H I absorbing gas in sub-galactic sized radio sources. A&A404:871–881. https://doi.org/10.1051/0004-6361:20030469. astro-ph/0304305
- Planck Collaboration, Ade PAR, Aghanim N, Arnaud M, Ashdown M, Aumont J, Baccigalupi C, Baker M, Balbi A, Banday AJ (2011a) Planck early results. I. The Planck mission. A&A536:A1. https://doi.org/10.1051/0004-6361/201116464. arXiv:1101.2022 [astro-ph.IM]
- Planck Collaboration, Ade PAR, Aghanim N, Arnaud M, Ashdown M, Aumont J, Baccigalupi C, Balbi A, Banday AJ, Barreiro RB (2011b) Planck early results. VII. The Early Release Compact Source Catalogue. A&A536:A7. https://doi.org/10.1051/0004-6361/201116474.arXiv:1101.2041 [astro-ph.CO]
- Podigachoski P, Barthel PD, Haas M, Leipski C, Wilkes B, Kuraszkiewicz J, Westhues C, Willner SP, Ashby MLN, Chini R, Clements DL, Fazio GG, Labiano A, Lawrence C, Meisenheimer K, Peletier RF, Siebenmorgen R, Verdoes Kleijn G (2015) Star formation in z > 1 3CR host galaxies as seen by Herschel. A&A575:A80. https://doi.org/10.1051/0004-6361/201425137.arXiv:1501.01434
- Podigachoski P, Barthel PD, Peletier RF, Steendam S (2016a) The far-infrared emission of the radio-loud quasar 3C 318. A&A585:A142. https://doi.org/10.1051/0004-6361/201527394. arXiv:1510.06066 [astro-ph.GA]
- Podigachoski P, Rocca-Volmerange B, Barthel P, Drouart G, Fioc M (2016b) Starbursts and dusty tori in distant 3CR radio galaxies. MNRAS462(4):4183–4196. https://doi.org/10.1093/mnras/stw1946.arXiv:1608.00805 [astro-ph.GA]
- Polatidis A, Wilkinson PN, Xu W, Readhead ACS, Pearson TJ, Taylor GB, Vermeulen RC (1999) Compact Symmetric Objects in a complete flux density limited sample. New A Rev.43:657–661. https://doi.org/10.1016/S1387-6473(99)00073-1
- Polatidis AG (2009) Expansion velocities and kinematic ages of Compact Symmetric Objects. Astron Nachr 330:149. https://doi.org/10.1002/asna. 200811143
- Polatidis AG, Conway JE (2003) Proper Motions in Compact Symmetric Objects. PASA20(1):69–74. https://doi.org/10.1071/AS02053. arXiv:astro-ph/0212122 [astro-ph]
- Polatidis AG, Conway JE, Owsianik I (2002) Proper Motions in Compact Symmetric Objects. In: Ros E, Porcas RW, Lobanov AP, Zensus JA (eds) Proceedings of the 6th EVN Symposium. p 139
- Principe G, Migliori G, Johnson TJ, D'Ammand o F, Giroletti M, Orienti M, Stanghellini C, Taylor GB, Torresi E, Cheung CC (2020) NGC 3894: a young radio galaxy seen by Fermi-LAT. A&A635:A185. https://doi.org/10.1051/0004-6361/201937049. arXiv:2003.01476 [astro-ph.GA]
- Privon GC, O'Dea CP, Baum SA, Axon DJ, Kharb P, Buchanan CL, Sparks

- W, Chiaberge M (2008) WFPC2 LRF Imaging of Emission-Line Nebulae in 3CR Radio Galaxies. ApJS175:423–461. https://doi.org/10.1086/525024.arXiv:0710.3105
- Rakshit S, Woo JH (2018) A Census of Ionized Gas Outflows in Type 1 AGNs: Gas Outflows in AGNs. V. ApJ865(1):5. https://doi.org/10.3847/1538-4357/aad9f8. arXiv:1808.03415 [astro-ph.GA]
- Ramos Almeida C, Tadhunter CN, Inskip KJ, Morganti R, Holt J, Dicken D (2011) The optical morphologies of the 2 Jy sample of radio galaxies: evidence for galaxy interactions. MNRAS410(3):1550–1576. https://doi.org/10.1111/j.1365-2966.2010.17542.x. arXiv:1008.2683 [astro-ph.CO]
- Ramos Almeida C, Bessiere PS, Tadhunter CN, Pérez-González PG, Barro G, Inskip KJ, Morganti R, Holt J, Dicken D (2012) Are luminous radio-loud active galactic nuclei triggered by galaxy interactions? MNRAS419(1):687–705. https://doi.org/10.1111/j.1365-2966.2011.19731.x. arXiv:1109.0021 [astro-ph.CO]
- Ramos Almeida C, Bessiere PS, Tadhunter CN, Inskip KJ, Morganti R, Dicken D, González-Serrano JI, Holt J (2013) The environments of luminous radio galaxies and type-2 quasars. MNRAS436(2):997–1016. https://doi.org/10.1093/mnras/stt1595. arXiv:1308.4725 [astro-ph.CO]
- Randall KE, Hopkins AM, Norris RP, Edwards PG (2011) An unbiased sample of bright southern compact steep spectrum and gigahertz peaked spectrum sources. MNRAS416:1135–1151. https://doi.org/10.1111/j.1365-2966.2011. 19116.x. arXiv:1105.4676
- Rastello S, Dallacasa D, Orienti M (2016) Multifrequency VLBA observations of two compact symmetric objects. Astron Nachr 337:42. https://doi.org/10.1002/asna.201512262
- Readhead ACS, Xu W, Pearson TJ, Wilkinson PN, Polatidis A (1993) Evidence for a Population of Short-Lived Powerful Radio Galaxies. In: American Astronomical Society Meeting Abstracts #182. Bulletin of the American Astronomical Society, vol 25. p 891
- Readhead ACS, Xu W, Pearson TJ, Wilkinson PN, Polatidis AG (1994) Compact Symmetric Objects. In: Zensus JA, Kellermann KI (eds) Compact Extragalactic Radio Sources. p 17
- Readhead ACS, Pearson TJ, Taylor GB, Wilkinson PN (1996) The Evolution of Extragalactic Radio Sources. In: Ekers RD, Fanti C, Padrielli L (eds) Extragalactic Radio Sources. IAU Symposium, vol 175. p 88
- Rees MJ (1989) The radio/optical alignment of high-z radio galaxies: triggering of star formation in radio lobes. MNRAS239:1P-4. https://doi.org/10.1093/mnras/239.1.1P
- Rejkuba M, Minniti D, Courbin F, Silva DR (2002) Radio-Optical Alignment and Recent Star Formation Associated with Ionized Filaments in the Halo of NGC 5128 (Centaurus A). ApJ564(2):688–695. https://doi.org/10.1086/324500. arXiv:astro-ph/0109407 [astro-ph]
- Reynaldi V, Feinstein C (2013) Shock ionization in the extended emission-line region of 3C 305: the last piece of the (optical) puzzle. MNRAS435(2):1350–1357. https://doi.org/10.1093/mnras/stt1377.

- arXiv:1307.7489 [astro-ph.CO]
- Reynaldi V, Feinstein C (2016) The fingerprints of photoionization and shock-ionization in two CSS sources. MNRAS455:2242–2252. https://doi.org/10.1093/mnras/stv2489. arXiv:1510.06979
- Reynolds CS, Begelman MC (1997) Intermittant Radio Galaxies and Source Statistics. ApJ487:L135–L138. https://doi.org/10.1086/310894.astro-ph/9707221
- Richards GT, Lacy M, Storrie-Lombardi LJ, Hall PB, Gallagher SC, Hines DC, Fan X, Papovich C, Vanden Berk DE, Trammell GB, Schneider DP, Vestergaard M, York DG, Jester S, Anderson SF, Budavári T, Szalay AS (2006) Spectral Energy Distributions and Multiwavelength Selection of Type 1 Quasars. ApJS166:470–497. https://doi.org/10.1086/506525. astro-ph/0601558
- Risaliti G, Woltjer L, Salvati M (2003) The nature of the absorbing torus in compact radio galaxies. A&A401:895–901. https://doi.org/10.1051/0004-6361:20030124. astro-ph/0301522
- Roche N, Humphrey A, Lagos P, Papaderos P, Silva M, Cardoso LrSM, Gomes JM (2016) MUSE three-dimensional spectroscopy and kinematics of the gigahertz peaked spectrum radio galaxy PKS 1934-63: interaction, recently triggered active galactic nucleus and star formation. MNRAS459(4):4259–4280. https://doi.org/10.1093/mnras/stw765.arXiv:1604.00309 [astro-ph.GA]
- Roettiger K, Burns JO, Clarke DA, Christiansen WA (1994) Relic Radio Emission in 3C 388. ApJ421:L23. https://doi.org/10.1086/187178
- Ross K, Callingham JR, Hurley-Walker N, Seymour N, Hancock P, Franzen TMO, Morgan J, White SV, Bell ME, Patil P (2020) Spectral Variability of Radio Sources at Low Frequencies. arXiv e-prints arXiv:2012.01842. arXiv:2012.01842 [astro-ph.GA]
- Rossetti A, Fanti C, Fanti R, Dallacasa D, Stanghellini C (2006) The B3-VLA CSS sample. VI. VLA images at 2 cm. A&A449:49-60. https://doi.org/10. 1051/0004-6361:20053945. arXiv:0806.1824
- Rossetti A, Dallacasa D, Fanti C, Fanti R, Mack KH (2008) The B3-VLA CSS sample. VII. WSRT polarisation observations and the ambient Faraday medium properties revisited. A&A487:865–883. https://doi.org/10.1051/0004-6361:20079047
- Rossetti A, Dallacasa D, Fanti C, Fanti R, Mack KH (2009) The B3-VLA CSS sample: Polarisation observations. Astron Nachr 330:165–166. https://doi.org/10.1002/asna.200811148
- Rownd BK, Young JS (1999) The Star Formation Efficiency within Galaxies. AJ118(2):670–704. https://doi.org/10.1086/300957
- Sabater J, Best PN, Hardcastle MJ, Shimwell TW, Tasse C, Williams WL, Brüggen M, Cochrane RK, Croston JH, de Gasperin F, Duncan KJ, Gürkan G, Mechev AP, Morabito LK, Prandoni I, Röttgering HJA, Smith DJB, Harwood JJ, Mingo B, Mooney S, Saxena A (2019) The LoTSS view of radio AGN in the local Universe. The most massive galaxies are always switched on. A&A622:A17. https://doi.org/10.1051/0004-6361/201833883.

- $arXiv:1811.05528 \ [astro-ph.GA]$
- Sadler EM (2016) GPS/CSS radio sources and their relation to other AGN. Astron Nachr 337:105. https://doi.org/10.1002/asna.201512274.arXiv:1512.01851
- Sadler EM, Ekers RD, Mahony EK, Mauch T, Murphy T (2014) The local radio-galaxy population at 20 GHz. MNRAS438:796–824. https://doi.org/10.1093/mnras/stt2239. arXiv:1304.0268
- Saikia DJ (1988) Compact Steep Spectrum Radio Sources. In: Miller HR, Wiita PJ (eds) Active Galactic Nuclei. Lecture Notes in Physics, vol 307. Springer, Berlin, p 317. https://doi.org/10.1007/3-540-19492-4_216
- Saikia DJ, Gupta N (2003) Polarization asymmetry in CSS sources: Evidence of AGN fuel? A&A405:499–504. https://doi.org/10.1051/0004-6361: 20030635. astro-ph/0304532
- Saikia DJ, Jamrozy M (2009) Recurrent activity in Active Galactic Nuclei. Bulletin of the Astronomical Society of India 37. arXiv:1002.1841 [astro-ph.CO]
- Saikia DJ, Salter CJ, Muxlow TWB (1987) A radio study of the compact steep-spectrum quasar 3C 2 (0003-003). MNRAS224:911-925. https://doi.org/10.1093/mnras/224.4.911
- Saikia DJ, Jeyakumar S, Wiita PJ, Sanghera HS, Spencer RE (1995) Compact steep-spectrum radio sources and unification schemes. MNRAS276:1215—1223. https://doi.org/10.1093/mnras/276.4.1215
- Saikia DJ, Jeyakumar S, Salter CJ, Thomasson P, Spencer RE, Mantovani F (2001) Compact steep-spectrum sources from the S4 sample. MNRAS321:37–43. https://doi.org/10.1046/j.1365-8711.2001.04017.x.astro-ph/0009175
- Saikia DJ, Thomasson P, Spencer RE, Mantovani F, Salter CJ, Jeyakumar S (2002) CSSs in a sample of B2 radio sources of intermediate strength. A&A391:149–157. https://doi.org/10.1051/0004-6361:20020807.astro-ph/0206049
- Saikia DJ, Jeyakumar S, Mantovani F, Salter CJ, Spencer RE, Thomasson P, Wiita PJ (2003) Symmetry Parameters of CSS Sources: Evidence of Fuelling? PASA20:50–56. https://doi.org/10.1071/AS02058. astro-ph/0305073
- Salomé Q, Salomé P, Combes F (2015) Jet-induced star formation in 3C 285 and Minkowski's Object. A&A574:A34. https://doi.org/10.1051/0004-6361/201424932. arXiv:1410.8367 [astro-ph.GA]
- Salomé Q, Salomé P, Miville-Deschênes MA, Combes F, Hamer S (2017) Inefficient jet-induced star formation in Centaurus A. High resolution ALMA observations of the northern filaments. A&A608:A98. https://doi.org/10.1051/0004-6361/201731429. arXiv:1710.09851 [astro-ph.GA]
- Salter CJ, Saikia DJ, Minchin R, Ghosh T, Chandola Y (2010) The Discovery of Host Galaxy H I Absorption in CTA 21. ApJ715(2):L117–L120. https://doi.org/10.1088/2041-8205/715/2/L117. arXiv:1004.4006 [astro-ph.CO]
- Salvesen G, Miller JM, Cackett E, Siemiginowska A (2009) A Deep XMM-Newton Observation of the Quasar 3C 287. ApJ692:753–757. https://doi.org/10.1088/0004-637X/692/1/753. arXiv:0809.4691

- Santoro F, Oonk JBR, Morganti R, Oosterloo T (2015) The jet-ISM interaction in the outer filament of Centaurus A. A&A574:A89. https://doi.org/10.1051/0004-6361/201425103. arXiv:1411.4639 [astro-ph.GA]
- Santoro F, Oonk JBR, Morganti R, Oosterloo TA, Tadhunter C (2016) Embedded star formation in the extended narrow line region of Centaurus A: Extreme mixing observed by MUSE. A&A590:A37. https://doi.org/10.1051/0004-6361/201628353. arXiv:1604.03891 [astro-ph.GA]
- Santoro F, Rose M, Morganti R, Tadhunter C, Oosterloo TA, Holt J (2018) Probing multi-phase outflows and AGN feedback in compact radio galaxies: the case of PKS B1934-63. A&A617:A139. https://doi.org/10.1051/0004-6361/201833248. arXiv:1806.09461
- Santoro F, Tadhunter C, Baron D, Morganti R, Holt J (2020) AGN-driven outflows and the AGN feedback efficiency in young radio galaxies. arXiv e-prints arXiv:2009.11175. arXiv:2009.11175 [astro-ph.GA]
- Saripalli L, Subrahmanyan R (2009) The Genesis of Morphologies in Extended Radio Sources: X-Shapes, Off-Axis Distortions, and Giant Radio Sources. ApJ695(1):156–170. https://doi.org/10.1088/0004-637X/695/1/156. arXiv:0811.1907 [astro-ph]
- Scharwächter J, Eckart A, Pfalzner S, Zuther J, Krips M, Straubmeier C (2004) A multi-particle model of the 3C 48 host. A&A414:497–501. https://doi.org/10.1051/0004-6361:20031658. astro-ph/0310740
- Schawinski K, Koss M, Berney S, Sartori LF (2015) Active galactic nuclei flicker: an observational estimate of the duration of black hole growth phases of ~10⁵ yr. MNRAS451(3):2517–2523. https://doi.org/10.1093/mnras/stv1136. arXiv:1505.06733 [astro-ph.GA]
- Schechter P (1976) An analytic expression for the luminosity function for galaxies. ApJ203:297–306. https://doi.org/10.1086/154079
- Scheuer PAG (1982) Morphology and power of radio sources. In: Heeschen DS, Wade CM (eds) Extragalactic Radio Sources. IAU Symposium, vol 97. pp 163–165
- Scheuer PAG (1995) Lobe asymmetry and the expansion speeds of radio sources. MNRAS277:331–340. https://doi.org/10.1093/mnras/277.1.331
- Schilizzi RT, Tian WW, Conway JE, Nan R, Miley GK, Barthel PD, Normandeau M, Dallacasa D, Gurvits LI (2001) VLBI, MERLIN and HST observations of the giant radio galaxy 3C 236. A&A368:398–407. https://doi.org/10.1051/0004-6361:20000288. astro-ph/0012231
- Schoenmakers AP, de Bruyn AG, Röttgering HJA, van der Laan H (1999) The Mpc-scale radio source associated with the GPS galaxy B1144+352. A&A341:44-57. astro-ph/9810178
- Schulz R, Kreikenbohm A, Kadler M, Ojha R, Ros E, Stevens J, Edwards PG, Carpenter B, Elsässer D, Gehrels N, Großberger C, Hase H, Horiuchi S, Lovell JEJ, Mannheim K, Markowitz A, Müller C, Phillips C, Plötz C, Quick J, Trüstedt J, Tzioumis AK, Wilms J (2016) The gamma-ray emitting radio-loud narrow-line Seyfert 1 galaxy PKS 2004-447. II. The radio view. A&A588:A146. https://doi.org/10.1051/0004-6361/201527404. arXiv:1511.02631 [astro-ph.HE]

Shabala SS, Ash S, Alexander P, Riley JM (2008) The duty cycle of local radio galaxies. MNRAS388(2):625–637. https://doi.org/10.1111/j.1365-2966. 2008.13459.x. arXiv:0805.4152 [astro-ph]

Shabala SS, Jurlin N, Morganti R, Brienza M, Hardcastle MJ, Godfrey LEH, Krause MGH, Turner RJ (2020) The duty cycle of radio galaxies revealed by LOFAR: remnant and restarted radio source populations in the Lockman Hole. MNRAS496(2):1706–1717. https://doi.org/10.1093/mnras/staa1172.arXiv:2004.08979 [astro-ph.GA]

Shen ZQ, Shang LL, Cai HB, Chen X, Jiang DR, Chen YJ, Liu X, Yang R, Kameno S, Hirabayashi H (2005) The Center of Activity in the Compact Steep-Spectrum Superluminal Source 3C 138. ApJ622:811–815. https://doi.org/10.1086/428284. astro-ph/0412549

Shih HY, Stockton A (2014) The Resolved Outflow from 3C 48. ApJ794:117. https://doi.org/10.1088/0004-637X/794/2/117

Shih HY, Stockton A, Kewley L (2013) Ionized Outflows from Compact Steep Spectrum Sources. ApJ772:138. https://doi.org/10.1088/0004-637X/772/2/138. arXiv:1306.5237

Shimwell TW, Röttgering HJA, Best PN, Williams WL, Dijkema TJ, de Gasperin F, Hardcastle MJ, Heald GH, Hoang DN, Horneffer A, Intema H, Mahony EK, Mandal S, Mechev AP, Morabito L, Oonk JBR, Rafferty D, Retana-Montenegro E, Sabater J, Tasse C, van Weeren RJ, Brüggen M, Brunetti G, Chyzy KT, Conway JE, Haverkorn M, Jackson N, Jarvis MJ, McKean JP, Miley GK, Morganti R, White GJ, Wise MW, van Bemmel IM, Beck R, Brienza M, Bonafede A, Calistro Rivera G, Cassano R, Clarke AO, Cseh D, Deller A, Drabent A, van Driel W, Engels D, Falcke H, Ferrari C, Fröhlich S, Garrett MA, Harwood JJ, Heesen V, Hoeft M, Horellou C, Israel FP, Kapińska AD, Kunert-Bajraszewska M, McKay DJ, Mohan NR, Orrú E, Pizzo RF, Prandoni I, Schwarz DJ, Shulevski A, Sipior M, Smith DJB, Sridhar SS, Steinmetz M, Stroe A, Varenius E, van der Werf PP, Zensus JA, Zwart JTL (2017) The LOFAR Two-metre Sky Survey. I. Survey description and preliminary data release. A&A598:A104. https://doi.org/10.1051/0004-6361/201629313. arXiv:1611.02700 [astro-ph.IM]

Shimwell TW, Tasse C, Hardcastle MJ, Mechev AP, Williams WL, Best PN, Röttgering HJA, Callingham JR, Dijkema TJ, de Gasperin F, Hoang DN, Hugo B, Mirmont M, Oonk JBR, Prandoni I, Rafferty D, Sabater J, Smirnov O, van Weeren RJ, White GJ, Atemkeng M, Bester L, Bonnassieux E, Brüggen M, Brunetti G, Chyzy KT, Cochrane R, Conway JE, Croston JH, Danezi A, Duncan K, Haverkorn M, Heald GH, Iacobelli M, Intema HT, Jackson N, Jamrozy M, Jarvis MJ, Lakhoo R, Mevius M, Miley GK, Morabito L, Morganti R, Nisbet D, Orrú E, Perkins S, Pizzo RF, Schrijvers C, Smith DJB, Vermeulen R, Wise MW, Alegre L, Bacon DJ, van Bemmel IM, Beswick RJ, Bonafede A, Botteon A, Bourke S, Brienza M, Calistro Rivera G, Cassano R, Clarke AO, Conselice CJ, Dettmar RJ, Drabent A, Dumba C, Emig KL, Enßlin TA, Ferrari C, Garrett MA, Génova-Santos RT, Goyal A, Gürkan G, Hale C, Harwood JJ, Heesen V, Hoeft M, Horellou C, Jackson C, Kokotanekov G, Kondapally R, Kunert-Bajraszewska M, Ma-

- hatma V, Mahony EK, Mandal S, McKean JP, Merloni A, Mingo B, Miskolczi A, Mooney S, Nikiel-Wroczyński B, O'Sullivan SP, Quinn J, Reich W, Roskowiński C, Rowlinson A, Savini F, Saxena A, Schwarz DJ, Shulevski A, Sridhar SS, Stacey HR, Urquhart S, van der Wiel MHD, Varenius E, Webster B, Wilber A (2019) The LOFAR Two-metre Sky Survey. II. First data release. A&A622:A1. https://doi.org/10.1051/0004-6361/201833559.arXiv:1811.07926
- Shulevski A, Morganti R, Oosterloo T, Struve C (2012) Recurrent radio emission and gas supply: the radio galaxy B2 0258+35. A&A545:A91. https://doi.org/10.1051/0004-6361/201219869. arXiv:1207.4348
- Siemiginowska A (2009) X-ray emission from GPS and CSS sources. Astron Nachr 330:264–269. https://doi.org/10.1002/asna.200811172. arXiv:0901.1327 [astro-ph.HE]
- Siemiginowska A, Bechtold J, Aldcroft TL, Elvis M, Harris DE, Dobrzycki A (2002) Chandra Discovery of a 300 Kiloparsec X-Ray Jet in the Gigahertz-peaked Spectrum Quasar PKS 1127-145. ApJ570:543–556. https://doi.org/10.1086/339629. astro-ph/0201116
- Siemiginowska A, Aldcroft TL, Bechtold J, Brunetti G, Elvis M, Stanghellini C (2003) X-ray Emission from Gigahertz Peaked/Compact Steep Spectrum Sources. PASA20:113–117. https://doi.org/10.1071/AS02052. astro-ph/0306288
- Siemiginowska A, Stawarz L, Cheung CC, Harris DE, Sikora M, Aldcroft TL, Bechtold J (2007) The 300 kpc Long X-Ray Jet in PKS 1127-145, z = 1.18 Quasar: Constraining X-Ray Emission Models. ApJ657:145–158. https://doi.org/10.1086/510898.astro-ph/0611406
- Siemiginowska A, LaMassa S, Aldcroft TL, Bechtold J, Elvis M (2008) X-Ray Properties of the Gigahertz Peaked and Compact Steep Spectrum Sources. ApJ684:811–821. https://doi.org/10.1086/589437. arXiv:0804.1564
- Siemiginowska A, Czerny B, Janiuk A, Stawarz L, Guainazzi M, Celotti A, Migliori G, Tengstrand O (2010) Intermittent Activity of Jets in AGN. In: Maraschi L, Ghisellini G, Della Ceca R, Tavecchio F (eds) Accretion and Ejection in AGN: a Global View. ASP Conference Series, vol 427. Astronomical Society of the Pacific, p 326. arXiv:1003.0129 [astro-ph.CO]
- Siemiginowska A, Sobolewska M, Migliori G, Guainazzi M, Hardcastle M, Ostorero L, Stawarz L (2016) X-Ray Properties of the Youngest Radio Sources and Their Environments. ApJ823:57. https://doi.org/10.3847/0004-637X/823/1/57. arXiv:1603.00947
- Sigl G, Torres DF, Anchordoqui LA, Romero GE (2001) Testing the correlation of ultrahigh energy cosmic rays with high redshift sources. Phys. Rev. D63(8):081302. https://doi.org/10.1103/PhysRevD.63.081302. arXiv:astro-ph/0008363 [astro-ph]
- Singh V, Chand H (2018) Investigating kpc-scale radio emission properties of narrow-line Seyfert 1 galaxies. MNRAS480(2):1796–1818. https://doi.org/10.1093/mnras/sty1818. arXiv:1807.01945 [astro-ph.GA]
- Singh V, Wadadekar Y, Ishwara-Chandra CH, Sirothia S, Sievers J, Beelen A, Omont A (2017) On the nature of infrared-faint radio sources in

- the Subaru X-ray Deep and Very Large Array-VIMOS VLT Deep Survey fields. MNRAS470(4):4956–4973. https://doi.org/10.1093/mnras/stx1536.arXiv:1706.05258 [astro-ph.GA]
- Sirothia SK, Dennefeld M, Saikia DJ, Dole H, Ricquebourg F, Roland J (2009) 325-MHz observations of the ELAIS-N1 field using the Giant Metrewave Radio Telescope. MNRAS395(1):269–281. https://doi.org/10.1111/j. 1365-2966.2009.14317.x. arXiv:0812.0813 [astro-ph]
- Smith EP, Heckman TM (1989) Multicolor Surface Photometry of Powerful Radio Galaxies. II. Morphology and Stellar Content. ApJ341:658. https://doi.org/10.1086/167524
- Snellen IAG, Schilizzi RT, Bremer MN, de Bruyn AG, Miley GK, Rottgering HJA, McMahon RG, Perez Fournon I (1998a) Optical and near-infrared imaging of faint Gigahertz Peaked Spectrum sources. MNRAS301:985–1000. https://doi.org/10.1046/j.1365-8711.1998.02100.x. astro-ph/9809069
- Snellen IAG, Schilizzi RT, de Bruyn AG, Miley GK, Rengelink RB, Roettgering HJ, Bremer MN (1998b) A new sample of faint Gigahertz Peaked Spectrum radio sources. A&AS131:435–449. https://doi.org/10.1051/aas: 1998281. astro-ph/9803140
- Snellen IAG, Schilizzi RT, Bremer MN, Miley GK, de Bruyn AG, Röttgering HJA (1999) Optical spectroscopy of faint gigahertz peaked-spectrum sources. MNRAS307:149–161. https://doi.org/10.1046/j.1365-8711.1999.02636.x. astro-ph/9903226
- Snellen IAG, Schilizzi RT, Miley GK, de Bruyn AG, Bremer MN, Röttgering HJA (2000) On the evolution of young radio-loud AGN. MNRAS319:445–456. https://doi.org/10.1046/j.1365-8711.2000.03935.x. astro-ph/0002130
- Snellen IAG, Lehnert MD, Bremer MN, Schilizzi RT (2002) A Parkes half-Jansky sample of GHz peaked spectrum galaxies. MNRAS337:981–992. https://doi.org/10.1046/j.1365-8711.2002.05978.x. astro-ph/0208368
- Snellen IAG, Mack KH, Schilizzi RT, Tschager W (2003) Constraining the Evolution of Young Radio-Loud AGN. PASA20:38–41. https://doi.org/10.1071/AS02041.astro-ph/0210313
- Snellen IAG, Mack KH, Schilizzi RT, Tschager W (2004) The CORALZ sample I. Young radio-loud active galactic nuclei at low redshift. MNRAS348:227–234. https://doi.org/10.1111/j.1365-2966.2004.07337.x
- Snellen IAG, Röttgering HJA, Barthel PD, Best PN, Brüggen M, Conway JE, Jarvis MJ, Lehnert MD, Miley GK, Morganti R (2009) Future investigations of GPS and CSS radio sources with LOFAR. Astron Nachr 330:297. https://doi.org/10.1002/asna.200811180
- Sobolewska M, Siemiginowska A, Guainazzi M, Hardcastle M, Migliori G, Ostorero L, Stawarz L (2019) The Impact of the Environment on the Early Stages of Radio Source Evolution. ApJ871:71. https://doi.org/10.3847/1538-4357/aaee78. arXiv:1812.02147 [astro-ph.HE]
- Somerville RS, Davé R (2015) Physical Models of Galaxy Formation in a Cosmological Framework. ARA&A53:51–113. https://doi.org/10.1146/annurev-astro-082812-140951. arXiv:1412.2712 [astro-ph.GA]
- Son D, Woo JH, Kim SC, Fu H, Kawakatu N, Bennert VN, Nagao T, Park

- D (2012) Accretion Properties of High- and Low-excitation Young Radio Galaxies. ApJ757:140. https://doi.org/10.1088/0004-637X/757/2/140. arXiv:1208.2025
- Spoelstra TAT, Patnaik AR, Gopal-Krishna (1985) A sample of 25 extragalactic radio sources having a spectrum peaked around 1 GHz (List 2). A&A152:38–41
- Spoon HWW, Farrah D, Lebouteiller V, González-Alfonso E, Bernard-Salas J, Urrutia T, Rigopoulou D, Westmoquette MS, Smith HA, Afonso J, Pearson C, Cormier D, Efstathiou A, Borys C, Verma A, Etxaluze M, Clements DL (2013) Diagnostics of AGN-Driven Molecular Outflows in ULIRGs from Herschel-PACS Observations of OH at 119 μ m. ApJ775(2):127. https://doi.org/10.1088/0004-637X/775/2/127. arXiv:1307.6224 [astro-ph.CO]
- Stanghellini C, O'Dea CP, Baum SA, Laurikainen E (1993) Optical CCD imaging of GHz-peaked-spectrum radio sources. ApJS88:1–21. https://doi.org/10.1086/191812
- Stanghellini C, Dallacasa D, O'Dea CP, Baum SA, Fanti C, Fanti R (1998a) The Parsec-Scale Radio Polarization of Three GHz-Peaked-Spectrum Radio Sources. In: Zensus JA, Taylor GB, Wrobel JM (eds) IAU Colloq. 164: Radio Emission from Galactic and Extragalactic Compact Sources. ASP Conference Series, vol 144. Astronomical Society of the Pacific, p 177
- Stanghellini C, O'Dea CP, Dallacasa D, Baum SA, Fanti R, Fanti C (1998b) A complete sample of GHz-peaked-spectrum radio sources and its radio properties. A&AS131:303–315. https://doi.org/10.1051/aas:1998270. astro-ph/9803222
- Stanghellini C, Dallacasa D, O'Dea CP, Baum SA, Fanti R, Fanti C (2001a) VLBA observations of GHz-Peaked-Spectrum radio sources at 15 GHz. A&A379:870–871. https://doi.org/10.1051/0004-6361:20011489
- Stanghellini C, Dallacasa D, O'Dea CP, Baum SA, Fanti R, Fanti C (2001b) VLBA observations of GHz-Peaked-Spectrum radio sources at 15 GHz. A&A377:377–388. https://doi.org/10.1051/0004-6361:20011101.astro-ph/0108185
- Stanghellini C, O'Dea CP, Dallacasa D, Cassaro P, Baum SA, Fanti R, Fanti C (2005) Extended emission around GPS radio sources. A&A443:891–902. https://doi.org/10.1051/0004-6361:20042226. astro-ph/0507499
- Stanghellini C, Dallacasa D, Orienti M (2009a) High Frequency Peakers: The faint sample. Astron Nachr 330:223. https://doi.org/10.1002/asna. 200811162. arXiv:0901.3068 [astro-ph.CO]
- Stanghellini C, Dallacasa D, Venturi T, An T, Hong XY (2009b) Transverse motions in CSOs? Astron Nachr 330:153. https://doi.org/10.1002/asna.200811144. arXiv:0901.3065 [astro-ph.CO]
- Stawarz L, Ostorero L, Begelman MC, Moderski R, Kataoka J, Wagner S (2008) Evolution of and High-Energy Emission from GHz-Peaked Spectrum Sources. ApJ680:911–925. https://doi.org/10.1086/587781. arXiv:0712.1220
- Steenbrugge KC, Blundell KM, Duffy P (2008) Multiwavelength study of Cygnus A II. X-ray inverse-Compton emission from a relic counterjet and implications for jet duty cycles. MNRAS388(4):1465–1472. https://doi.org/10.1016/jet.2016-1472.

- //doi.org/10.1111/j.1365-2966.2008.13412.x. arXiv:0805.2172 [astro-ph]
- Steffen W, Gómez JL, Raga AC, Williams RJR (1997) Jet-Cloud Interactions and the Brightening of the Narrow-Line Region in Seyfert Galaxies. ApJ491(2):L73–L76. https://doi.org/10.1086/311066.arXiv:astro-ph/9710178 [astro-ph]
- Stickel M, Kuehr H (1994) An update of the optical identification status of the S4 radio source catalogue. A&AS103:349–363
- Stockton A, Canalizo G, Fu H, Keel W (2007) The Nature of Optical Features in the Inner Region of the 3C 48 Host Galaxy. ApJ659:195–204. https://doi.org/10.1086/511952.astro-ph/0701539
- Stone RB, Richards GT (2019) Narrow, intrinsic C IV absorption in quasars as it relates to outflows, orientation, and radio properties. MNRAS488(4):5916–5934. https://doi.org/10.1093/mnras/stz2111. arXiv:1907.11876 [astro-ph.GA]
- Storchi-Bergmann T, Schnorr-Müller A (2019) Observational constraints on the feeding of supermassive black holes. Nature Astronomy 3:48–61. https://doi.org/10.1038/s41550-018-0611-0. arXiv:1904.03338 [astro-ph.GA]
- Stuardi C, Missaglia V, Massaro F, Ricci F, Liuzzo E, Paggi A, Kraft RP, Tremblay GR, Baum SA, O'Dea CP, Wilkes BJ, Kuraszkiewicz J, Forman WR, Harris DE (2018) The 3CR Chandra Snapshot Survey: Extragalactic Radio Sources with Redshifts between 1 and 1.5. ApJS235(2):32. https://doi.org/10.3847/1538-4365/aaafcf. arXiv:1806.11125 [astro-ph.HE]
- Sutherland RS, Bicknell GV (2007) Interaction of jets with the ISM of radio galaxies. Ap&SS311(1-3):293–303. https://doi.org/10.1007/s10509-007-9580-y. arXiv:0707.3669 [astro-ph]
- Tabara H, Inoue M (1980) A catalogue of linear polarization of radio sources. A&AS39:379–393
- Tadhunter C (2007) The significance of AGN-induced outflows in nearby radio galaxies. New A Rev.51(1-2):153–159. https://doi.org/10.1016/j.newar. 2006.11.020
- Tadhunter C (2016a) Radio AGN in the local universe: unification, triggering and evolution. A&A Rev.24:10. https://doi.org/10.1007/s00159-016-0094-x. arXiv:1605.08773
- Tadhunter C (2016b) The impact of compact radio sources on their host galaxies: observations. Astron Nachr 337:159. https://doi.org/10.1002/asna. 201512286
- Tadhunter C, Wills K, Morganti R, Oosterloo T, Dickson R (2001) Emission-line outflows in PKS1549-79: the effects of the early stages of radio-source evolution? MNRAS327:227-232. https://doi.org/10.1046/j.1365-8711.2001.04708.x. astro-ph/0105146
- Tadhunter C, Dickson R, Morganti R, Robinson TG, Wills K, Villar-Martin M, Hughes M (2002) The origin of the UV excess in powerful radio galaxies: spectroscopy and polarimetry of a complete sample of intermediate-redshift radio galaxies. MNRAS330(4):977–996. https://doi.org/10.1046/j. 1365-8711.2002.05153.x. arXiv:astro-ph/0201391 [astro-ph]
- Tadhunter C, Holt J, González Delgado R, Rodríguez Zaurín J, Villar-Martín

- M, Morganti R, Emonts B, Ramos Almeida C, Inskip K (2011) Starburst radio galaxies: general properties, evolutionary histories and triggering. MNRAS412:960–978. https://doi.org/10.1111/j.1365-2966.2010.17958.x. arXiv:1011.2096
- Tadhunter C, Dicken D, Morganti R, Konyves V, Ysard N, Nesvadba N, Almeida CR (2014) The dust masses of powerful radio galaxies: clues to the triggering of their activity. MNRAS445:L51–L55. https://doi.org/10.1093/mnrasl/slu135. arXiv:1408.3637 [astro-ph.GA]
- Tadhunter CN, Scarrott SM, Draper P, Rolph C (1992) The optical polarizations of high- and intermediate-redshift radio galaxies. MNRAS256(4):53P–58P. https://doi.org/10.1093/mnras/256.1.53P
- Tadhunter CN, Dickson RC, Shaw MA (1996) Young stars and scattered light in the powerful radio galaxy 3C 321. MNRAS281(2):591–603. https://doi.org/10.1093/mnras/281.2.591
- Takami H, Horiuchi S (2011) The production of ultra high energy cosmic rays during the early epochs of radio-loud AGN. Astroparticle Physics 34:749–754. https://doi.org/10.1016/j.astropartphys.2011.01.014. arXiv:1010.2788 [astro-ph.HE]
- Taylor GB, Vermeulen RC (1997) Bi-Directional Relativistic Jets of the Radio Galaxy 1946+708: Constraints on the Hubble Constant. ApJ485:L9–L12. https://doi.org/10.1086/310800. astro-ph/9706011
- Taylor GB, Marr JM, Pearson TJ, Readhead ACS (2000) Kinematic Age Estimates for Four Compact Symmetric Objects from the Pearson-Readhead Survey. ApJ541:112–119. https://doi.org/10.1086/309428. astro-ph/0005209
- Taylor GB, Fassnacht CD, Sjouwerman LO, Myers ST, Ulvestad JS, Walker RC, Fomalont EB, Pearson TJ, Readhead ACS, Gehrels N, Michelson PF (2005) VLBA Imaging Polarimetry of Active Galactic Nuclei: An Automated Approach. ApJS159:27–40. https://doi.org/10.1086/430255. astro-ph/0503234
- Tchekhovskoy A, Narayan R, McKinney JC (2010) Black Hole Spin and The Radio Loud/Quiet Dichotomy of Active Galactic Nuclei. ApJ711(1):50–63. https://doi.org/10.1088/0004-637X/711/1/50. arXiv:0911.2228 [astro-ph.HE]
- Tengstrand O, Guainazzi M, Siemiginowska A, Fonseca Bonilla N, Labiano A, Worrall DM, Grandi P, Piconcelli E (2009) The X-ray view of giga-hertz peaked spectrum radio galaxies. A&A501:89–102. https://doi.org/10.1051/0004-6361/200811284. arXiv:0903.2444
- Thomasson P, Saikia DJ, Muxlow TWB (2003) 3C459: a highly asymmetric radio galaxy with a starburst. MNRAS341(1):91–99. https://doi.org/10.1046/j.1365-8711.2003.06393.x. arXiv:astro-ph/0305176 [astro-ph]
- Tingay SJ, de Kool M (2003) An Investigation of Synchrotron Self-absorption and Free-Free Absorption Models in Explanation of the Gigahertz-peaked Spectrum of PKS 1718-649. AJ126:723–733. https://doi.org/10.1086/376600
- Tingay SJ, Edwards PG (2015) The multifrequency parsec-scale structure of

- PKS 2254-367 (IC 1459): a luminosity-dependent break in morphology for the precursors of radio galaxies? MNRAS448(1):252-257. https://doi.org/10.1093/mnras/stu2756. arXiv:1501.04393 [astro-ph.GA]
- Tingay SJ, Jauncey DL, Reynolds JE, Tzioumis AK, King EA, Preston RA, Lovell JEJ, McCulloch PM, Costa ME, Nicolson G, Koekemoer A, Tornikoski M, Kedziora-Chudczer L, Campbell-Wilson D (1997) The Nearest GHz Peaked-Spectrum Radio Galaxy, PKS 1718-649. AJ113:2025–2030. https://doi.org/10.1086/118414
- Tingay SJ, Edwards PG, Tzioumis AK (2003) Identification of a new low-redshift GHz-peaked spectrum radio source and implications for the GHz-peaked spectrum class. MNRAS346:327–331. https://doi.org/10.1046/j.1365-2966.2003.07098.x
- Tingay SJ, Macquart JP, Collier JD, Rees G, Callingham JR, Stevens J, Carretti E, Wayth RB, Wong GF, Trott CM, McKinley B, Bernardi G, Bowman JD, Briggs F, Cappallo RJ, Corey BE, Deshpande AA, Emrich D, Gaensler BM, Goeke R, Greenhill LJ, Hazelton BJ, Johnston-Hollitt M, Kaplan DL, Kasper JC, Kratzenberg E, Lonsdale CJ, Lynch MJ, McWhirter SR, Mitchell DA, Morales MF, Morgan E, Oberoi D, Ord SM, Prabu T, Rogers AEE, Roshi A, Udaya Shankar N, Srivani KS, Subrahmanyan R, Waterson M, Webster RL, Whitney AR, Williams A, Williams CL (2015) The Spectral Variability of the GHz-Peaked Spectrum Radio Source PKS 1718-649 and a Comparison of Absorption Models. AJ149:74. https://doi.org/10.1088/0004-6256/149/2/74. arXiv:1412.4216
- Tinti S, de Zotti G (2006) Constraints on evolutionary properties of GHz Peaked Spectrum galaxies. A&A445:889–899. https://doi.org/10.1051/0004-6361:20053752. astro-ph/0509439
- Tinti S, Dallacasa D, de Zotti G, Celotti A, Stanghellini C (2005) High Frequency Peakers: Young radio sources or flaring blazars? A&A432:31–43. https://doi.org/10.1051/0004-6361:20041620. astro-ph/0410663
- Torniainen I, Tornikoski M, Teräsranta H, Aller MF, Aller HD (2005) Long term variability of gigahertz-peaked spectrum sources and candidates. A&A435:839–856. https://doi.org/10.1051/0004-6361:20041886
- Torniainen I, Tornikoski M, Lähteenmäki A, Aller MF, Aller HD, Mingaliev MG (2007) Radio continuum spectra of gigahertz-peaked spectrum galaxies. A&A469:451–457. https://doi.org/10.1051/0004-6361:20066892
- Torniainen I, Tornikoski M, Turunen M, Lainela M, Lähteenmäki A, Hovatta T, Mingaliev MG, Aller MF, Aller HD (2008) Cluster analyses of gigahertz-peaked spectrum sources with self-organising maps. A&A482:483–498. https://doi.org/10.1051/0004-6361:20079222
- Tornikoski M, Jussila I, Johansson P, Lainela M, Valtaoja E (2001) Radio Spectra and Variability of Gigahertz-Peaked Spectrum Radio Sources and Candidates. AJ121:1306–1318. https://doi.org/10.1086/319417
- Tornikoski M, Torniainen I, Lähteenmäki A, Hovatta T, Nieppola E, Turunen M, Lainela M, Valtaoja E, Aller MF, Aller HD, Mingaliev M, Trushkin S (2009) Long-term radio behaviour of GPS sources and candidates. Astron Nachr 330:128. https://doi.org/10.1002/asna.200811139

- Torresi E, Grandi P, Capetti A, Baldi RD, Giovannini G (2018) X-ray study of a sample of FR0 radio galaxies: unveiling the nature of the central engine. MNRAS476(4):5535–5547. https://doi.org/10.1093/mnras/sty520.arXiv:1802.08581 [astro-ph.HE]
- Tortora C, Antonuccio-Delogu V, Kaviraj S, Silk J, Romeo AD, Becciani U (2009) AGN jet-induced feedback in galaxies II. Galaxy colours from a multicloud simulation. MNRAS396(1):61–77. https://doi.org/10.1111/j. 1365-2966.2009.14718.x. arXiv:0903.0397 [astro-ph.GA]
- Tran HD, Cohen MH, Ogle PM, Goodrich RW, di Serego Alighieri S (1998) Scattered Radiation from Obscured Quasars in Distant Radio Galaxies. ApJ500(2):660–672. https://doi.org/10.1086/305752. arXiv:astro-ph/9801063 [astro-ph]
- Tremblay SE, Taylor GB, Helmboldt JF, Fassnacht CD, Pearson TJ (2008) A Shrinking Compact Symmetric Object: J11584+2450? ApJ684:153–159. https://doi.org/10.1086/590377. arXiv:0806.3955
- Tremblay SE, Taylor GB, Helmboldt JF, Fassnacht CD, Romani RW (2009) Identifying Compact Symmetric Objects from the VLBA Imaging and Polarization Survey. Astron Nachr 330:206. https://doi.org/10.1002/asna. 200811157. arXiv:0905.2982 [astro-ph.GA]
- Tribble PC (1991) Depolarization of extended radio sources by a foreground Faraday screen. MNRAS250:726. https://doi.org/10.1093/mnras/250.4.726
- Tschager W, Schilizzi RT, Röttgering HJA, Snellen IAG, Miley GK (2000) The GHz-peaked spectrum radio galaxy 2021+614: detection of slow motion in a compact symmetric object. A&A360:887-895. astro-ph/0007068
- Tzioumis AK, Jauncey DL, Preston RA, Meier DL, Nicolson GD, Batchelor R, Gates J, Hamilton PA, Harvey BR, Haynes RF, Johnson B, McCulloch P, Moorey G, Morabito DD, Niell AE, Robertson JG, Royle GWR, Skjerve L, Slade MA, Slee OB, Watkinson A, Wehrle AE, Wright AE (1989) VLBI observations at 2.3 GHz of the compact galaxy 1934-638. AJ98:36–43. https://doi.org/10.1086/115124
- Ulvestad JS, Wilson AS (1989) Radio Structures of Seyfert Galaxies. VII. Extension of a Distance-limited Sample. ApJ343:659. https://doi.org/10.1086/167737
- Urry CM, Padovani P (1995) Unified Schemes for Radio-Loud Active Galactic Nuclei. PASP107:803. https://doi.org/10.1086/133630. arXiv:astro-ph/9506063 [astro-ph]
- Vaddi S, O'Dea CP, Baum SA, Whitmore S, Ahmed R, Pierce K, Leary S (2016) Constraints on Feedback in the Local Universe: The Relation between Star Formation and AGN Activity in Early-type Galaxies. ApJ818(2):182. https://doi.org/10.3847/0004-637X/818/2/182.arXiv:1601.00344 [astro-ph.GA]
- van Breugel W (1984) Steep Spectrum Radio Cores and Far-Sightedness. In: Fanti R, Kellermann KI, Setti G (eds) VLBI and Compact Radio Sources. IAU Symposium, vol 110. p 59
- van Breugel W, Miley G, Heckman T (1984) Studies of kiloparsec-scale, steep-spectrum radio cores. I VLA maps. AJ89:5–22. https://doi.org/10.1086/

113480

- van Breugel W, Filippenko AV, Heckman T, Miley G (1985) Minkowski's object: a starburst triggered by a radio jet. ApJ293:83–93. https://doi.org/10.1086/163216
- van Breugel WJM, Dey A (1993) Induced Star Formation in a Radio Lobe of 3C 285? ApJ414:563. https://doi.org/10.1086/173103
- van der Laan H (1966) A Model for Variable Extragalactic Radio Sources. Nature211(5054):1131–1133. https://doi.org/10.1038/2111131a0
- Vantyghem AN, McNamara BR, Russell HR, Main RA, Nulsen PEJ, Wise MW, Hoekstra H, Gitti M (2014) Cycling of the powerful AGN in MS 0735.6+7421 and the duty cycle of radio AGN in clusters. MNRAS442(4):3192-3205. https://doi.org/10.1093/mnras/stu1030.arXiv:1405.6208 [astro-ph.GA]
- Vedantham HK, Readhead ACS, Hovatta T, Pearson TJ, Blandford RD, Gurwell MA, Lähteenmäki A, Max-Moerbeck W, Pavlidou V, Ravi V, Reeves RA, Richards JL, Tornikoski M, Zensus JA (2017) Symmetric Achromatic Variability in Active Galaxies: A Powerful New Gravitational Lensing Probe? ApJ845(2):89. https://doi.org/10.3847/1538-4357/aa745c.arXiv:1702.06582 [astro-ph.HE]
- Venturi T, Dallacasa D, Stefanachi F (2004) Radio galaxies in cooling core clusters. Renewed activity in the nucleus of 3C 317? A&A422:515–522. https://doi.org/10.1051/0004-6361:20040089. arXiv:astro-ph/0404571 [astro-ph]
- Vermeulen RC, Pihlström YM, Tschager W, de Vries WH, Conway JE, Barthel PD, Baum SA, Braun R, Bremer MN, Miley GK, O'Dea CP, Röttgering HJA, Schilizzi RT, Snellen IAG, Taylor GB (2003) Observations of H I absorbing gas in compact radio sources at cosmological redshifts. A&A404:861–870. https://doi.org/10.1051/0004-6361:20030468.astro-ph/0304291
- Vermeulen RC, Labiano A, Barthel PD, Baum SA, de Vries WH, O'Dea CP (2006) Atomic hydrogen in the one-sided "compact double" radio galaxy 2050+364. A&A447:489–498. https://doi.org/10.1051/0004-6361:20053857.astro-ph/0510440
- Vestergaard M (2003) Occurrence and Global Properties of Narrow C IV λ1549 Å Absorption Lines in Moderate-Redshift Quasars. ApJ599(1):116–139. https://doi.org/10.1086/379159. arXiv:astro-ph/0309550 [astro-ph]
- Vigotti M, Grueff G, Perley R, Clark BG, Bridle AH (1989) Structures, spectral indexes, and optical identifications of radio sources selected from the B3 catalogue. AJ98:419–499. https://doi.org/10.1086/115153
- Vink J, Snellen I, Mack KH, Schilizzi R (2006) The X-ray properties of young radio-loud AGN. MNRAS367:928–936. https://doi.org/10.1111/j. 1365-2966.2006.10036.x. astro-ph/0601141
- Virmani A, Bhattacharya S, Jain P, Razzaque S, Ralston JP, Mckay DW (2002) Angular correlation of ultra-high energy cosmic rays with compact radio-loud quasars. Astroparticle Physics 17:489–495. https://doi.org/10.1016/S0927-6505(01)00177-3. astro-ph/0010235
- Volvach AE, Kardashev NS, Larionov MG, Volvach LN (2016) Characteristics

- of GPS sources in the Planck survey. Astronomy Reports 60:781-791. https://doi.org/10.1134/S1063772916080096
- Wagner AY, Bicknell GV (2011) Relativistic Jet Feedback in Evolving Galaxies. ApJ728:29. https://doi.org/10.1088/0004-637X/728/1/29.arXiv:1012.1092
- Wagner AY, Bicknell GV, Umemura M, Sutherland RS, Silk J (2016) Galaxy-scale AGN feedback theory. Astron Nachr 337(1-2):167. https://doi.org/10.1002/asna.201512287. arXiv:1510.03594 [astro-ph.GA]
- Wang Z, Wiita PJ, Hooda JS (2000) Radio Jet Interactions with Massive Clouds. ApJ534:201–212. https://doi.org/10.1086/308743
- Wayth RB, Lenc E, Bell ME, Callingham JR, Dwarakanath KS, Franzen TMO, For BQ, Gaensler B, Hancock P, Hindson L, Hurley-Walker N, Jackson CA, Johnston-Hollitt M, Kapińska AD, McKinley B, Morgan J, Offringa AR, Procopio P, Staveley-Smith L, Wu C, Zheng Q, Trott CM, Bernardi G, Bowman JD, Briggs F, Cappallo RJ, Corey BE, Deshpande AA, Emrich D, Goeke R, Greenhill LJ, Hazelton BJ, Kaplan DL, Kasper JC, Kratzenberg E, Lonsdale CJ, Lynch MJ, McWhirter SR, Mitchell DA, Morales MF, Morgan E, Oberoi D, Ord SM, Prabu T, Rogers AEE, Roshi A, Shankar NU, Srivani KS, Subrahmanyan R, Tingay SJ, Waterson M, Webster RL, Whitney AR, Williams A, Williams CL (2015) GLEAM: The GaLactic and Extragalactic All-Sky MWA Survey. PASA32:e025. https://doi.org/10.1017/pasa.2015.26.arXiv:1505.06041 [astro-ph.IM]
- Westhues C, Haas M, Barthel P, Wilkes BJ, Willner SP, Kuraszkiewicz J, Podigachoski P, Leipski C, Meisenheimer K, Siebenmorgen R, Chini R (2016) Star Formation in 3CR Radio Galaxies and Quasars at z < 1. AJ151(5):120. https://doi.org/10.3847/0004-6256/151/5/120.arXiv:1602.07443 [astro-ph.GA]
- White RL, Becker RH (1992) A new catalog of 30,239 1.4 GHz sources. ApJS79:331–467. https://doi.org/10.1086/191656
- Whittam IH, Riley JM, Green DA, Jarvis MJ (2016) The faint source population at 15.7 GHz III. A high-frequency study of HERGs and LERGs. MNRAS462(2):2122–2137. https://doi.org/10.1093/mnras/stw1725. arXiv:1607.03709 [astro-ph.GA]
- Whittam IH, Prescott M, McAlpine K, Jarvis MJ, Heywood I (2018) The Stripe 82 1-2 GHz Very Large Array Snapshot Survey: host galaxy properties and accretion rates of radio galaxies. MNRAS480(1):358–370. https://doi.org/10.1093/mnras/sty1787. arXiv:1806.10143 [astro-ph.GA]
- Wiita PJ (2004) Jet Propagation Through Irregular Media and the Impact of Lobes on Galaxy Formation. Ap&SS293(1):235–245. https://doi.org/10.1023/B:ASTR.0000044672.94932.c5
- Wilkinson PN, Booth RS, Cornwell TJ, Clark RR (1984) Peculiar radio structure in the quasar 3C380. Nature308(5960):619–621. https://doi.org/10.1038/308619a0
- Wilkinson PN, Polatidis AG, Readhead ACS, Xu W, Pearson TJ (1994) Two-sided ejection in powerful radio sources: The compact symmetric objects. ApJ432:L87–L90. https://doi.org/10.1086/187518

- Willett KW, Stocke JT, Darling J, Perlman ES (2010) Spitzer Mid-Infrared Spectroscopy of Compact Symmetric Objects: What Powers Radio-Loud Active Galactic Nuclei? ApJ713:1393–1412. https://doi.org/10.1088/0004-637X/713/2/1393. arXiv:1004.0952 [astro-ph.HE]
- Williams WL, Calistro Rivera G, Best PN, Hardcastle MJ, Röttgering HJA, Duncan KJ, de Gasperin F, Jarvis MJ, Miley GK, Mahony EK, Morabito LK, Nisbet DM, Prand oni I, Smith DJB, Tasse C, White GJ (2018) LOFAR-Boötes: properties of high- and low-excitation radio galaxies at 0.5 < z < 2.0. MNRAS475(3):3429–3452. https://doi.org/10.1093/mnras/sty026. arXiv:1711.10504 [astro-ph.GA]
- Willott CJ, Martínez-Sansigre A, Rawlings S (2007) Molecular Gas Observations of the Reddened Quasar 3C 318. AJ133:564–567. https://doi.org/10.1086/510291. astro-ph/0610564
- Wills BJ, Pollock JT, Aller HD, Aller MF, Balonek TJ, Barvainis RE, Binzel RP, Chaffee FH, Dent WA, Douglas JN (1983) The QSO 1156+295: a multifrequency study of recent activity. ApJ274:62–85. https://doi.org/10.1086/161426
- Wills KA, Tadhunter CN, Robinson TG, Morganti R (2002) The ultraviolet excess in nearby powerful radio galaxies: evidence for a young stellar component. MNRAS333(1):211–221. https://doi.org/10.1046/j.1365-8711.2002.05397.x
- Wing JD, Blanton EL (2011) Galaxy Cluster Environments of Radio Sources. AJ141(3):88. https://doi.org/10.1088/0004-6256/141/3/88. arXiv:1008.1099 [astro-ph.CO]
- Wójtowicz A, Stawarz I, Cheung CC, Ostorero L, Kosmaczewski E, Siemiginowska A (2020) On the Jet Production Efficiency in a Sample of the Youngest Radio Galaxies. ApJ892(2):116. https://doi.org/10.3847/1538-4357/ab7930. arXiv:1911.01197 [astro-ph.HE]
- Wold M, Lacy M, Lilje PB, Serjeant S (2000) Clustering of galaxies around radio quasars at $0.5 \lesssim z \lesssim 0.8$. MNRAS316(2):267–282. https://doi.org/10.1046/j.1365-8711.2000.03473.x. arXiv:astro-ph/9912070 [astro-ph]
- Wołowska A, Kunert-Bajraszewska M, Mooley K, Hallinan G (2017) Changing-look AGNs or short-lived radio sources? Frontiers in Astronomy and Space Sciences 4:38. https://doi.org/10.3389/fspas.2017.00038. arXiv:1712.00251
- Woo JH, Bae HJ, Son D, Karouzos M (2016) The Prevalence of Gas Outflows in Type 2 AGNs. ApJ817(2):108. https://doi.org/10.3847/0004-637X/817/2/108. arXiv:1511.05142 [astro-ph.GA]
- Worrall DM, Hardcastle MJ, Pearson TJ, Readhead ACS (2004) The relationship between the X-ray and radio components in the compact steep-spectrum quasar 3C 48. MNRAS347:632–644. https://doi.org/10.1111/j. 1365-2966.2004.07243.x. astro-ph/0309737
- Wright EL, Eisenhardt PRM, Mainzer AK, Ressler ME, Cutri RM, Jarrett T, Kirkpatrick JD, Padgett D, McMillan RS, Skrutskie M, Stanford SA, Cohen M, Walker RG, Mather JC, Leisawitz D, Gautier I Thomas N, McLean I, Benford D, Lonsdale CJ, Blain A, Mendez B, Irace WR, Duval V, Liu F, Royer D, Heinrichsen I, Howard J, Shannon M, Kendall M, Walsh AL,

- Larsen M, Cardon JG, Schick S, Schwalm M, Abid M, Fabinsky B, Naes L, Tsai CW (2010) The Wide-field Infrared Survey Explorer (WISE): Mission Description and Initial On-orbit Performance. AJ140(6):1868–1881. https://doi.org/10.1088/0004-6256/140/6/1868. arXiv:1008.0031 [astro-ph.IM]
- Wu F, An T, Baan WA, Hong XY, Stanghellini C, Frey S, Xu HG, Liu X, Wang JY (2013) Kinematics of the compact symmetric object OQ 208 revisited. A&A550:A113. https://doi.org/10.1051/0004-6361/ 201219700. arXiv:1211.4287
- Wu Q (2009a) Observational Evidence for Young Radio Galaxies is Triggered by Accretion Disk Instability. ApJ701:L95–L99. https://doi.org/10.1088/0004-637X/701/2/L95. arXiv:0907.2234 [astro-ph.HE]
- Wu Q (2009b) The black hole mass, Eddington ratio and M_{BH} - $\sigma_{[OIII]}$ relation in young radio galaxies. MNRAS398:1905–1914. https://doi.org/10.1111/j. 1365-2966.2009.15127.x. arXiv:0905.3663
- Xu C, Livio M, Baum S (1999) Radio-loud and Radio-quiet Active Galactic Nuclei. AJ118(3):1169–1176. https://doi.org/10.1086/301007. arXiv:astro-ph/9905322 [astro-ph]
- Xu D, Komossa S, Zhou H, Lu H, Li C, Grupe D, Wang J, Yuan W (2012) Correlation Analysis of a Large Sample of Narrow-line Seyfert 1 Galaxies: Linking Central Engine and Host Properties. AJ143(4):83. https://doi.org/ 10.1088/0004-6256/143/4/83. arXiv:1201.2810 [astro-ph.CO]
- Yang X, Liu X, Yang J, Mi L, Cui L, An T, Hong X, Ho LC (2017) VLBA 24 and 43 GHz observations of massive binary black hole candidate PKS 1155 + 251. MNRAS471(2):1873–1878. https://doi.org/10.1093/mnras/stx1743.arXiv:1707.03121 [astro-ph.GA]
- Yao S, Komossa S (2020) Spectroscopic classification, variability and SED of the Fermi-detected CSS 3C 286: the radio-loudest NLS1 galaxy? arXiv e-prints arXiv:2012.01785 [astro-ph.HE]
- Young JS, Schloerb FP, Kenney JD, Lord SD (1986) CO Observations of Infrared Bright Galaxies: The Efficiency of Star Formation. ApJ304:443. https://doi.org/10.1086/164179
- Yuan W, Zhou HY, Komossa S, Dong XB, Wang TG, Lu HL, Bai JM (2008) A Population of Radio-Loud Narrow-Line Seyfert 1 Galaxies with Blazar-Like Properties? ApJ685(2):801–827. https://doi.org/10.1086/591046. arXiv:0806.3755 [astro-ph]
- Zatsepin GT, Kuz'min VA (1966) Upper Limit of the Spectrum of Cosmic Rays. Soviet Journal of Experimental and Theoretical Physics Letters 4:78
- Zhang HY, Gabuzda DC, Nan RD, Jin CJ (2004) Parsec-scale rotation-measure distribution in the quasar 3C 147 at 8 GHz. A&A415:477–481. https://doi.org/10.1051/0004-6361:20034313
- Zhang J, Zhang HM, Gan YY, Yi TF, Wang JF, Liang EW (2020) Jet Properties of Compact Steep-spectrum Sources and an Eddington-ratio-driven Unification Scheme of Jet Radiation in Active Galactic Nuclei. ApJ899(1):2. https://doi.org/10.3847/1538-4357/aba2cd. arXiv:2005.11535 [astro-ph.HE]
- Zhao JH, Sumi DM, Burns JO, Duric N (1993) 3C 317: an Amorphous Radio

- Source in the Cooling Flow Cluster Abell 2052. ApJ416:51. https://doi.org/10.1086/173214
- Zinn PC, Middelberg E, Ibar E (2011) Infrared-faint radio sources: a cosmological view. AGN number counts, the cosmic X-ray background and SMBH formation. A&A531:A14. https://doi.org/10.1051/0004-6361/201016264. arXiv:1104.0564 [astro-ph.CO]
- Zinn PC, Middelberg E, Norris RP, Dettmar RJ (2013) Active Galactic Nucleus Feedback Works Both Ways. ApJ774(1):66. https://doi.org/10.1088/0004-637X/774/1/66. arXiv:1306.6468 [astro-ph.CO]
- Zovaro HRM, Nesvadba NPH, Sharp R, Bicknell GV, Groves B, Mukherjee D, Wagner AY (2019a) Searching for signs of jet-driven negative feedback in the nearby radio galaxy UGC 05771. MNRAS489(4):4944–4961. https://doi.org/10.1093/mnras/stz2459. arXiv:1909.00144 [astro-ph.GA]
- Zovaro HRM, Sharp R, Nesvadba NPH, Bicknell GV, Mukherjee D, Wagner AY, Groves B, Krishna S (2019b) Jets blowing bubbles in the young radio galaxy 4C 31.04. MNRAShttps://doi.org/10.1093/mnras/stz233. arXiv:1811.08971
- Zovaro HRM, Sharp R, Nesvadba NPH, Kewley L, Sutherland R, Taylor P, Groves B, Wagner AY, Mukherjee D, Bicknell GV (2020) Unravelling the enigmatic ISM conditions in Minkowski's object. MNRAS499(4):4940–4960. https://doi.org/10.1093/mnras/staa3121. arXiv:2010.03139 [astro-ph.GA]
- Zuther J, Eckart A, Scharwächter J, Krips M, Straubmeier C (2004) NIR observations of the QSO 3C 48 host galaxy. A&A414:919–926. https://doi.org/10.1051/0004-6361:20031677. astro-ph/0311007